THERMAL CHARACTERISTICS OF AN ALUMUNUM CLOSED-LOOP PULSATING HEAT PIPE CHARGED WITH AMMONIA

Md Shahidul Haque

A thesis submitted for partial fulfillment of the requirements for the degree of

MASTER OF SCIENCE IN MECHANICAL ENGINEERING

DEPARTMENT OF MECHANICAL ENGINEERING

BANGLADESH UNIVERSITY OF ENGINEERING AND TECHNOLOGY

Dhaka-1000, Bangladesh

December 2011.

CERTIFICATE OF APPROVAL

The thesis titled "**THERMAL CHARACTERISTICS OF AN ALUMUNUM CLOSED-LOOP PULSATING HEAT PIPE CHARGED WITH AMMONIA"** submitted by **Md Shahidul Haque**, Roll No: 0409102016F, Session: April 2009 has been accepted as satisfactory in partial fulfillment of the requirements for the degree of Master of Science in Mechanical Engineering on …….

BOARD OF EXAMINERS

_____ Chairman

Dr. M. Mahbubur Razzaque
Professor
Department of Mechanical Engineering, BUET, Dhaka

_____ Member

Dr M M Alam (Ex- Officio)
Professor and Head
Department of Mechanical Engineering, BUET, Dhaka

_____ Member

Dr. Mohammad Ali
Professor
Department of Mechanical Engineering, BUET, Dhaka

_____ Member

Dr. S. Reaz Ahmed
Professor
Department of Mechanical Engineering , BUET, Dhaka

_____ Member

Dr A K M Sadrul Islam (External)
Professor
Dept of Mcchanical and Chemical Engineering, IUT,Dhaka

CANDIDATE'S DECLARATION

It is hereby declared that this thesis or any part of it has not been submitted elsewhere for the award of any degree or diploma

Signature of the Candidate

_____

Md Shahidul Haque

ACKNOWLEDGEMENT

The author would like to express his sincerest gratitude to advisor *Dr. Muhammed Mahbubur Razzaque,* Professor, Department of Mechanical Engineering, Bangladesh University of Engineering and Technology, Dhaka for his kind supervision, guidance, encouragement and inspection throughout the entire research period.

The author also expresses thankful gratitude to *Dr. Chowdhury Md. Feroz*, former Professor, Mechanical Engineering Department, Bangladesh University of Engineering and Technology, Dhaka, who always guided and encouraged him in the course of this work. The author has been benefited a lot from his visions and advices not only in studies but also in experiences. The author must acknowledge particular debts to *Syful Ahmed ,Tanjheel Hasan Mahdi and Mohammad Abdullah Yousuf Khan*, final year students of BUET who helped the author in conducting the experiment. Special thanks goes to the members of *Fuel Testing Lab*, *Measurement, Instrumentation & Control Engg. Lab , Heat transfer lab and different shops.*

A lot of thanks are due for *Md. Abdul Awal*, Senior Lab Attendant of Fuel Testing Laboratory for his cooperation all through the research work. Thanks are also given to *Md. Masudur Rahman,* Assistant Instrument Engineer, Instrumentation and measurement lab and *Mr. Alauddin Fakir* of Heat Transfer Lab of Mechanical Engineering Department, Bangladesh University of Engineering and Technology, Dhaka for his cooperation.

Md Shahidul Haque

ABSTRACT

Pulsating heat pipe is a two-phase heat transfer device that uses pulsating motion to transfer heat from a source and passively move it to a condenser or radiator. In the recent past, many researches have been carried out on Pulsating Heat Pipes (PHPs) to enhance heat transfer through passive two-phase heat transfer mechanism. Although a complete theoretical understanding of operational characteristics of this device is not yet achieved, there are many emerging applications, ranging from electronics thermal management to compact heat exchangers. For a better theoretical understanding, it is vital to generate experimental data under various operating boundary conditions. In this background, this study aims for thermal analysis of a closed loop pulsating heat pipe based on heat input, inclination, fill ratio. So, a closed loop pulsating heat pipe is designed and fabricated with Aluminium. This closed loop Aluminium PHP with ammonia as working fluid is experimentally investigated for variable varying inclination and fill ratios. The experimental apparatus consists of a 8.862m long 3mm inner diameter closed loop Aluminum pipe meandering back and forth into an electrically heated block of Aluminum. One end of the PHPs is inserted inside the heater and the other end of it is placed in air. Heat transfer characteristics of PHPs are determined experimentally, based on the heat transfer principles. Response curves in terms of heat transfer rate, heat transfer coefficient and thermal resistance are obtained for different inclinations and liquid ammonia fill ratios. The overall heat transfer coefficient and thermal resistance of the system is determined to show the heat transfer capability of the PHP. The results show that, the performance of the heat pipe varies substantially for different inclinations and fill ratios.

NOMENCLATURE

Symbol	Meaning	Unit
A	Surface Area	m^2
g	Acceleration due to gravity	m/s^2
Q	Heat Load	Watt
T_{con}/ T_{eva}	Average Condenser / Evaporator Temperature	ºC
M	Mass	kg
P	Inside pressure of PHP	psig
T_{sat}	Saturation Temperature	ºC
ρ_l	Liquid Density	kg/m^3
ρ_v	Vapor density	kg/m^3
σ	Surface Tension	N/m
L	Length	m
V	Voltage	V
I	Current	Amp
t	Time	min
S_{Al}	Heat capacity of aluminum heating block	J/kgK
ΔT	Temperature Difference	℃
U	Overall heat transfer coefficient	W/m^2 ℃
k	Thermal conductivity	W/m ℃
R	Thermal resistance	℃/W
θ	Inclination	°(Degree)
V/V_{max}	Fill Ratio	-
Δt	Time Difference	min
D,d	Diameter of Pipe	m
B_o	Bond number	-

ABBREVIATIONS

CLPHP	Closed Loop Pulsating Heat Pipe
OLPHP	Open Loop Pulsating Heat Pipe
ID	Inner Diameter
OD	Outer Diameter
PHP	Pulsating Heat Pipe

SUBCRIPTS

con	Condenser
eva	Evaporator
l	Liquid
v	vapor
a	Ambient
ad	Adiabatic
ea	Evaporator to ambient
ca	Condenser to ambient
crit	critical
sat	saturation
i	inner
o	outer
ei	Evaporator inner surface
ci	Condenser inner surface
co	Condenser outer surface
elec	Electricity
w	wall
ins	insulator
php	PHP
bloc/Al	Aluminium block

Contents

Table of Contents

Figures

List Of Tables

Chapter 1

Introduction

1.1 Motivation

With the advancement of micro and nano technologies the electronic equipments are becoming smaller and smaller day by day; the power densities in the electronic equipments are increasing rapidly. It is becoming very important to facilitate optimum cooling in a small electronic device because integrated circuit lifetime increases with increasing cooling rate. It is a trade off situation: either to enlarge the package to accept additional cooling or to sacrifice IC lifetime. This is a great challenge in thermal design management. Among other cooling techniques, heat pipes emerged as the most appropriate and cost effective thermal design solution due to its excellent heat transfer capability, high efficiency and structural simplicity.

Thermal management of electronics is becoming very important and the limits are being stressed in every aspect of design. Modern development requires low thermal resistance from chip to heat sink, high heat transport capability of up to 250 W, high heat flux spreading up to 60 W/cm^2, mechanical and thermal compatibility, long term reliability, miniaturization, and low cost. These demands pose a simultaneous challenge of managing increased power levels and fluxes [1]. The thermal management problems of microelectronic components will worsen with further miniaturization. The size of microelectronic components is being reduced day by day with the development of electronics. Consequently, in the last decade, the number of active semi-conductor devices per unit chip area has almost quadrupled. This reduction in size also brings severe limitations to the conventional cooling techniques. Development of efficient thermal management scheme is essential to dissipate these high heat fluxes and maintain suitable operating temperature of the device. High power density and space constraint in most of the modern electronic devices, specifically in personal computers and telecommunications systems, placed constraint on the size of heat pipes. Development of this has accelerated the phase change techniques such as pool boiling, jet impingement cooling and more recently

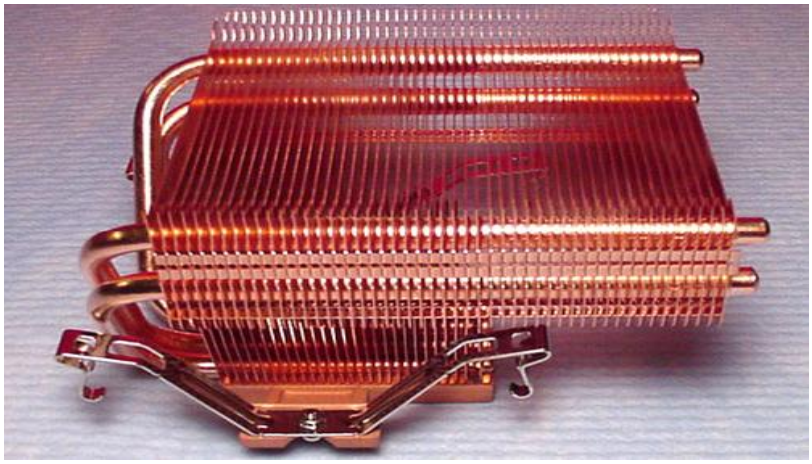

Figure 1.1: Heat pipe

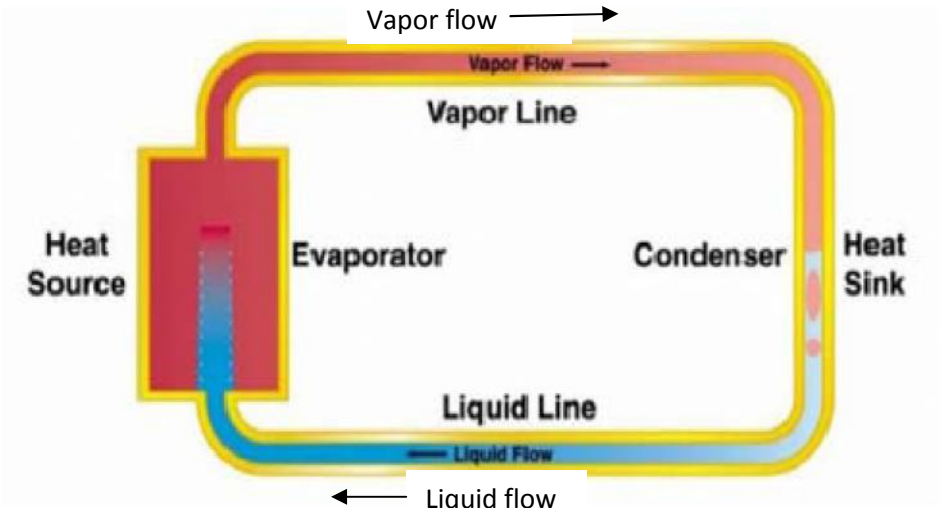

Figure 1.2: Liquid vapor circulation inside a heat pipe

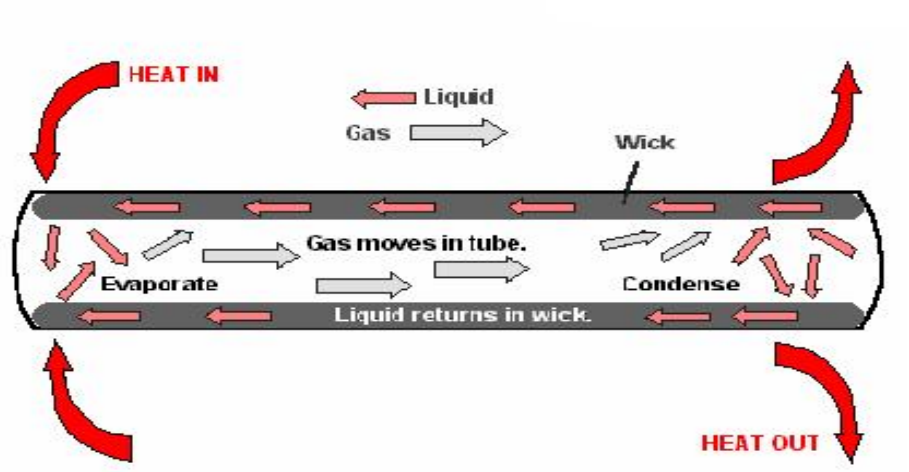

Figure 1.3: Operation of Heat pipe with wick structure

mini/micro channel flow boiling concepts [2]. The looped parallel heat pipe (LPHP) was developed to overcome poor performances of single tube heat pipe (STHP). Parallel heat pipes in various configurations and designs, have played a decisive role in many applications. In line with these developments, pulsating heat pipes introduced in the early nineties [3-4] have become a very promising heat transfer technology for electronics.

A heat pipe shown in fig 1.1 is a heat transfer device that employs both conduction and phase transition to efficiently manage the transfer of heat between two solid surfaces. It generally uses the gravitational force as the driving force for the flow of the working fluid. Heat pipes shown in fig 1.2are pencil-sized metal tubes that move heat from one end of the tube to the other without the aid of a pump. Within the heat pipe, heat is absorbed to vaporize a small amount of fluid at the hot end of the pipe; the fluid travels to the other, slightly cooler end and condenses before returning to the hot end through a capillary wick as shown in fig 1.3; thus the process continues to repeat. The device efficiently transfers large quantities of heat. Now-a-days heat pipe is widely used in computer, telecommunication and other various electronics equipment. It is a light weight device with no moving part. It is silent in operation and has several hundred times heat transport capacity compared to the best metallic heat conductor like silver and copper. Heat pipes are often called the "superconductors" of heat, as they possess an extra ordinary heat transfer capacity with almost no heat loss.

Pulsating Heat Pipe (PHP) is a special kind of heat pipe where slug-plug motion of the working fluid plays the most important role not the gravitational force. The unique feature of PHPs is that there is no wick structure to return the condensate to the evaporator section, and, therefore, there is no counter flow between the liquid and the vapor. It is considered as being a potentially useful option in the thermal management and control of electrical and electronic devices . It is a relatively new and simple two-phase heat transfer device [5]. A PHP has no moving parts, no wick structure and it can transfer heat even when the heat source, relative to gravity,

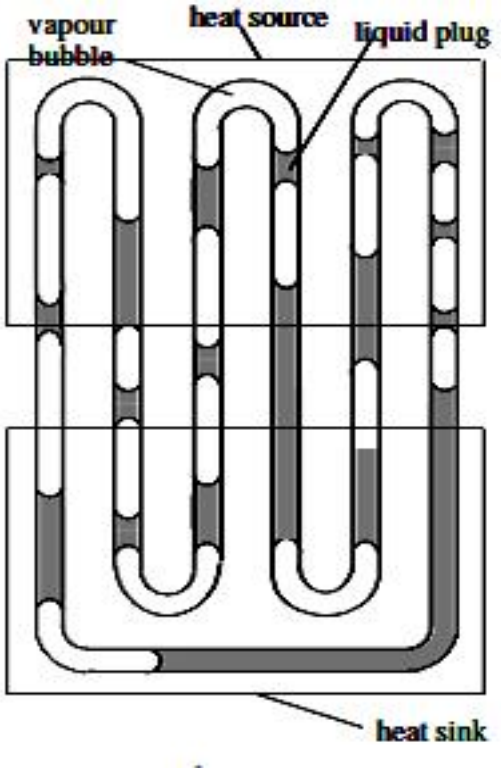

Figure 1.4: Pulsating Heat pipe (wickless structure)

is above the heat sink [6]. It consists essentially of a relatively long but small diameter pipe meandering in a serpentine fashion between the heat source and the heat sink. The pipe is sealed, evacuated and then charged with a working fluid. Provided the diameter is small enough the fluid forms a system of discrete liquid plugs and vapor bubbles that move in a random fashion back and forth between the heat source and the heat sink. A qualitative experimental analysis and flow visualization of the movement of the liquid plugs and vapor bubbles in a PHP has been addressed [7]. A number of attempts have been made to mathematically model a PHP [8-10]. It is suggested that boiling and condensation contribute towards the motion of the bubbles and plugs; the major mode of heat transfer is not due to the latent heat transfer but rather due to sensible heat transfer between the wall and the liquid plugs as they move back and forth in the pipe [12 & 13]. Thermal designers have widely accepted Closed Loop PHP [CLPHP] for their thermal design solution and the area of application of CLPHP has increased day by day. At this time however a comprehensive theory and reliable data or tools for the design of PHPs for a specific cooling application is as yet not available [14-16]. So a thorough comprehension of the dependence of the heat transfer capacity of CLPHP on

geometry and other factors influencing its performance is indispensable for further development.

Looking into the available literature, it can be seen that six major thermo-mechanical parameters have emerged as the primary design parameters affecting the PHP system dynamics [17]. These include:· internal diameter of the PHP tube,· input heat flux to the device, volumetric filling ratio of the working fluid, total number of turns, device orientation with respect to gravity, and thermo-physical properties of the working fluid. Other conditions which influence the operation are: ·use of direction control check valves, tube cross sectional shape, tube material and fluid combination, and rigidity of the tube material etc. Apart from these variables, the performance is also strongly linked with the flow patterns existing inside the device. Various flow patterns other than capillary slug flow, e.g. bubbly flow, developing or semi-annular flow and fully developed annular flow (in case of CLPHPs) have also been reported which have a significant effect on the thermal performance of the device [18-25]. The state of the art strongly suggests that a comprehensive theory of the complex thermo hydrodynamic phenomena governing the operation of PHPs is not yet available. Authoritative quantitative database explicitly connecting the thermal performance with individual influence parameters is limited but growing continuously.

1.2 Objectives

The objective of this thesis is to present the experimental data of an ammonia-charged pulsating heat pipe. Such data are important because ammonia is a particularly efficient heat transfer fluid and no published result of its usage in a PHP is found in literature. Further, in an attempt to better understand the functioning of a PHP, the thermo-fluid dynamics of a simple liquid plug and vapor bubble system will be investigated. The main objectives of this experimental study are:

(a) To study the heat transfer performance of a Closed Loop Pulsating Heat pipe [CLPHP].

(b) To study the temperature profile and the heat transfer rate at different sections of the CLPHP as a function of time, fill ratio and inclination angle.

(c) To evaluate the heat transfer coefficient and thermal resistance of CLPHP for different heat input, fill ratio and inclination angles.

(d) To compare the maximum overall heat transfer coefficient and thermal resistance of CLPHP for different fill ratio and inclination angles.

(e) To develop an empirical correlation that correlates the experimental data.

1.3 Scope of the Present Study

In the present study, thermal analysis of a thin walled Aluminum CLPHP has been presented. The investigation has the objective to find out the thermal performance of the CLPHP with different fill ratio and orientations. Such findings are useful both for understanding the thermo-fluid transport phenomena inside the CLPHP capillary tube and for the practical design and operation of CLPHPs.

In this thesis, development of heat pipe, modern trend of heat pipes and the basic mechanism and design parameters of pulsating heat pipes are reviewed in chapter 2. Experimental setup, experimental procedure, data collection and calculation procedure are discussed in chapter 3. Experimental results are discussed and an empirical correlation is developed in chapter 4. Chapter 5 contains the conclusions and recommendations for further work.

Chapter 2

Literature Review

2.1 The Early History

In 1939, E. Schmidt, a German engineer, reported that heat transfer rate of a copper tube filled with ammonia or carbon dioxide near its critical point is more than 400 times greater than that of a solid rod of copper with same dimensions and at the same temperature difference between the hot and the cold regions. But the limitation of that experiment is that it can operate only in vertical position.

The idea of heat pipe was first suggested by Gaugler [26] in 1942. According to Gaugler, the objective of the invention was "The evaporation of the liquid to a point above the place where the condensation or the giving off the heat takes place without expanding upon the liquid any additional work to lift the liquid to an elevation above the point at which condensation takes place". A capillary structure was proposed as the means for returning the liquid from the condenser to the evaporator, and Gaugler suggested that, one form of this structure might be a sintered iron wick.

This device received little attention until 1964, when Grover and his colleagues at Los Alamos National Laboratories published the results of an independent investigation and first applied the term heat pipe. Grover [27] provided limited theoretical analysis and presented results of experiments carried out on stainless steel heat pipes with a wire mesh wick and sodium as working fluid. Lithium and silver were also mentioned as working fluids.

The first commercial organization to work on heat pipes was RCA [28]. During the two year period between mid 1964 to mid 1966 they made heat pipes using glass, copper, nickel, stainless steel and molybdenum. Working fluids included water, cesium, sodium, lithium, bismuth etc. During 1967 and 1968 several articles appeared in the United States scientific press indicating a broad area of application of the heat pipes for electronic cooling, air conditioning, engine cooling and others. In 1968, heat pipe was first used in space for satellite thermal control on GEOS-B,

launched from Vandenberg Air Force base. The purpose of the heat pipe was to minimize the temperature difference between various transponders in the satellite. In 1969, NASA developed a new type of heat pipe called rotating heat pipe in which the wick was omitted. These heat pipes were utilized for cooling motor rotors and turbine blade rotors.

Most of the work on heat pipes described so far has been associated with liquid metal working fluids and, for low temperature, water, acetone, alcohols, etc. With the need for cooled detectors in satellite infrared scanning systems cryogenic heat pipes began to receive particular attention. The most common working fluid in these heat pipes was nitrogen, which was acceptable for temperature ranges between 77 and 100°K. Liquid oxygen was also used for this temperature range. The Rutherford High Energy Laboratory (RHEL) was the first organization in the United Kingdom to operate cryogenic heat pipes, liquid hydrogen units being developed for cooling targets at the RHEL. Later RHEL developed a helium heat pipe operating at 4.2 °K.

By 1970 a wide variety of heat pipes were commercially available from a number of companies in the United States. RCA, Thermo-Electron, and Noren Products were among several firms marketing a range of ‘standard’ as well as “customized” heat pipes. During the next few years several manufacturers were established in the United Kingdom and a number of companies specializing in heat pipe heat recovery systems, based primarily on technology from the United States, have entered what is becoming an increasingly competitive market. While much development work was concentrated on ‘conventional’ heat pipes, increasing interest was seen in the rotating heat pipe and in research into electro-hydro-dynamics for liquid transport. The proposed use of ‘inverse’ thermal siphons and an emphasis on the advantages (and possible limitations) for gravity-assisted heat pipes have stood out as areas of considerable importance. The reason for the growing interest in these topics is not difficult to find. Heat pipes in terrestrial applications have, probably in the majority of cases, proved particularly viable when gravity, in addition to capillary action has aided condensate return to the evaporator.

Loop heat pipes were invented in the former Soviet Union in the early 1980s. Thermacore Inc. brought expertise in the design and fabrication of loop heat pipes to

the United States in 1990. During the past several years, the ability to fabricate all aspects of loop heat pipes were transferred to Thermacore Inc. and its sister company, Dynatherm Corp.

2.2 Development of Pulsating Heat Pipe

Since the introduction of conventional heat pipe in 1960s, various geometries, working fluids, and wick structures have been proposed [29]. In the last 20 years, new types of heat pipes—such as capillary pumped loops and loop heat pipes—were introduced, seeking to separate the liquid and vapor flows to overcome certain limitations inherent in conventional heat pipes. In the 1990s, Akachi et al. and Polášek, F [5] invented a new type of heat pipe known as the pulsating or oscillating heat pipe (PHP or OHP). The most popular applications of PHP are found in electronics cooling because it may be capable of dissipating the high heat fluxes required by next generation electronics. Other proposed applications include using PHPs to preheat air or pump water. This section will describe the operation of pulsating heat pipes, summarize the research and development over the past decade, and discuss the issues surrounding them that have yet to be resolved.

Pulsating heat pipes, like conventional heat pipes, are closed, two-phase systems capable of transporting heat without any additional power input, but they significantly differ from conventional heat pipes in several ways. A typical PHP is a small meandering tube that is partially filled with a working fluid [30]. The tube is bent back and forth parallel to itself, and the ends of the tube may be connected to one another in a closed loop, or pinched off and welded shut in an open loop. It is generally agreed that the closed-loop PHP has better heat transfer performance [31, 32]. For this reason, most experimental work is done with closed-loop PHPs. In addition to the oscillatory flow, the working fluid can also be circulated in the closed-loop PHP, resulting in heat transfer enhancement. Although an addition of a check valve could improve the heat transfer performance of the PHPs by making the working fluid move in a specific direction, it is difficult and expensive to install these valves. Consequently, the closed-loop PHP without a check valve becomes the most favorable choice for the PHP structures. Recently, PHPs with a sintered metal wick have been prototyped by Zuo et al. [33] and analyzed by Holley and Faghri [34]. The

wick should aid in heat transfer and liquid distribution. There has also been some exploration into pulsating heat pipes in which one or both ends are left open without being sealed [35-37].

According to the previous investigations, the maximum heat transport capacity of a heat pipe with 0.01- 0.5 mm hydraulic radius was 0.03 - 0.5 W and the heat flux was 1 W/cm^2 of the surface area of the evaporator. It was reported that the maximum heat transport capacity is 4 - 5 W for a flat micro heat pipe of 1 mm hydraulic diameter. Faghri [29] mentioned that it was necessary to improve the maximum heat transport capacity in order to cover the thermal load encountered in the most main ICs of the current computers.

In 1991, Merrigane at Los Alamos National Laboratory tested alumina borosilicate covered stainless steel-sodium heat pipes to use in high temperature radiators. The tests indicated radiation heat rejection rates from the fabric-covered surface was strongly affected by the emittance of the underlying metal substrate. In the same year, Rankine at Los Alamos National Laboratory presented the results of studies on a thermionic reactor concept that using a combined beryllium and zirconium hydride moderator allows heat pipe cooling of a compact thermionic fuel element.

Gottschlich at Wright-Patterson Air Force Base described the cooling of gas turbine engine vanes using heat pipes. A heat pipe flight test was done on a Hitchhiker canister abroad the Space Shuttle Discovery (STS-53) in December 1992. The canister housed two oxygen heat pipe designs. These heat pipes, cooled by five Stirling-cycle cryocoolers, were developed to demonstrate heat rejection techniques for the spacecraft infrared sensors.

In 1993, Woloshun described the design, fabrication, and ground test at Los Alamos National Laboratory of three stainless steel-potassium heat pipes: one with a homogeneous screen wick, one with an arterial wick, and the last with an annular gap wick. This experiment, sponsored by the US Air Force Philips Laboratory, flew abroad STS-77 in May 1996, becoming the first American-built liquid metal heat pipes to operate in micro gravity conditions. In 1995, Judd investigated the use of heat pipes to regulate the temperature of a carbide cutting tool on an engine lathe.

Acrolab in Windsor, Ontario manufactured heat pipes to isothermalize molds and extruders used in the plastics and rubber industries.

A family of these devices has been produced to begin to address several applications, such as cooling of avionics in aircraft and missiles, aircraft-anti-icing, regulation of temperature of spacecraft, and solar heating to produce domestic hot water. Development of a Loop heat pipe (LHP) anti icing system was done in NASA Lewis Research Center. Loop heat pipes are used to passively transport engine waste heat forward to supply heat to critical surfaces to prevent ice formations. Because waste heat is used here, there is no power penalty and engine efficiency remains high.

Heat pipes are not in general a low cost solution to the cooling problem, but they are most effective and have great potential as power level and volume requirement increase. For these reasons heat pipes have been applied up to now mainly in applications with special working conditions and requirements, such as in space thermal control, in aircraft devices, in traction devices, in audio amplifiers, in cooling of closed cabinets, in harsh environmental conditions etc. Heat pipes, because of their high thermal conductivity, provide an essential isothermal environment with very small temperature gradients between the individual components.

2.3 The Modern Trends

A breakthrough innovation in the application of heat pipe technology in modern times came through the miniaturization and effectiveness of heat pipes. Studies on the application of pulsating heat pipes of inner diameter around 3 mm for cooling of the electronics items have been actively conducted by the American and Japanese enterprises specializing in heat pipes. Recently, researchers performed experimental investigation on cooling characteristics of PHP of 3 or 4 mm diameter with wick and wickless structures and water, ethanol, ammonia, etc. as working fluids. The parameters of their experiment were heat input, fill ratio, inclination, coolant flow rate, structure of the pipes and length of the condenser. They claimed that the heat transfer rate increases with the increasing condenser length. The experimental data prove that the radially rotating high-temperature micro heat pipe has a high effective thermal conductance, which is 60–100 times higher than the thermal conductivity of

copper, and a large heat transfer capacity that is more than 300 W. Investigation on high performance pulsating heat pipes were carried on with new capillary structure – notched fins, capillary fins and flooded sheet fin. The heat pipe with notched fins has the lowest internal thermal resistance at similar operating temperatures. Zhang in 2002[39] have carried out test and comparison to the starting performance, maximum transfer power and heat transfer performance under condition of antigravity of the heat pipes with three different structural wicks (sintered, mesh and fiber). They found that all structures of wicks have little influence on the heat transfer capability of heat pipe with the aid of gravity. Under condition of antigravity, the structure of wicks has obvious influence on the heat transfer capability of heat pipes.

2.4 Pulsating Heat Pipes

Pulsating heat pipes (PHPs) or oscillating heat pipes (OHPs) are characterized by the following basic features [23]:

(a) No wick structure
(b) At least one heat receiving (evaporator) zone
(c) At least one heat dissipating (condenser) zone
(d) An optional 'adiabatic' section separating the evaporator and the condenser zones
(e) Meandering tube of capillary dimensions with many turns filled partially with a suitable working fluid.
(f) Self-excited thermally driven oscillations
(g) Surface tension predominates; although gravity may affect the performance
(h) Latent as well as sensible heat transport possible by the self-oscillating working fluid.

This tube may be of two types:

- Closed Loop: tube ends are connected to each other in an endless loop [Fig 2.1(a)].
- Open Loop: tube ends are not connected to each other; essentially one long tube bent in multiple turns with both ends sealed after filling the working fluid [Fig 2.1(b)].

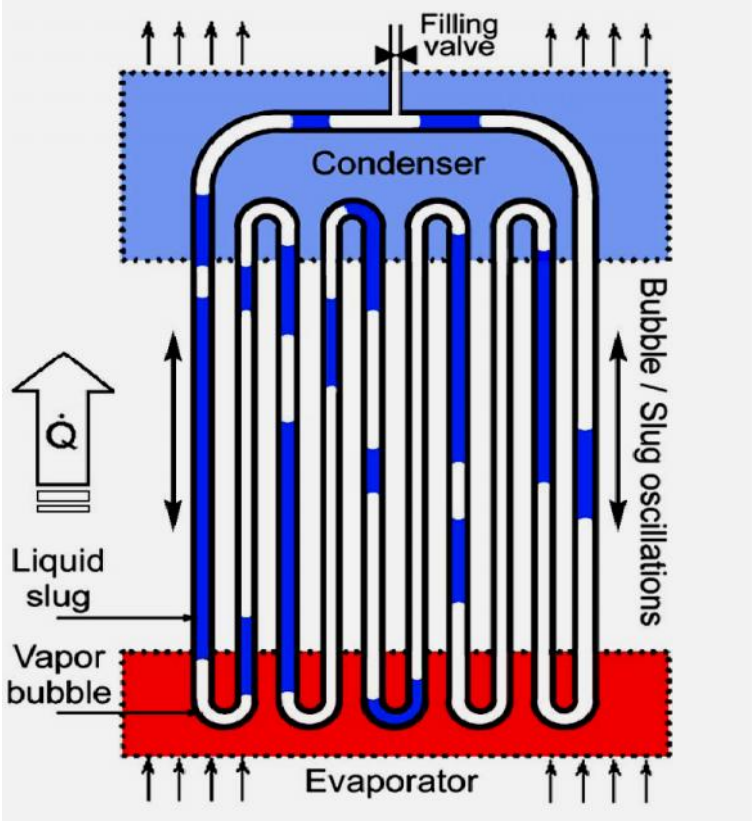

(a) CLPHP

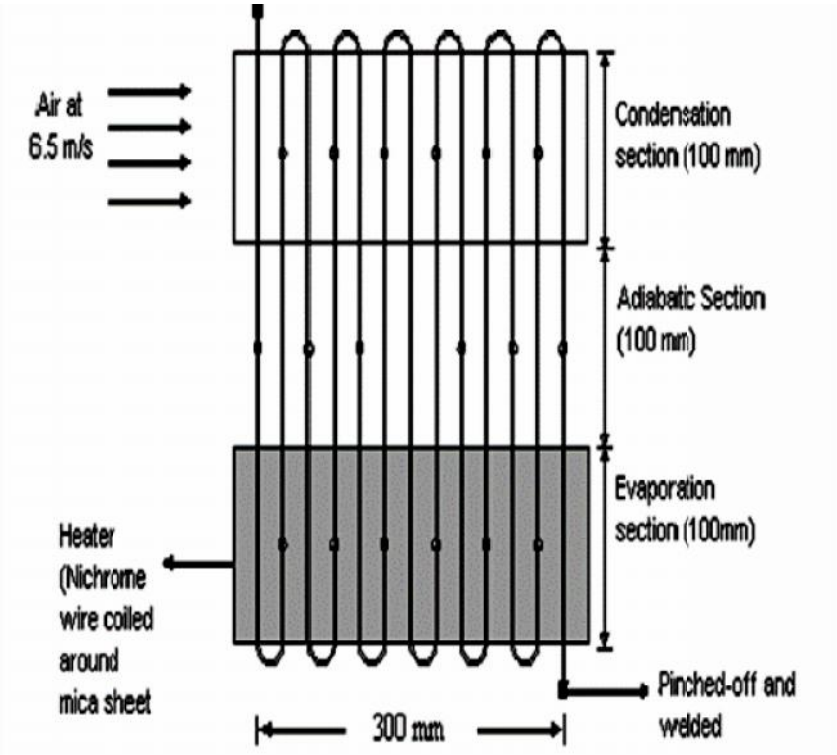

(b) OLPHP

Figure 2.1: Schematic representation of pulsating heat pipe (a) Closed loop PHP (b) Open loop PHP

2.5 Working Mechanism of Pulsating Heat Pipe

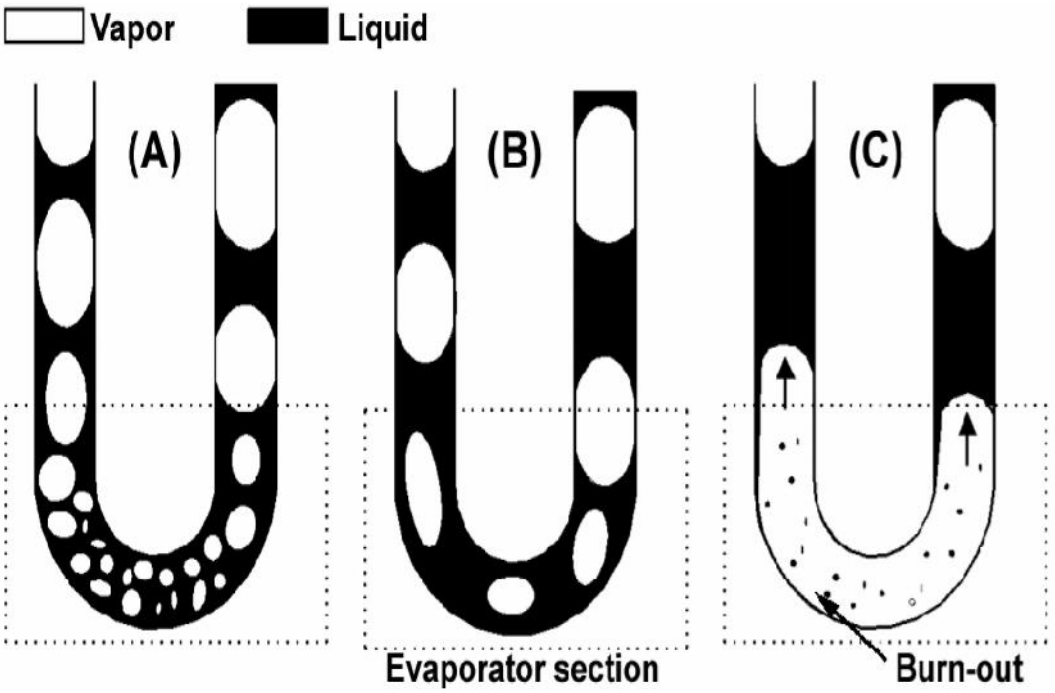

Figure 2.2 Operational states of CLPHP

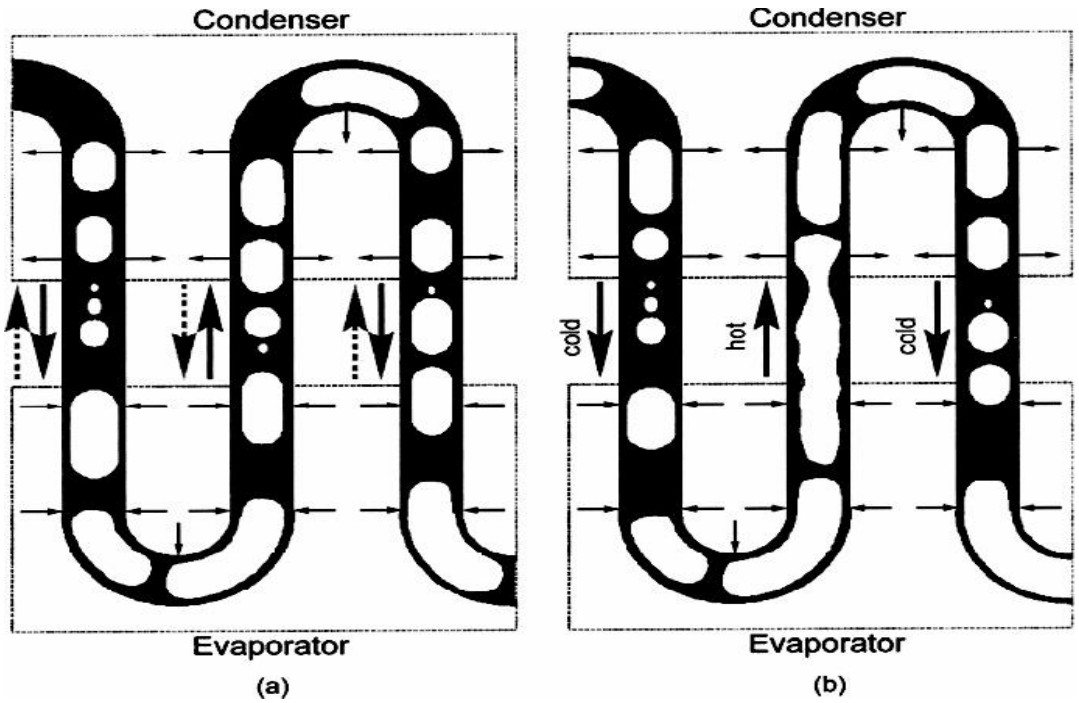

Figure 2.2: Bubble pattern in pulsating heat pipes

A PHP is essentially a non-equilibrium heat transfer device. The liquid and vapor slug transport results because of the pressure pulsations in the system. Since these pressure pulsations are fully thermally driven, because of the inherent constructions of the device, there is no external mechanical power source required for the fluid transport. The size of bubble in loop are shown figure 2.2. At lower heat input the size of bubble plugs are very small [Fig 2.2(A)] but with the increase of heat input the size of bubbles increases increasing the heat transfer [Fig 2.2(B)]. If the temperature increases too much then dry out or burn out may occur in the evaporator section [Fig 2.2(C)]. In an actual working PHP, there exists a
temperature gradient between the evaporator and the condenser sections. At lower heat input there is no fixed flow pattern of bubbles within the PHP rather the bubbles oscillates inside the pipes [Fig 2.3(a)] but a further increase in heating power results in 'stable' oscillations whose amplitude increases with increase in input power. Eventually, the fluid oscillations in alternate tubes come in phase with each other thereby resulting in an overall fluid circulation in the device [Fig 2.3(b)].

2.6 Design Parameters

Various experimental investigations indicated the following main variables affecting PHP performance:

•**Geometric Variables**: Overall length of the PHP, diameter/size and shape of the tube, length and number of turns of evaporator/condenser/adiabatic section.

•**Physical Variables:** Quantity of the working fluid (filling ratio), physical properties of the working fluid and tube material.

•**Operational Variables:** Open loop or closed loop operation, heating and cooling methodology, orientation of the PHP during operation, use of check valves.

It is evident that there are multiple variables which simultaneously affect the operation and performance of PHPs. So far as capillary slug flow exists inside the entire device, it has been demonstrated that latent heat will not play a significant role in the device performance. Nevertheless, bubbles are certainly needed for self-sustained thermally driven oscillations. The performance not only depends on a large

number of parameters described above, but also on the flow pattern. This makes it more difficult to undertake mathematical modeling using conventional techniques.

2.7 Performance Influencing Parameters

Looking into the available literature, it can be seen that six major thermo-mechanical parameters have emerged as the primary design parameters affecting the PHP system dynamics. These include:

- Internal diameter of the PHP tube
- Input heat flux to the device
- Volumetric filling ratio of the working fluid
- Total number of turns
- Device orientation with respect to gravity
- Working fluid thermo-physical properties

Other conditions which influence the operation are:

- Use of flow direction control check valves
- Tube cross sectional shape
- Tube material and fluid combination
- Rigidity of the tube material
- Flow patterns existing inside the device [37].

2.7.1 Tube Diameter

The internal tube diameter is one of the parameters which essentially define a PHP. The physical behavior adheres to the 'pulsating' mode only under a certain range of diameters. The critical Bond number (or Eötvös) criterion gives the tentative design rule for the diameter. The Bond number (or alternatively the Eötvös number) is the ratio of surface tension and gravity forces and defined as follows,

$$(E\ddot{o})_{crit} = (B_0)^2_{crit} \approx \frac{D^2_{crit} \times g \times (\rho_l - \rho_v)}{\sigma}$$

If the Bond number exceeds a particular critical value (Bo_{crit} ≈2) stable liquid slugs will not form and the device will not function as a pulsating heat pipe. For Bo > 2, the heat transfer limitation comes from nucleate pool boiling and counter-current flow limitations. A theoretical maximum tolerable inner diameter, D_{max}, of a PHP capillary tube was derived based on the balance of capillary and gravity forces by Akachi and Polasek [5],

$$D_{max} = D_{crit} = 2 \times \sqrt{\frac{\sigma}{g \times (\rho_l - \rho_v)}}$$

where σ, g, and ρ are surface tension, gravitational acceleration, and density, respectively.

As the PHP tube diameter increases beyond the D_{max}, ($D >> D_{max}$ or $D \geq D_{max}$) the surface tension is reduced and all the working fluid will tend to stratify by gravity and the heat pipe will stop functioning as a PHP, and the device may operate as an interconnected array of two- phase thermo-siphons [Fig 2.4 (case A and case B)]. If $D < D_{max}$, surface tension forces tend to dominate and stable liquid slugs are formed [Fig 2.4 (case C)].

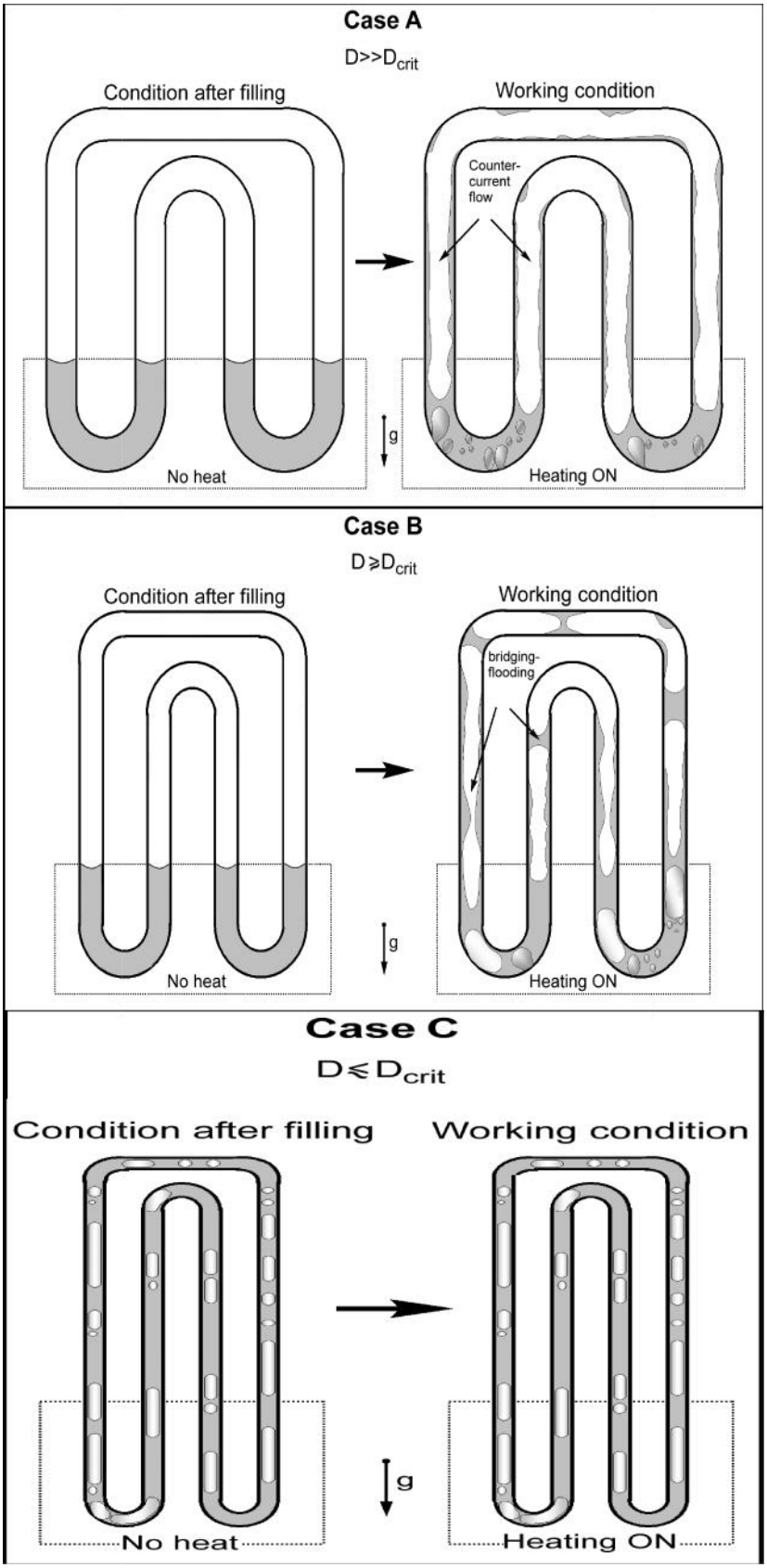

Figure 2.4: Effect of diameter on fluid distribution inside the circular tube of CLPHP under adiabatic and operating conditions

2.7.2 Heat flux

Low heat flux normally leads to generation of very small bubbles in the evaporator region, a process phenomenologically similar to nucleate pool boiling. As the input heat flux surpasses a critical value, oscillations are initiated in the beginning, these oscillations are abrupt and there is no specified flow circulation in the tube loop. The flow pattern remains oscillating capillary slug flow. A further increase in heating power results in 'stable' oscillations whose amplitude increases with increase in input power. Eventually, the fluid oscillations in alternate tubes come in phase with each other thereby resulting in an overall fluid circulation in the device. The direction that the flow takes is arbitrary for a given experimental run [Fig 2.3 (a, b)]. Increase in heater power further increases the circulation velocity by increasing the bubble size and movement velocity of bubbles [Fig 2.5]. The flow direction tends to remain more fixed. Initially the flow is a capillary slug flow [Fig2.6 (a, b)]. This marks the beginning of a flow transition from capillary slug flow in the entire device to a combination for capillary slug flow in the down-header tubes (from condenser to the evaporator) and semi-annular/ annular flow in the up-header tubes (from evaporator to the condenser) [Fig 2.6 (c, d)]. The slugs in the cold down-headers keep shrinking in size with further increase in the input heat power [Fig 2.6 e]. As the vapor volumetric fraction increases in the annular flow up-headers, since the net void fraction must remain effectively constant, the down-header bubbles must shrink in size. The results also indicate that the pulsating unstable slug flow behavior is again stabilized after a certain higher input heat flux.

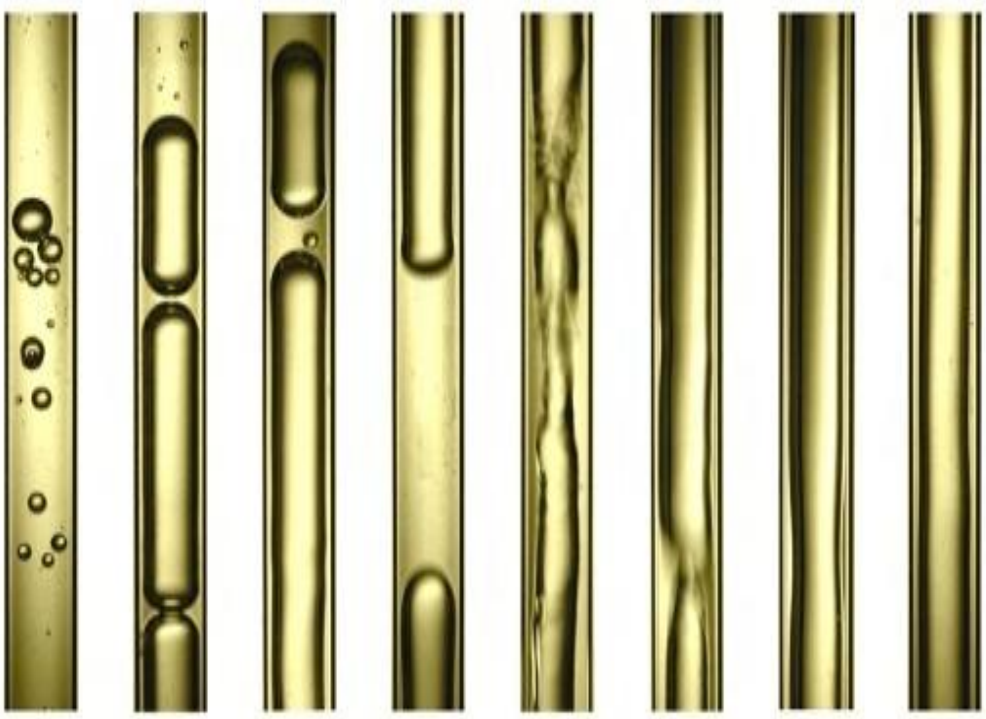

Figure 2.5: Changing Patterns of bubble flow from evaporator through tube with increase of heat flow

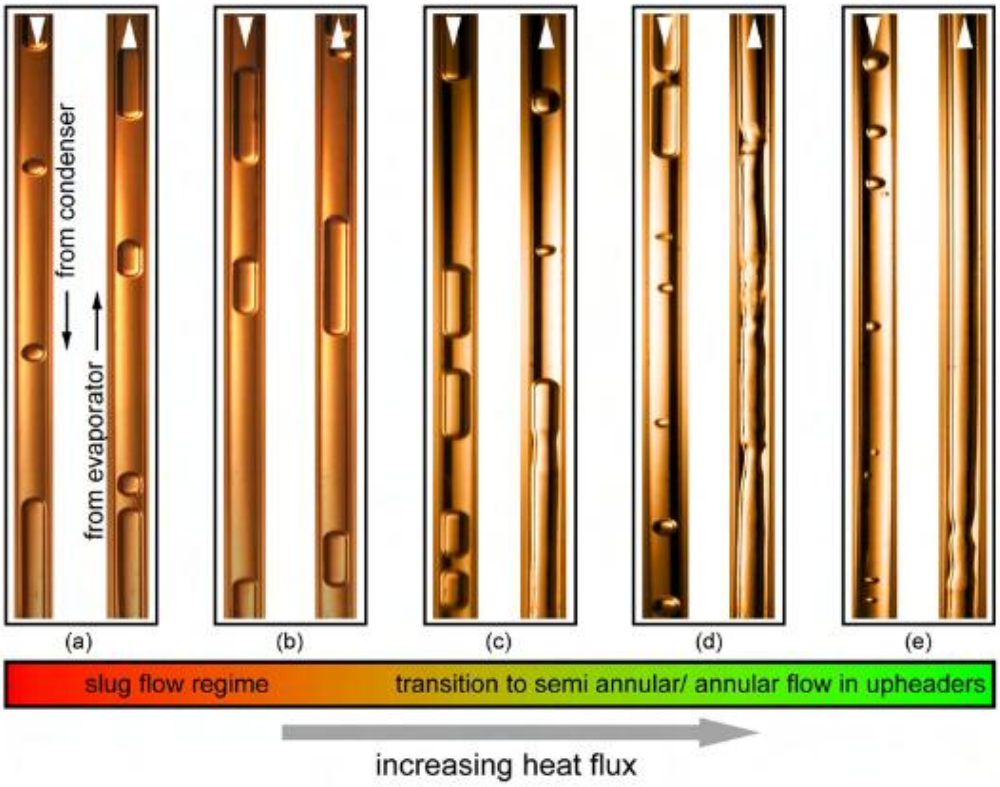

Figure 2.6: Pattern of bubble flow from evaporator and condenser through tube with increase of heat flux

2.7.3 Working Fluid Fill Ratio

Immediately after filling the CLPHP, the working fluid naturally distributes itself into various liquid vapor plug-bubble systems in a random fashion.

Experimental results indicate that there is an optimum filling ratio for proper PHP operation (in the pulsating mode of operation). This optimum, however, is not sharply defined but generally is around 50% filling of charge. A too high filling ratio above the optimum leads to a decrease in the overall degree of freedom as there are not enough bubbles for liquid pumping.

A 100% filled CLPHP is identical in operation to a single-phase thermo-siphon. In this case, the liquid starts circulating inside the device due to a density difference associated with the temperature gradient. The buoyancy force must overcome the liquid phase viscous dissipation and the wall shear stresses to set the liquid into circulation, causing a net sensible heat transfer from the heater to the cooler.

A 0% filled CLPHP with only bare tubes having no working fluid inside, is a poor conduction mode heat transfer device obviously having a very undesirable high thermal resistance.

2.7.4 Total Number of Turns

If a same system is cooled by a CLPHP, then in this case, instead of bare copper rods there are copper pipes partially filled with a working fluid. The heat transfer primarily takes place due to liquid convection, provided the CLPHP is optimally operating in the true pulsating regime. For a given heat throughput requirement, an optimum number of turns must exist after which the pulsating effect of the fluid inside, and the heat transfer advantage there-of, will start to diminish.

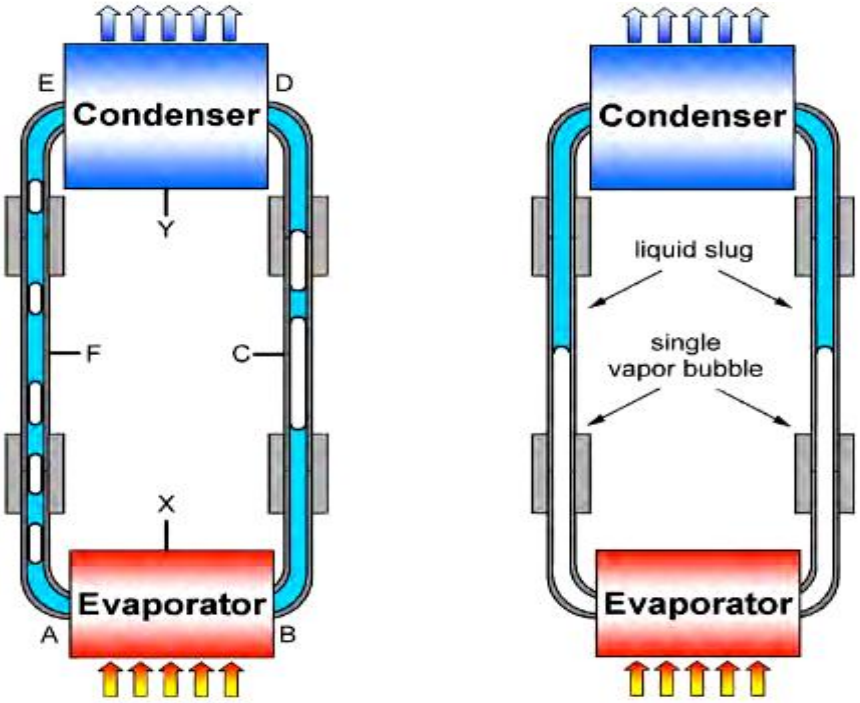

Fig 2.7: (a)Natural distribution of bubble in single loop CLPHP (b) Stop over phenomenon in single loop CLPHP

The initial partial filling of the loop leads to a natural volumetric distribution of phases in the two tube sections [Fig 2.7 (a)]. As the heating power is switched on, the system starts to oscillate in the usual manner. If there is only one turn bubble agglomeration takes place leading to the formation of a single large bubble which envelopes the entire evaporator section Then oscillations die down completely and all macro motion of the fluid inside the tube stops leading to an increase of the evaporator temperature. This condition essentially leads to a dry out and small perturbations cannot amplify to make the system operate self-sustained [Fig 2.7(b)]. As the number of turns keeps increasing, the probability of such a tendency towards complete stopover will essentially diminish, approaching practically zero as the number of turns exceeds a certain critical value.

Chapter 3

Experimental Setup and Process

A closed loop pulsating heat pipe and the experimental facility have been designed, and fabricated as shown in Figure 3.1 and 3.2. The detailed description of experimental apparatus and experimental procedure are illustrated in the following sections of this chapter.

3.1 Experimental Apparatus

A pulsating heat pipe configured as closed loop was built using Aluminum tubing of 4.0 mm OD, 3.0 mm ID and 8.862 m length to form 14 parallel channels with 13 bends. The detailed dimensions of the closed loop pulsating heat pipe system are listed in Table 3.1. The evaporator section of the heat pipe was placed inside a grooved Aluminum block. Grooves were exactly of same dimension of the heat pipe to avoid any gap between the block and the pipe tubing to ensure smooth heat flow to the PHP. A heater coil was placed inside the Aluminum block which acted as heat source. The CLPHP was built with 3 sections: evaporator, adiabatic and condenser. The evaporator section is about 210 mm long, the adiabatic is 120 mm long and the condenser is 324 mm long. The apparatus was placed on a stand that can be rotated at different orientations. The stand was constructed with wood to avoid heat conduction. For the tests at 0° (vertical), 30°, 45° and 60° setting, the evaporator section was below the condenser section and for 180° setting, the evaporator section was above the condenser section. For the tests under horizontal orientation (90°), all sections were on the same plane. Both evaporator and adiabatic sections were thermally insulated, while the condenser section was open to the surrounding air. The condenser section was cooled by natural flow of air. Aluminium pipes were bend by applying heat to avoid any deformation of cross section. Here air gap between the PHP tube and the Aluminium block would act as a resistance to heat flow between the tube wall and the heating block which will hinder smooth heat flow from the evaporator to the working fluid.To avoid this the slot inside the heating block was grooved as nearer to the outer dia of the tube as possible. To cut this groove a special

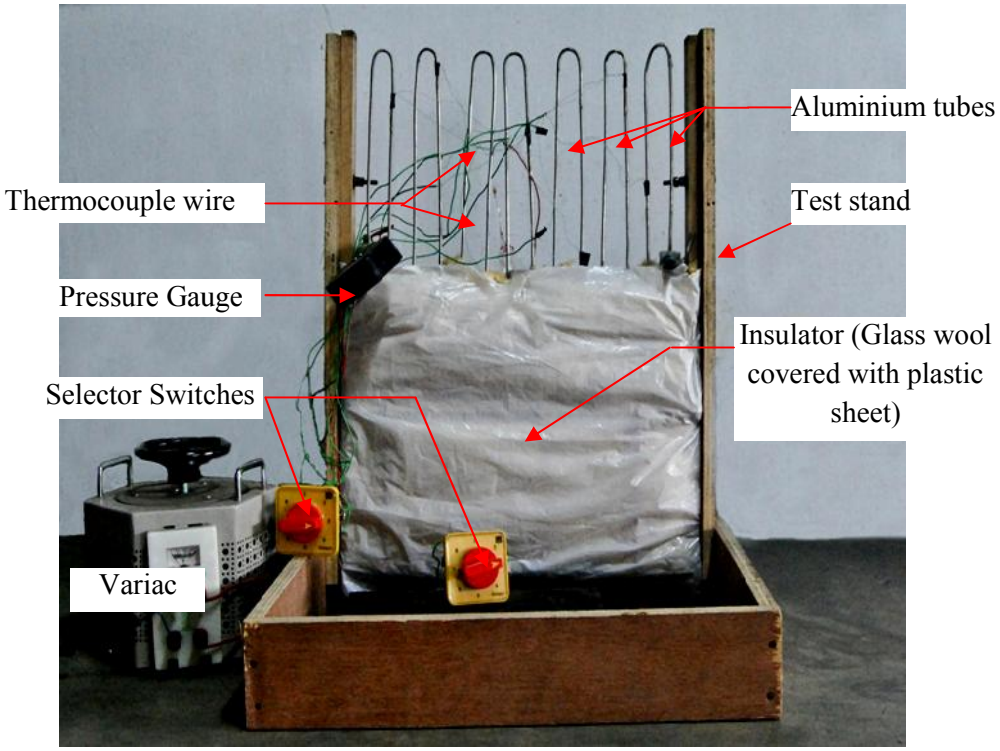

Fig 3.1: Photograph of the experimental setup

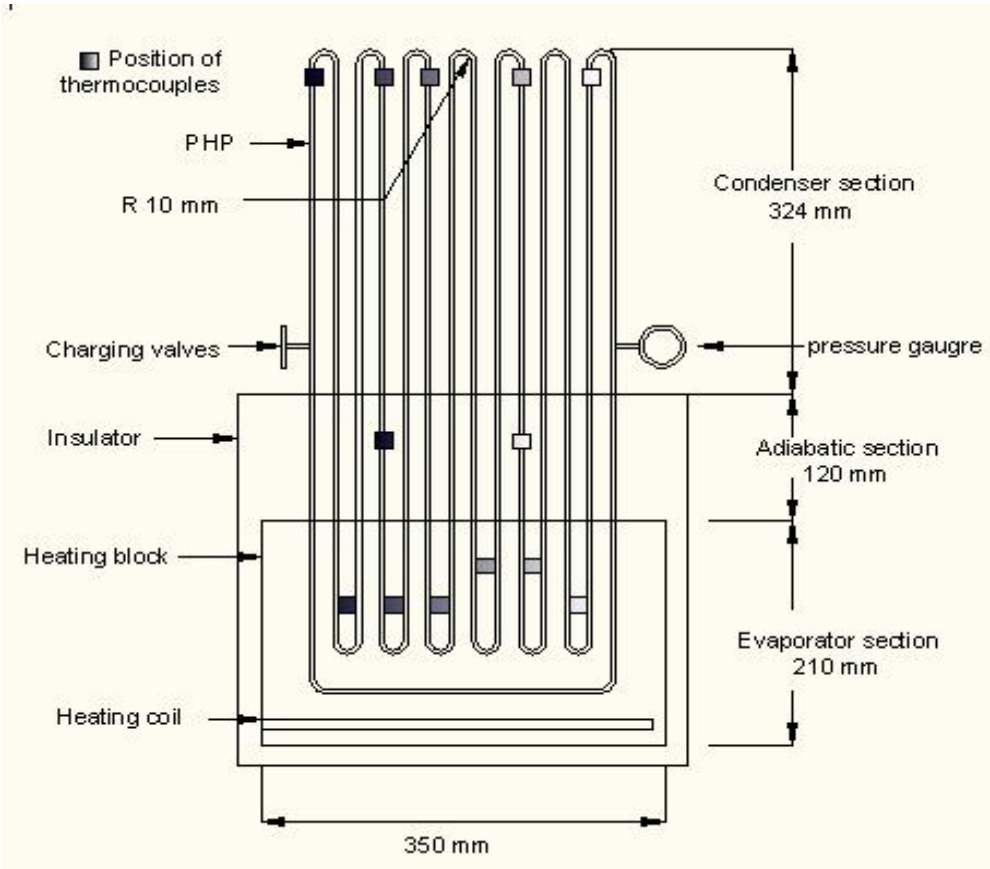

Fig 3.2: Schematic diagram of the CLPHP system.

machine called Jig boring machine was used whose accuracy was very high uoto 10 micron. Practically the dia of groove was a bit lower than the dia of outer tube so that when two parts of heating block are clamped together the tubes were under pressure to avoid any air gar between them. A hole was drilled in the Aluminium block to heat it with a heater. A special type of paper was used which act as insulator to electricity but which will not hinder the flowing of heat from the heater to the block. Thermocouples were attached to evaporator, adiabatic and condenser section to monitor the temperature at various section. Rotating frame was made of wood to avoid any heat loss by conduction.

3.1.1 Heat Pipe and Heating Block

Different sections of the closed loop pulsating heat pipe (CLPHP) are:
Evaporator section: It consists of an electric coil and an Aluminum heat pipe inserted inside a grooved Aluminum block. Heat is added to the heat pipe by the electric heater.

Condenser section: Heat is removed from the heat pipe through the condenser section by natural convection of air.

Adiabatic section: This section is between the evaporator and condenser sections and is covered with glass wool.

Table 3.1 Detail dimensions of the CLPHP system

Parameters	**Symbol**	**Dimensions (m)**
Heating block	block	0.35x0.21x0.035
Insulation	ins	0.39x0.35x0.075
Total length of tube	L_{PHP}	8.862
Length of tube in evaporator section	L_e	2.502
Length of tube in condenser section	L_c	4.68
Length of tube in adiabatic section	L_{ad}	1.68
Inner diameter of the tube	d_i	0.003
Outer diameter of the tube	d_o	0.004

3.1.2 Different Components

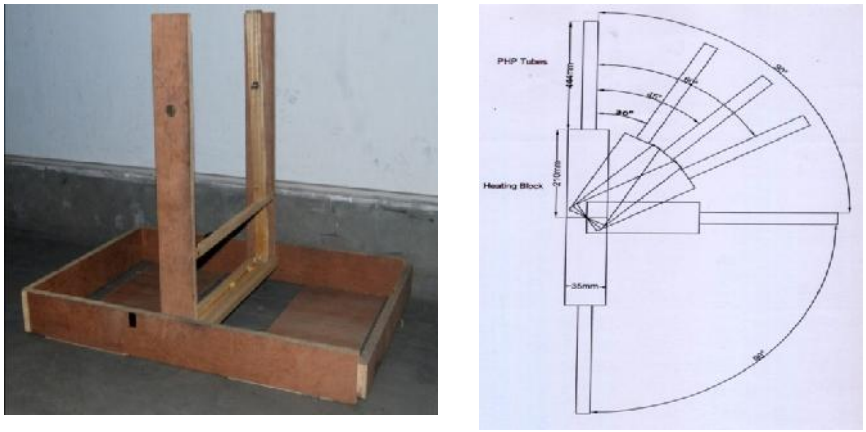

Fig 3.3: Rotating stand

Stand:

It is a wooden stand with a wooden base. The stand holds the test equipment on the base and can be rotated to any angle. A photograph of the stand and base are shown in Fig 3.3.

Heating Arrangement:

AC supply is used in this experiment as the electric source. Then a variac is used to control the current and voltage for supplying electricity to the heater.

Specifications	
Model No.	J8/T10091
Input Voltage	220 V
Output Voltage	0-250V
Output current	8A
Frequency	50 Hz
Mass	11 kg

Fig 3.4: Variac

A heater coil is fabricated by winding a nicrome wire on ceramic beeds. A piece of nicrome wire of 0.25mm diameter wound at constant interval of 1.50 mm is used as heater, which is wrapped by insulating clothes to hinder the electricity from passing through the heating blocks. The heater coil is shown in Fig 3.5

Fig 3.5 Heater coil

The aluminum block conducts heat from the wire to the PHP. It is 35 cm long, 21 cm wide , 3.5 cm thick and weighing 7.5 kg. To ensure high heat conductivity, the aluminum block is covered with insulating glass wool. The aluminum block in Fig 3.6 is grooved to ease the placement of the tubes of the PHP.

Fig 3.6: Grooved Aluminum Block

Cooling of Condenser:

The condenser section was cooled by natural flow of air. A digital anemometer was used to measure the air flow rate.

3.1.3 Temperature Measurement

The wall temperature at various points on the CLPHP was measured by a digital thermocouple thermometer (K-type, made in China). A photograph of digital thermometer is shown in Figure 3.7.

Specifications	
Manufacturer	INSTEK
Model No.	GDM-451
Temperature range	(-40~1000) ˚C

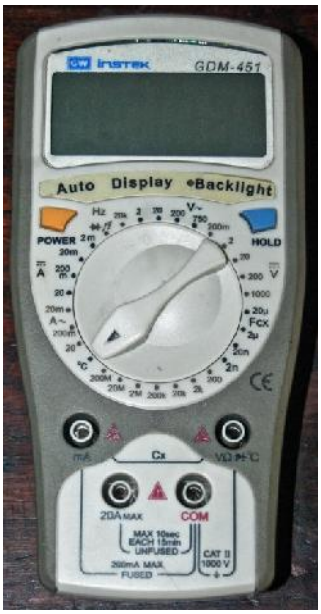

Fig 3.7: Digital Thermometer

In this experiment, fourteen K-type Chromel Alumel thermocouple were used. Seven calibrated K type thermocouples (0.2 mm diameter) were glued to the Aluminum block at different positions of the evaporator, two were glued in the adiabatic section and five were in the condenser section near the tip.

The thermocouples were first calibrated using a standard thermometer. Temperatures were recorded in boiling water of 100°, melting ice of 0°C and some other temperatures with the standard thermometer and thermocouples. The actual temperature from the standard thermometer and the corresponding temperature obtained from thermocouple were plotted and the relationship was found linear. Calibration curves of different thermocouples are shown below.

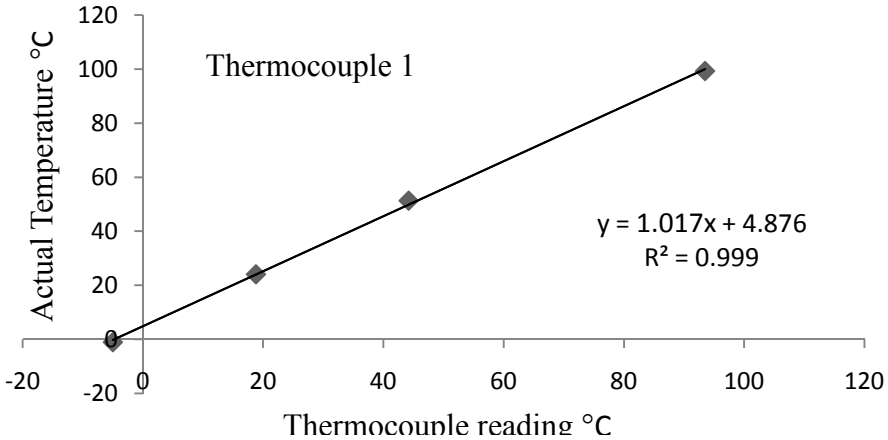

Figure 3.8.1: Calibration curve of Thermocouple 1

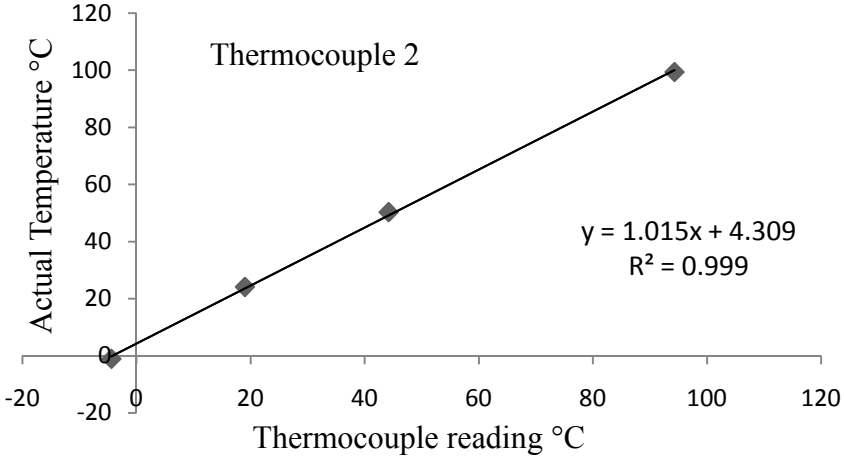

Figure 3.8.2: Calibration curve of Thermocouple 2

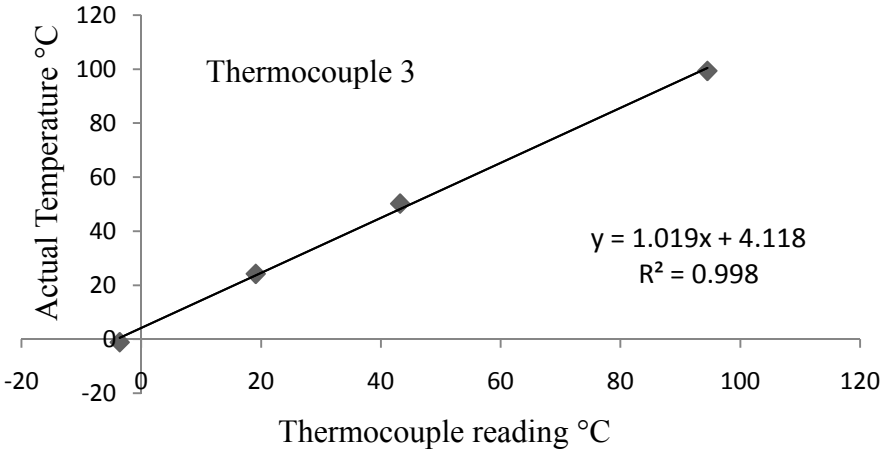

Figure 3.8.3: Calibration curve of Thermocouple 3

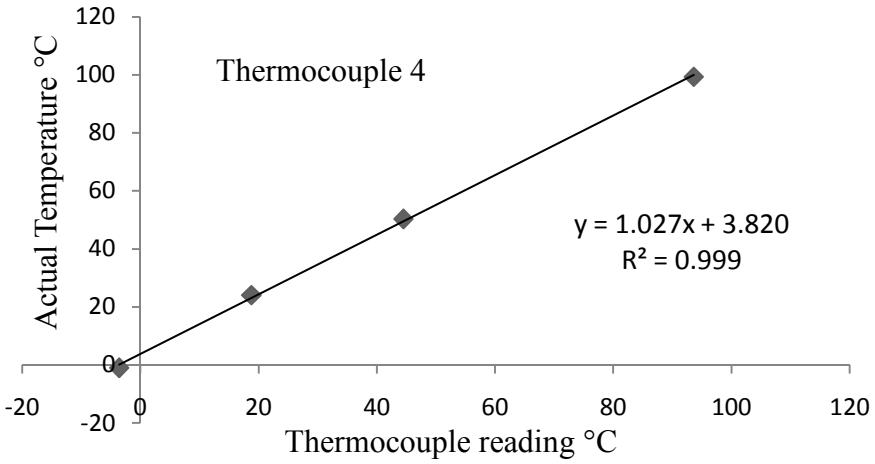

Figure 3.8.4: Calibration curve of Thermocouple 4

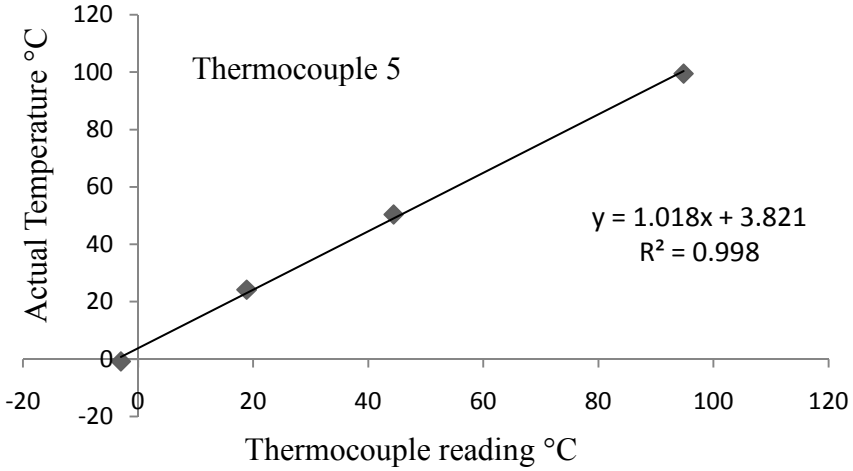

Figure 3.8.5: Calibration curve of Thermocouple 5

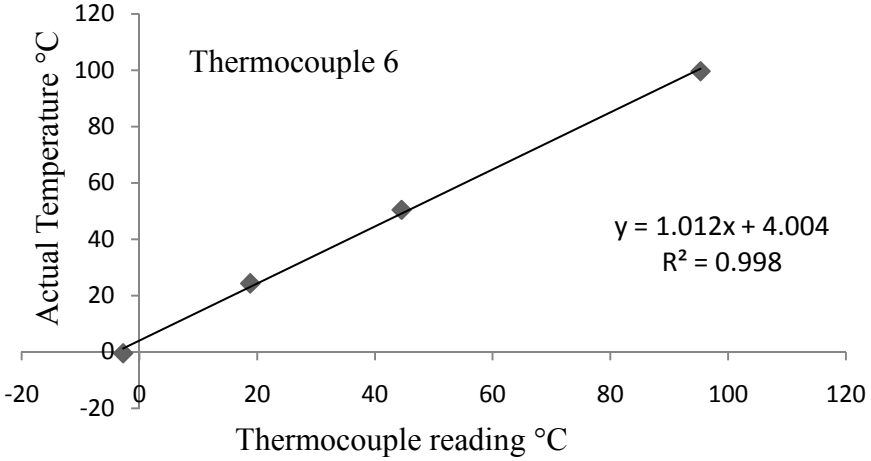

Figure 3.8.6: Calibration curve of Thermocouple 6

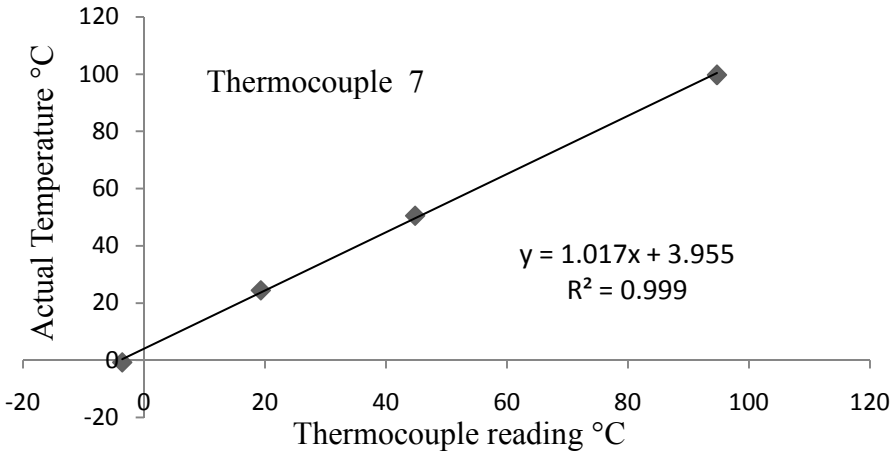

Figure 3.8.7: Calibration curve of Thermocouple 7

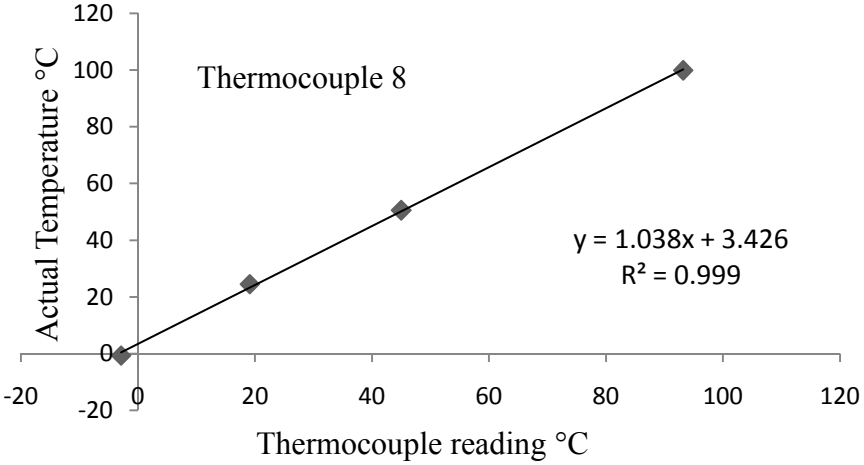

Figure 3.8.8: Calibration curve of Thermocouple 8

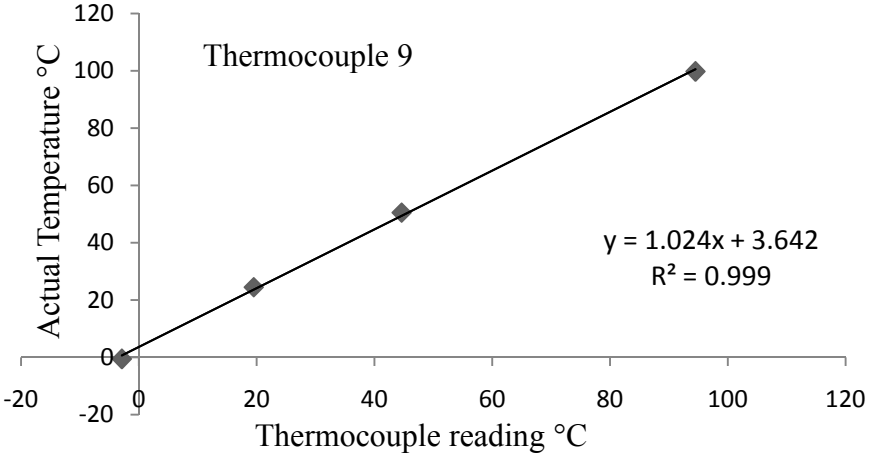

Figure 3.8.9: Calibration curve of Thermocouple 9

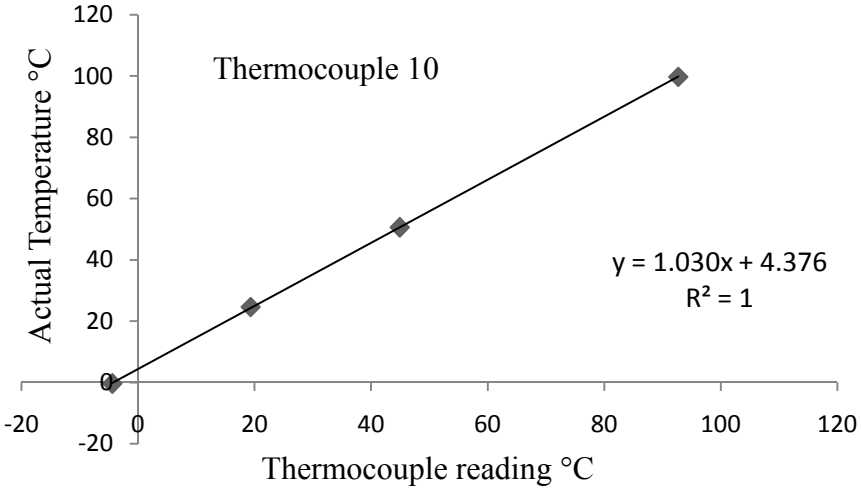

Figure 3.8.10: Calibration curve of Thermocouple 10

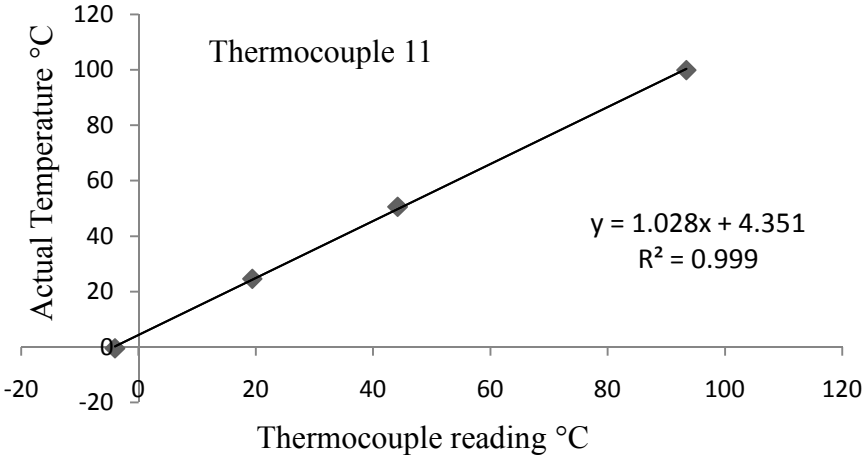

Figure 3.8.11: Calibration curve of Thermocouple 11

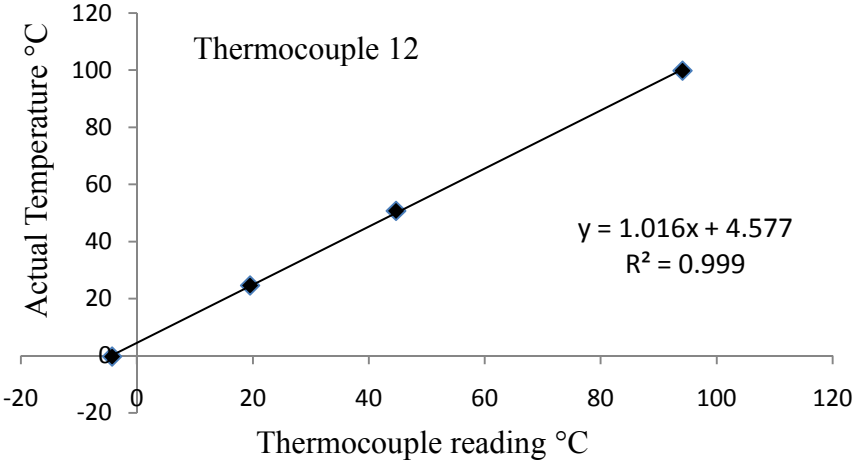

Figure 3.8.12: Calibration curve of Thermocouple 12

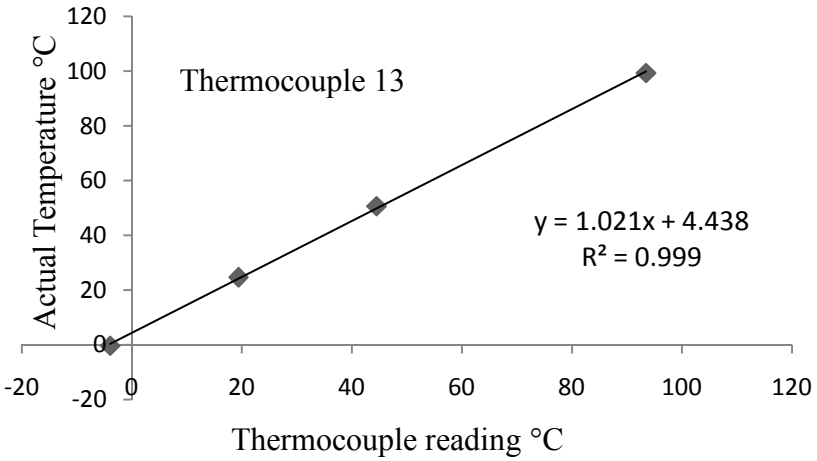

Figure 3.8.13: Calibration curve of Thermocouple 13

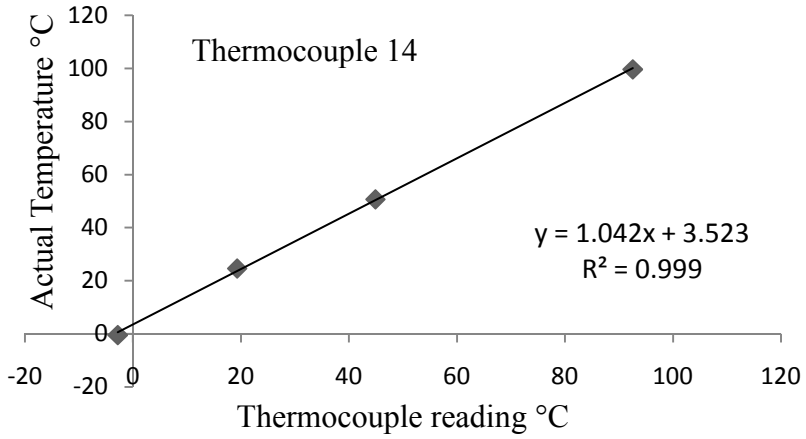

Figure 3.8.14: Calibration curve of Thermocouple 14

Selector switch.

Two 8 point selector switches were used in the experiment to select different thermocouple points on the heat pipe for measurement of temperature. A photo of the selector switch is shown in Figure 3.9.

Fig 3.9: Selector Switch

3.1.4 Pressure measurement

The volume of the working fluid increases when heat is applied to the PHP. If the PHP is operated as a closed loop constant volume system, the pressure inside it will increase continuously. To monitor and record the pressure profile of the PHP, a pressure gauge shown in Fig 3.10 is used.

Specifications	
Manufacturer	HAWK
Working fluid	Ammonia
Lowest pressure	30 in Hg VAC
Highest pressure	300 psi

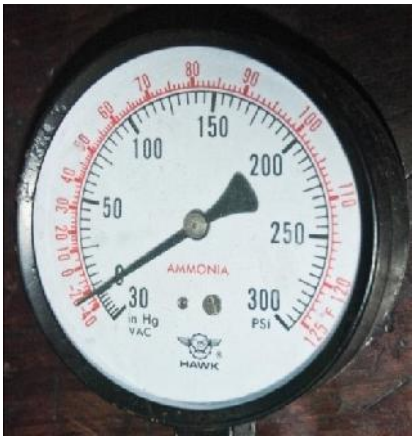

Fig 3.10: Pressure Gauge

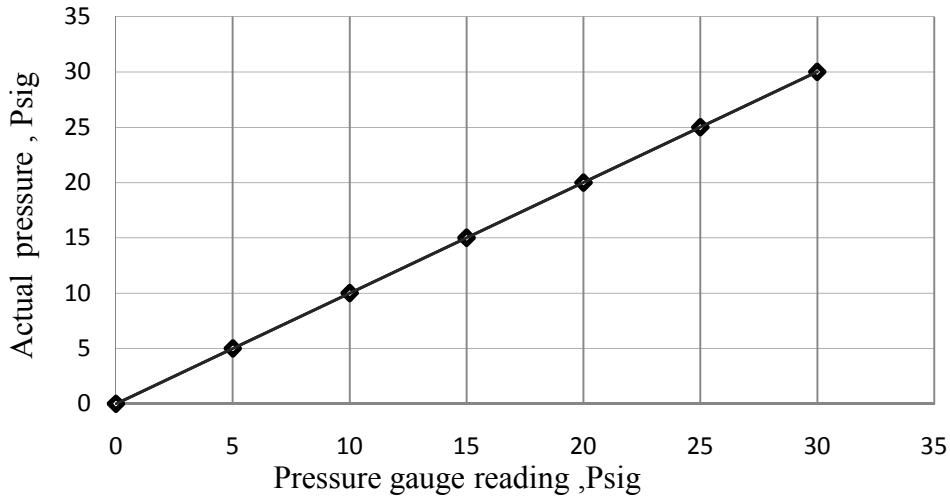

Figure 3.10.1: Calibration curve of the Pressure gauge

3.1.5 Evacuation of the PHP

To evacuate the PHP, a vacuum pump is used. Using the vacuum pump, vacuum is created inside the PHP and then the working fluid is charged. The pump is shown in fig 3.11. The lowest vacuum that could be created by the vacuum pump was 3.7 psig.

Specifications	
Manufacturer	VACUUBRAND GMBH
Manufacturer country	Germany
Pressure	4*10-4 mbar
Volume flow rate	2.2 m^3/h
Sl. No.	22929216

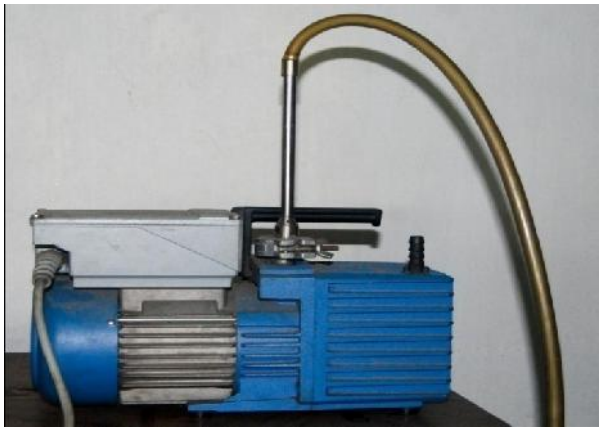

Fig 3.11: Vacuum Pump

3.2 Experimental Procedure

The tests were conducted in room environment, with temperature ranging between 24-28^{o}C. The evaporator section was in contact with Aluminum plate heated by nicrome wire wound ceramic heater to deliver the desired heat load. The heat load was provided by an AC power supply and was controlled by a variac. 14 K-type thermocouples placed at different locations on the device were used to monitor the temperature during the tests. A total of 7 thermocouples were located at evaporator section. The Temperatures were recorded at every 10-20 minutes. The input electric energy was kept constant at 36 W. Measurement was taken at different inclinations (0°, 30°, 45°, 60° , 90° and 180°). The test was conducted at three fill ratio, such as 40%, 60% and 80%.

Thermocouple connections are shown in Fig 3.12. One selector switch was used to monitor the temperature of condenser section and another selector switch was used to monitor the temperature of evaporator and adiabatic sections. Seven different points were used to monitor condenser temperature, five different points to monitor evaporator temperature and two different points for adiabatic section temperature. The common positive and negative terminals were connected to the digital thermometer. Keeping the knob of the selector switch to any desired point the temperature of that point could be monitored.

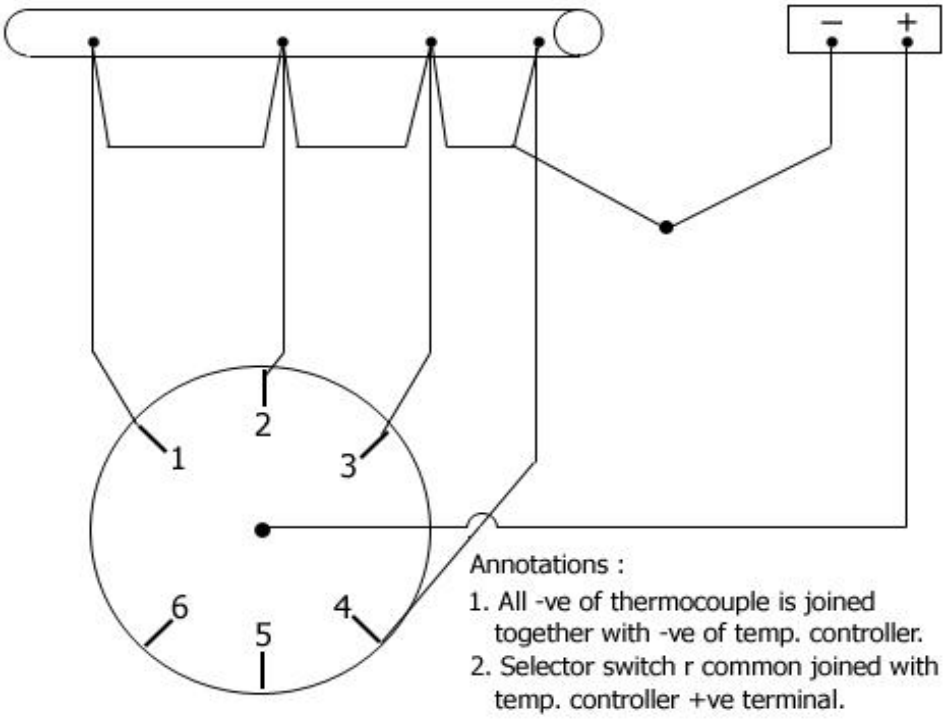

Fig 3.12:Thermocouple connections

3.3. Data Collection and Calculation

Temperatures at different sections (evaporator, adiabatic and condenser) are measured by the help of thermocouple, digital thermometer and selector switch. The temperature at different sections are monitored and recorded at every 20 minutes till the steady state is reached. Below 90˚ inclination the system reaches steady state after about 260 minutes. Beyond 90˚ inclination it takes more time to reach steady state and a stable steady state is not attained. In all test runs, the rise of temperature was monitored and recorded for 260 min. The values of heat transfer coefficient and thermal resistance at different inclinations and fill ratio were calculated from the recorded temperature.

Total electrical heat input to the CLPHP is shared by the Aluminum block, tube wall and the working fluid (i.e. the CLPHP). So, the heat transfer rate by the CLPHP may be calculated by the following heat balance equation.

$$Q_{elec} = Q_{block} + Q_{php} + Q_{w} \qquad (3.1)$$

$$Q_{php}(W) = Q_{elec} - Q_{block} - Q_w \quad (3.2)$$

Where,

Q_{elec} = Electric heat input

Q_{block} = Heat absorbed by the block

Q_w = Heat conducted through the PHP tube wall

Q_{php} = Heat transfer by the working fluid, i.e. the CLPHP

The rate of heat absorbed by the Aluminium block is regulated by applying a constant Electric heat input. Heat absorbed by the block acts as the heat source for the PHP and gradually raises its temperature. After certain time, temperature becomes steady and at this state,

$$Q_{block}(W) = \frac{M_{Al} S_{Al} \Delta T_{Al}}{\Delta t} \quad (3.3)$$

Where, M_{Al} = the mass of Aluminium block

S_{Al} = Specific heat of Aluminium

ΔT_{Al} = Rise of temperature at time interval Δt

Conduction heat transfer through the PHP wall from the evaporator to the condenser section may be derived from the Fourier's law of heat conduction.

$$Q_w(W) = KA\frac{\Delta T}{\Delta x} \quad (3.4)$$

Here,

Cross sectional area of n number of Aluminum tubes,

$A = n\pi(d_o^2 - d_i^2)/4$

Temperature difference between the evaporator and the condenser,

$\Delta T = T_{eva} - T_{con}$

Length of the PHP wall between the evaporator and the condenser,

$\Delta x = L_{ad}$

Thermal conductivity of Aluminum,

$K = k_{Al}$

Substituting all of these in the Fourier's law (eq. 3.4), we get,

$$Q_w(W) = -KA\frac{\Delta T}{\Delta x} = -k_{Al}\frac{n\pi(d_o^2 - d_i^2)}{4}\frac{(T_{eva} - T_{con})}{L_{ad}} \quad (3.5)$$

In the current test set up,

n = No of Aluminum pipes = 14

d_o = Outer diameter of the Aluminum pipe = 0.004 m

d_i = Inner diameter of the Aluminum pipe = 0.003 m

T_{eva} = Average temperature of evaporator section

T_{con} = Average temperature of condenser section

L_{ad}= Length of the PHP wall between the evaporator and the condenser section = 0.12 m

k_{Al} = Thermal conductivity of Aluminum = 250 W/m ˚C

In the evaporator section, heat is transferred from the PHP tube wall to the working fluid and it may be determined by the Newton's Law of Cooling.

$$Q_e(W) = hAdT = h_{fe} A_{ei} (T_{eva} - T_{fe}) \quad (3.6)$$

Where, A_{ei} = Inner surface area of the evaporator, $m^2 = \pi d_i L_e$

T_{eva} = Average evaporator temperature, ˚C

T_{fe} = Average temperature of fluid in the evaporator, ˚C

h_{fe} = Convective heat transfer coefficient between the evaporator inner surface and the working fluid, $W/m^2\,^oC$

Assuming no addition or loss of heat in the adiabatic section, the heat absorbed by the working fluid in the evaporator section should be completely transferred to the condenser section. In the condenser section, heat is transferred from the working fluid to the condenser wall and it may again be determined by the Newton's Law of Cooling.

$$Q_c(W) = hAdT = h_{fc} A_{ci} (T_{fc} - T_{con}) \quad (3.7)$$

Where, A_{ci} = Inner surface area of the condenser, $m^2 = \pi d_i L_c$

T_{con} = Average condenser temperature, ˚C

T_{fc} = Average temperature of fluid in the condenser, ˚C

h_{fc} = Convective heat transfer coefficient between the condenser inner surface and the working fluid, $W/m^2\,^oC$

Equation 3.6 shows that the thermal resistance in the evaporator section is $1/(hA_{ei})$. Similarly, equation 3.7 shows that the thermal resistance in the condenser section is

$1/(hA_{ci})$. So, the overall thermal resistance from evaporator inner wall to the condenser inner wall is $1/(hA_{ei})+ 1/(hA_{ci})$.So it can be written

$$Q_{php} = \frac{(T_{eva}-T_{con})}{\frac{1}{hA_{ei}}+\frac{1}{hA_{ci}}} = h\frac{(T_{eva}-T_{con})}{\frac{1}{A_{ei}}+\frac{1}{A_{ci}}} \quad (3.8)$$

In steady state, considering the overall heat flow path from the evaporator to the condenser via the working fluid, one may write,

$$Q_e = Q_{php} = Q_c$$

Rearranging equation 3.8, we get,

$$h = \frac{Q_{php}}{(T_{eva}-T_{con})}\left[\frac{1}{A_{ei}}+\frac{1}{A_{ci}}\right] \quad (3.9)$$

The overall heat transfer coefficient, *h* in equation 3.9 involves heat transfer by both convection and phase change. Hence, to differentiate it from the convective heat transfer coefficient between the working fluid and the solid wall, the overall heat transfer coefficient is denoted by U and equation 3.9 is rewritten as,

$$U_{php}\left(\frac{W}{m^2}°C\right) = \frac{Q_{php}}{T_{eva}-T_{con}}\left(\frac{1}{A_{ei}}+\frac{1}{A_{ci}}\right) \quad (3.10)$$

Where,

$$A_{ei}(m^2) = \pi d_i L_{eva}\ , \qquad A_{ci}\,(m^2) = \pi d_i L_{con}$$

Combined thermal resistance of the working fluid is defined as the ratio of the difference in thermal potential (i.e. temperature) to the heat flow rate, i.e.

$$R_{combined}(°C/W) = \frac{T_{eva}-T_{con}}{Q_{php}} \quad (3.11)$$

The heat that is transferred from the evaporator section to the condenser section is transferred to the environment by natural convection heat transfer. Convection heat transfer to the surrounding air from the condenser section may be determined by

$$Q_{con}(W) = hAdT = h_{ca}A_{co}\,(T_{con} - T_a) \quad (3.12)$$

Where, A_{co} = Outer surface area of the condenser, $m^2 = \pi d_o L_{con}$

T_{con} = Average condenser temperature, ˚C

T_a = Ambient temperature, ˚C

h_{ca} = Convective heat transfer coefficient between the condenser surface and ambient air, $W/m^2\,^oC$

Chapter 4

Results and Discussion

Altogether eighteen experimental run has been undertaken with the CLPHP for three fill ratio, the summary of which is shown in Table 4.1. At each fill ratio inclination was set at six different angles between 0^0 and 180^0. Temperature was measured at different sections of the CLPHP. Heat transfer rate by working fluid , Q_{php}(Watt), Overall heat transfer coefficient , U(W/m² °C) and Overall thermal resistance, R(°C/W) are determined from the measured data of temperature. Data for fill ratio= 0.4 and inclination = 0° was taken twice to check the repeatability and the temperature reading was found within ±1.5 °C of the previous reading.

Table 4.1: Summary of the experimental runs

Fill Ratio V/V_{max}	Inclination Angle (θ)	Q_{php}(Watt)	Thermal Resistance R (°C/W)	Overall Heat Transfer Coefficient U_{php} (W/m² °C)
0.4	0°	34.387	0.083	782.308
	30°	34.451	0.078	834.782
	45°	33.651	0.091	712.268
	60°	33.644	0.106	614.436
	90°	33.012	0.260	250.612
	180°	28.520	0.808	80.652
0.6	0°	33.858	0.082	796.091
	30°	34.127	0.078	835.796
	45°	33.741	0.089	733.575
	60°	33.407	0.103	633.702
	90°	32.378	0.194	335.155
	180°	27.272	0.787	82.760
0.8	0°	33.571	0.106	616.425
	30°	33.446	0.101	642.327
	45°	33.199	0.180	362.793
	60°	33.081	0.261	249.660
	90°	30.881	0.560	116.359
	180°	24.233	1.011	64.429

4.1 Temperature Rise

A constant heat input of 36 W was applied in the heating block and temperature rise in various sections was monitored till steady state was reached. This is carried out for three different fill ratio, namely, 0.4, 0.6 and 0.8 and at 0°, 30°, 45°, 60°, 90° and 180° inclinations. The time-histories of temperature rise at various sections of the CLPHP are shown in figures 4.1.1 to 4.1.6 for fill ratio 0.4. The time-histories of temperature rise for fill ratio 0.6 are shown in figures 4.1.7 to 4.1.12, whereas those for fill ratio 0.8 are shown in figures 4.1.14 to 4.1.18. The data for these figures are given in Tables 4 to 39 in the Appendix B.

It is evident from these figures that for the same heat input the temperature of various sections increases in the same fashion for fill ratio 0.4 as shown in figures 4.1.1 to 4.1.3. In all sections, the rate of temperature rise is very close to each other for inclinations below 90^o. For inclination 90^o and above, the rate of temperature rise increases in the evaporator section whereas it decreases in the condenser section. It implies that the rate of heat transfer is lower at inclination 90^o and above.

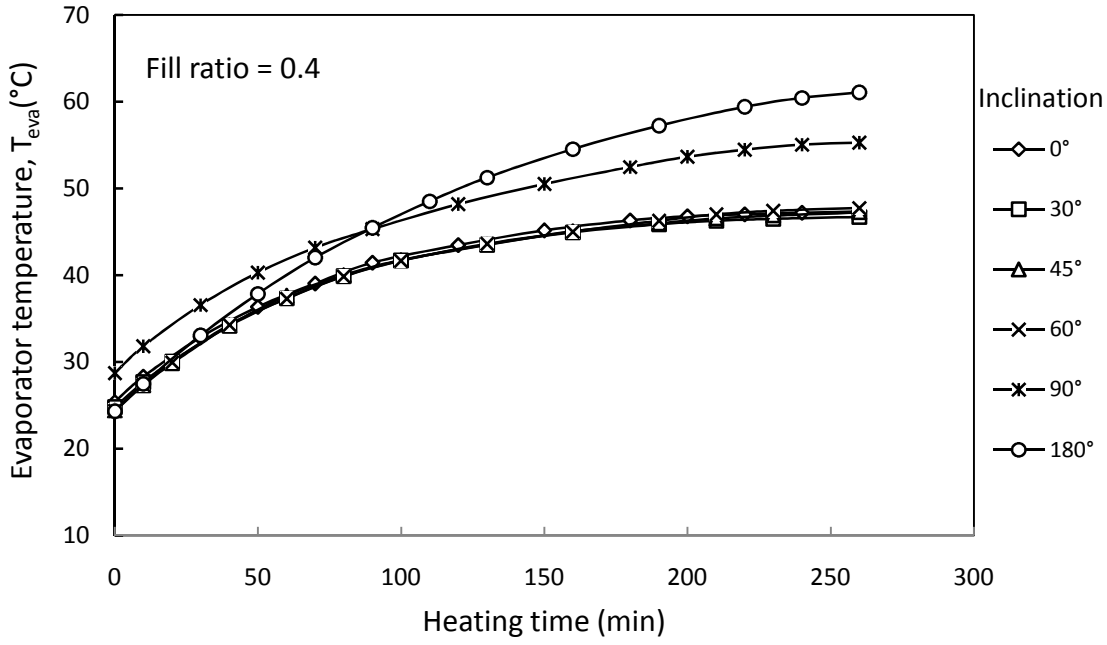

Figure 4.1.1: Increase in the evaporator temperature with time at different inclinations for fill ratio = 0.4.

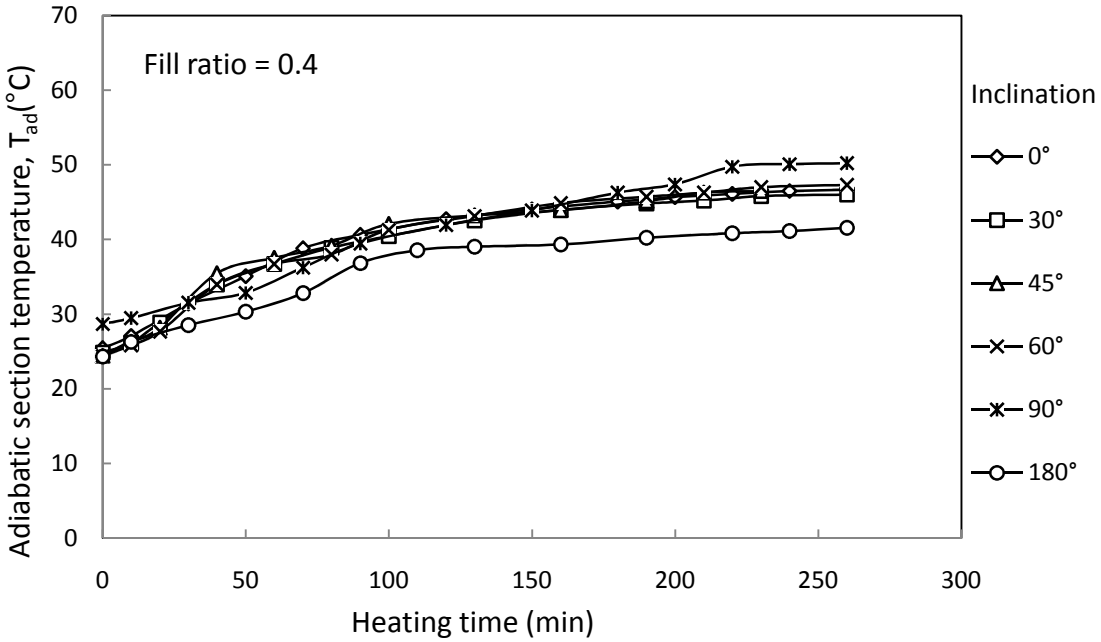

Figure 4.1.2: Increase in the adiabatic section temperature with time at different inclinations for fill ratio = 0.4.

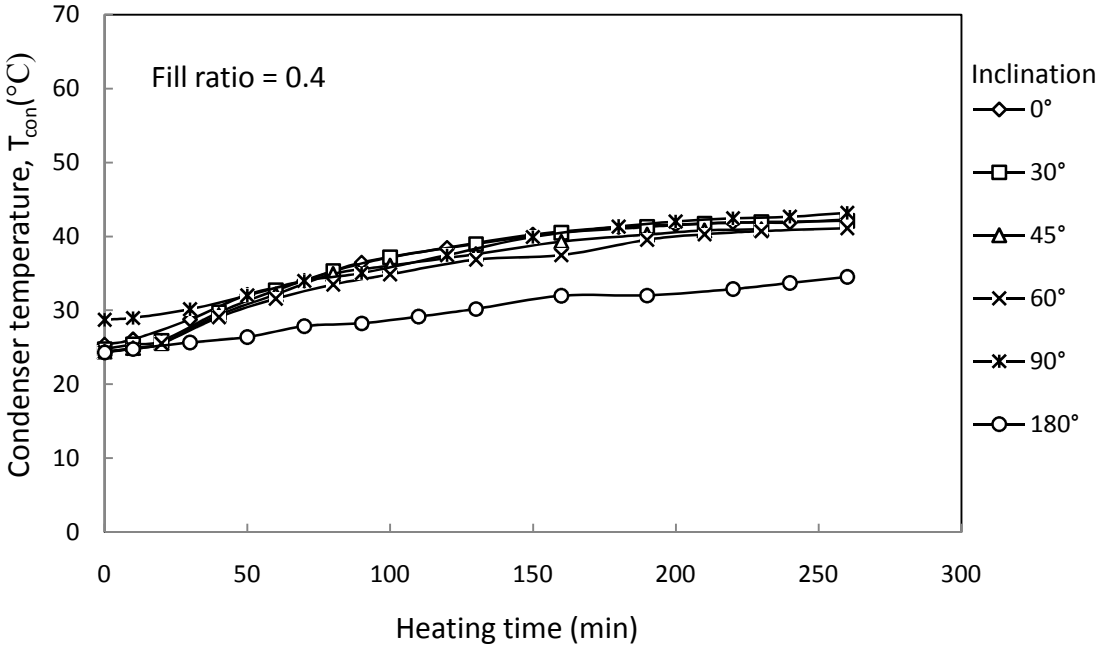

Figure 4.1.3: Increase in the condenser temperature with time at different inclinations for fill ratio = 0.4.

The rate of increase of temperature at three sections of the CLPHP is compared in figures 4.1.4 to 4.1.6 for three different inclinations but at a fill ratio of 0.4.

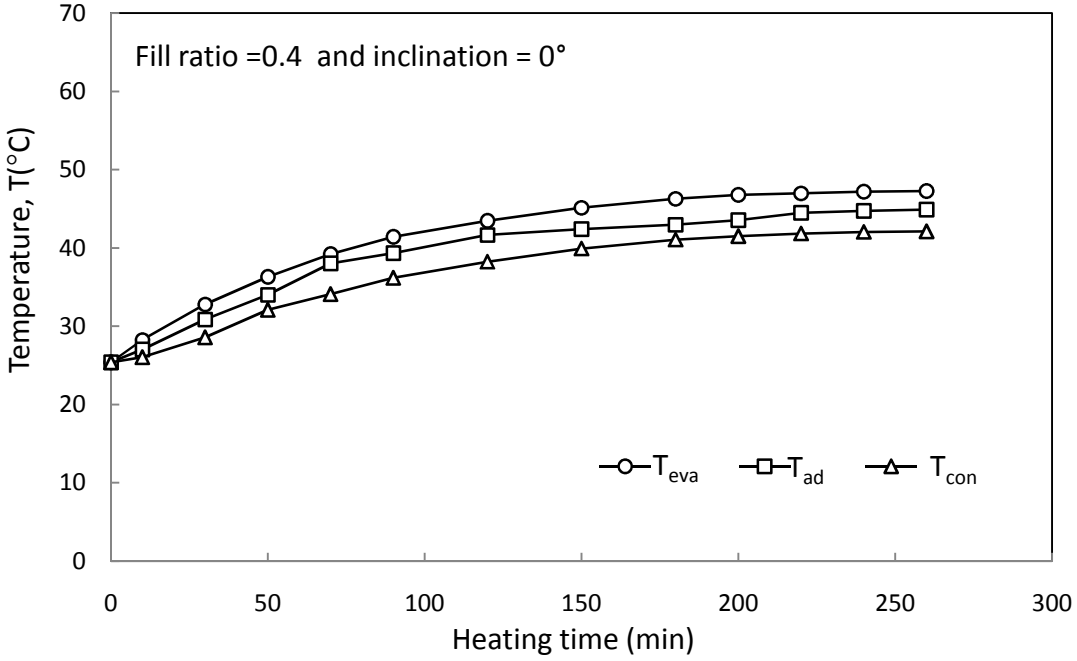

Figure 4.1.4: Comparison of the rates of increase of temperature with time in the three sections of the CLPHP for fill ratio = 0.4 and inclination = 0° (Vertical position).

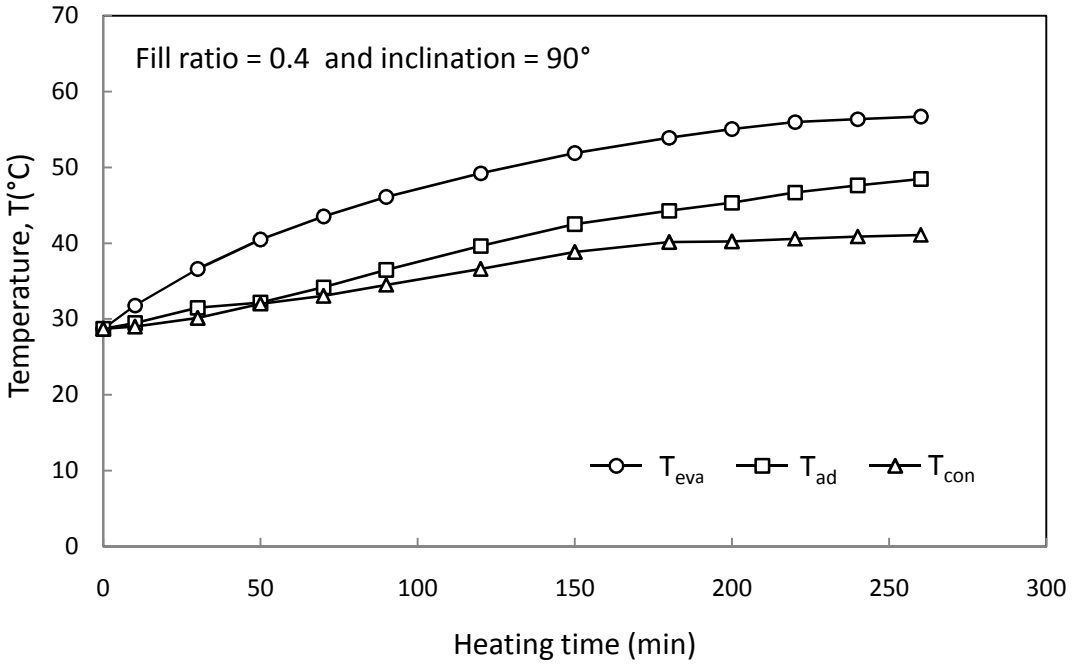

Figure 4.1.5: Comparison of the rates of increase of temperature with time in the three sections of the CLPHP for fill ratio = 0.4 and inclination = 90° (Horizontal position).

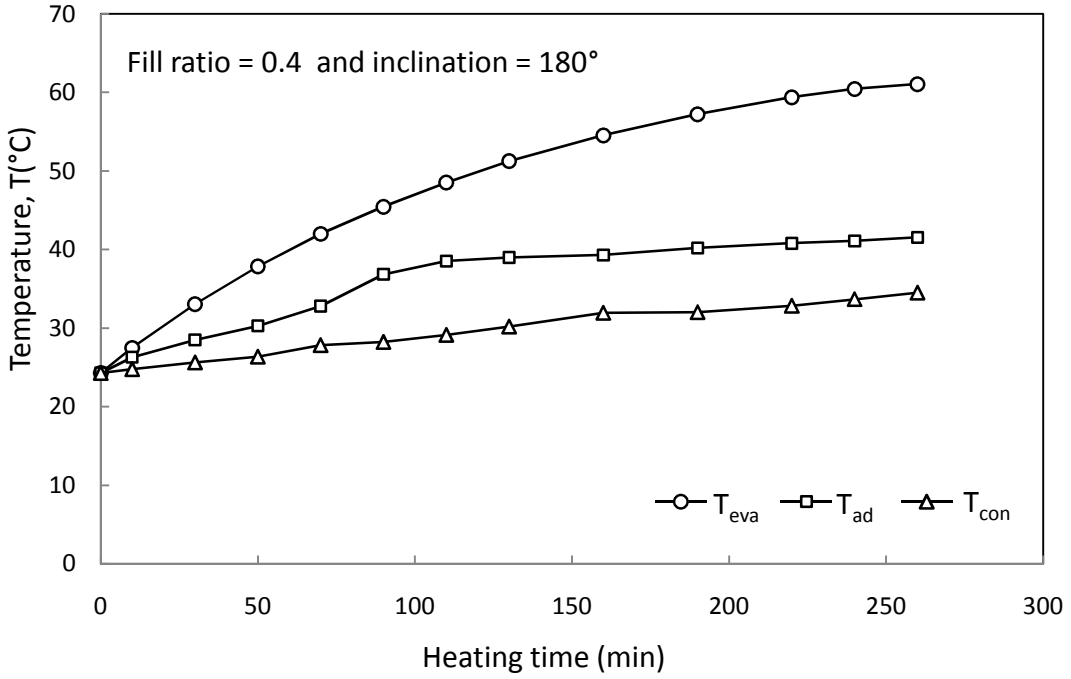

Figure 4.1.6: Comparison of the rates of increase of temperature with time in the three sections of the CLPHP for fill ratio = 0.4 and inclination = 180° (Heat source above the heat sink).

It is seen from the above figures that the difference in temperature between the evaporator and the condenser sections is uniform throughout the experimental range for 0° inclination. But for 90° and 180° inclinations this difference in temperature gradually increases with time. This observation again implies that the heat transfer rate decreases with increase of inclination above 90°.

Similar results are shown in figures 4.1.7 to 4.1.9 for fill ratio = 0.6 and in figures 4.1.10 to 4.1.12 for fill ratio = 0.8. For all inclinations below 90^o, the patterns of the rate of temperature rise are both qualitatively and quantitatively similar for the three fill ratio, i.e. 0.4, 0.6 and 0.8. However, for inclination 90^o and above, the patterns are only qualitatively similar.

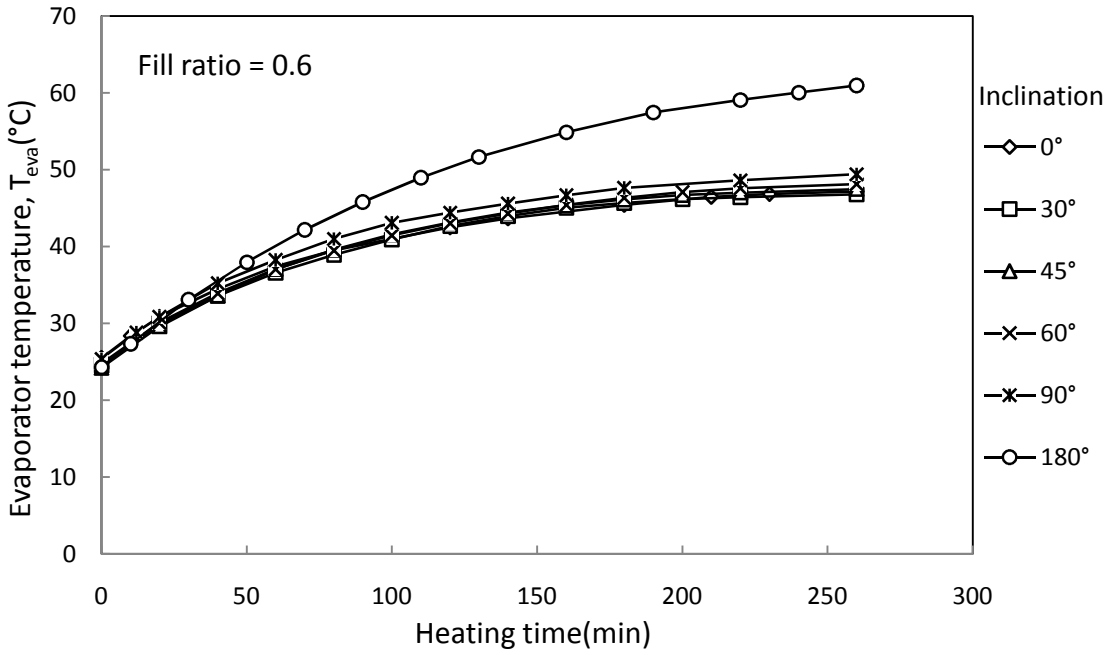

Figure 4.1.7: Increase in the evaporator temperature with time at different inclinations for fill ratio = 0.6.

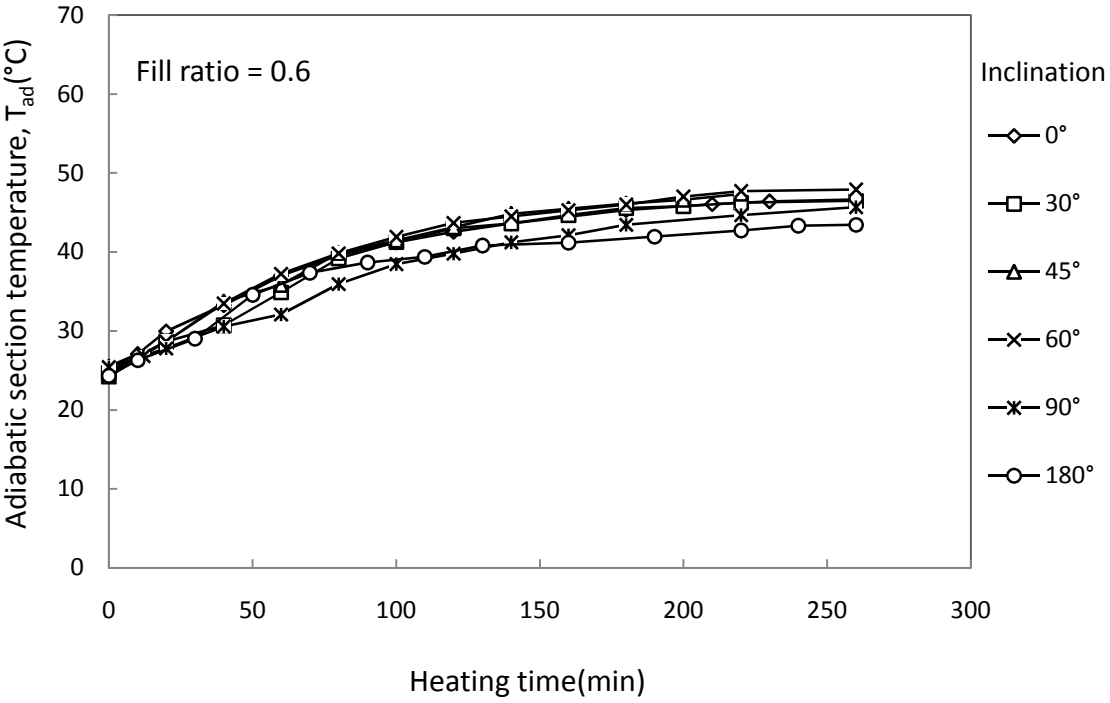

Figure 4.1.8: Increase in the adiabatic section temperature with time at different inclinations for fill ratio = 0.6.

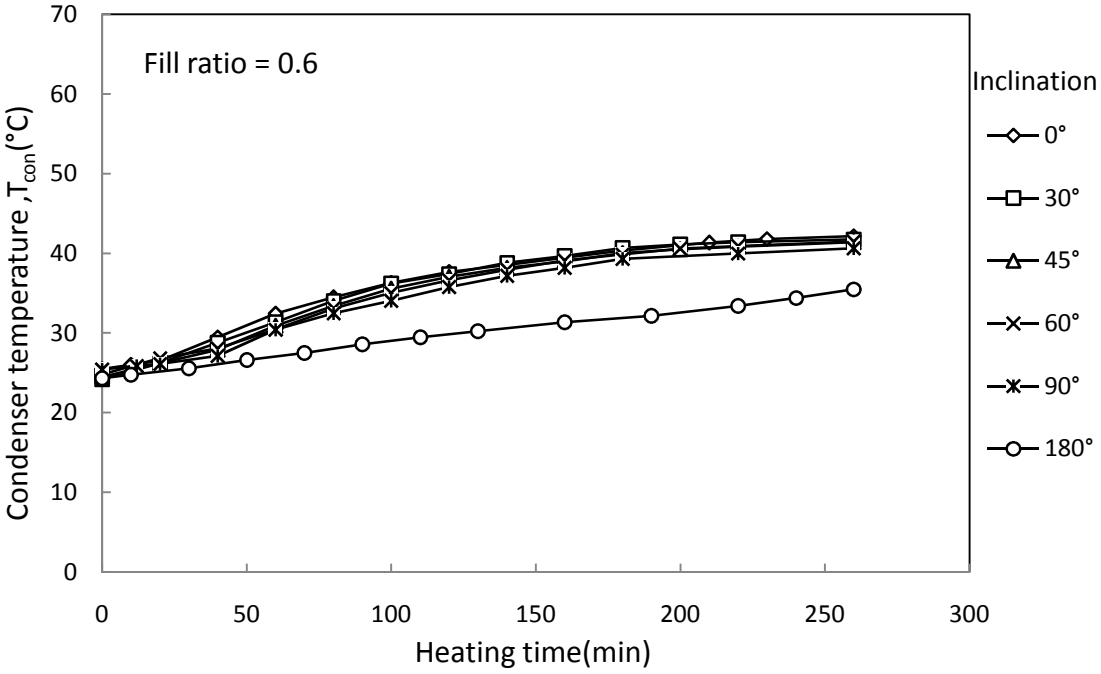

Figure 4.1.9: Increase in the condenser temperature with time at different inclinations for fill ratio = 0.6.

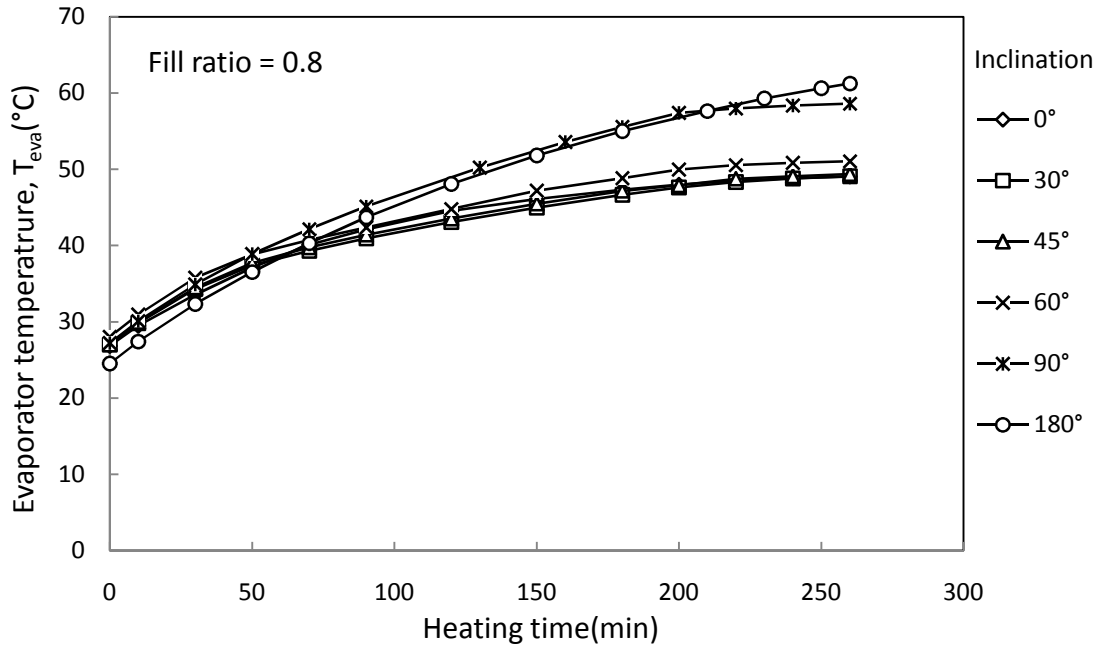

Figure 4.1.10: Increase in the evaporator temperature with time at different inclinations for fill ratio = 0.8.

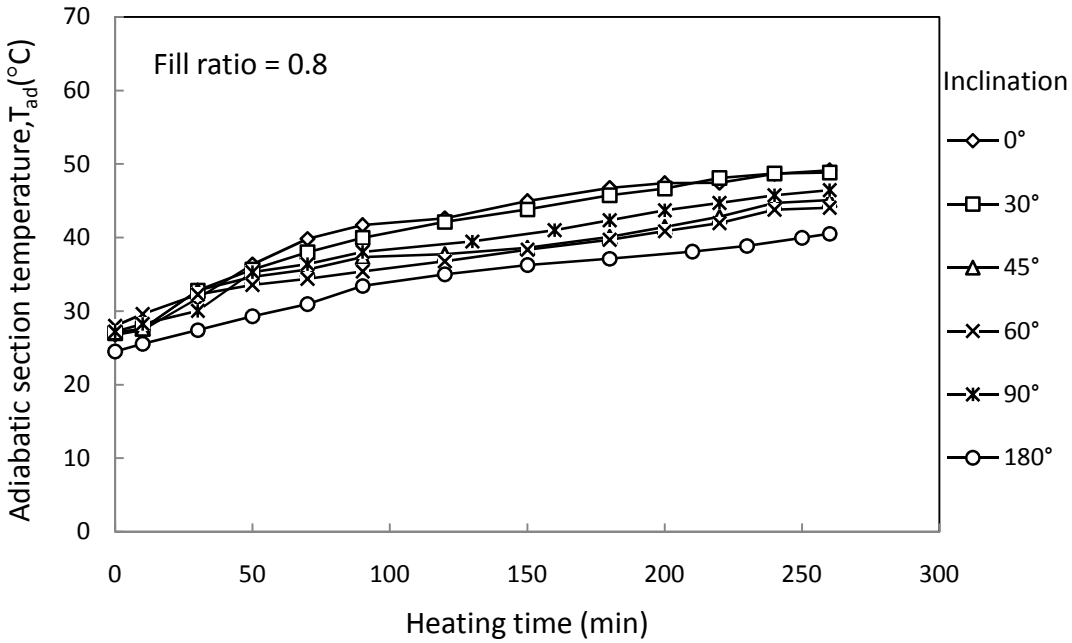

Figure 4.1.11: Increase in the adiabatic section temperature with time at different inclinations for fill ratio = 0.8.

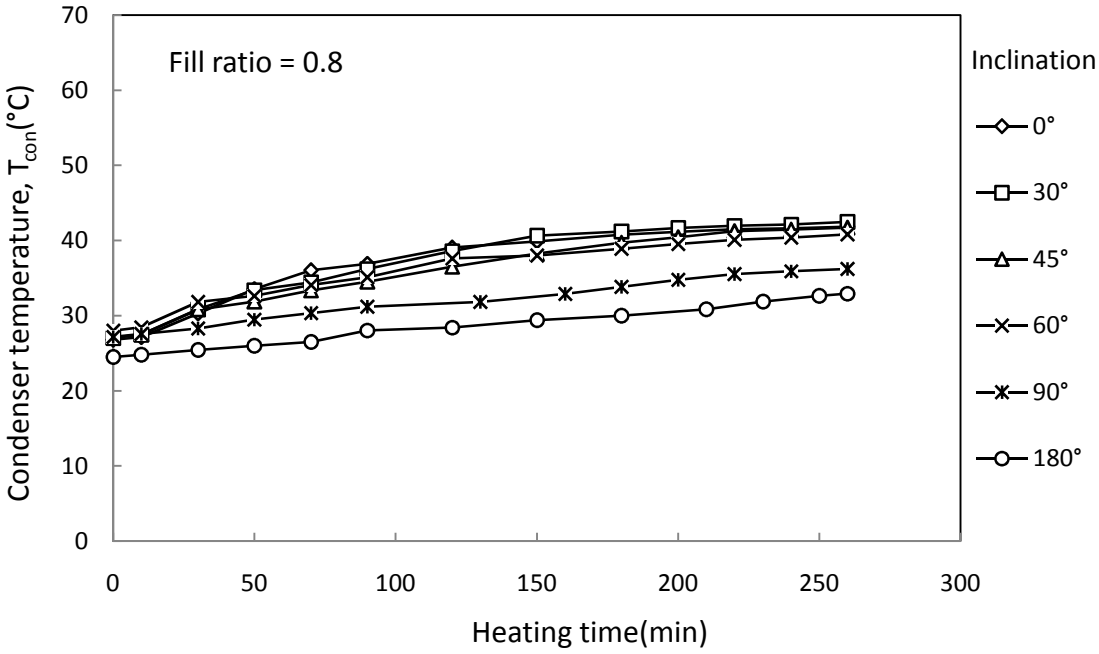

Figure 4.1.12: Increase in the condenser temperature with time at different inclinations for fill ratio = 0.8.

The rate of increase of temperature at three sections of the CLPHP is compared in figures 4.1.13 to 4.1.15 for fill ratio = 0.6 and in figures 4.1.16 to 4.1.18 for fill ratio = 0.8 for inclination 0^0 , 90^0 , 180^0.

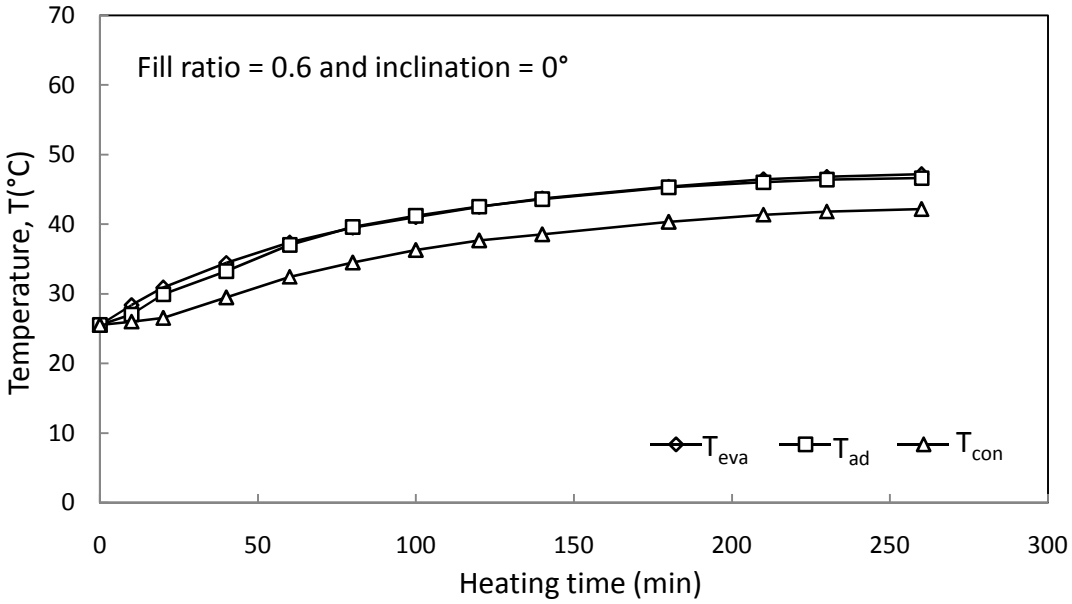

Figure 4.1.13: Comparison of the rates of increase of temperature with time in the three sections of the CLPHP for fill ratio = 0.6 and inclination = 0° (Vertical position).

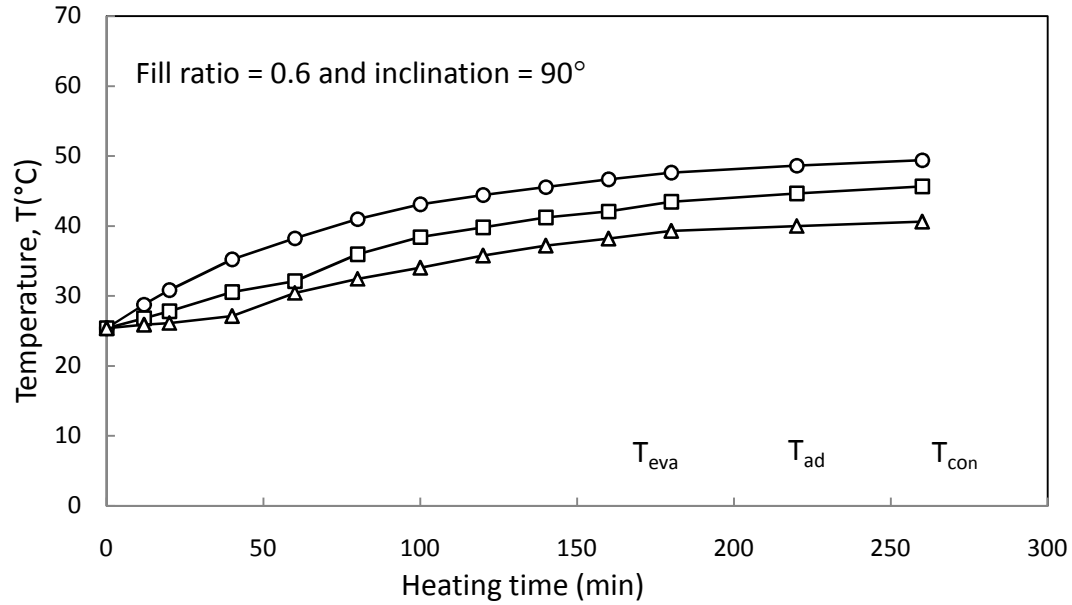

Figure 4.1.14: Comparison of the rates of increase of temperature with time in the three sections of the CLPHP for fill ratio = 0.6 and inclination = 90° (Horizontal position).

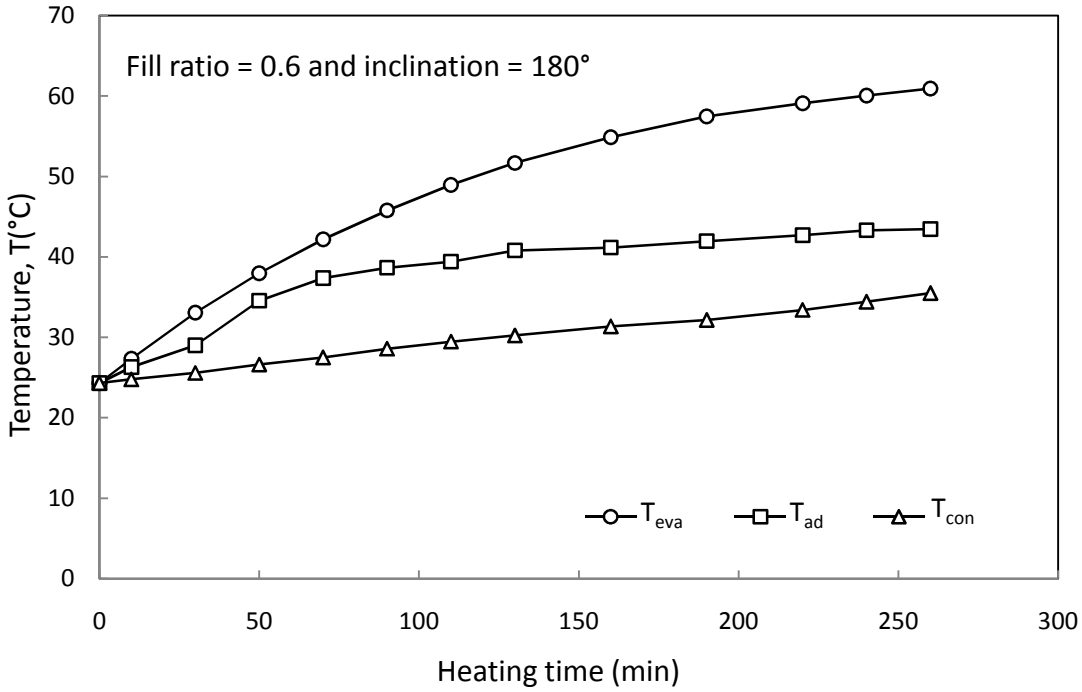

Figure 4.1.15: Comparison of the rates of increase of temperature with time in the three sections of the CLPHP for fill ratio = 0.6 and inclination = 180° (Heat source above the heat sink).

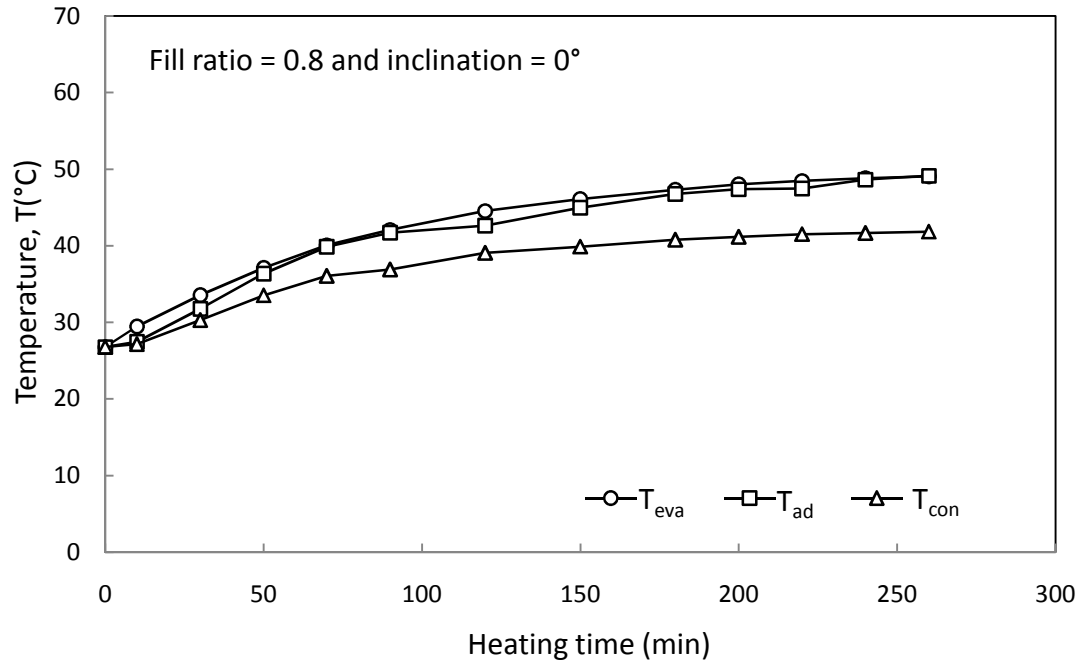

Figure 4.1.16: Comparison of the rates of increase of temperature with time in the three sections of the CLPHP for fill ratio = 0.8 and inclination = 0° (Vertical position).

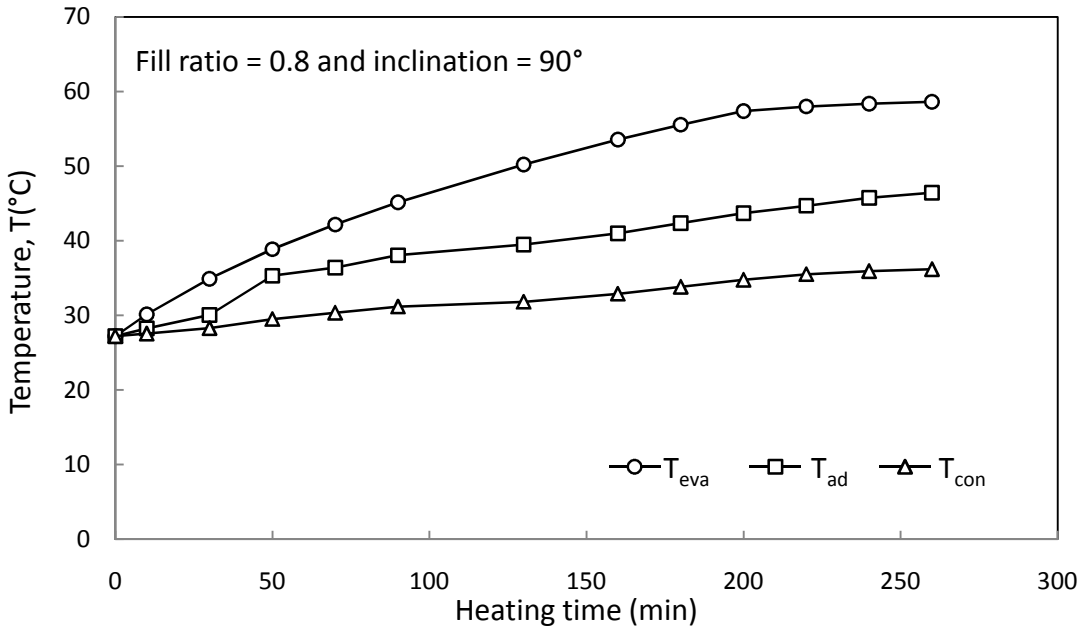

Figure 4.1.17: Comparison of the rates of increase of temperature with time in the three sections of the CLPHP for fill ratio = 0.8 and inclination = 90° (Horizontal position).

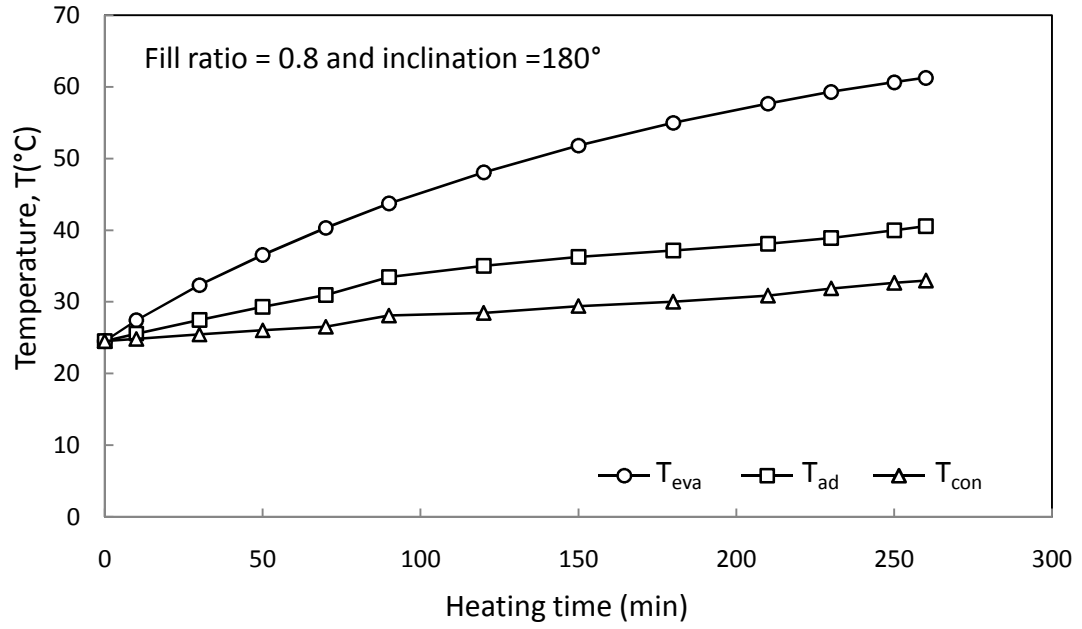

Figure 4.1.18: Comparison of the rates of increase of temperature with time in the three sections of the CLPHP for fill ratio = 0.8 and inclination = 180° (Heat source above the heat sink).

It is seen from the above figures 4.1.13 to 4.1.18, that as with fill ratio =0.4, the difference in temperature between the evaporator and the condenser sections for the other two fill ratio is also uniform throughout the experimental range for 0° inclination. But for 90° and 180° inclinations this difference in temperature gradually increases with time though the rate of increase of temperature difference with 90^o is very small. This observation again implies that the heat transfer rate decreases with increase of inclination above 90°.

The rate of increase of temperature at evaporator and condenser sections of the CLPHP for fill ratio 0.4 , 0.6 and 0.8 at inclinations 0^0 , 30^0 , 45^0 , 60^0 , 90^0 and 180^0 is compared in figures 4.1.19 to 4.1.20 .

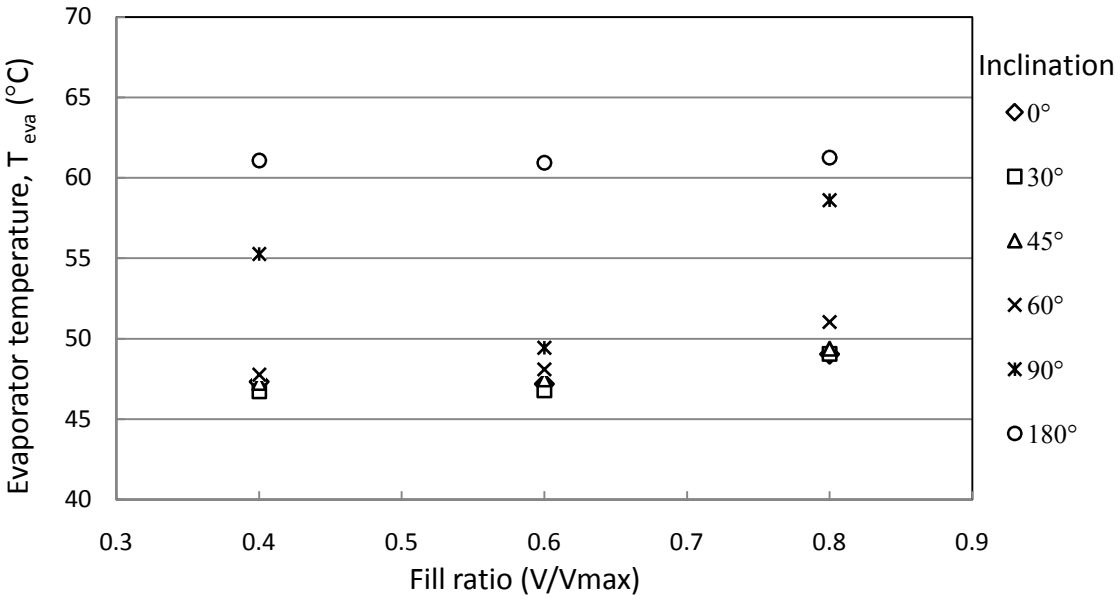

Figure 4.1.19: Effect of fill ratio(V/Vmax) on evaporator temperature T_{eva} (°C) in CLPHP at different inclination.

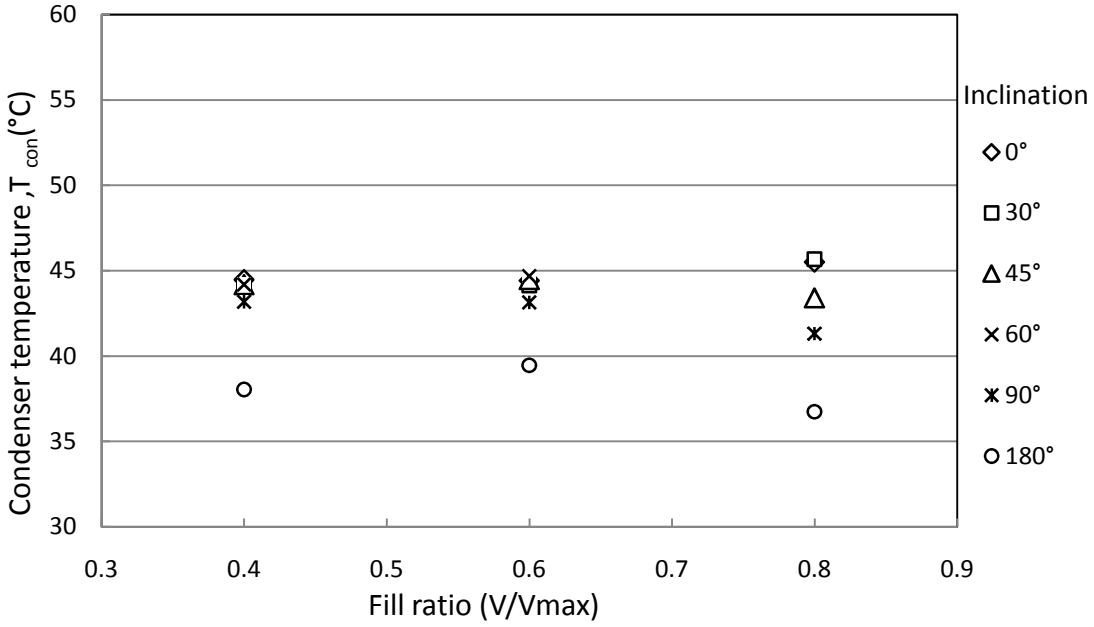

Figure 4.1.20: Effect of fill ratio(V/Vmax) on condenser temperature T_{con}(°C) in CLPHP at different inclination.

It is seen from the above figures 4.1.19 to 4.1.20 that with fill ratio =0.4 and 0.6 for inclination angle below 90^o the evaporator temperature is qualitatively and quantitavely same but for fill ratio 0.8 it is higher.For inclination angle 90^o and above evaporator section temperature is much higher for all fill ratios.The condenser sections temperature for all fill ratios is lower for inclination angle 90° and 180° . This observation implies that the heat transfer rate is lower at fill ratio 0.8 compared to fill ratio 0.4 and 0.6. It also decreases with increase of inclination above 90°. It is also evident from figure 4.1.19(b) that the temperature of evaporator section for fill ratios 0.4 and 0.6 is slightly lower in inclination angle 30°.

The rate of increase of temperature at evaporator and condenser sections of the CLPHP at inclination angle 0^0 , 30^0 , 45^0 , 60^0 , 90^0 and 180^0 for fill ratio 0.4 , 0.6 and 0.8 is compared in figures 4.1.21 to 4.1.22 .

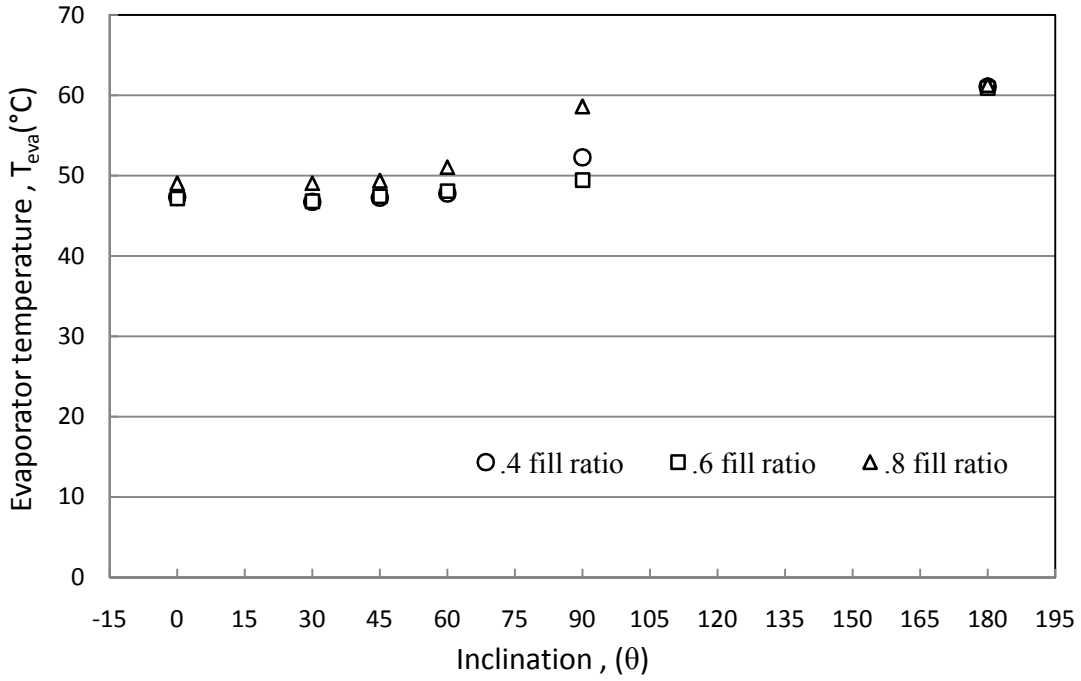

Figure 4.1.21: Effect of inclination , θ on evaporator temperature T_{eva}(°C) of CLPHP for different fill ratio at constant heat input.

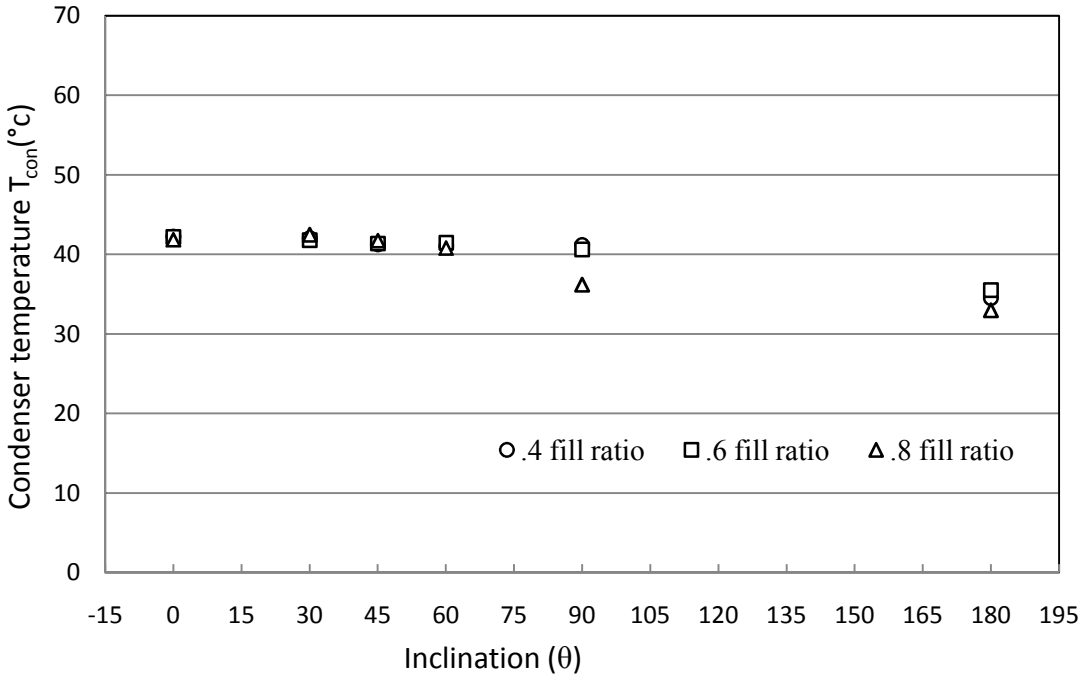

Figure 4.1.22: Effect of inclination ,θ on condenser temperature T_{con}(°c) of CLPHP for different fill ratio at constant heat input.

It is seen from the above figures 4.1.21 to 4.1.22 that for inclination angle below 90^o the evaporator temperature is nearly same with fill ratio =0.4 , 0.6 but for fill ratio 0.8 it is higher.For inclination angle 180^o evaporator section temperature is much higher for all fill ratios.The condenser section temperature at inclinations 0^o , 30^o , 45^o , 60^o for all fill ratios is approximately same but at inclination 90^o and 180° condenser section temperature is lower for fill ratio 0.8. This observation implies that the heat transfer rate is lower at inclination 90^o and 180° compared to other inclinations.

4.2 Heat Transfer rate by Working Fluid ,Q_{php}(Watt)

Heat transfer rate through the CLPHP at various fill ratio and inclinations are calculated by the procedure described in section 3.3 of the previous chapter and sample calculation is shown in the appendix D. Figures 4.2.1 - 4.2.9 compare the calculated heat transfer rate through the CLPHP and heat transfer to the environment from the condenser for a fixed heat input of 36 W.

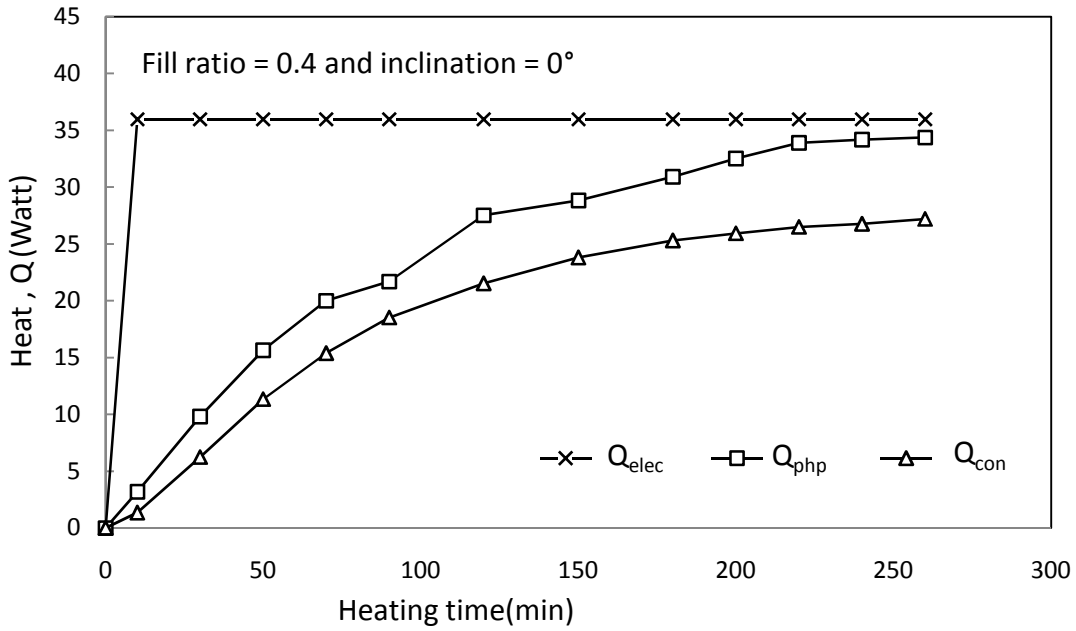

Figure 4.2.1: Comperative study of electrical heat input 36(Watt), heat transferred by working fluid, Q_{php} (Watt) and heat transfer from condenser section Q_{con} (Watt) with time in CLPHP for fill ratio = 0.4 and inclination = 0° (Vertical position).

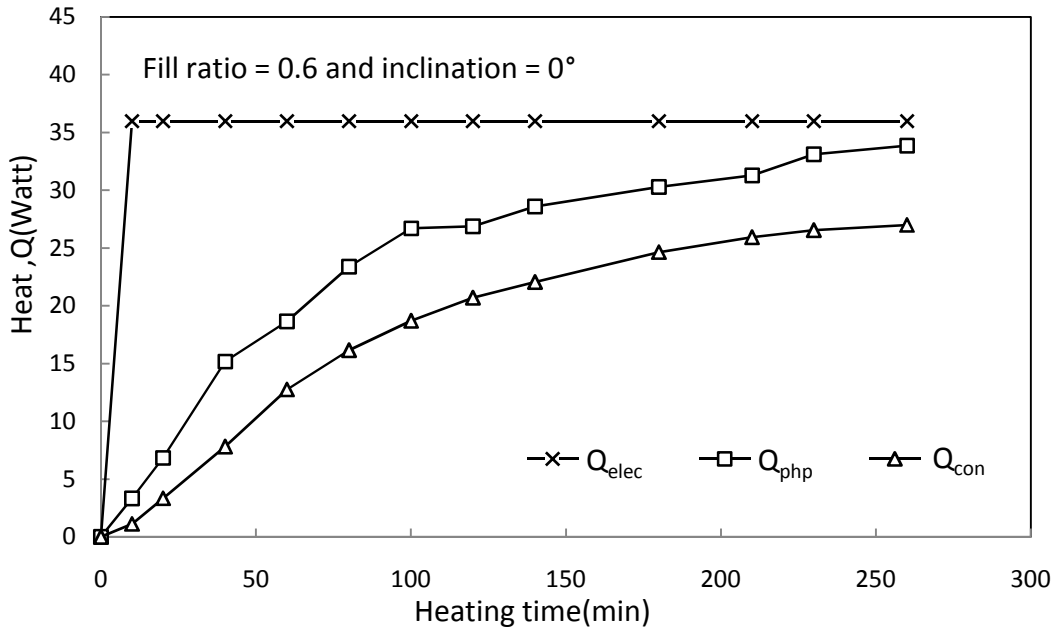

Figure 4.2.2: Comperative study of electrical heat input 36(Watt), heat transferred by working fluid, Q_{php} (Watt) and heat transfer from condenser section Q_{con}(Watt) with time in CLPHP for fill ratio = 0.6 and inclination = 0° (Vertical position).

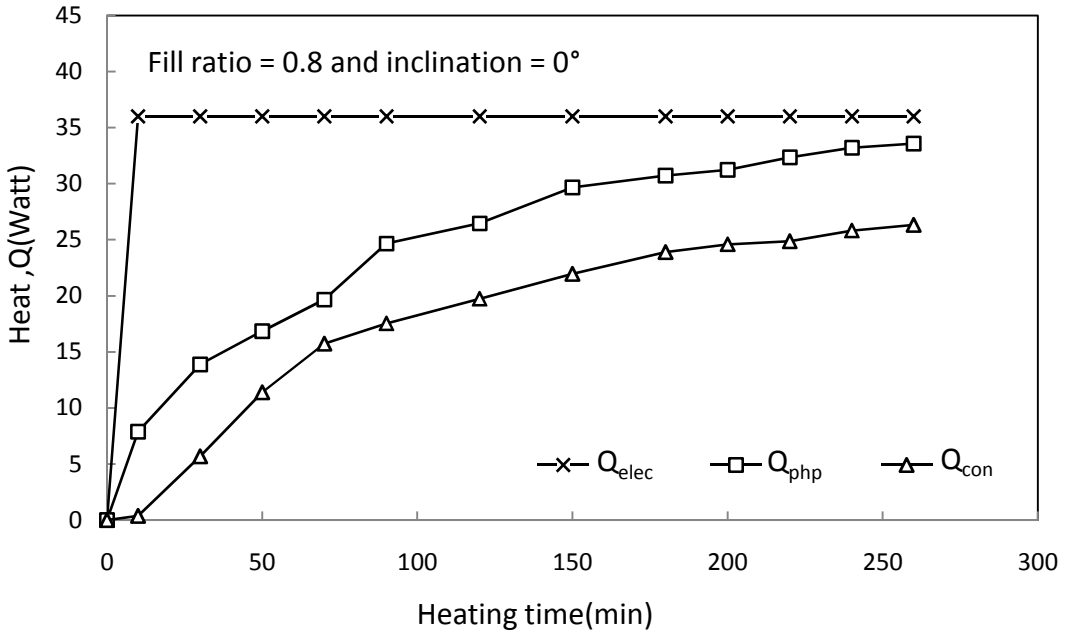

Figure 4.2.3: Comperative study of electrical heat input 36(Watt), heat transferred by working fluid, Q_{php} (Watt) and heat transfer from condenser section Q_{con}(Watt) with time in CLPHP for fill ratio = 0.8 and inclination = 0° (Vertical position).

It is obserbed from fig 4.2.1 to 4.2.3 above that within the test period Q_{php} reach nearer to heat input and the difference between Q_{php} and Q_{con} are simillar for all fill ratios at 0° inclination which indicate that heat transfer rate is approximately same for all fill ratios at 0° inclination

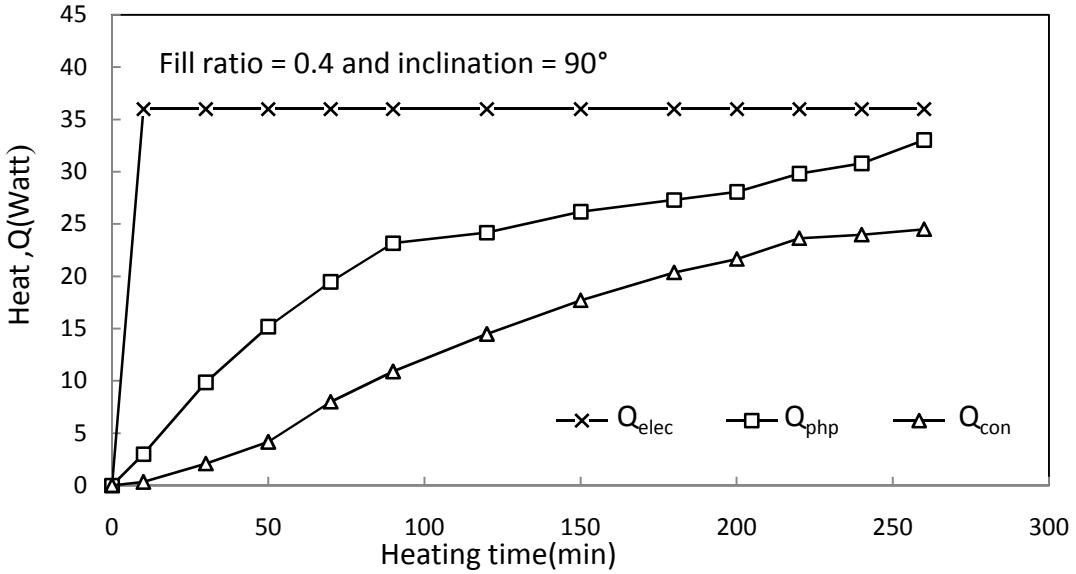

Figure 4.2.4: Comperative study of electrical heat input 36(Watt), heat transferred by working fluid, Q_{php} (Watt) and heat transfer from condenser section Q_{con}(Watt) with time in CLPHP for fill ratio = 0.4 and inclination = 90° (Horizontal position).

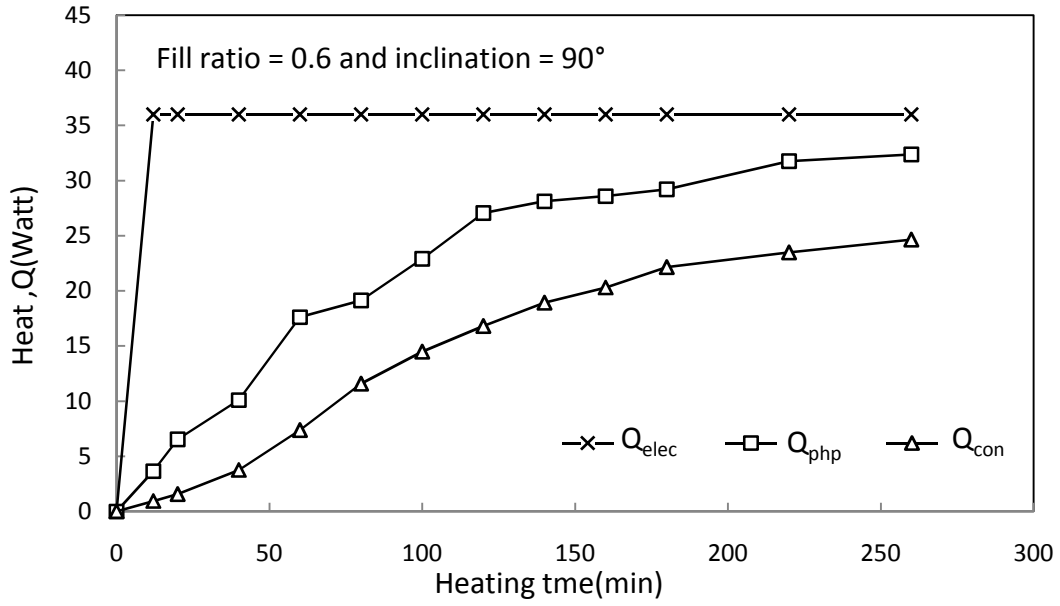

Figure 4.2.5: Comperative study of electrical heat input 36(Watt), heat transferred by working fluid, Q_{php} (Watt) and heat transfer from condenser section Q_{con}(Watt) with time in CLPHP for fill ratio = 0.6 and inclination = 90° (Horizontal position).

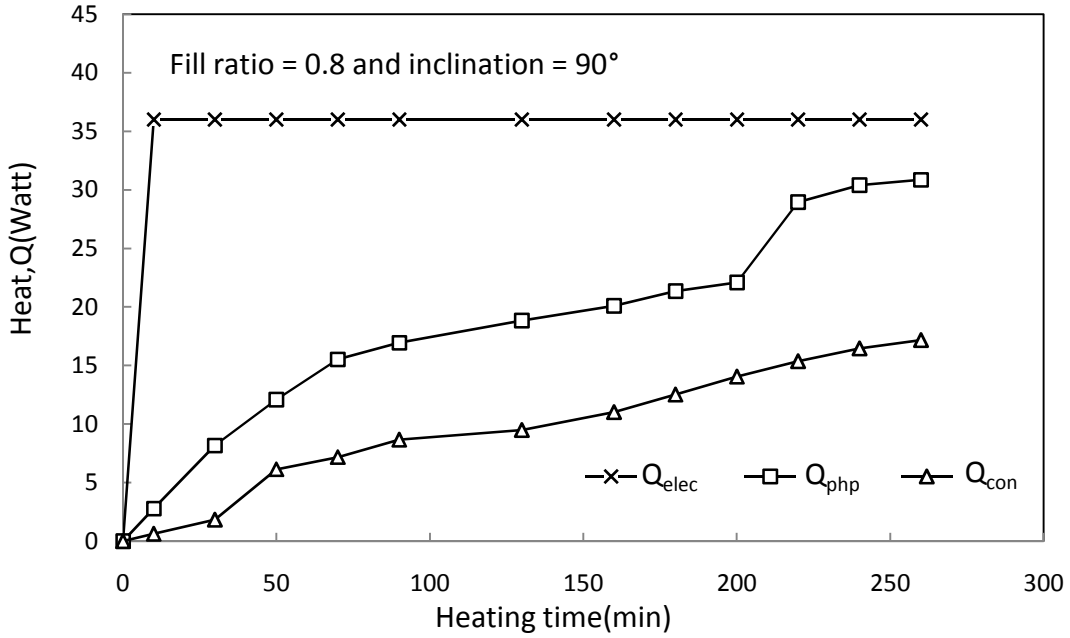

Figure 4.2.6: Comperative study of electrical heat input 36(Watt), heat transferred by working fluid, Q_{php} (Watt) and heat transfer from condenser section Q_{con}(Watt) with time in CLPHP for fill ratio = 0.8 and inclination = 90° (Horizontal position).

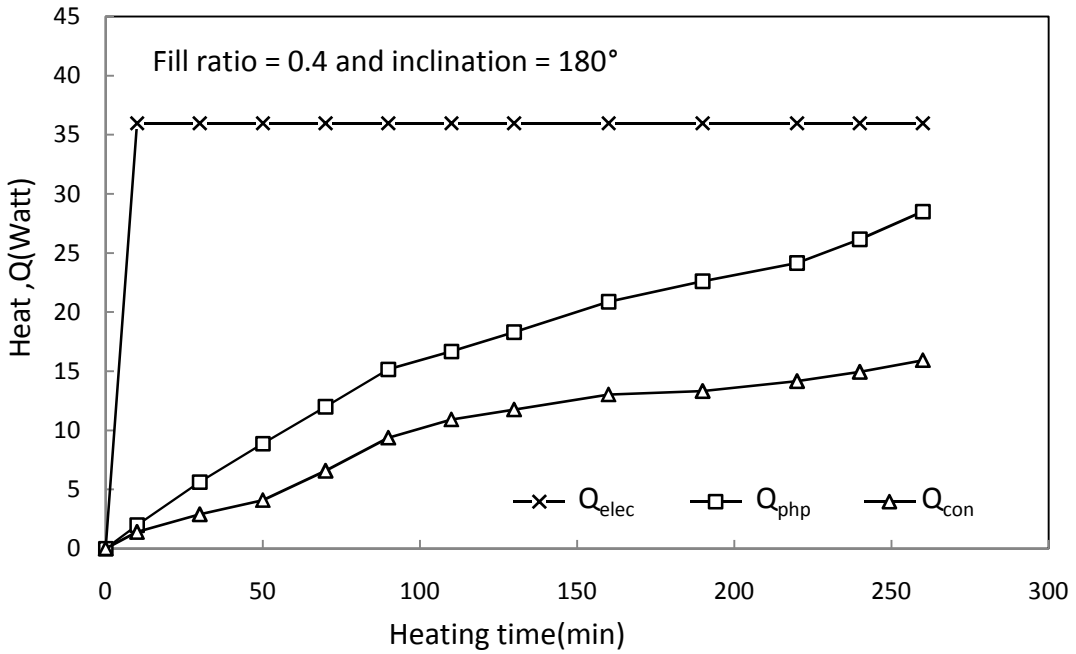

Figure 4.2.7: Comperative study of electrical heat input 36(Watt), heat transferred by working fluid, Q_{php} (Watt) and heat transfer from condenser section Q_{con}(Watt) with time in CLPHP for fill ratio = 0.4 and inclination = 180° (Heat source above the heat sink).

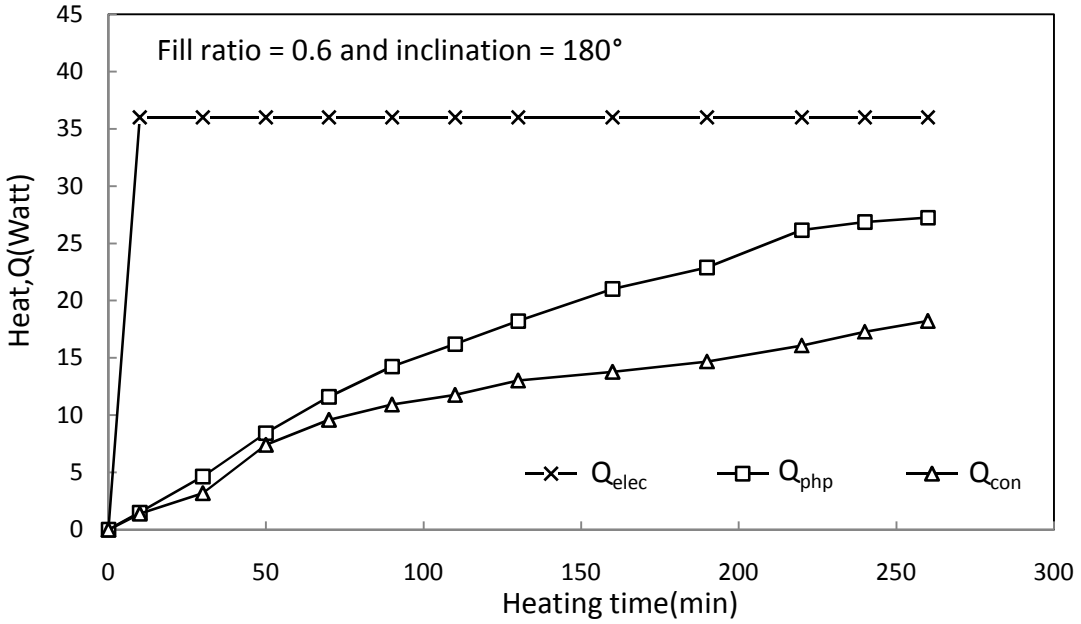

Figure 4.2.8: Comperative study of electrical heat input 36(Watt), heat transferred by working fluid, Q_{php} (Watt) and heat transfer from condenser section Q_{con}(Watt) with time in CLPHP for fill ratio =0.6 and inclination=180°(Heat source above the heat sink).

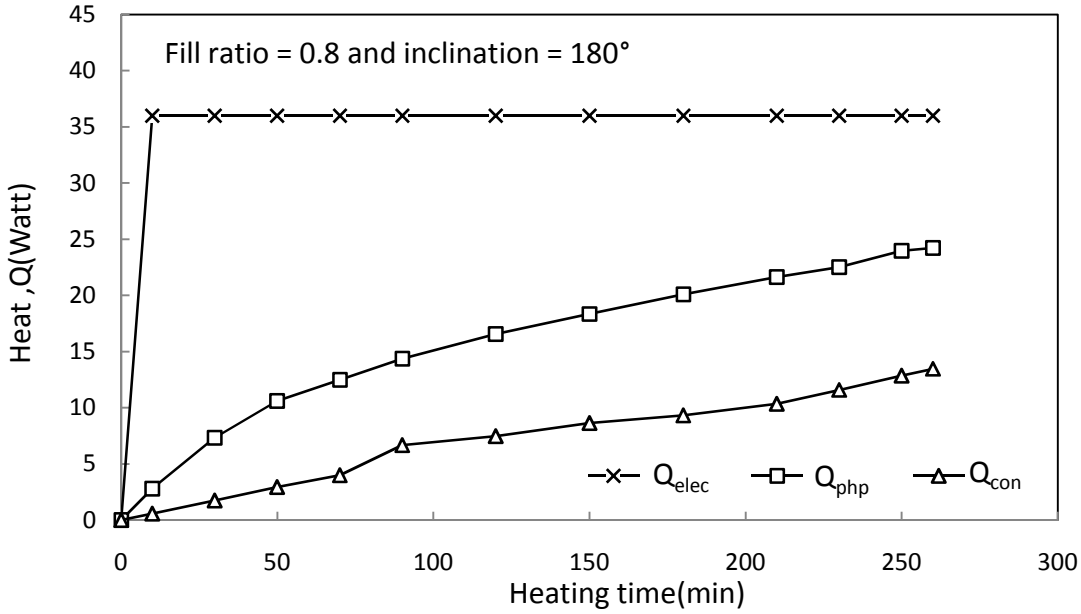

Figure 4.2.9: Comperative study of electrical heat input 36(Watt), heat transferred by working fluid, Q_{php} (Watt) and heat transfer from condenser section Q_{con}(Watt) with time in CLPHP for fill ratio=0.8 and inclination=180°(Heat source above the heat sink).

Similar result is observed for all fill ratios at 90° inclination as seen in fig 4.2.4 to 4.2.6. From fig 4.2.7 to 4.2.9 it is observed that though the difference between Q_{php} and Q_{con} at inclination 180° are similar to other inclinations but Q_{php} is much lower than heat input and still to reach steady state position.It indicates that hear transfer rate is slower at 180° inclination.

Fig 4.2.10 to 4.2.15 below compares the increase of Q_{php} with heating time for fill ratios 0.4 , 0.6 and 0.8 at inclination angles 0°,30°,45°,60°,90° and180°.

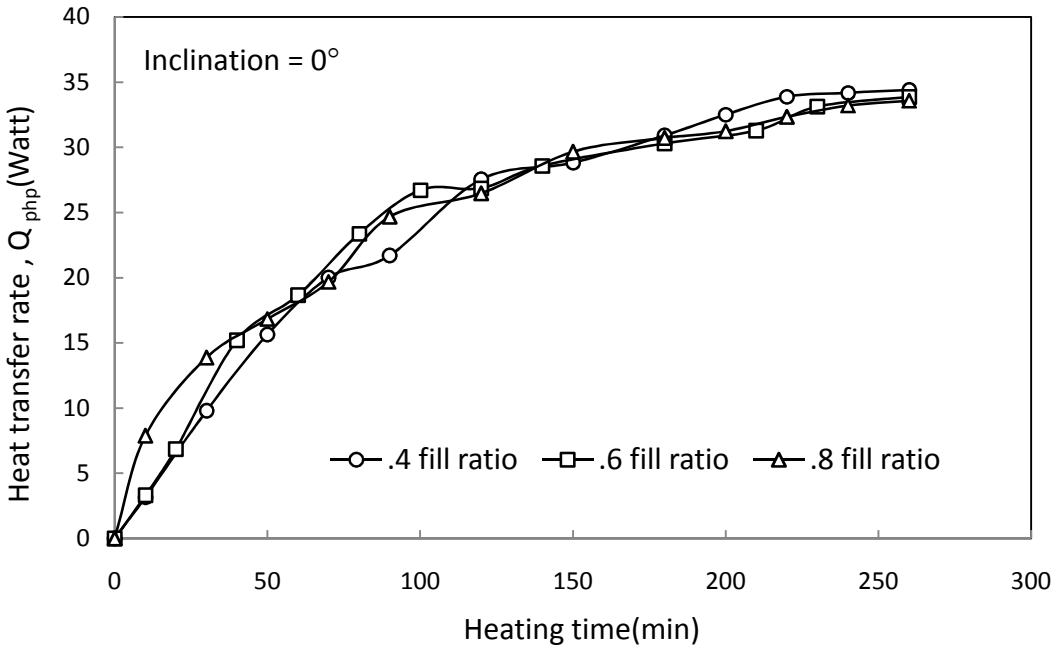

Figure 4.2.10: Heat transfer rate by working fluid , Q_{php} (Watt) with time for different fill ratio at inclination = 0° (Vertical position).

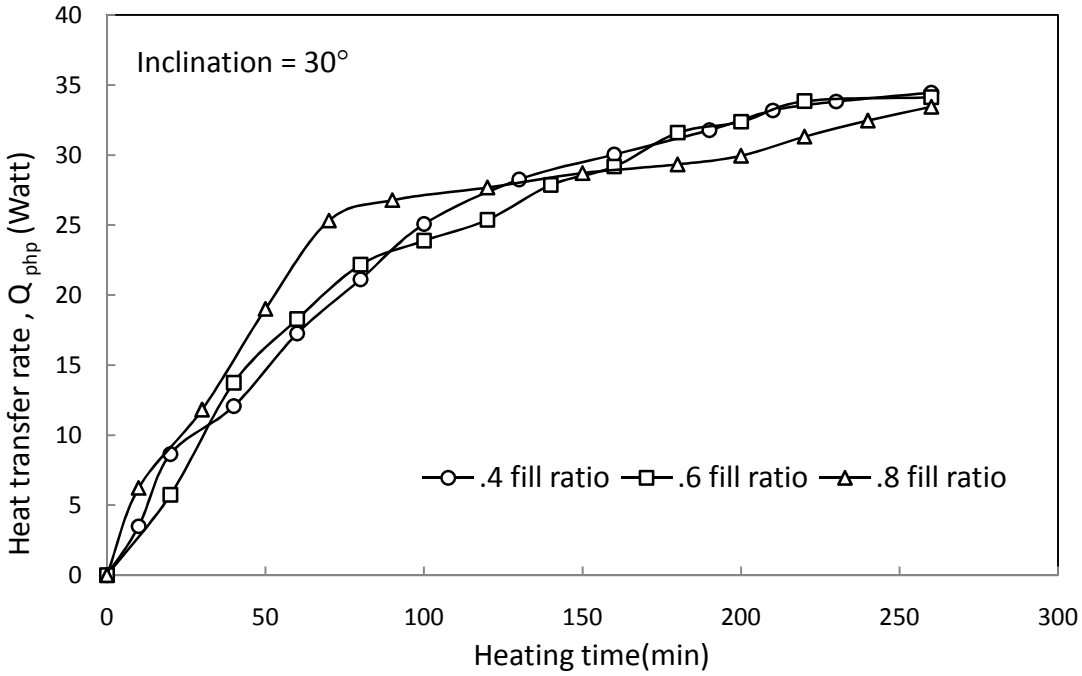

Figure 4.2.11: Heat transfer rate by working fluid, Q_{php} (Watt) with time for different fill ratio at inclination = 30°.

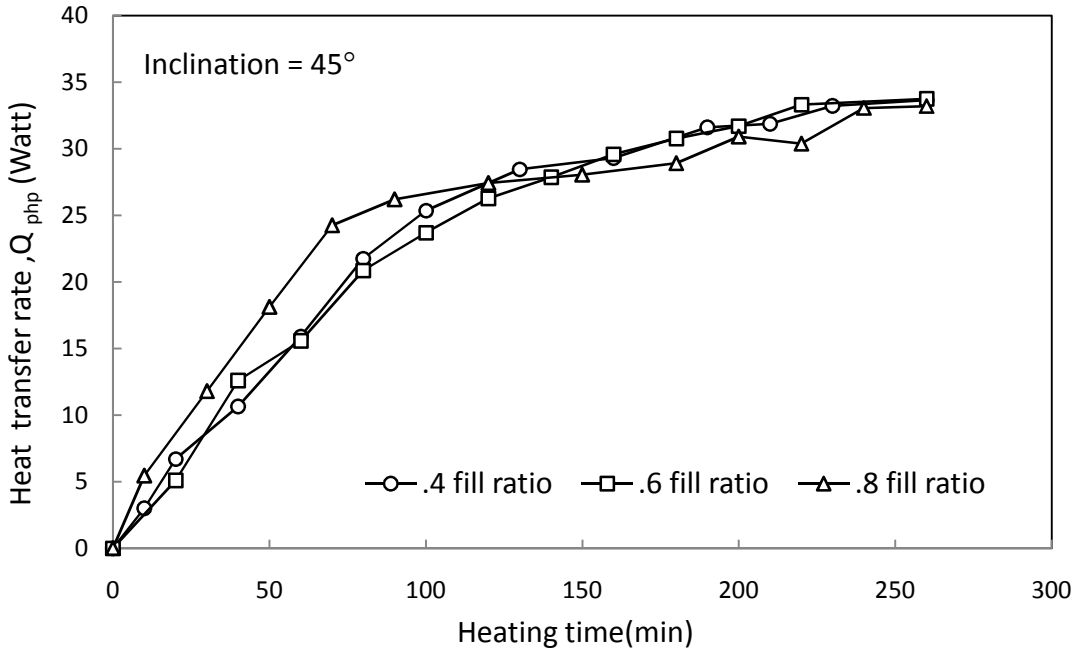

Figure 4.2.12: Heat transfer rate by working fluid , Q_{php} (Watt)with time for different fill ratio at inclination = 45°.

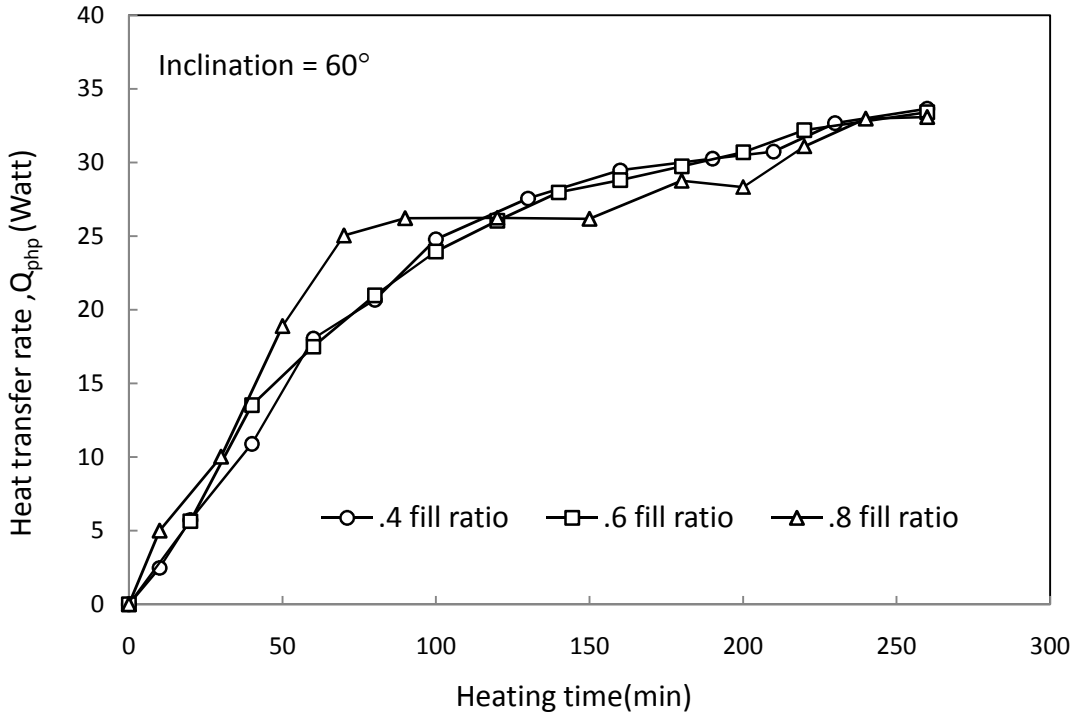

Figure 4.2.13: Heat transfer rate by working fluid, Q_{php} (Watt) with time for different fill ratio at inclination = 60°.

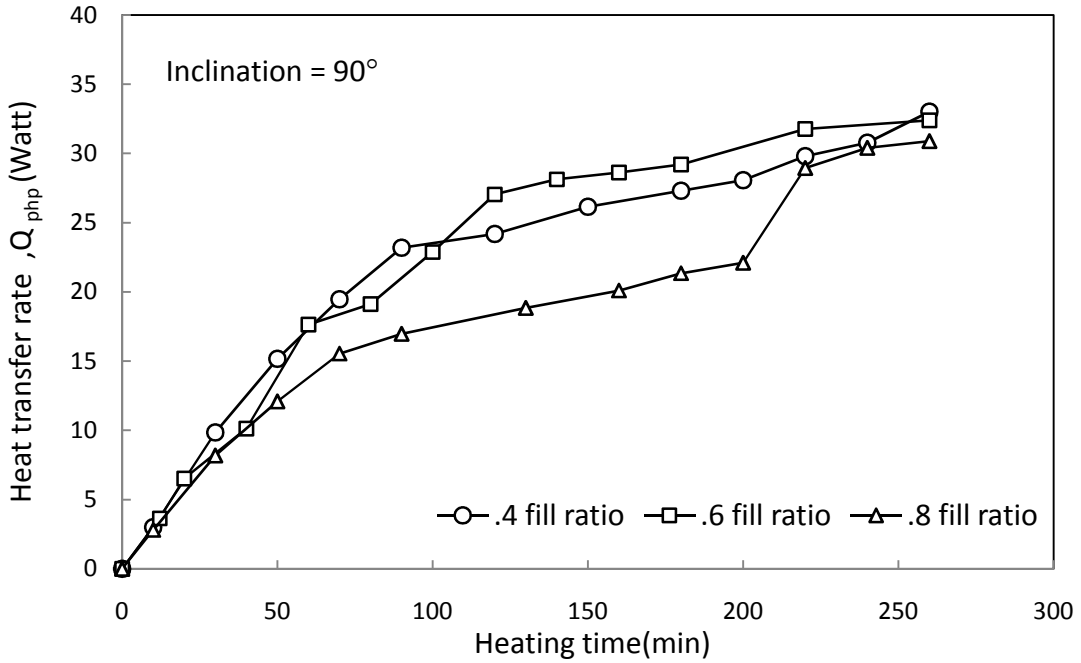

Figure 4.2.14: Heat transfer rate by working fluid ,Q_{php} (Watt) with time for different fill ratio at inclination = 90° (Horizontal position) .

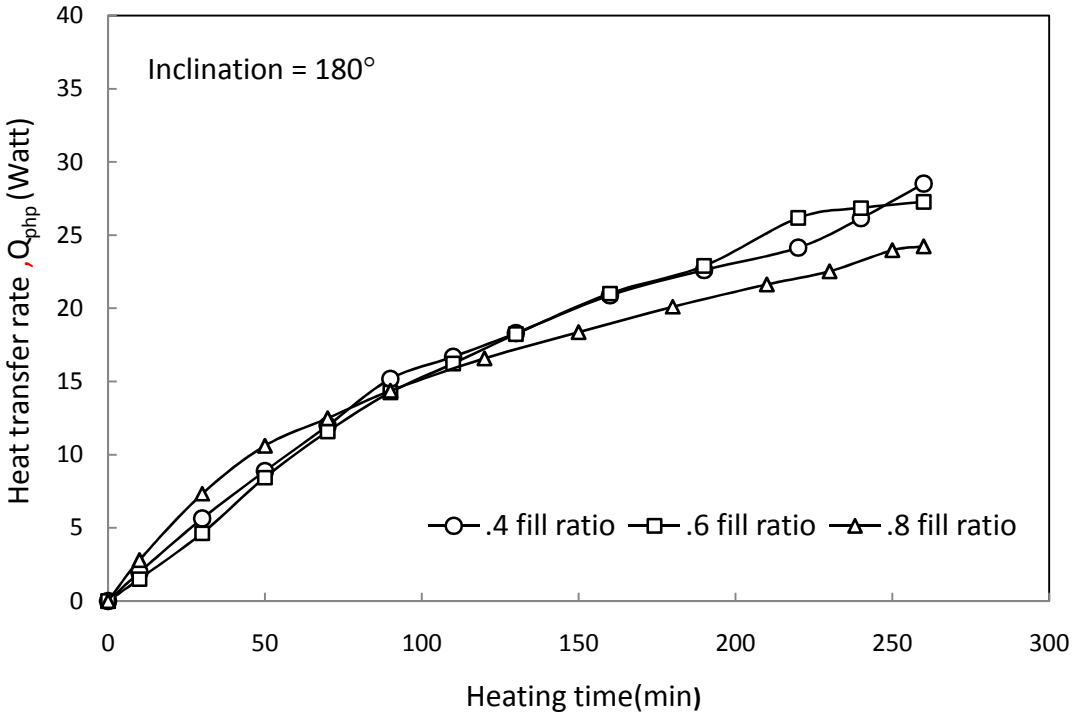

Figure 4.2.15: Heat transfer rate by working fluid, Q_{php} (Watt) with time for different fill ratio at inclination = 180° (Heat source above the heat sink.)

It is observed from fig 4.2.10 to 4.2.15 above that initially the rate of increase of Q_{php} at fill ratio 0.8 is higher than fill ratio 0.4 and 0.6 for inclination 0°, 30°, 45°, 60°, 90° and 180° but with increase of time this rate gradually decrease for a fixed heat input and ultimately heat transfer rate for fill ratio 0.8 is lower than fill ratio 0.4 and 0.6 for all inclination. It is also observed from above figures that the rate of increase of Q_{php} for fill ratio 0.4 and 0.6 at constant heat input is almost same and as seen in fig 4.2.15 that at inclination angle 180° for all fill ratio heat transfer rate is low compared to other inclination.

Fig 4.2.16 to 4.2.18 below compares the increase in Q_{php} with time at inclinations 0°, 30°, 45°, 60°, 90°and 180° for fill ratio 0.4 , 0.6 and 0.8.

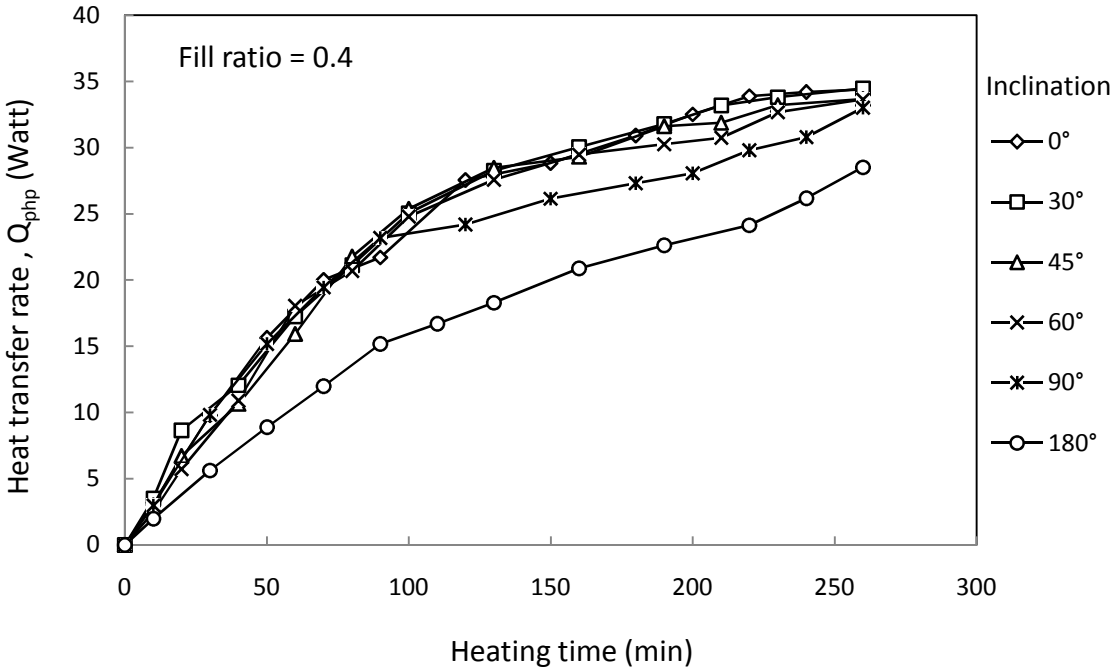

Figure 4.2.16: Heat transfer rate by working fluid, Q_{php} (Watt) with time in CLPHP at different inclination for fill ratio = 0.4.

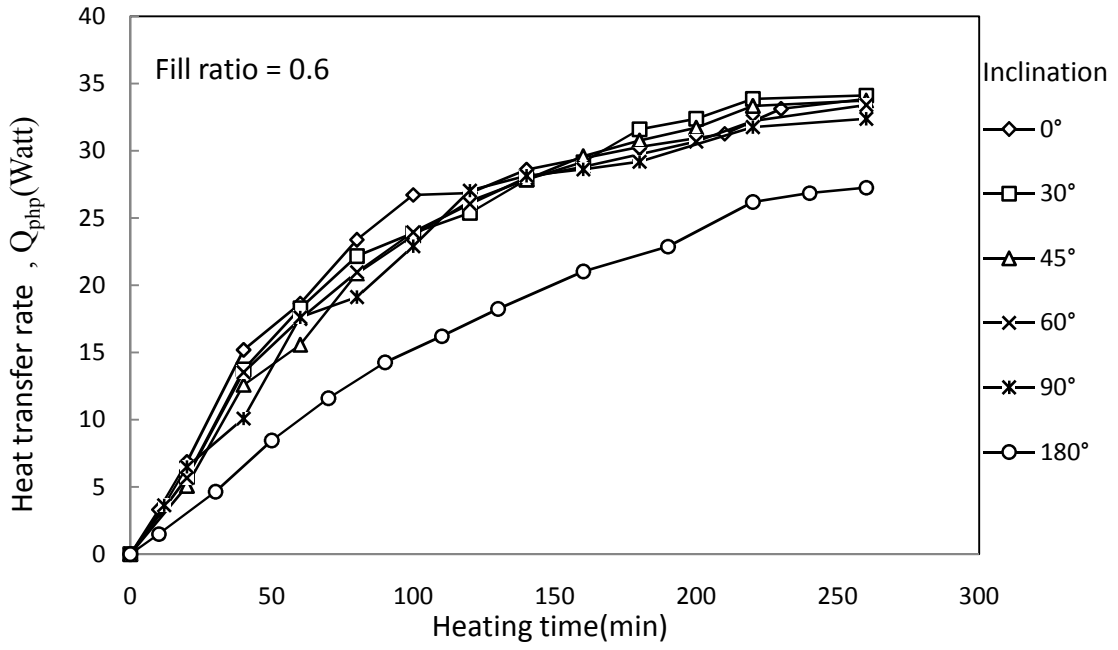

Figure 4.2.17: Heat transfer rate by working fluid, Q_{php} (Watt) with time in CLPHP at different inclination for fill ratio = 0.6.

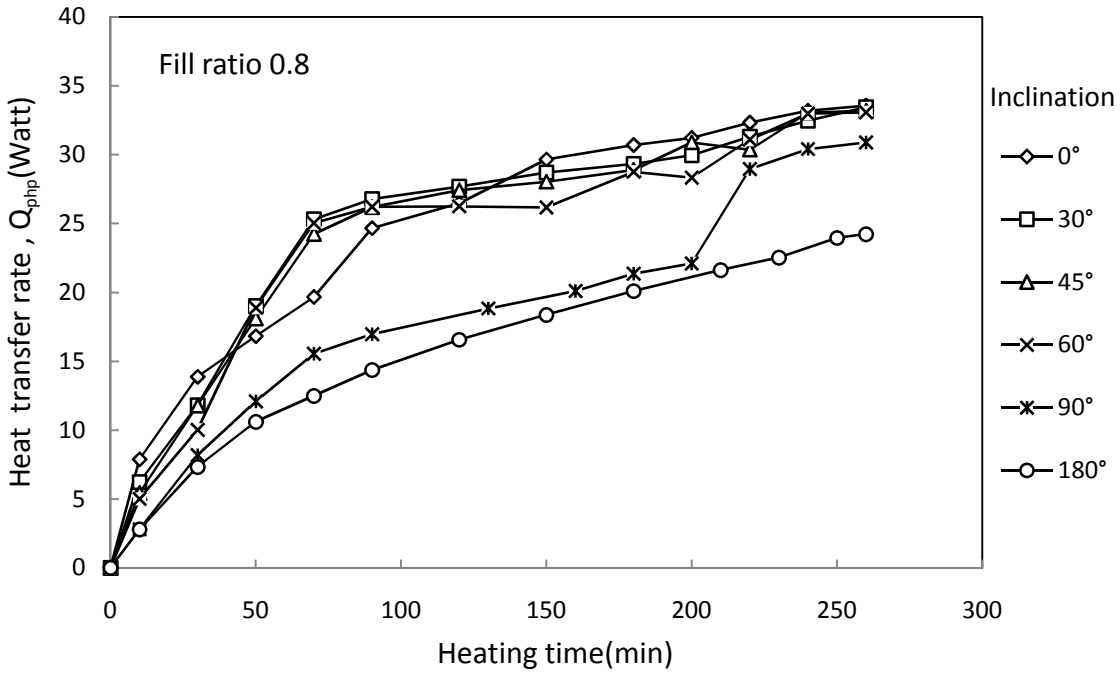

Figure 4.2.18: Heat transfer rate by working fluid, Q_{php} (Watt) with time in CLPHP at different inclination for fill ratio = 0.8

It is observed from fig4.2.16 above that the increase in Q_{php} for inclinations 0°, 30°, 45° and 60° are qualitatively and quantitatively same for fill ratio 0.4. The same result is observed at fill ratios 0.6 and 0.8 for inclination 0°, 30°, 45° and 60° . But for inclinations 90° and 180° the increase in Q_{php} is much slower compared to other inclinations for all fill ratios. From fig 4.2.16 and 4.2.17 it is also observed that increase in Q_{php} is nearly same for fill ratios 0.4 and 0.6 though it is slightly low in case of 0.8 fill ratio. Thus we can say that the rate of increase of Q_{php} is independent of fill ratio at fill ratios 0.4 and 0.6 and inclination 0°, 30°, 45° and 60°.

Fig 4.2.19 below shows change in Heat flux with fill ratios at inclinations 0°, 30°, 45°, 60°, 90°and 180° .

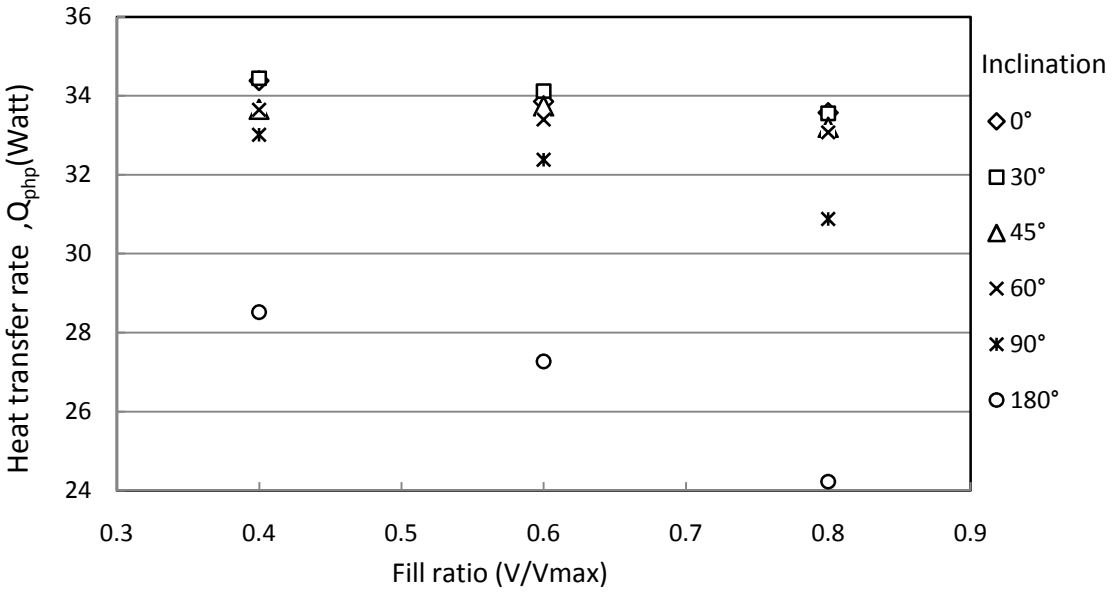

Figure 4.2.19: Effect of fill ratio(V/Vmax) on Heat transfer rate by working fluid , Q_{php} (Watt) at different inclination .

From fig 4.2.19 above it is observed that for all fill ratios the Heat transfer rate, Q_{php} at inclinations 0°, 30°, 45°and 60° in are very close to each other though it is slightly lower for fill ratio 0.8 . It is also observed that for all fill ratios heat transfer rate, Q_{php} at inclinations 90°and 180° is much lower and it is lowest for fill ratio 0.8.So we can say that at fill ratios 0.4 and 0.6 heat transfer rate, Q_{php} is independent of inclination below 90° .

Effect of various inclination on heat transfer rate of CLPHP are shown in fig 4.2.20 below

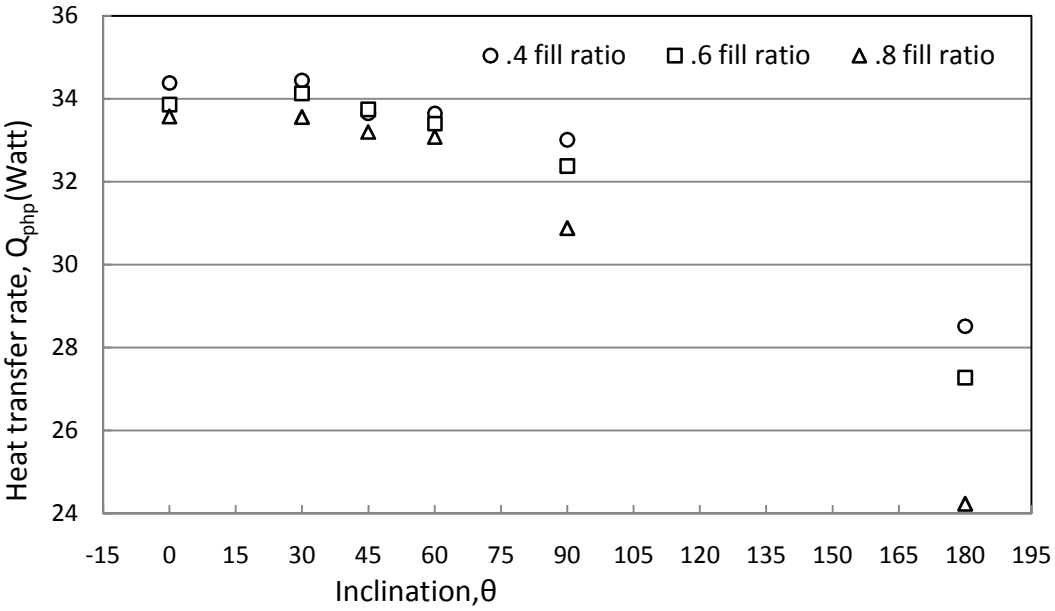

Figure 4.2.20: Effect of inclination , θ on heat transfer rate by working fluid, Q_{php} (Watt) of CLPHP for different fill ratio at constant heat input.

It is observed that for all inclination below 90° heat transfer rate by working fluid, Q_{php} for fill ratio 0.4 , 0.6 and 0.8 is approximately same though Q_{php} for 0.8 is slightly lower .For inclination 90° and 180° this Q_{php} is lower compared to other inclination. From fig it is also clear that Q_{php} for inclination 180° and fill ratio 0.8 is the lowest.

4.3 Overall Heat Transfer coefficient , U(W/m² °C)

Variation of overall Heat transfer coefficient of CLPHP with time , fill ratio and inclination for a heat input are shown in fig 4.3.1, 4.3.11 and calculation of this overall hear transfer is shown in appendix D.

Change in overall heat transfer coefficient of CLPHP with time for inclination 0°,30°,45°,60° ,90° and 180° at various fill ratio are shown in fig 4.3.1 to fig 4.3.3.

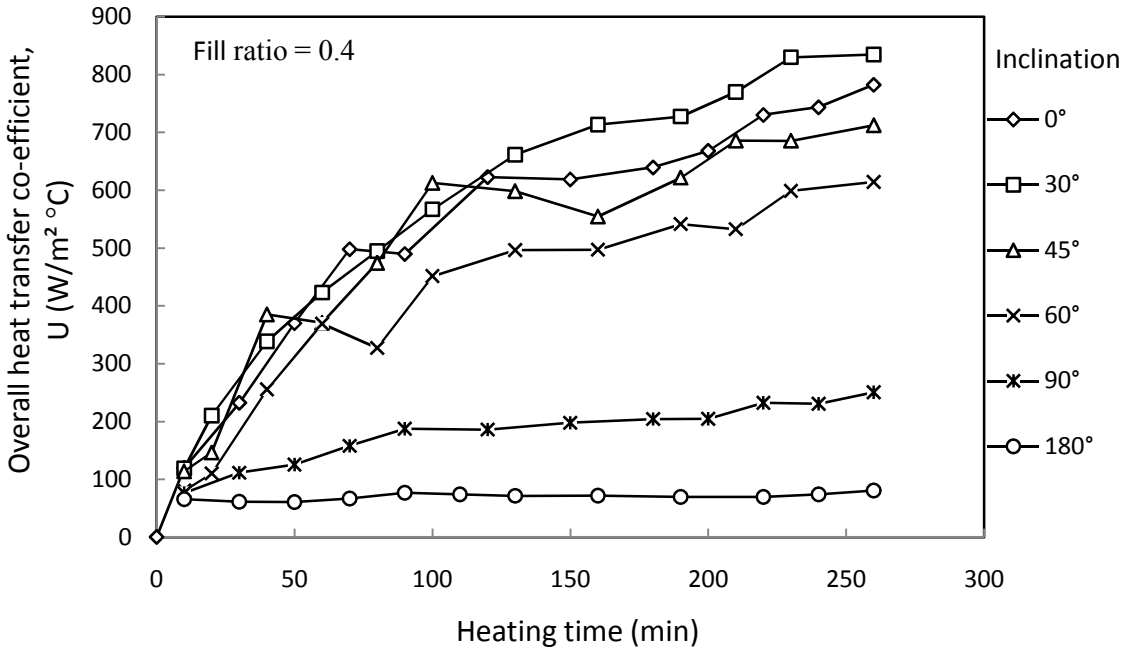

Figure 4.3.1: Change in overall heat transfer co-efficient,U(W/m² °C) with time in CLPHP at different inclination for fill ratio = 0.4.

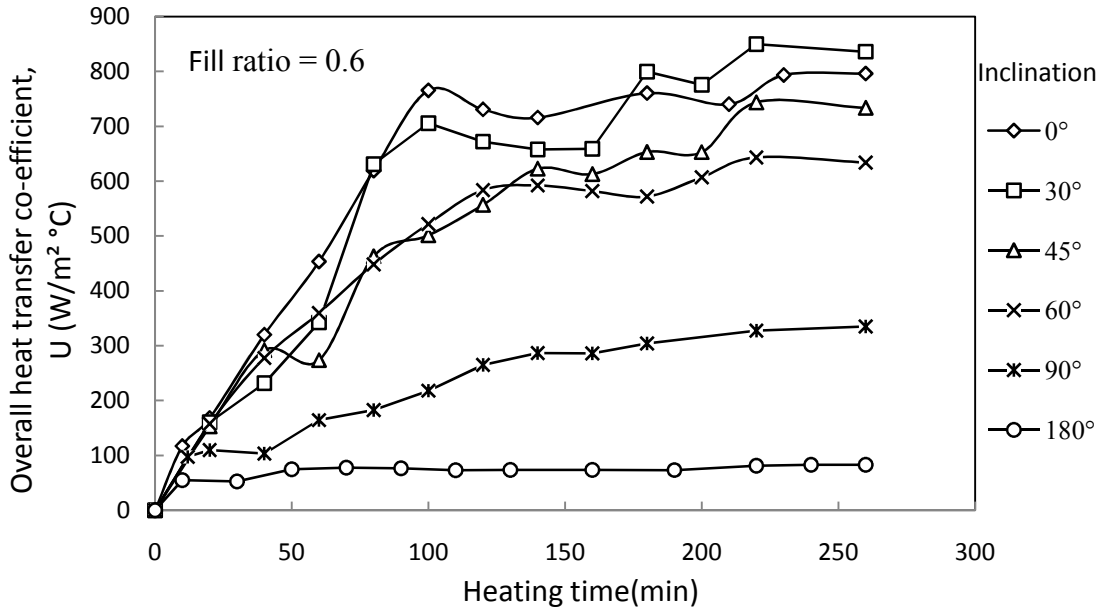

Figure 4.3.2: Change in overall heat transfer co-efficient,U(W/m² °C) with time in CLPHP at different inclination for fill ratio = 0.6.

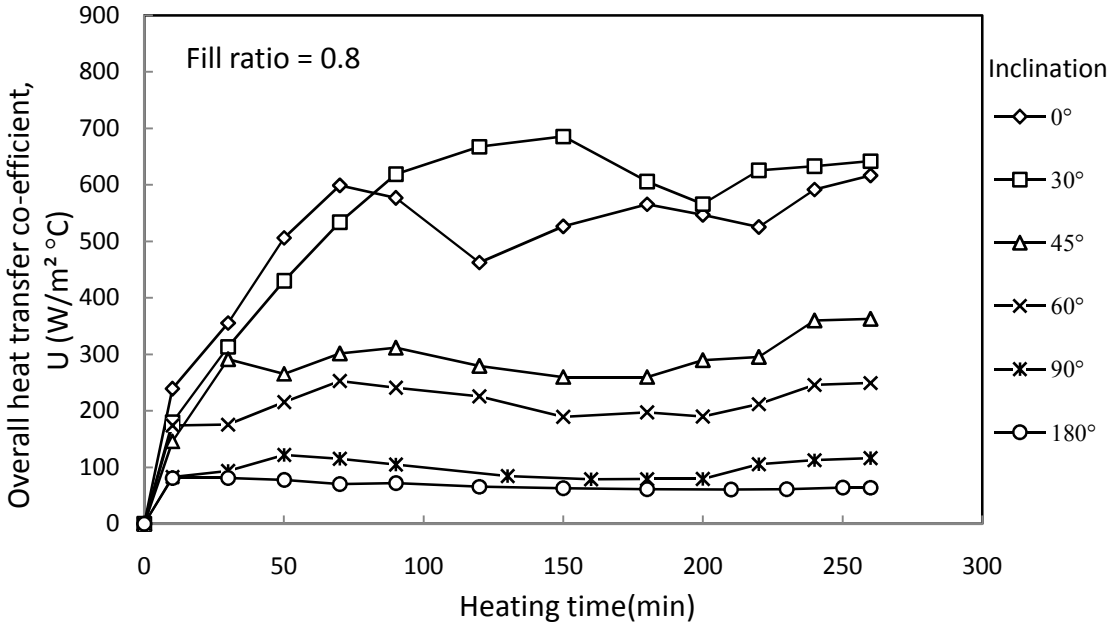

Figure 4.3.3: Change in overall heat transfer co-efficient,U(W/m² °C) with time in CLPHP at different inclination for fill ratio = 0.8.

It is observed from fig 4.3.1 that at fill ratio 0.4 the rate of increase of heat transfer follow similar trend for inclination 0°,30°,45°and 60° and also it is higher than inclination 90° and 180°. The same result is also observed at fill ratio 0.6 and 0.8 fill ratio. The graph also shows that at 0° , 30° inclination the value of U is little higher than other inclination and then with increase in inclination of CLPHP the value of U decrease . At 90° inclination it is lower and at 180° inclination it is lowest.

Fig 4.3.4 - 4.3.9 compares the rate of increase of heat transfer coefficient ,U with heating time for different fill ratios at various inclinations.

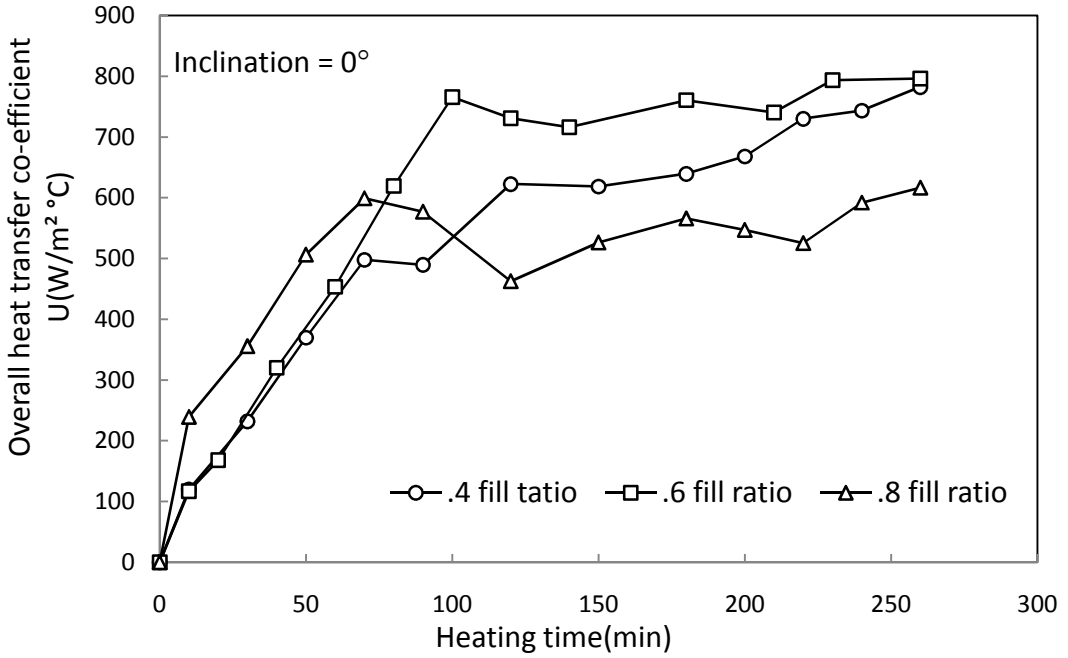

Figure 4.3.4: Change in overall heat transfer co-efficient ,U(W/m² °C) with time in CLPHP for different fill ratio at inclination(Vertical position) = 0°.

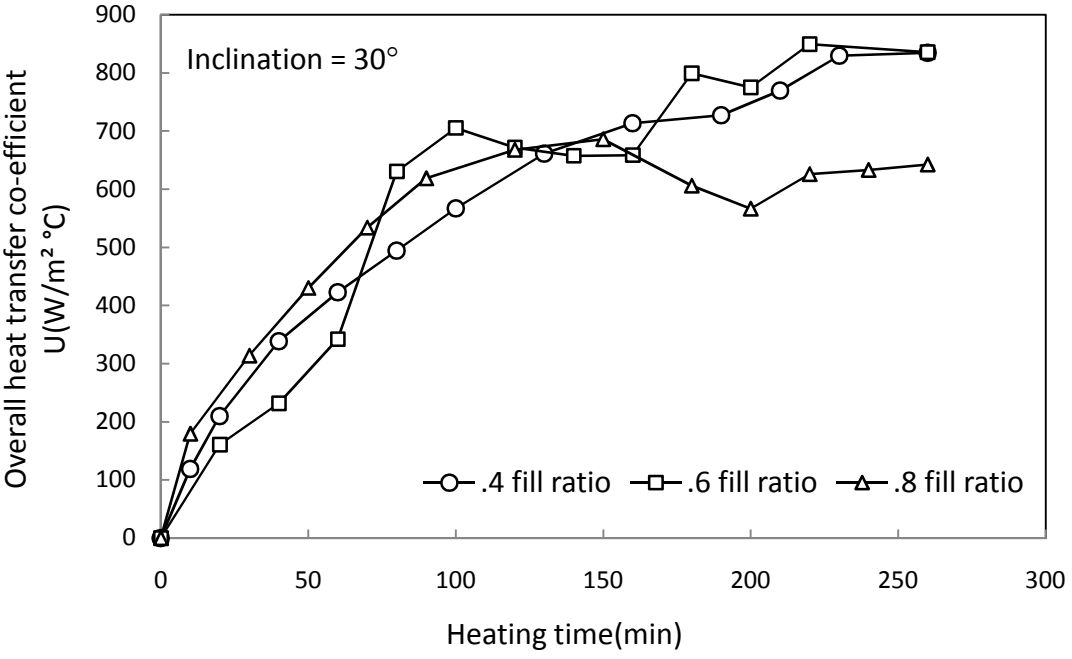

Figure 4.3.5: Change in overall heat transfer co-efficient ,U(W/m² °C) with time in CLPHP for different fill ratio at inclination = 30°.

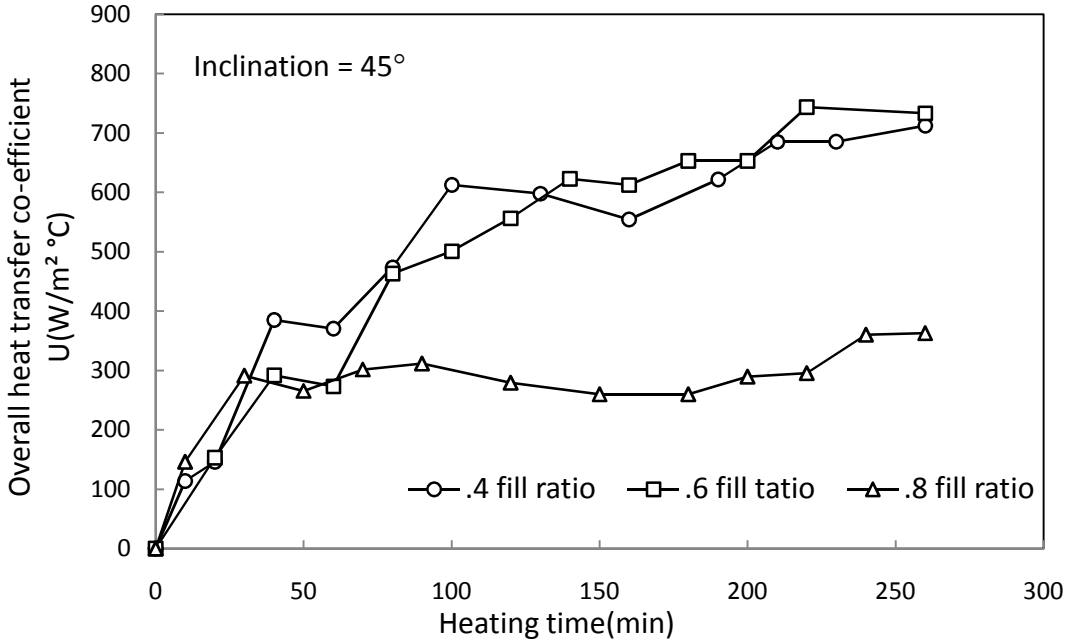

Figure 4.3.6: Change in overall heat transfer co-efficient ,U(W/m² °C) with time in CLPHP for different fill ratio at inclination = 45°.

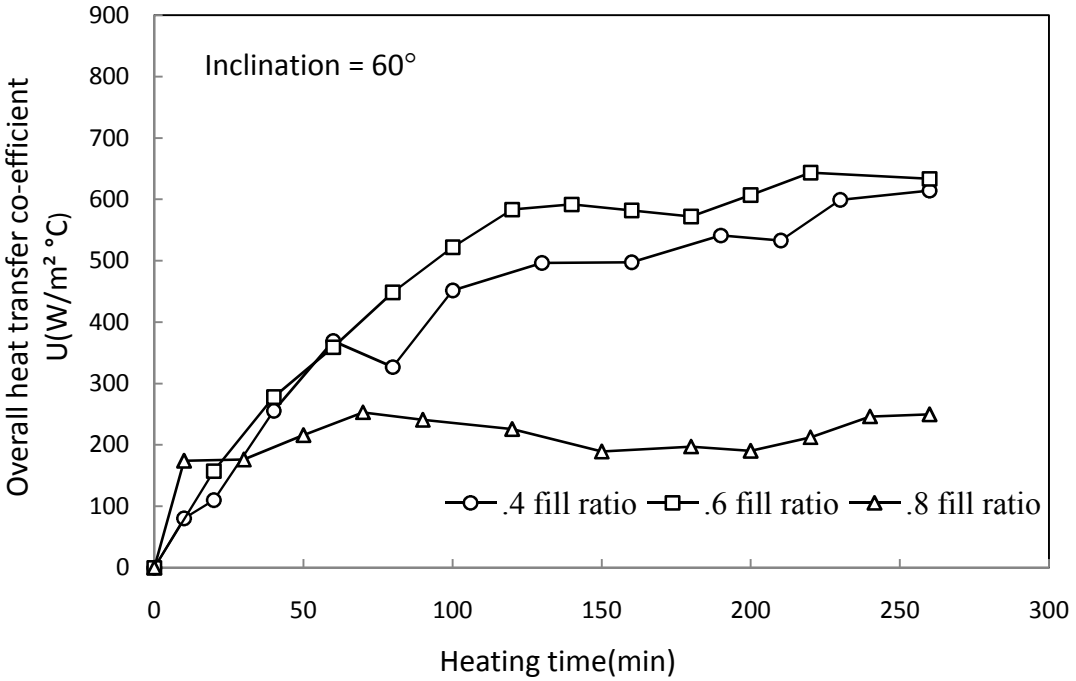

Figure 4.3.7: Change in overall heat transfer co-efficient ,U(W/m² °C) with time in CLPHP for different fill ratio at inclination = 60°.

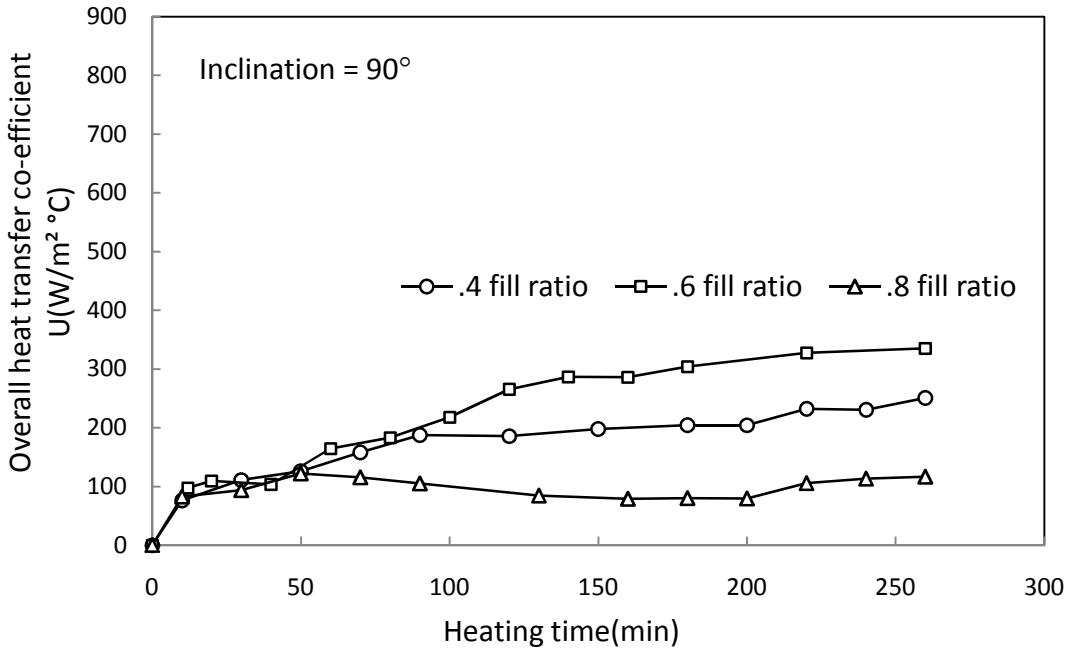

Figure 4.3.8: Change in overall heat transfer co-efficient ,U(W/m² °C) with time in CLPHP for different fill ratio at inclination = 90° (Horizontal position).

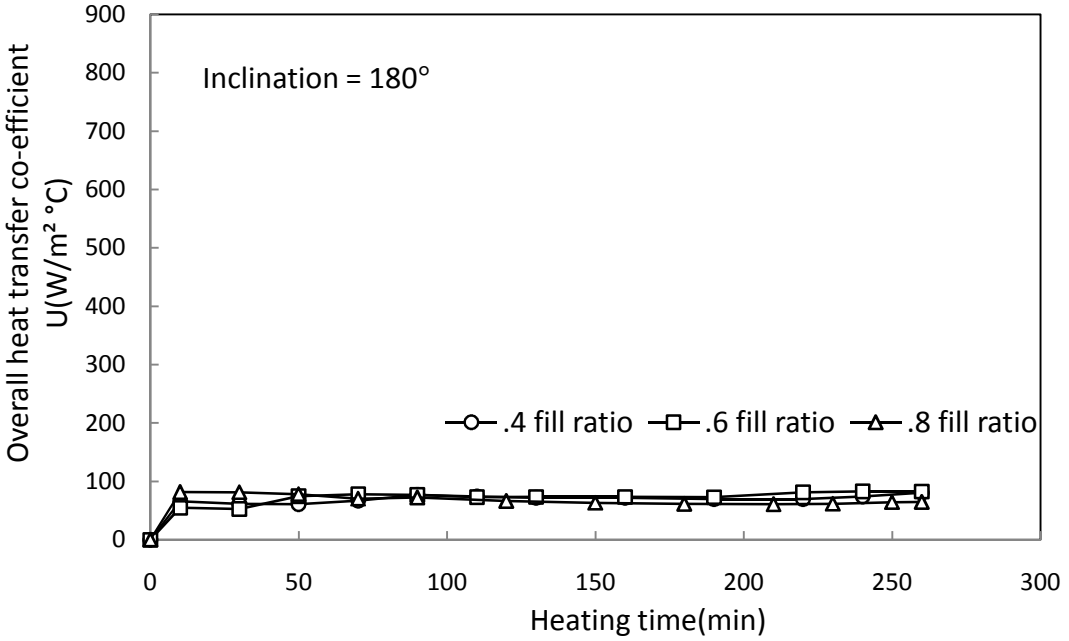

Figure 4.3.9: Change in overall heat transfer co-efficient ,U(W/m² °C) with time in CLPHP for different fill ratio at inclination =180° (Heat source above the heat sink).

It is observed from above fig 4.3.4 - 4.3.7 that rate of increase of heat transfer coefficient, U for fill ratio 0.4 and 0.6 is similar at inclination 0°,30°,45°and 60° and the value is higher than fill ratio 0.8. As shown in fig 4.3.8 and 4.3.9 , U is very low for all fill ratio at 90° and 180° inclination and at 180° inclination for all fill ratio the value is very low and approximately equal.

Figure 4.3.10 below shows the effect of fill ratio on overall heat transfer coefficient, U at different inclination angle.

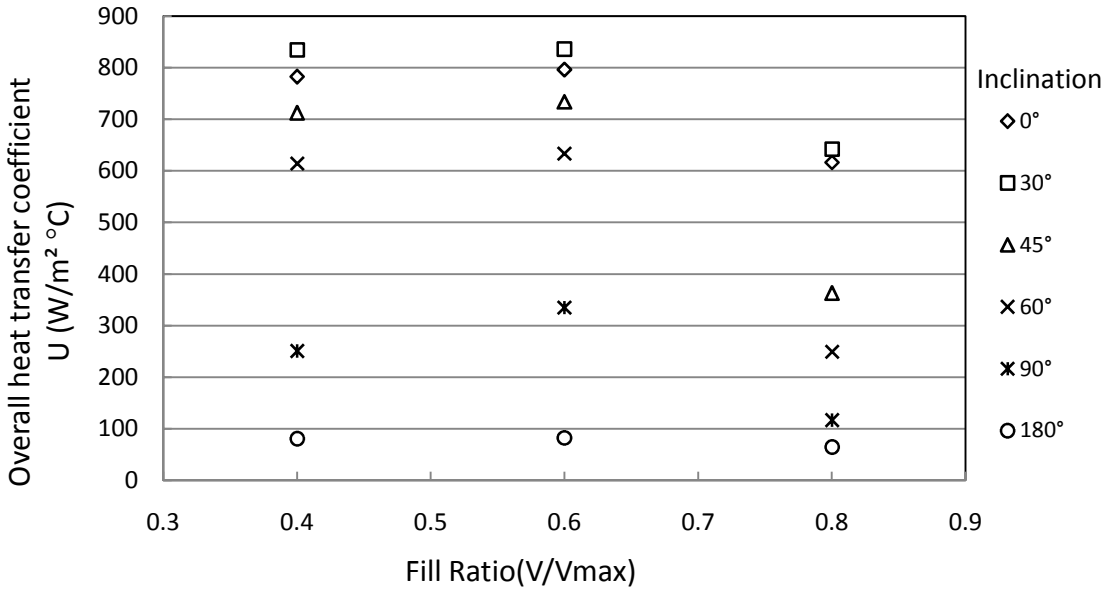

Figure 4.3.10: Change in overall heat transfer co-efficient ,U(W/m² °C) with fill ratio (V/Vmax) in CLPHP at different inclination .

From figure above, it is evident that overall heat transfer coefficient for a fixed heat input are similar for fill ratio 0.4 and 0.6 at all inclination though it is low for fill ratio 0.8. Overall heat transfer coefficient for fill ratio 0.4 and 0.6 are close to each other below inclination 90°.For all fill ratio overall heat transfer coefficient is lower at inclination 90° and above compared to other inclination. At inclination 180° the value of heat transfer coefficient is the lowest and approximately same for all fill ratio.

Fig 4.3.11 compares the change in overall heat transfer coefficient with inclination at different fill ratio

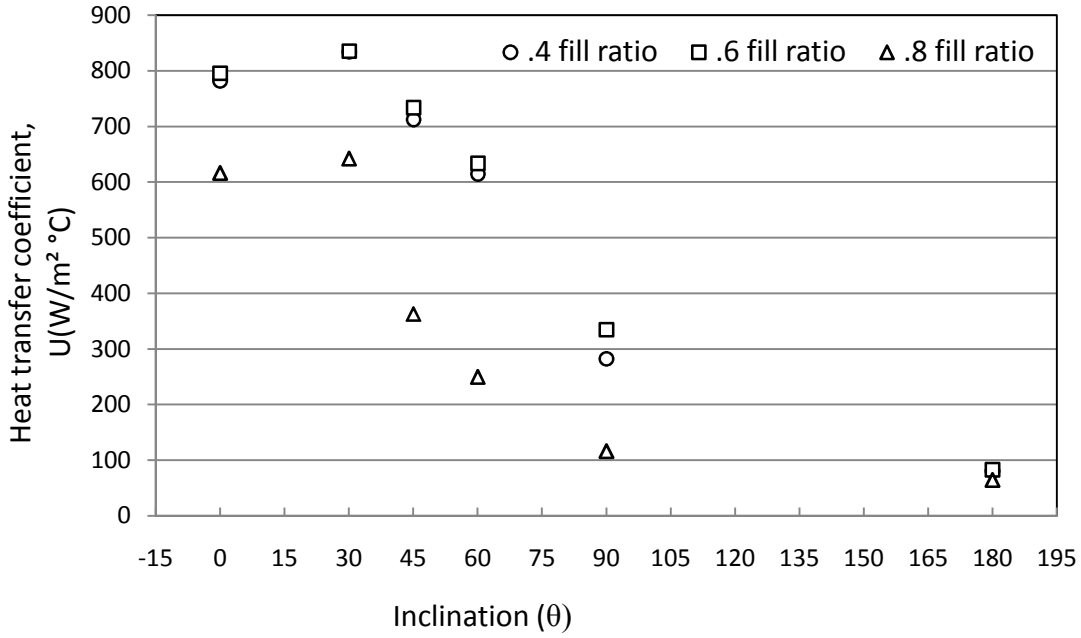

Figure 4.3.11: Effect of inclination, θ on heat transfer coefficient, U of CLPHP for different fill ratio at constant heat input.

It is observed from above fig that overall heat transfer coefficient for all inclination nearly same for fill ratio 0.4 and 0.6 but this value is low for fill ratio 0.8. At inclination 90° and above the value of U is lower compared to other inclination. At inclination 180° the value of heat transfer coefficient is very low and approximately same for all fill ratios.

4.4 Thermal Resistance , R (°C/W) of CLPHP

Change in thermal resistance to heat flow through the CLPHP at various fill ratio and inclinations are calculated following the calculation procedure described in section 3.3 of the previous chapter and sample calculation is shown in the appendix D. Variation of thermal resistance of CLPHP with heating time, fill ratio and inclination for a specific heat input are shown in fig 4.4.1 to 4.4.11

Fig 4.4.1 to 4.4.3 compare the change in thermal resistance to heat flow with heating time at various inclination for fill ratio 0.4 , 0.6 and 0.8.

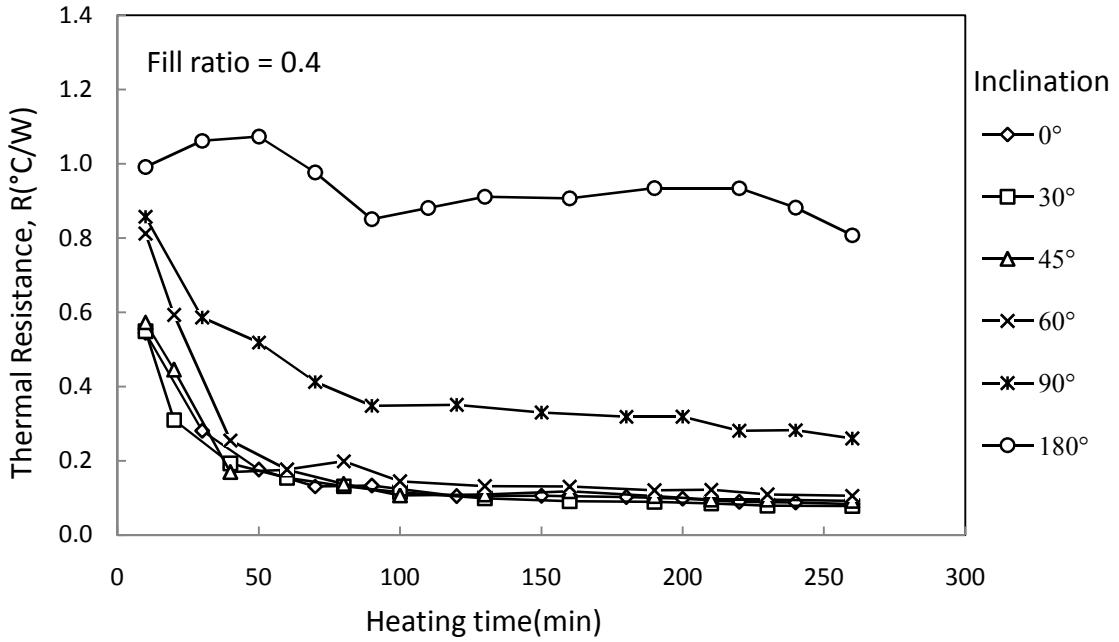

Figure 4.4.1: Change in thermal resistance,R (°C/W) with time in CLPHP at different inclination for fill ratio = 0.4.

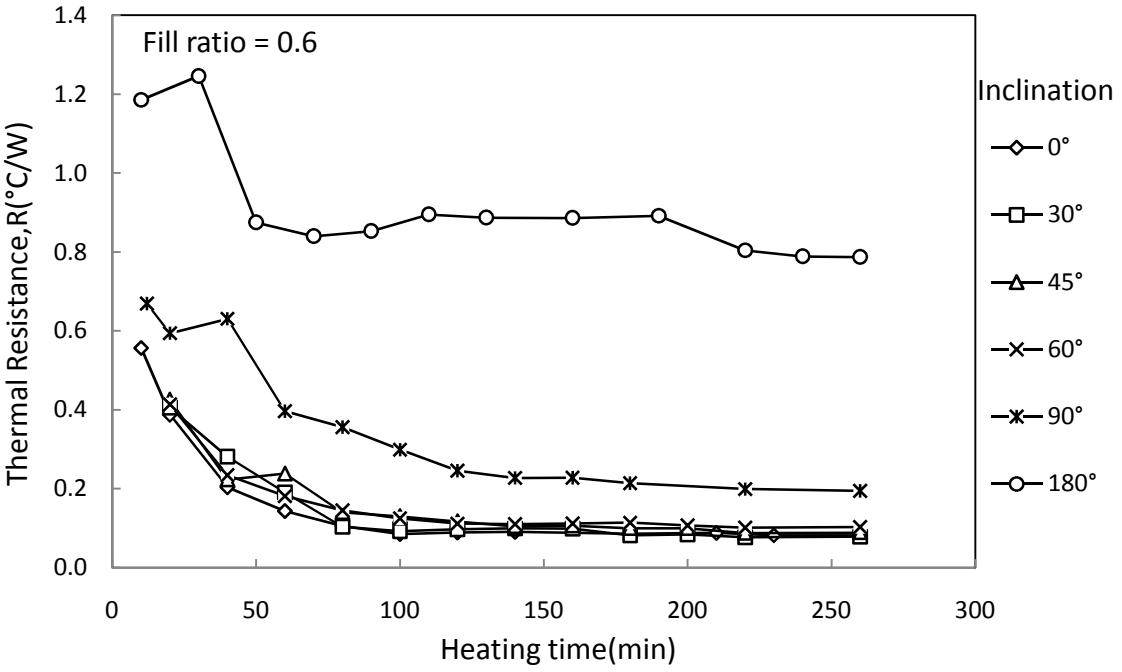

Figure 4.4.2: Change in thermal resistance,R (°C/W) with time in CLPHP at different inclination for fill ratio = 0.6.

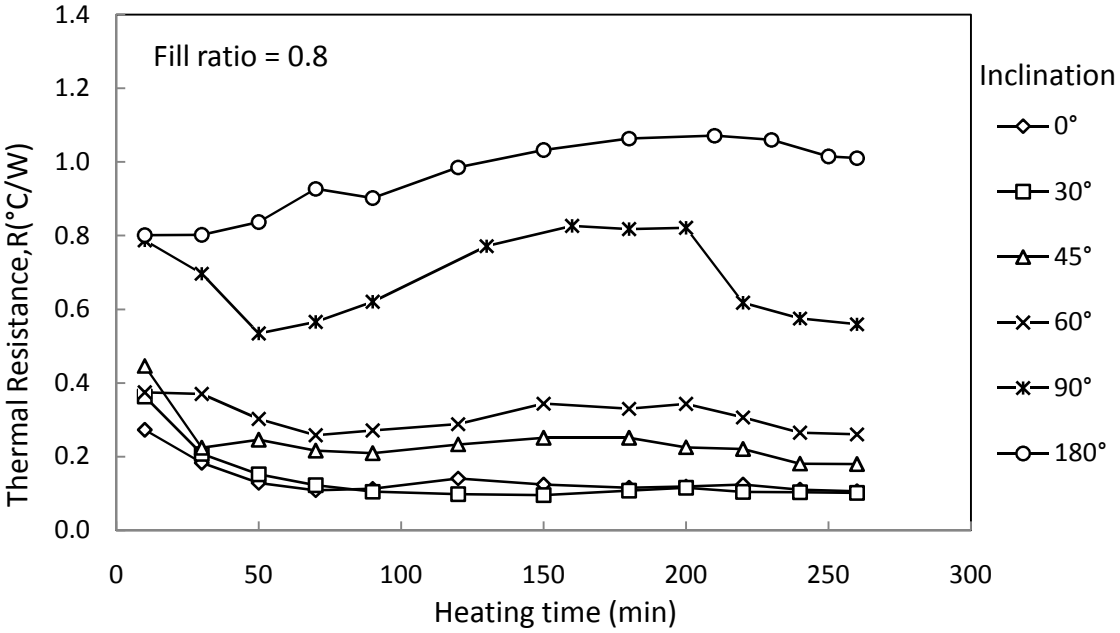

Figure 4.4.3: Change in thermal resistance,R (°C/W) with time in CLPHP at different inclination for fill ratio = 0.8.

It is ovserved from fig 4.4.1 that with the increase of heating time thermal resistance to heat flow decrease.The rate of decrease follows the similar trend for all inclination below inclination 90°.For inclination below 90° the value to thermal resistance are low compared to inclination 90° and above. The same result is also observed for fill ratio 0.6 and 0.8 As shown in fig 4.4.1 and 4.4.2, At fill ratio 0.4 and 0.6 for inclination 180° thermal resistance to heat flow decrease with heating time but in case of fill ratio 0.8 thermal resistance to heat flow increase with increase to heating time,shown in fig 4.4.3. It is also observed that for fill ratio 0.8 the rate of decrease of thermal resistance is much lower compared to fill ratio 0.4 and 0.6 .

Fig 4.4.4 to 4.4.9 shows the decrease in thermal resistance ,R of CLPHP with time for various fill ratio at different inclination

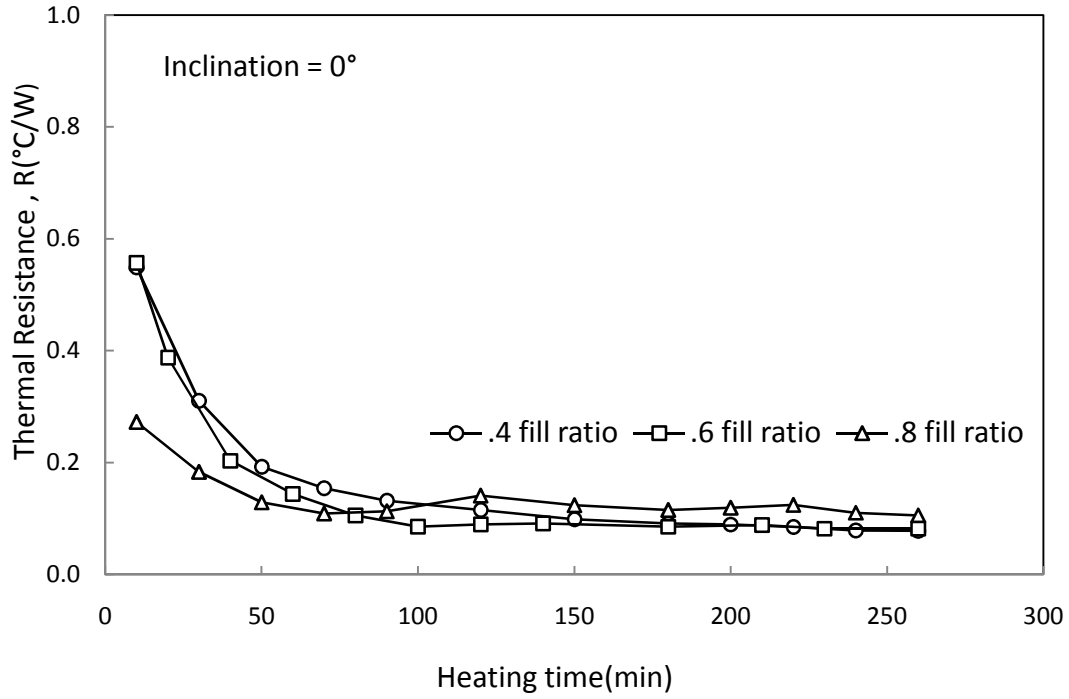

Figure 4.4.4: Change in thermal resistance, R(°C/W) with time in CLPHP for different fill ratio at inclination = 0° (Vertical position).

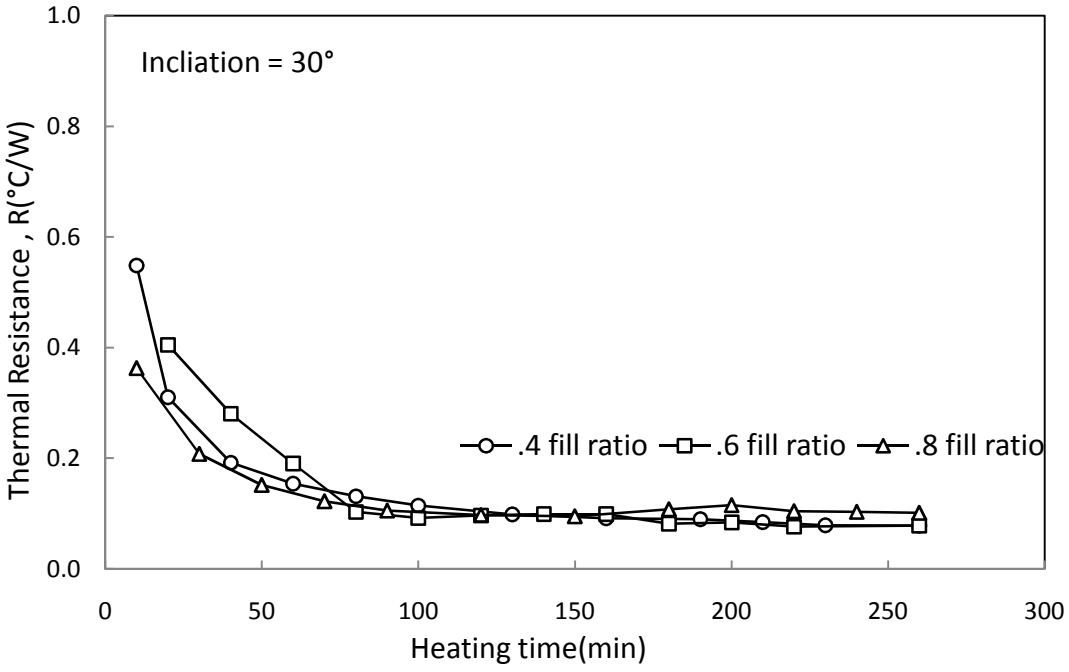

Figure 4.4.5: Change in thermal resistance, R(°C/W) with time in CLPHP for different fill ratio at inclination = 30°.

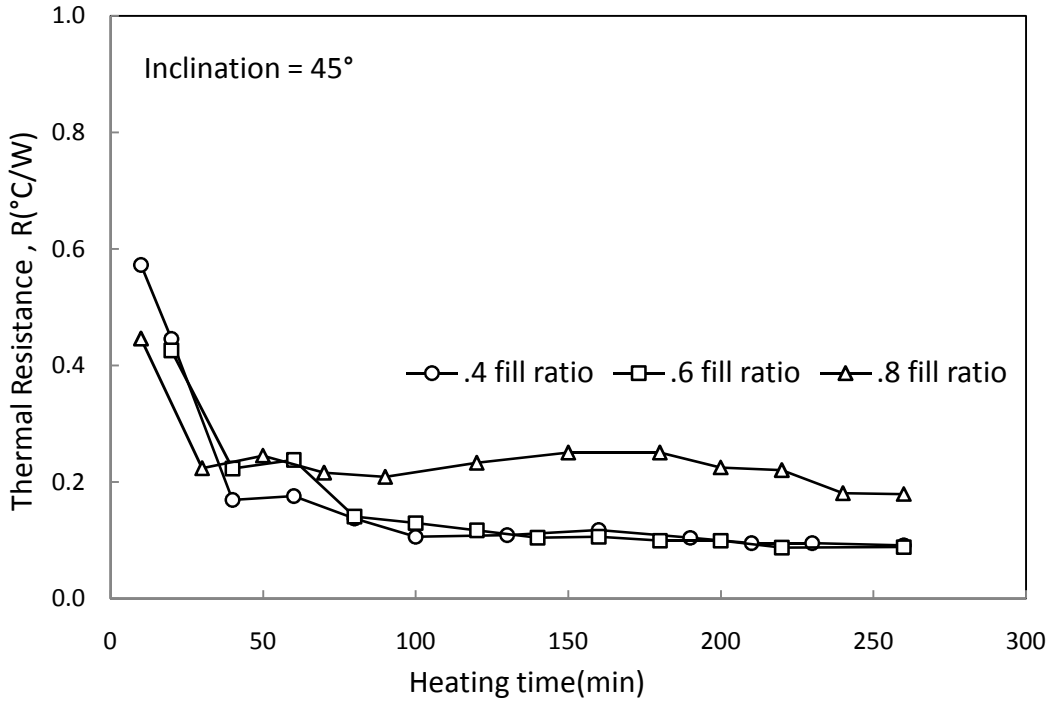

Figure 4.4.6: Change in thermal resistance, R(°C/W) with time in CLPHP for different fill ratio at inclination = 45°.

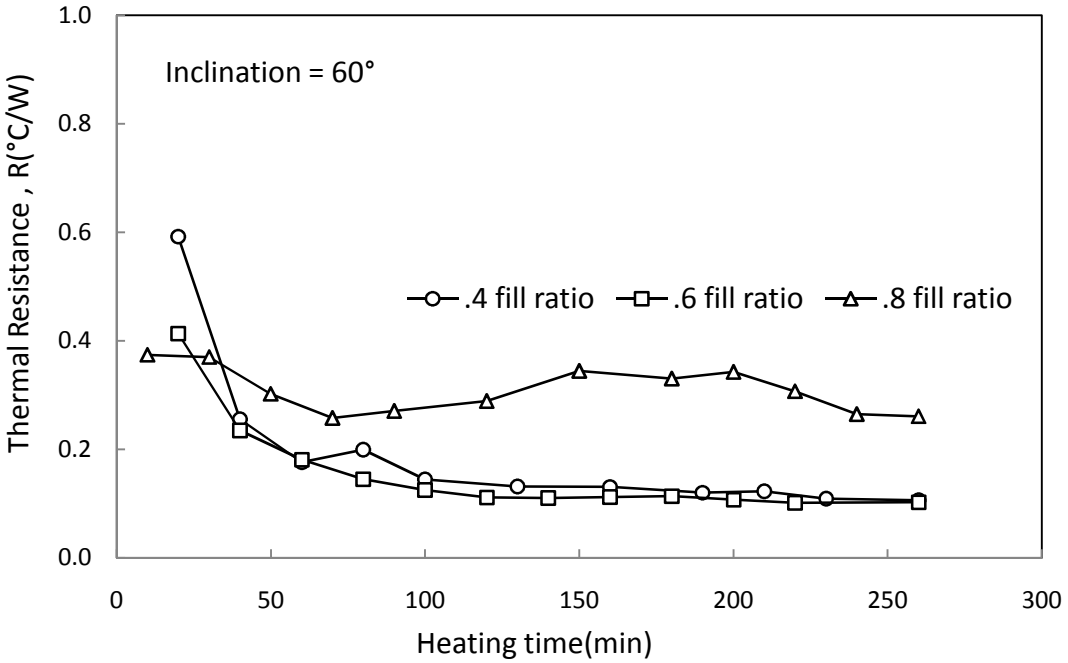

Figure 4.4.7: Change in thermal resistance R(°C/W) with time in CLPHP for different fill ratio at inclination = 60°.

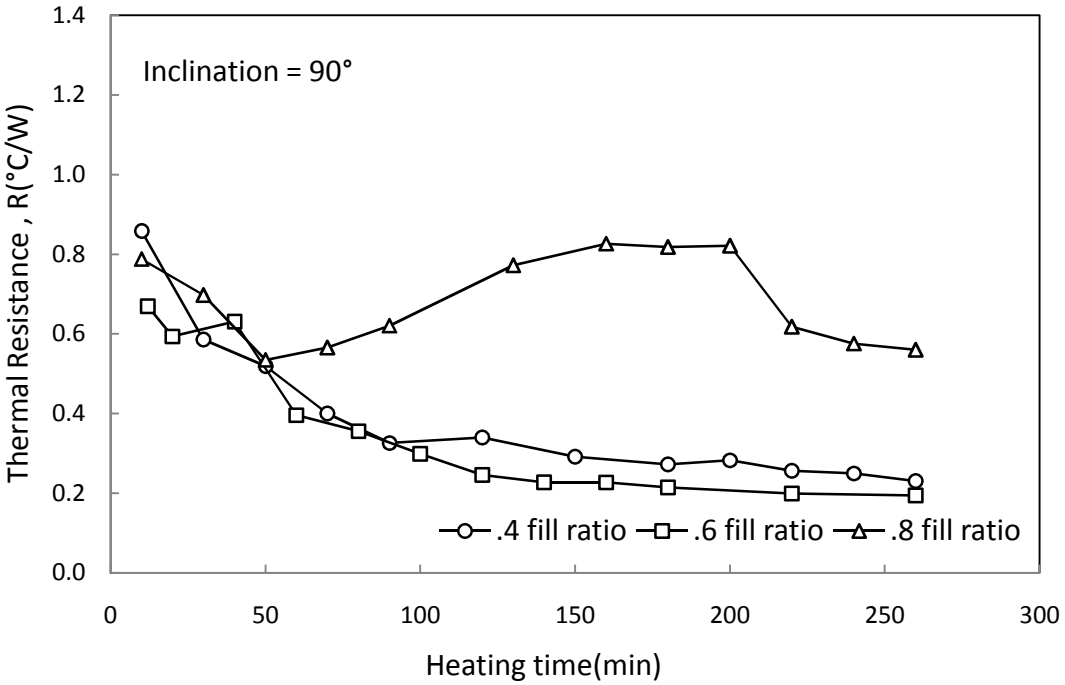

Figure 4.4.8: Change in thermal resistance, R(°C/W) with time in CLPHP for different fill ratio at inclination = 90° (Horizontal position).

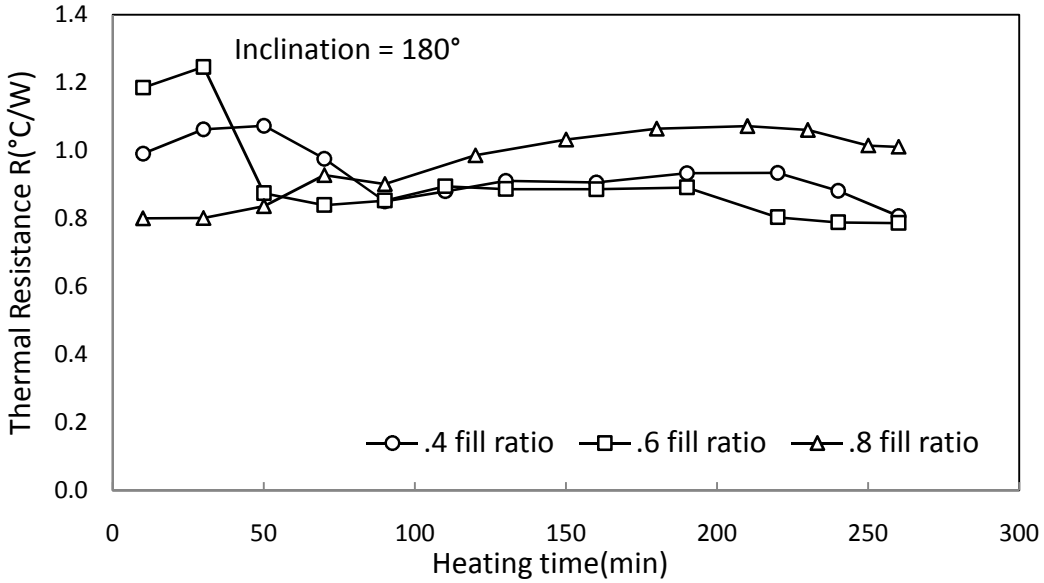

Figure 4.4.9: Change in thermal resistance, R(°C/W) with time in CLPHP for different fill ratio at inclination = 180° (Heat source above the heat sink) .

Fig 4.4.4 to 4.4.9 above shows that the rate of decrease of thermal resistance of fill ratio 0.4 and 0.6 follows similar trend at all inclination but the rate of decrease is

much lower for fill ratio 0.8 at inclination 0°,30°,45°,60°.Fig 4.4.9 shows that the thermal resistance to heat flow increase with heating time at inclination 180°.

Change in thermal resistance, R(°C/W) with fill ratio(V/Vmax) at different inclination of CLPHP are compared in fig 4.4.10.

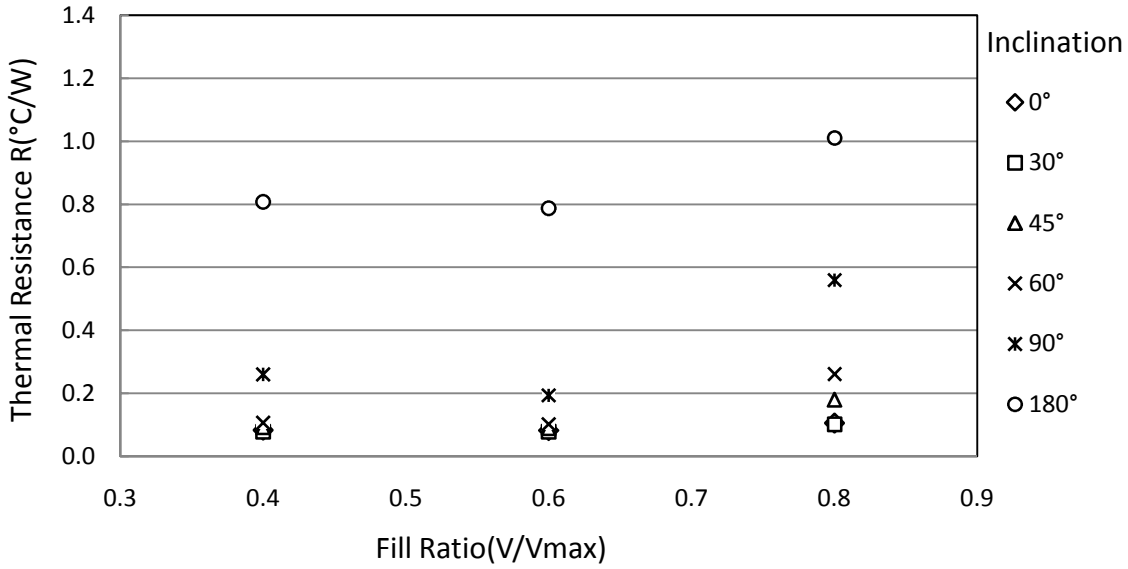

Figure 4.4.10: Effect of fill ratio(V/Vmax) on thermal resistance, R(°C/W) in CLPHP at different inclination .

From the fig above it is clear that thermal resistance for fill ratio 0.4 and 0.6 is approximately same at inclination below 90°. At fill ratio 0.8 this value is not same but very close to each other. Thermal resistance, R is much higher at fill ratio 0.4 , 0.6 and 0.8 for inclination 90° and above. At fill ratio 0.8 and inclination thermal resistance is the highest.

CLPHP is tested at six different inclination. Thermal resistance, R(°C/W) at different inclination for different fill ratio(V/Vmax) of CLPHP are compared in fig 4.4.11.

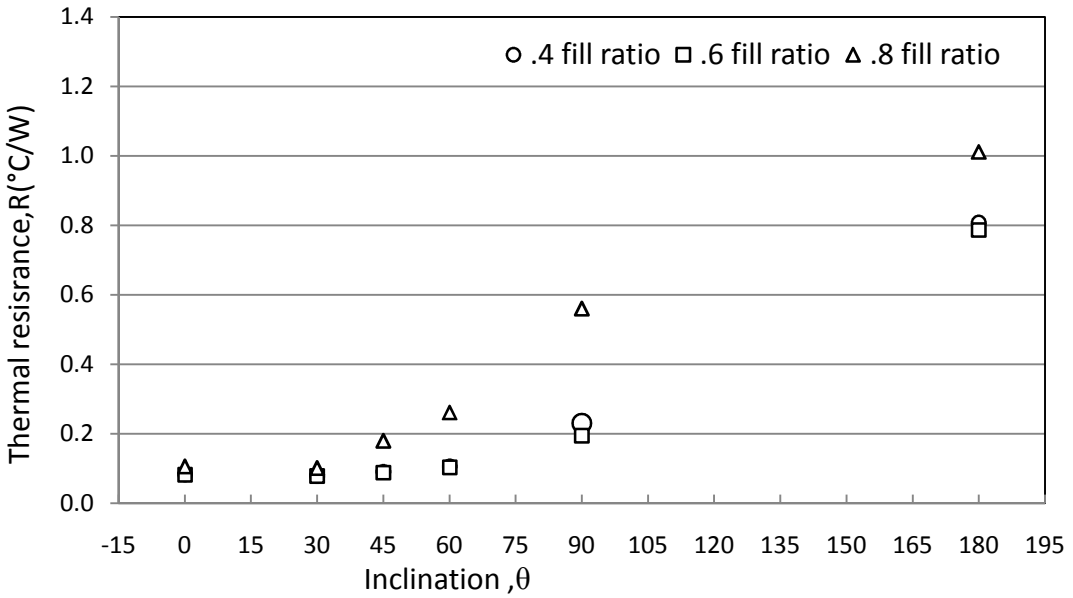

Figure 4.4.11: Effect of inclination ,θ on thermal resistance of CLPHP for different fill ratio at constant heat input.

From figure 4.4.11 it is evident that thermal resistance is minimum for an inclination of 0° and 30° when ammonia is used as working fluid. But as the inclination goes on increasing , thermal resistance to heat flow increase. At $30°<\theta<90°$ this thermal resistance increased gradually but at $90°\leq\theta\leq180°$ this thermal resistance increases more rapidly. At 180° inclination this resistance is maximum. At this position the lower portion(condenser) of PHP is occupied with liquid ammonia and the upper portion (evaporator) is occupied with ammonia vapor.

4.5 Internal Pressure of CLPHP

The pressure developed in the PHP is measured by a pressure gauge attached with the PHP. Figure 4.5.1 to 4.5.9 shows the effect of heat input on the pressure of working fluid though this pressure is not uniform throughout the PHP.

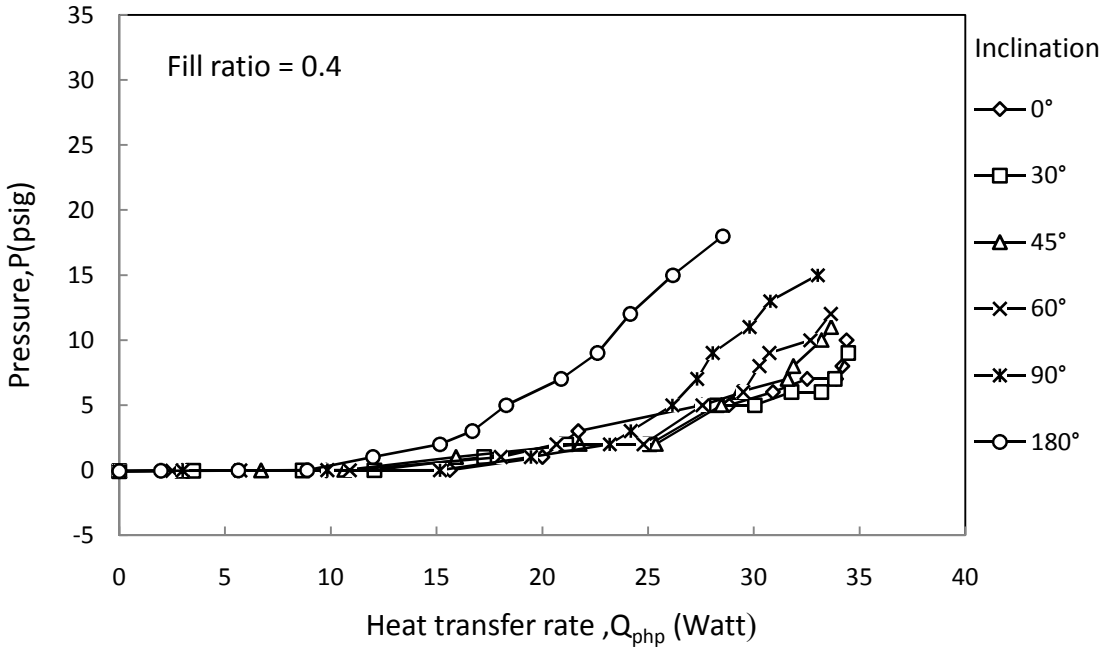

Figure 4.5.1: Change in pressre,P with Heat transfer rate ,Q_{php} (Watt)in CLPHP at different inclination for fill ratio = 0.4.

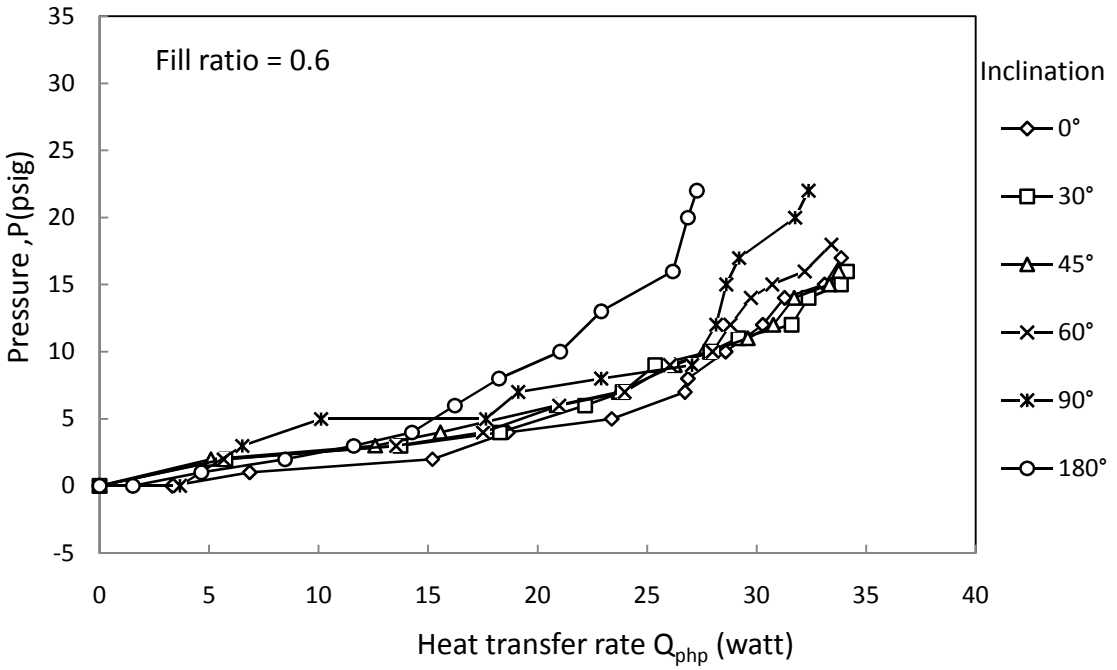

Figure 4.5.2: Change in pressre,P with Heattransfer rate ,Q_{php} (Watt) in CLPHP at different inclination for fill ratio = 0.6.

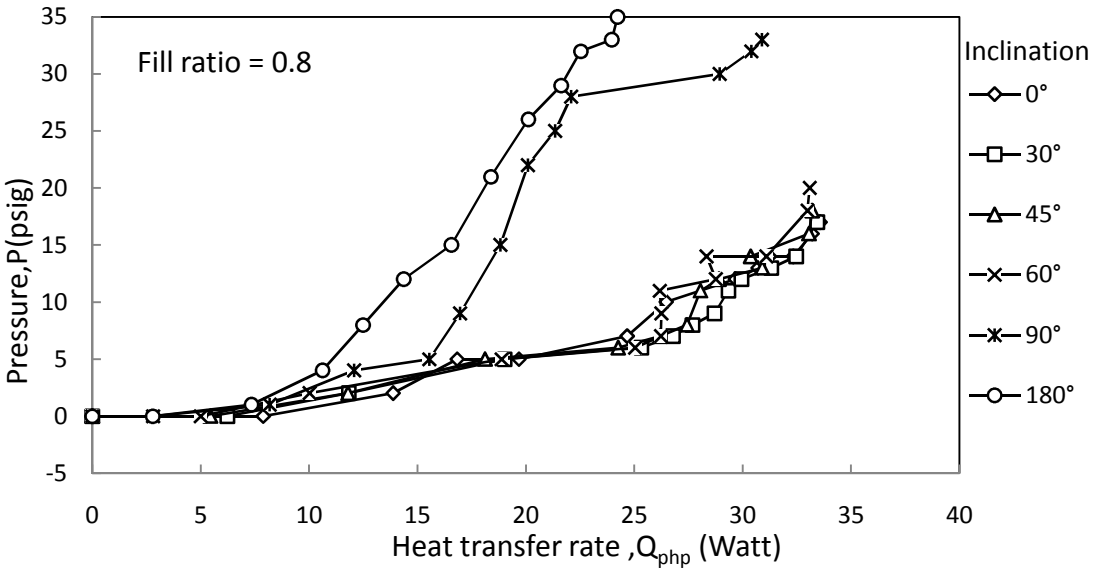

Figure 4.5.3: Change in pressre,P with Heattransfer rate ,Q_{php} (Watt) in CLPHP at different inclination for fill ratio = 0.8.

Fig 4.5.1- 4.5.3 shows that for a particular fill ratio with the increase of heat input the pressure increases and for inclination more than 90° this pressure increase more rapidly. For fill ratio 0.4 and inclination 90°, pressure increases up to 15 psig and for fill ratio 0.6 and inclination 90°, pressure increases up to 22psig, but for fill ratio 0.8 and inclination 90° pressure increases drastically up to 35 psig. So, working with higher fill ratio needs sturdy structure with delicate sealing.

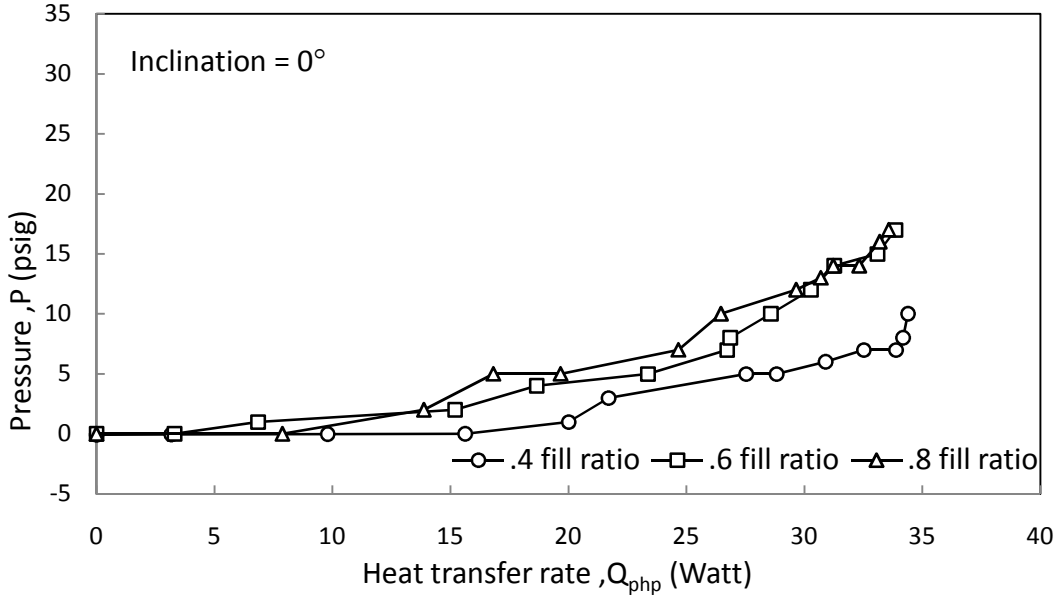

Figure 4.5.4: Effect of Heat transfer rate ,Q_{php} (Watt) on internal pressure of CLPHP for different fill ratio at inclination = 0° (vertical position) and constant heat input.

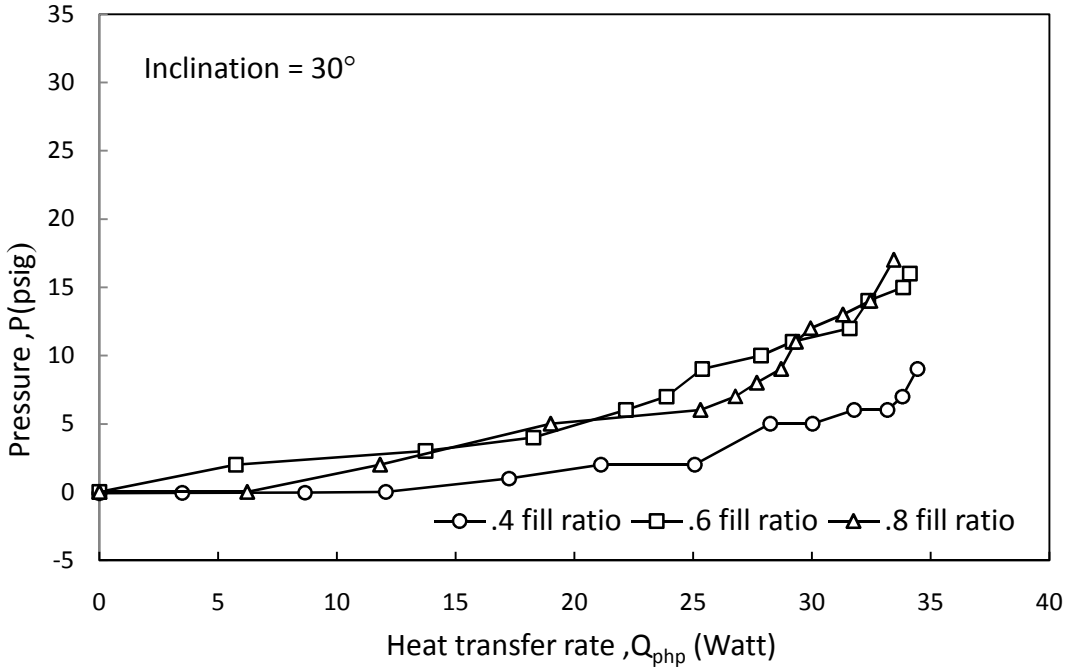

Figure 4.5.5: Effect of Heat transfer rate ,Q_{php} (Watt) on internal pressure of CLPHP for different fill ratio at inclination = 30° and constant heat input.

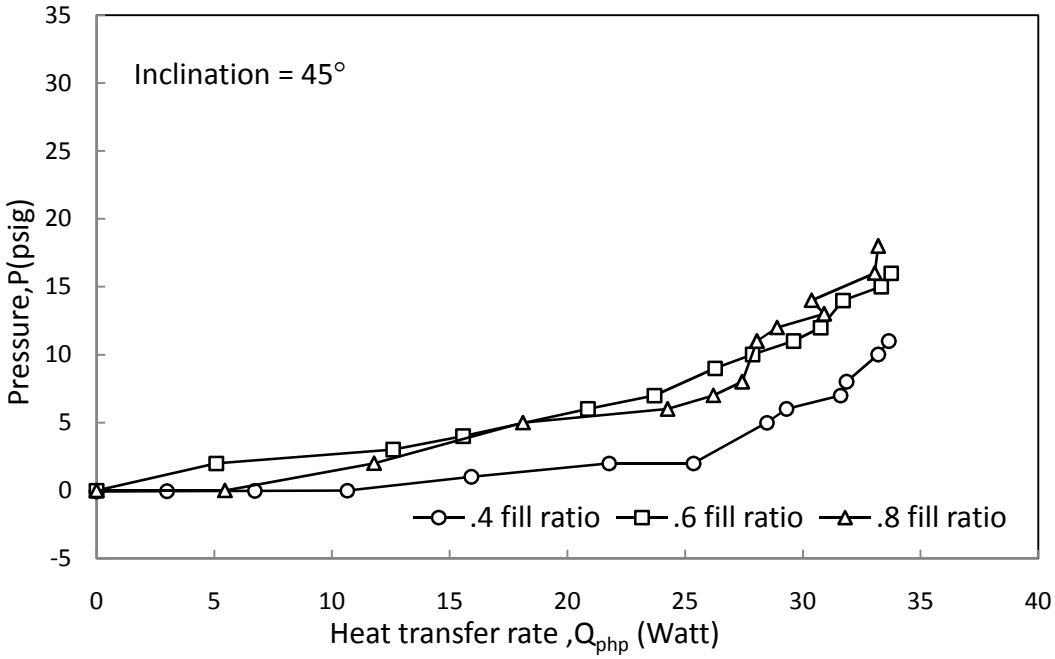

Figure 4.5.6: Effect of Heat transfer rate ,Q_{php} (Watt) on internal pressure of CLPHP for different fill ratio at inclination = 45°and constant heat input.

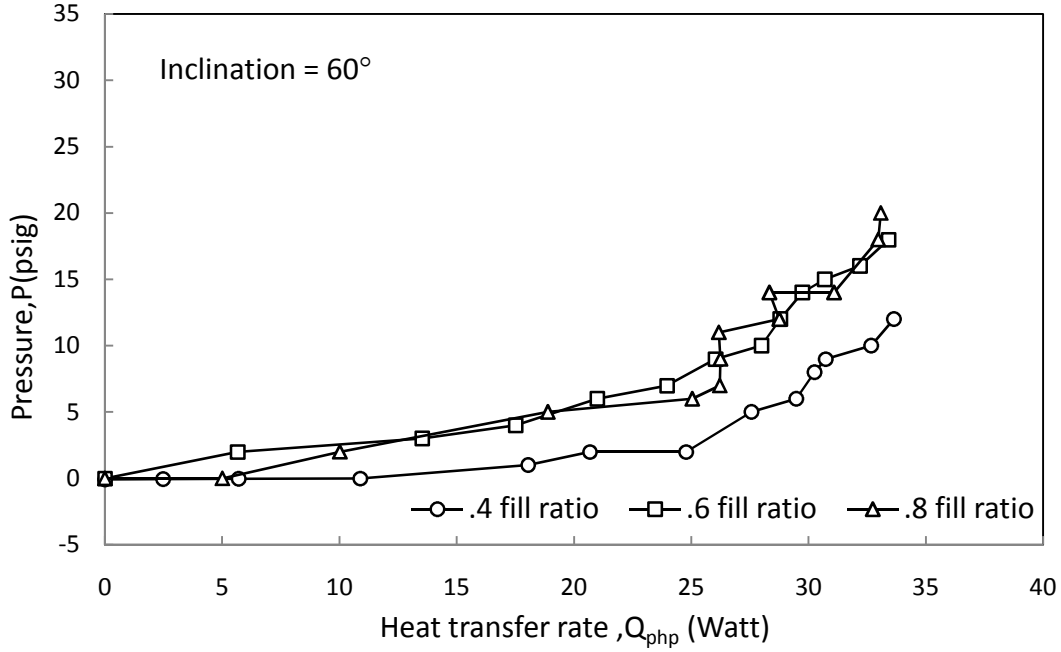

Figure 4.5.7: Effect of heat transfer rate, Q_{php} (watt) on internal pressure of CLPHP for different fill ratio at inclination = 60° and constant heat input.

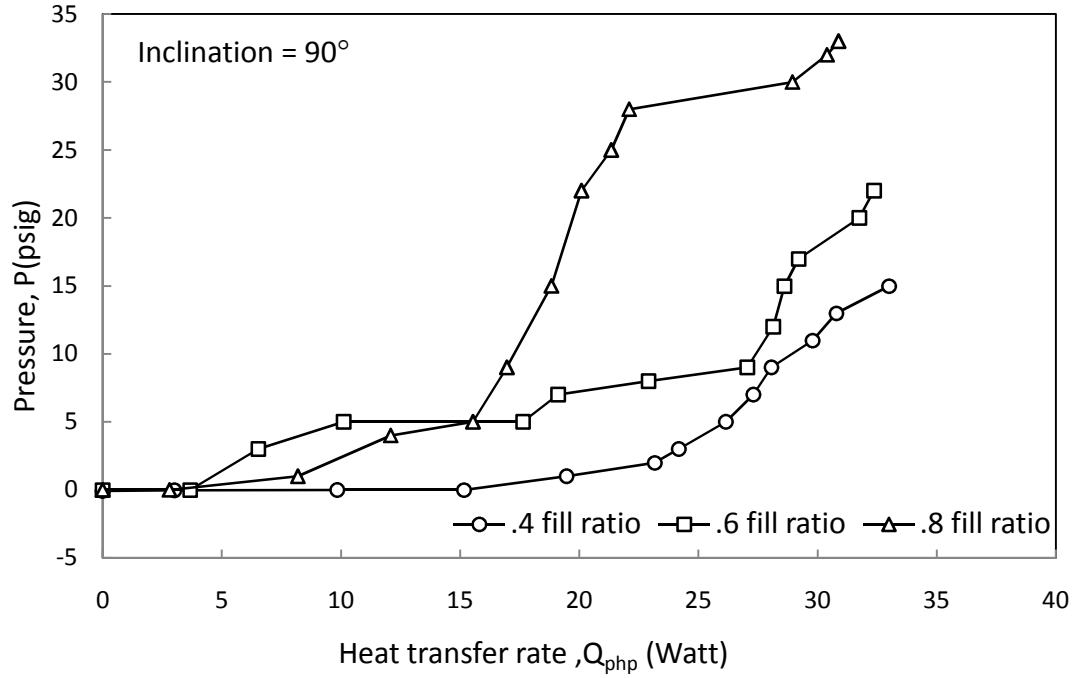

Figure 4.5.8: Effect of Heat transfer rate ,Q_{php} (Watt) on internal pressure of CLPHP for different fill ratio at inclination = 90° (horizontal position) and constant heat input.

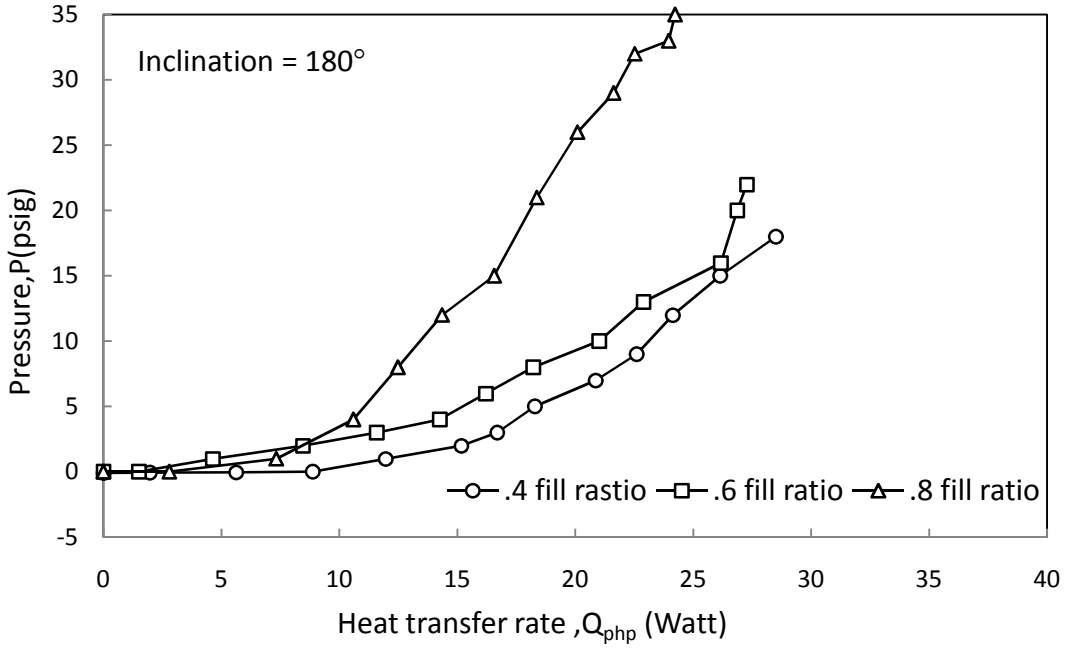

Figure 4.5.9: Effect of Heat transfer rate ,Q_{php} (Watt) on internal pressure of CLPHP for different fill ratio at inclination = 180° (Heat source above the heat sink) and constant heat input.

Fig 4.11.4 to 4.11.9 depict the effect of inclination on the pressure developed in CLPHP. There is no significant change in pressure for different fill ratio below inclination 60°. But with the increase of inclination beyond 90° the pressure increases significantly. For fill ratio 0.8 and inclination 180° pressure increases upto 35 psig.

4.6 Relation between Heat transfer rate by the working fluid, Q_{php} and Heat Transferred to Surrounding by the condenser.

Fig 4.12.1 to fig 4.12.9 shows relation between heat absorbed by evaporator and transferred to atmosphere at different inclination angle and fill ratio. At .4 and .6 fill ratio for inclination angle below 90° the relation is smooth. Qcon (Watt) is lower than Q_{php} (Watt) .This is due to thermal resistance of CLPHP, heat loss through insulator and air flow through laboratory. At all fill ratio for inclination ≥90°(Fig 4.12.1 to 4.12.3) and at fill ratio 0.8 for all inclinations (Fig 4.12.4 4.12.9) the difference between Q_{php} and Q_{con} is higher because of increased thermal resistance of CLPHP at these conditions.

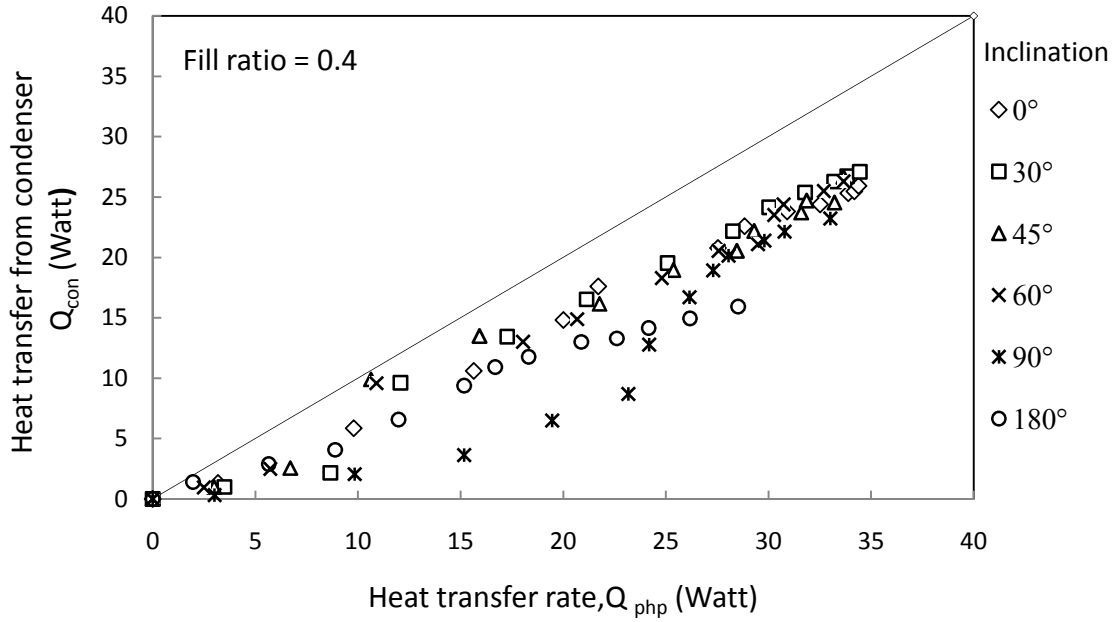

Figure 4.6.1: Comparison of heat transfer rate Q_{php} as calculated from electrical power input and Q_{con} as calculated from heat transfer to the environment(natural convection) for different inclination at fill ratio = 0.4

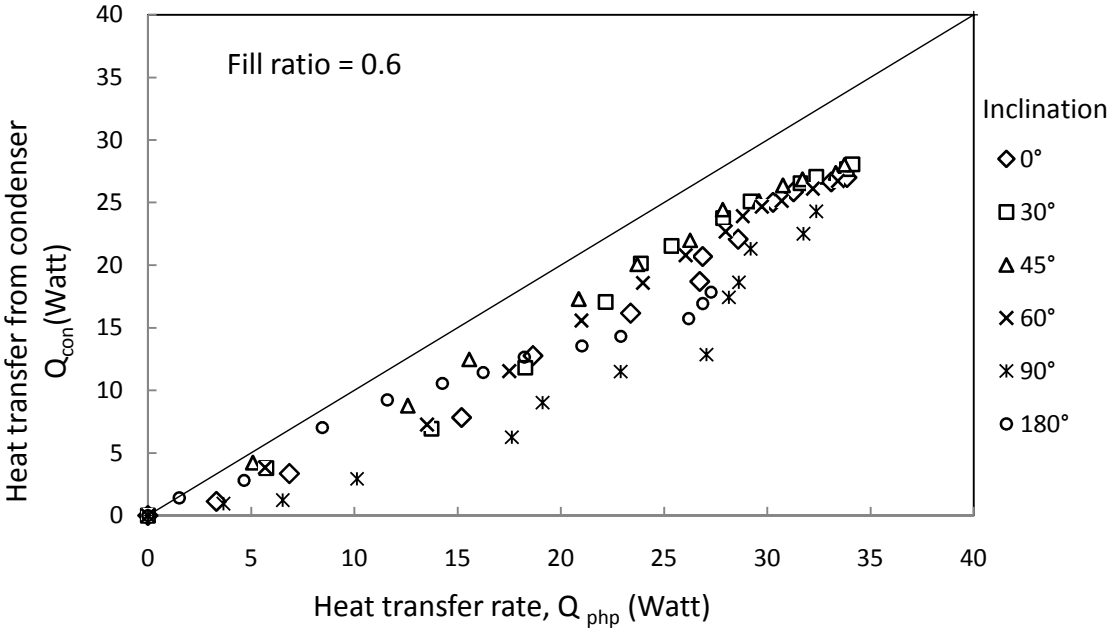

Figure 4.6.2: Comparison of heat transfer rate Q_{php} as calculated from electrical power input and Q_{con} as calculated from heat transfer to the environment(natural convection) for different inclination at fill ratio = 0.6

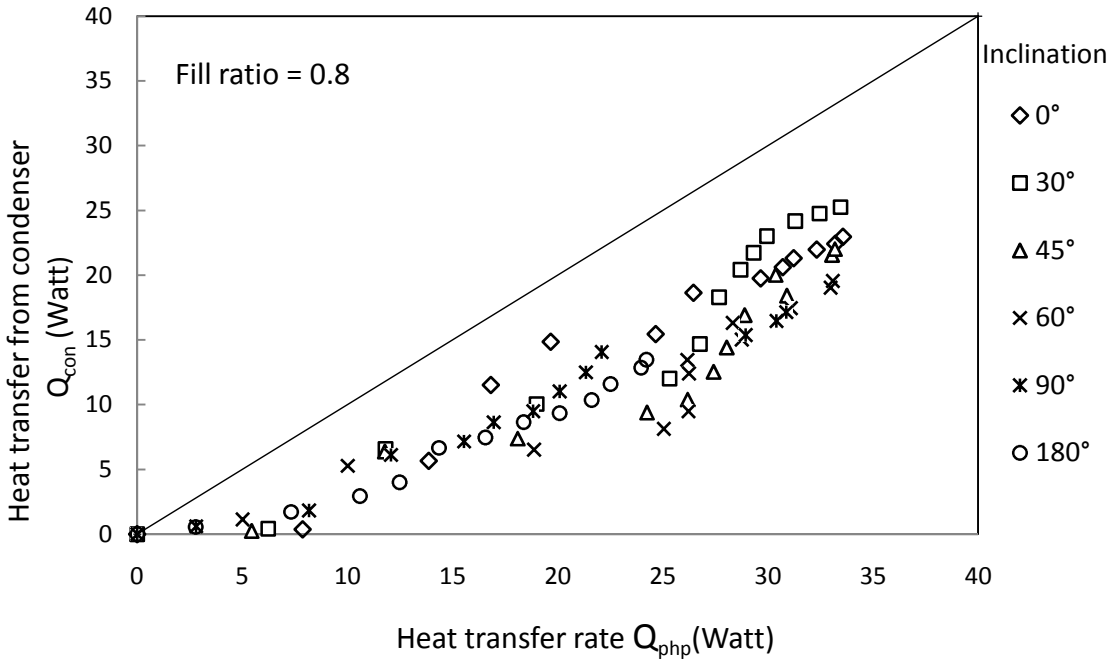

Figure 4.6.3: Comparison of heat transfer rate Q_{php} as calculated from electrical power input and Q_{con} as calculated from heat transfer to the environment(natural convection) for different inclination at fill ratio = 0.8

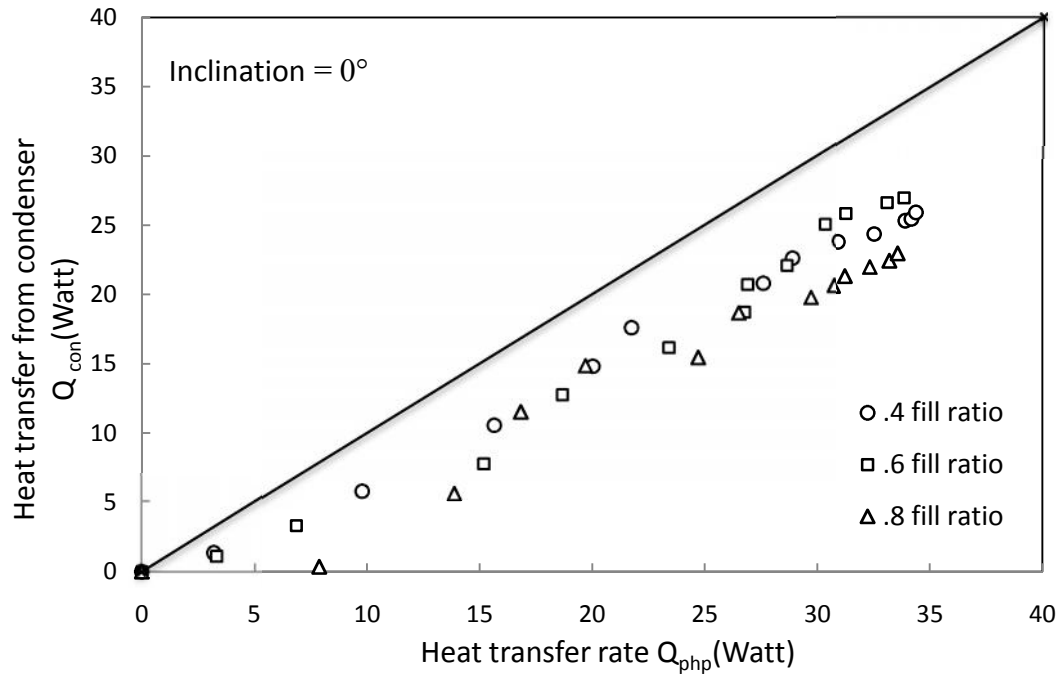

Figure 4.6.4: Comparison of heat transfer rate Q_{php} as calculated from electrical power input and Q_{con} as calculated from heat transfer to the environment(natural convection) for different fill ratio at inclination = 0°

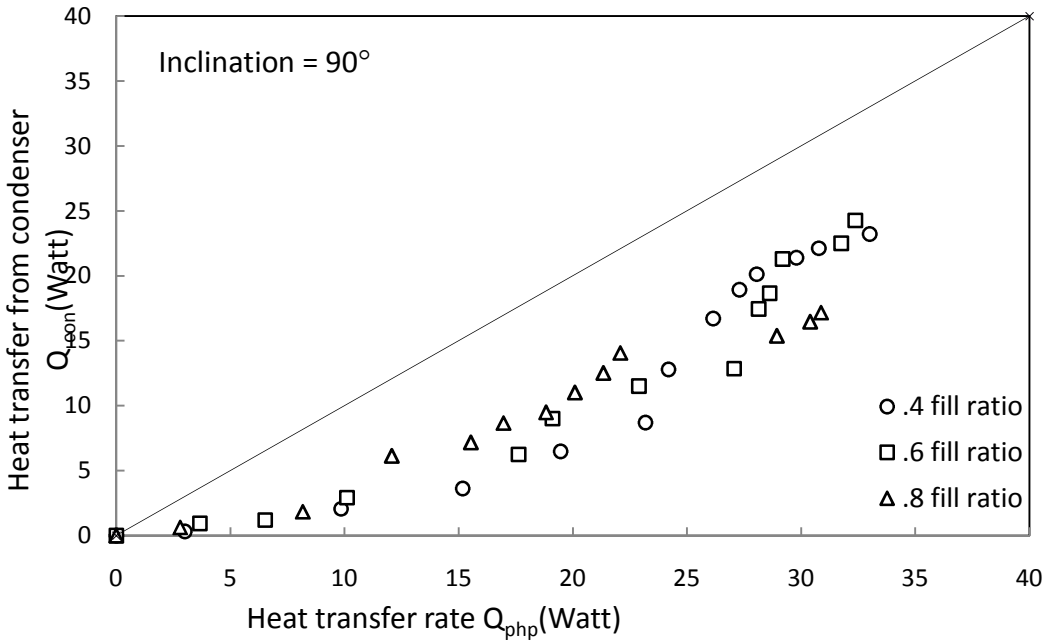

Figure 4.6.5: Comparison of heat transfer rate Q_{php} as calculated from electrical power input and Q_{con} as calculated from heat transfer to the environment(natural convection) for different fill ratio at inclination = 90°

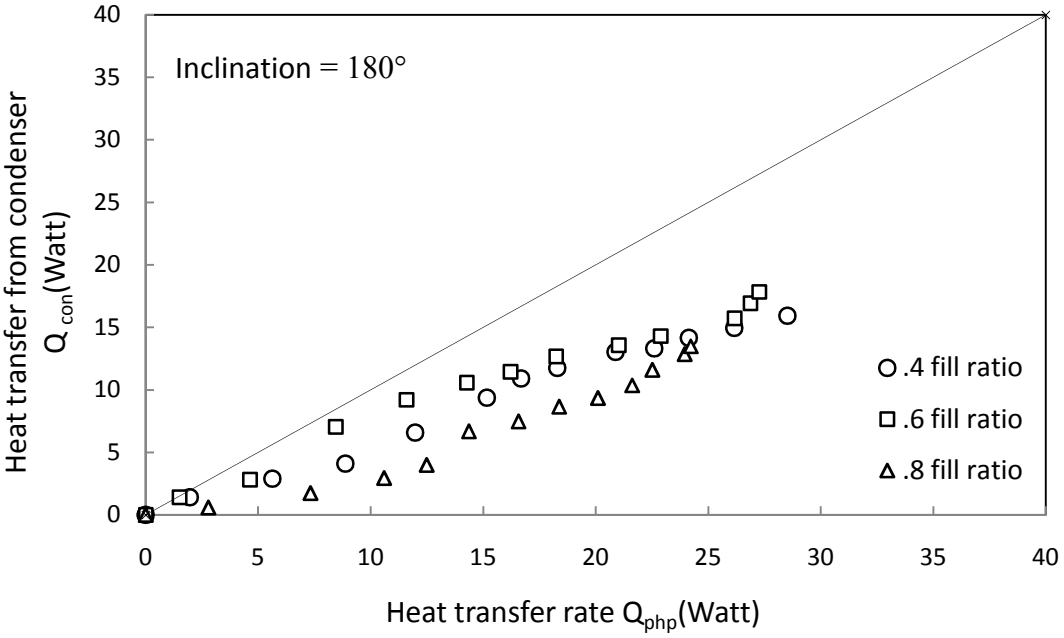

Figure 4.6.6: Comparison of heat transfer rate Q_{php} as calculated from electrical power input and Q_{con} as calculated from heat transfer to the environment (natural convection) for different fill ratio at inclination =180°

4.7 Comperison of Experimental result with other results

Fig 3 and 4 shows the change in thermal resistance with heat input in different experiment.

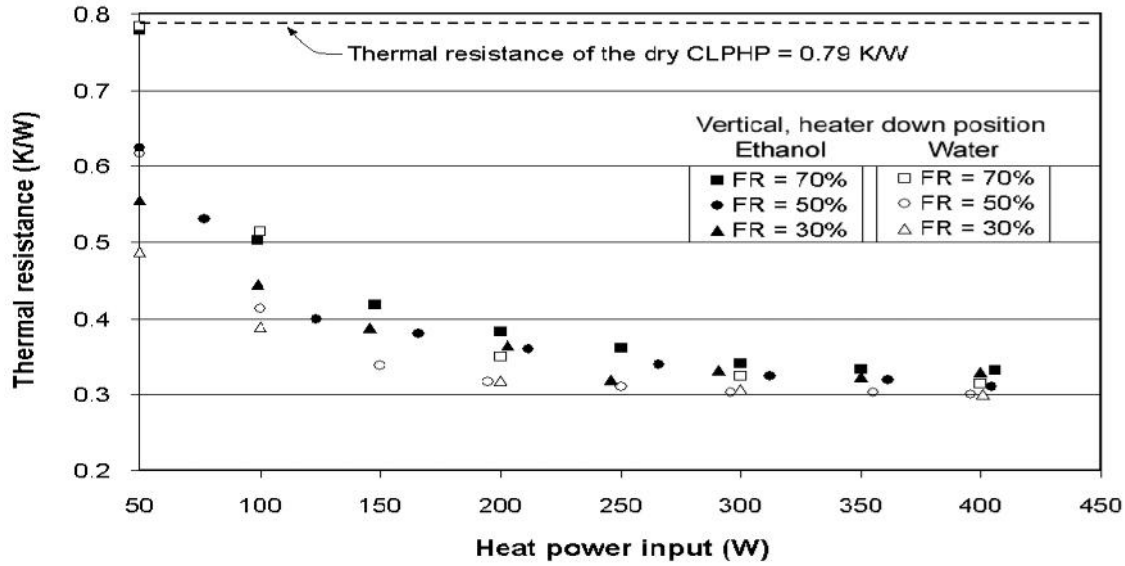

Fig 4.7.1 Change in thermal resistance with heat input in Copper CLPHP shown by Sameer Khandaker

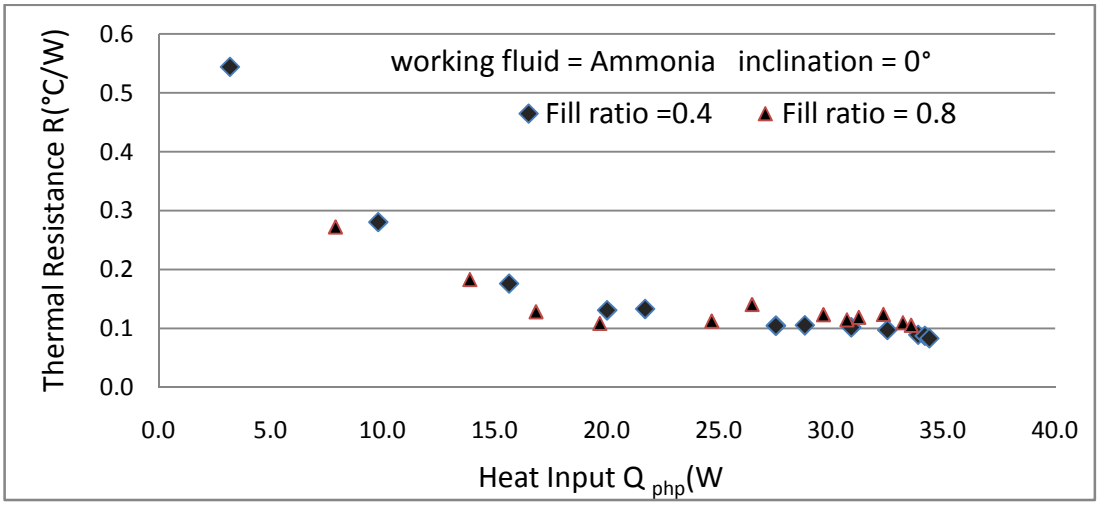

Fig 4.7.2 Change in thermal resistance with heat input in Aluminium CLPHP for different fill ratios described in this paper.

It is also observed from fig 4.7.2 that thermal resistance decrease with increase in heat input for all fill ratios It is also observed from fig 4.7.1 above that thermal resistance of PHP decrease with increase in heat input for different fill ratio.It is also observed that thermal resistance is comparatively low in case of Ammonia charged Aluminium CLPHP.

Fig. 6 and 7 below shows change in heat transfer rate with fill ratio in different experiment.

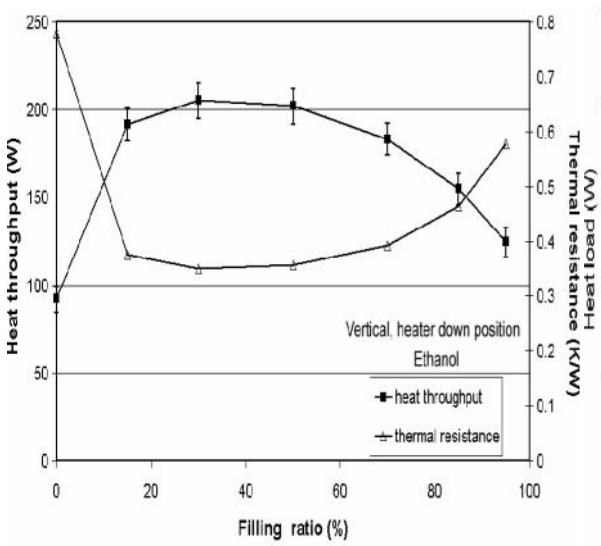

Fig 4.7.3(a) Change in Heat throughput And thermal resistance with Fill ratio in Cupper CLPHP charged with Ethanol shown by Sameer Khandaker

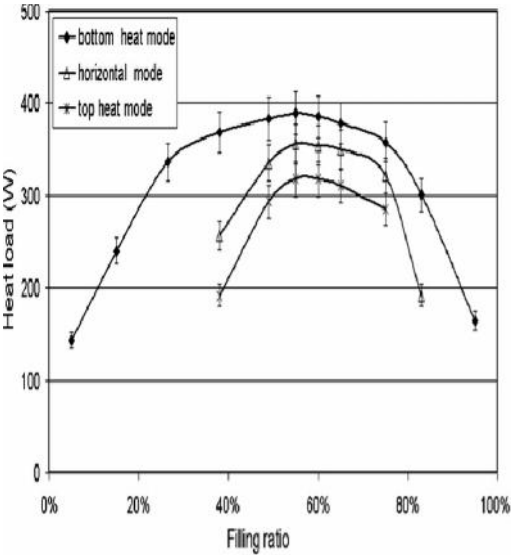

(b) Variation of heat load for Te=110 °C with respect to filling ratio of ethanol charged Cupper PHP (2×2 mm^2)shown by H. Yang and S. Khandekar.

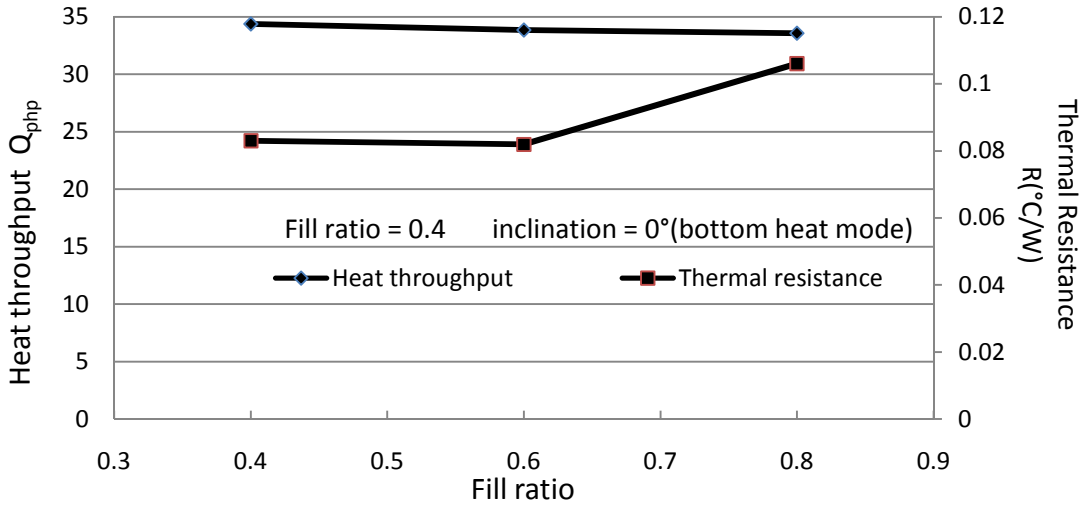

Fig 4.7.4 Change in heat throughput and thermal resistance with Fill ratio in Aluminium CLPHP charged with ammonia.

In the experiment heat throughput is in the chronological order of 0.4 , 0.6 and 0.8 shown in fig 4.7.4 above. It is observed from S. Khandaker erxperiment that fill ratio 0.4 has higher Heat through put than fill ratio 0.6 shown in fig 4.7.3(a) and from H. Yang and S. Khandekar that fill ratio 0.4 has lower heat through put than fill ratio 0.6 shown in fig 4.7.3(b).Here the variation of heat input for fill ratio 0.4 and 0.6

varies due to the variation of cross section of tubes but in both the cases fill ratio 0.8 has lower heat throughput than fill ratio 0.4 and 0.6. Thus the experimental result obtained in this paper is similar to other two experimental results.

4.8 Development of Empirical Correlation

From the analysis of experimental results of closed loop Pulsating Heat Pipe (CLPHP) discussed in this Chapter, the thermal performance of CLPHP depends on various parameters such as heat input, heat transfer coefficient, condenser inclination, evaporator temperature, ambient temperature and fill ratio. In order to correlate the data obtained from the present experimental investigation, some dimensionless group such as heat input ratio, temperature difference ratio, ratio of condenser inclination and fill ratio are proposed. To determine the dependency of overall heat transfer ratio on the other dimensionless groups, the following steps are considers.

4.8.1 Effect of Heat Input

The present experimental investigations were carried out with different heat inputs. From the experimental results, it is found that, with the increase of heat input, the heat transfer rate is increased. For the analysis of heat transfer performance for different heat input, a ratio of heat input to the maximum heat input can be considered as

$$Heat\ Input\ Ratio = \left(\frac{Q}{Q_{\max}} \right)$$

Thus the correlation can be assumed as

$$\frac{U}{U_{\max}} \propto \left(\frac{Q}{Q_{\max}} \right)^{n_1} \quad \text{..... (4.1)}$$

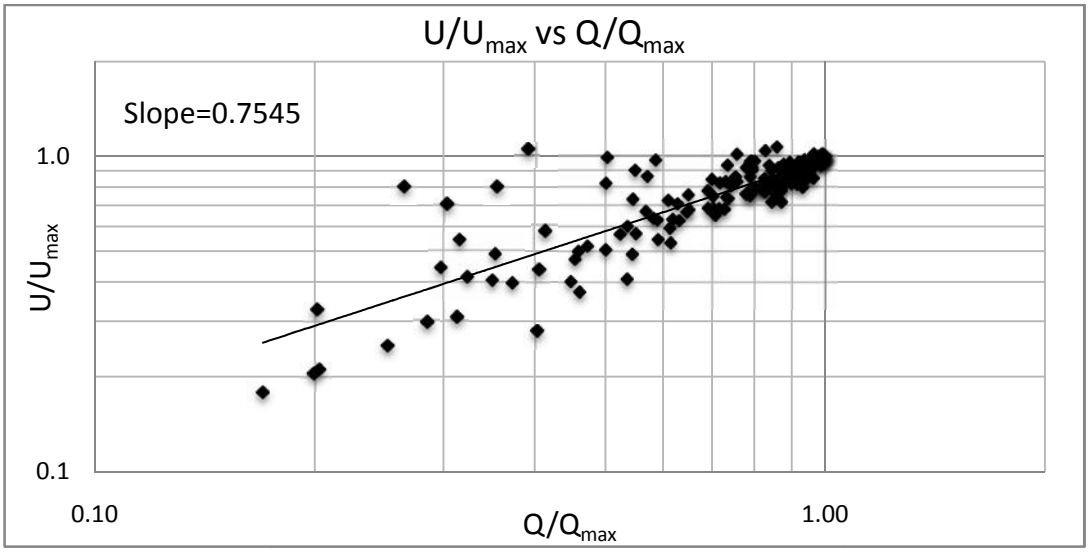

Figure 4.8.1: Determination of exponent 'n_1'

In this case, using conventional techniques, the exponent n_1 was determined by plotting (U/U_{max}) vs. (Q/Q_{max}) from the present experimental data as shown in figure 4.1 and the average of the slope was found $n_1 = 0.7545$. So the correlation became:

$$\frac{U}{U_{max}} \alpha \left(\frac{Q}{Q_{max}}\right)^{.7545} \quad \text{..... .....} \quad (4.2)$$

4.8.2 Effect of Evaporator and Ambient Temperature

In the heat pipes, the heat is transferred by the evaporation and condensation of working fluid from evaporator and condenser section respectively. Heat transfer can be occurred by the convection which is directly depends to the temperature differential of the evaporator and condenser section. From the experimental date, it is evident that, with the increase of temperature differential of evaporator to condenser section, the overall heat transfer coefficient also increases. From this, a dimensionless group can be assumed as following:

$$\text{Ratio of Temperature} = \frac{T_{eva} - Ta}{T_{eva}}$$

This dimensionless parameter also should include the contribution of heat transfer performance of Looped Parallel Micro Heat Pipes (LPMHP). By including this dimensionless group the correlating equation became,

$$\frac{U}{U_{max}} \alpha \left(\frac{Q}{Q_{max}}\right)^{.7545} \left(\frac{T_{eva} - T_a}{T_{eva}}\right)^{n_2} \quad \text{.....} \quad (4.3)$$

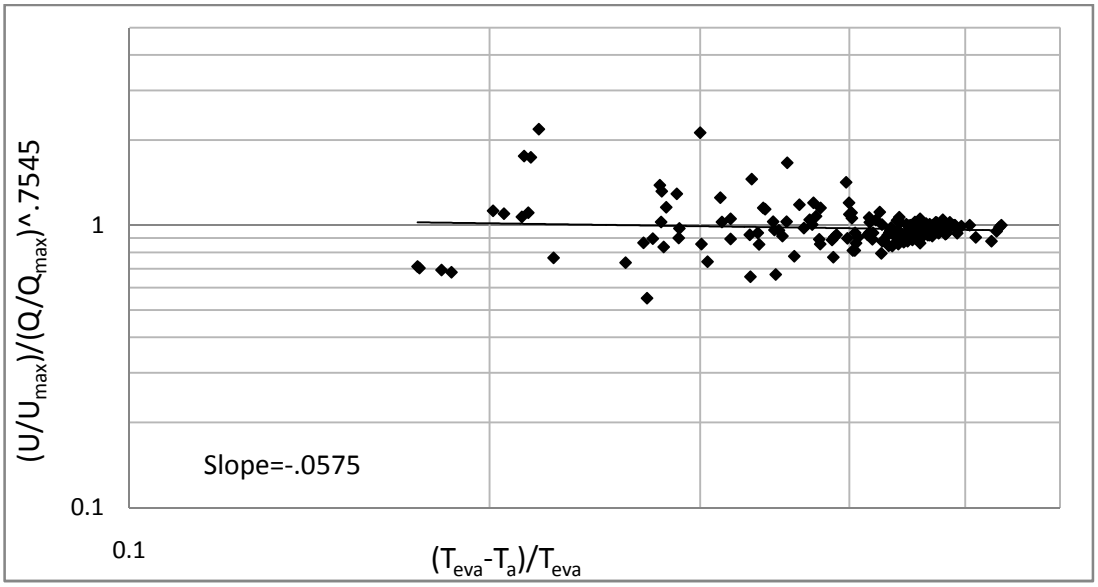

Figure 4.8.2: Determination of exponent 'n_2'

In this case also using conventional techniques, the exponent n_2 of the dimensionless heat transfer ratio was determined by plotting $[U/U_{max}] / [(Q/Q_{max})^{0.7545}]$ vs. $(T_{eva}-T_a)/T_{eva}$) of the present experimental data as shown in figure 4.2. The average value of the exponent was found to be, $n_2 = -.0575$. So the Correlation became:

$$\frac{U}{U_{max}} \alpha \left(\frac{Q}{Q_{max}}\right)^{.7545} \left(\frac{T_{eva}-T_a}{T_{eva}}\right)^{-.0575} \quad \ldots\ldots\ldots\ldots \quad (4.4)$$

4.8.3 Effect of Inclination of CLPHP

In the heat transfer performance of looped parallel micro heat pipe, the condenser inclination has an effect. For considering the effect of condenser inclination at the transport section, a dimensionless group can be assumed as

$$Condenser\ Inclination\ effect = \left(1 + \frac{\theta}{\theta_{max}}\right)$$

Here, θ is the various condenser inclination and θ_{max} is the maximum inclination angle which is at the horizontal position ($\theta_{max} = 90^o$). By including this dimensionless group the correlating equation became,

$$\frac{U}{U_{max}} \alpha \left(\frac{Q}{Q_{max}}\right)^{.7545} \left(\frac{T_{eva}-T_a}{T_{eva}}\right)^{-.0575} \left(\frac{\theta}{\theta_{max}}\right)^{n_3} \quad \ldots\ldots\ldots \quad (4.5)$$

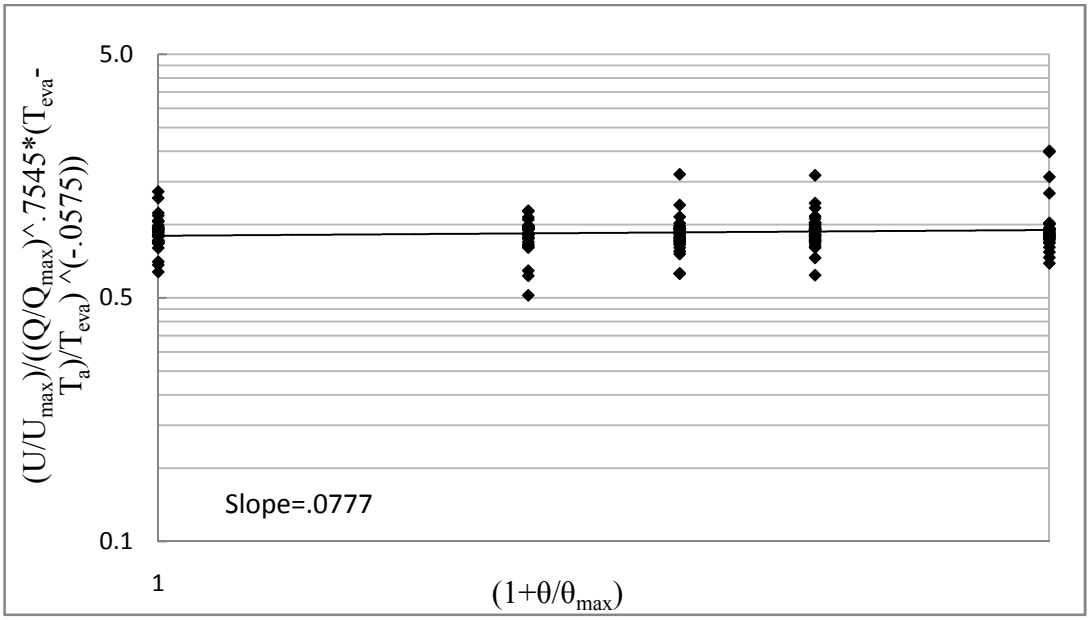

Figure 4.8.3: Determination of exponent 'n_3'

In this case also using conventional techniques, exponent n_3 of the group $(1+\theta/\theta_{max})$ was determined by plotting $[U/U_{max}] / (Q/Q_{max})^{07545}$ X $[(T_{eva}-T_a)/T_{eva})]^{.0575}$vs. $(1+\theta/\theta_{max})$ of the present experimental data as shown in figure 4.3. The average value of the exponent was found to be, $n_3 \approx 0.0777$. So the final Correlation became:

$$\frac{U}{U_{max}} \alpha \left(\frac{Q}{Q_{max}}\right)^{.7545} \left(\frac{T_{eva}-T_a}{T_{eva}}\right)^{-.0575} \left(\frac{\theta}{\theta_{max}}\right)^{.0777} \quad \text{.....(4.6)}$$

4.8.4 Effect of CLPHP Fill Ratio.

The fill ratio V/V_{max} has an effect on the heat transfer performance CLPHP. For considering the effect of fill ratio at the transport section, a dimensionless group can be assumed as V/V_{max}. Here, V is the various fill ratio and V_{max} is the maximum fill ratio in the experiment. By including this dimensionless group the correlating equation became,

$$\frac{U}{U_{max}} \alpha \left(\frac{Q}{Q_{max}}\right)^{.7545} \left(\frac{T_{eva}-T_a}{T_{eva}}\right)^{-.0575} \left(\frac{\theta}{\theta_{max}}\right)^{.0777} \left(\frac{V}{V_{max}}\right)^{n_4} \text{.....4.7}$$

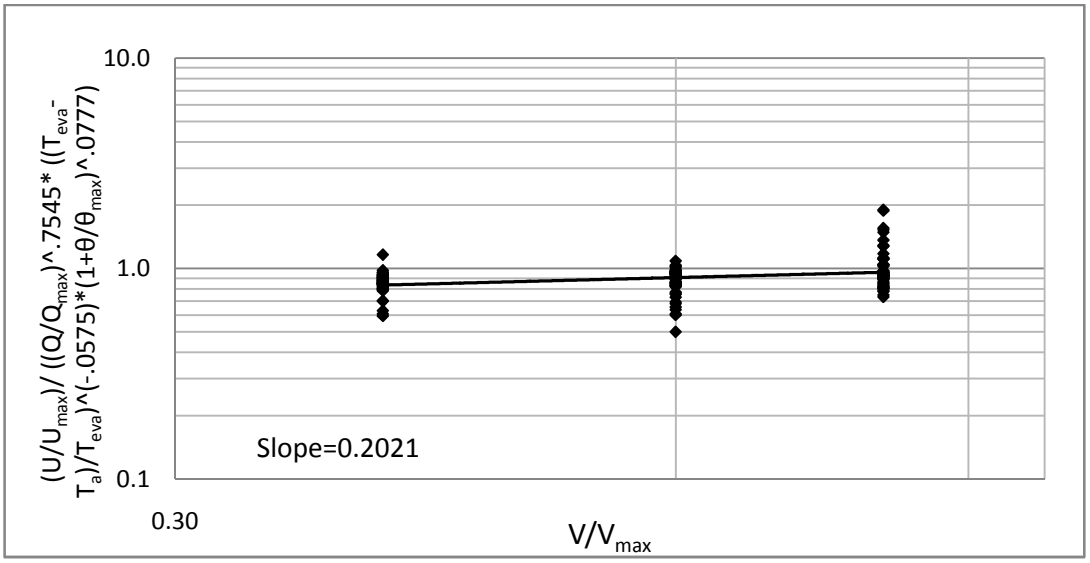

Figure 4.8.4: Determination of exponent 'n_4'

In this case also using conventional techniques, exponent n_4 of the group (V/Vmax) was determined by plotting $(U/U_{max})/[(Q/Q_{max})^{07545}X[(T_{eva}-T_a)/T_{eva})]^{.0575}$ $X(1+\theta/\theta_{max})^{.0777}$ vs (V/V_{max}) of the present experimental data as shown in figure 4.4 The average value of the exponent was found to be, n_4 = 0.2021. So the final Correlation became:

$$\frac{U}{U_{max}}\alpha\left(\frac{Q}{Q_{max}}\right)^{.7545}\left(\frac{T_{eva}-T_a}{T_{eva}}\right)^{-.0575}\left(\frac{\theta}{\theta_{max}}\right)^{.0777}\left(\frac{V}{V_{max}}\right)^{.2021} \quad \text{.....4.8}$$

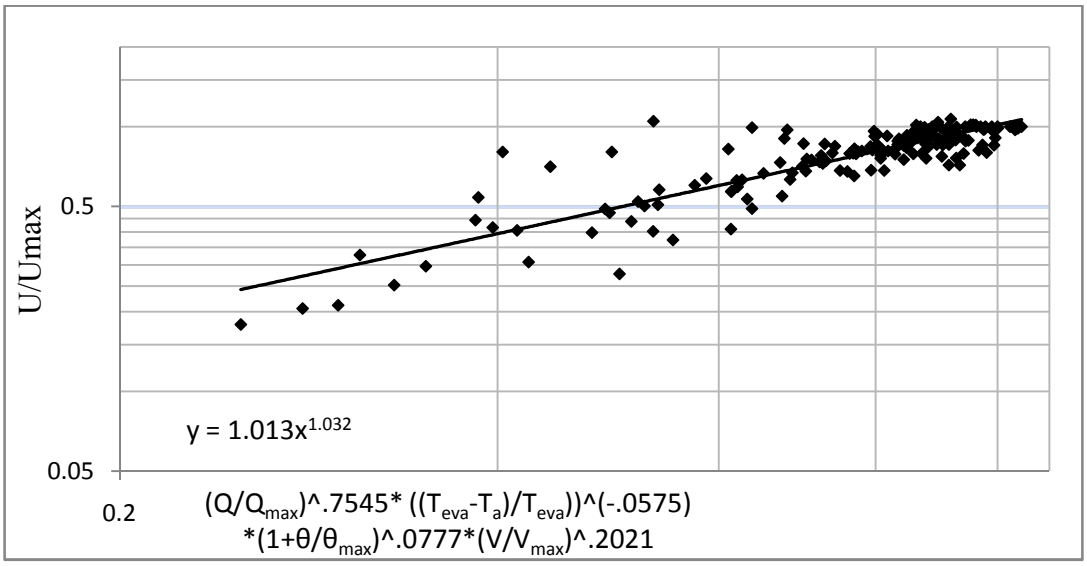

Figure 4.8.5: Graphical representation of correlation for CLPHP.

4.8.5 Proposed Correlation

In this final correlation (equation 5.8), we found that the exponent of [$(T_{eva}-T_a)/T_{eva})^{(-.0575)}$] and $(1+\theta/\theta_{max})$ is very close to zero. In this case, if we neglect these two terms, thus the correlation becomes:

$$\frac{U}{U_{max}} \alpha \left(\frac{Q}{Q_{max}}\right)^{0.7545}\left(\frac{V}{V_{max}}\right)^{0.2021} \quad \text{..... 4.9}$$

Then the graphical representation of the simplified correlations for CLPHP is shown in figure 4.6. The complete correlation for pulsating heat pipe is given by the following equation:

$$\frac{U}{U_{max}} = 1.085\left(\frac{Q}{Q_{max}}\right)^{0.7545}\left(\frac{V}{V_{max}}\right)^{0.2021} \quad \text{.....4.10}$$

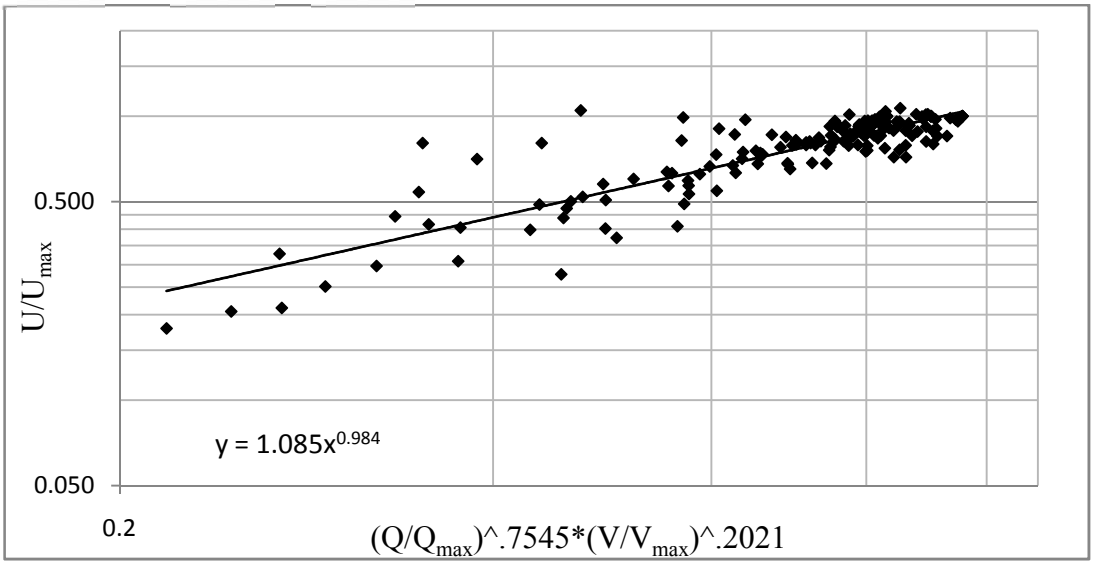

Figure 4.8.6: Proposed Correlation

4.9 Proposed Applications for Pulsating Heat Pipes

Thermal conductivity (k_{Al}) and convective heat transfer coefficient (h_{Al}) of Aluminium is 250 W/m°C and 25 W/m² °C respectively. But we have got the overall heat transfer coefficient of CLPHP (U) within the range of 615 to 830 W/m²-°C for fill ratio 0.4 and 0.6 at inclination below 90°.For fill ratio 0.8 this value is within 250 to 615 W/m² °C at inclination below 90°.At inclination above 90° this value is within 116 to 335 W/m² °C which is still much higher than conductive and convective heat transfer coefficient of Aluminium. The value of overall heat transfer coefficient is 64 W/m² °C which is the lowest of all. Since the overall heat transfer coefficient for PHP is much higher for inclination below 90° at fill ratio 0.4 and 0.6 hence it can be used efficiently in small equipments where space is not sufficient to install conventional heat exchanger.

Chapter 5

Conclusions and Recommendations

5.1 Conclusions

The present study shows an experimental investigation on thermal analysis of a Closed Loop Pulsating Heat Pipe. Tests are performed for ammonia as working fluids at ˚ inclination 0 (vertical), 30˚, 45˚, 60˚, 90˚ (horizontal) and 180˚ (Heat source above the heat sink) in natural cooling modes. temperature of evaporation, condensation and adiabatic section are measure. With these data heat transfer rate, overall heat transfer coefficient, thermal resistance and inside pressure are calculated to compare the performance of the heat pipe for different conditions. The conclusions that could be taken from this investigation are as follows:

(a) At the beginning the oscillation of working fluid inside the tube are abrupt and there is no specific circulation direction in the tube loop. Increase in heating power results in stable oscillations. A further increase in heat input increase the circulation velocity which ultimately enhance heat transfer rate. Eventually the fluid oscillation in alternate tubes come in phase with others and thus heat transfer rate gradually increase.

(b) The pulsating motion of working fluid and vapor inside the tube is responsible for transferring heat from the evaporator to the condenser. At low heat flux the number and size of bubbles produced by the working fluid is small and few which is sufficient enough to carry the heat from the evaporator section to the condenser section but with the increase of heat input more and larger bubbles are required to carry the heat to condenser section which could not be produced in fill ratio 0.8 due to lack of available space. Hence heat transfer at fill ratio 0.8 is lower than fill ratio 0.4 and 0.6.

(c) Time required to reach steady state is nearly same for 0.4 and 0.6 fill ratios but it increases for 0.8 fill ratio because of shortage of sufficient space for producing

bubbles to transmit the heat to the condenser. There is no significant change of the time required to reach steady state with the change of inclination from vertical (0˚ inclination) upto horizontal (90˚ inclination) but from 90˚ to 180˚ inclination time require to reach steady state is more due to shortage of sufficient liquid to produce bubble in the evaporator section which is actually responsible to carry heat to the condenser section. For all fill ratios heat transfer rate for inclination 0˚and 30˚ is higher than other inclination because at this angle bubble face less resistance to flow upward to the condenser section.

(d) 0° and 30˚ inclination gives better overall heat transfer coefficient than other setup orientations. After 0˚ and 30˚ with the increase of inclination overall heat transfer coefficient decrease and at 90° inclination the value is lower because at this stage the bubble do not get enough bouncy force to move up and transfer the heat to condenser section.

(e) At 180° inclination evaporator section is above the condenser section. Ammonia vapor is trapped in the evaporator section and evaporator section of PHP does not get enough liquid to produce bubble which is responsible to transfer heat from the evaporator to the condenser. Heat generated in evaporator section is trapped in vapor which could not be circulated due to absent of circulation of the working fluid. Thus temperature and pressure in the evaporator section increase rapidly.

(f) Thermal resistance of PHP for fill ratio 0.8 is higher than fill ratio 0.4 and 0.6. With the increase of heat input thermal resistance of PHP for fill ratio 0.8 decreases slowly than fill ratio 0.4 and 0.6 . At inclination 90˚and 180° the rate of decrease of thermal resistance is low than any other inclination and at inclination 180˚and fill ratio 0.8 thermal resistance of PHP increase rather than decrease with the increase of heat input.

(g) The pressure of ammonia-charged PHP increases linearly with temperature below inclination 90˚. This increase in pressure is low for lower fill ratio. For high fill ratio pressure is also higher for a constant heat input. For fill ratio 0.8 pressure increases rapidly at inclinations 90˚ to 180˚ because at these inclinations the vapor is

trapped in the evaporator section and temperature of working fluid vapor increases more rapidly raising its volume and ultimately the pressure inside the PHP increases.

5.2 Recommendations

Although the information gained from the experimental work has been sufficient to cover the objectives of the thesis proposal, but a certain number of problems also require further attention. These are given below:

(a) Detailed flow visualization is required to improve basic understanding of the fluid flow and heat transfer process in the device.

(b) For precise temperature reading, data logger should be used.

(c) The investigation can be further carried out by varying the length of evaporator, condenser and transition section to determine the optimum size of the CLPHP

(d) The entire investigation can also be repeated by changing the cooling condition such as forced convection at the condenser section. Air velocity could be varied to test the thermal performance and also water cooling could be incorporated for comparing heat transfer performance between air and water cooling of heat pipe.

(e) CLPHP of different hydraulic diameters can also be investigated and the effects of hydraulic diameter variation on thermal performance can be included in the correlation.

(f) Performance of CLPHP can be invested by changing the no of turns.

(g) Numerical analysis of the results of CLPHP at different inclination, fill ratio and working fluid can also be performed to correlate experimental results of this study.

REFERENCES

1. Azar K., "The histry of power Dissipation", Electronic cooling , Vol. 6, No. 1, 2000.

2. Cao, Y.and Gao, M. "Wickless network heat pipes for high heat flux spreading applications", International Journal of Heat and Mass transfer, Vol. 45, pp. 2539-2547, 2002.

3. Lin, S., Sefiane K. and Christy J., "Prospects of Confined Flow Boiling in Thermal Management of Microsystems", Applied Thermal Engg. Vol. 22, pp. 825-837, 2002.

4. Khandekar, S., Groll, M., Charoensawan, P., Rittidech S. and Terdtoon, P., "Closed and Open Loop Pulsating Heat Pipes", Proc. 13th Int. Heat Pipe Conf., Sanghai, Chaina, , pp.1-14 , 2004.

5. Akachi, H. and Polášek, F., "Pulsating Heat Pipes", 5thInt. Heat Pipe Symposium, Melbourne, Australia, 17 - 20 November 1996.

6. Dobson, R. T. and Graf, G., "Thermal Characterisation of an Ammonia-charged Pulsating Heat Pipe", Proc. 7th IHPS. pp.460-466 , 2003

7. Polášek, F. and Zelko M, "Thermal control of electronic components by heat pipes and thermosyphons", A historical overview, Proc. 10 Int. Heat Pipe Conf., Stuttgart, Germany, 21-25 September 1997.

8. Tong, B. Y., Wong, T. N. and Ooi, K. T., " Closed-loop pulsating heat pipe", Applied Thermal Engineering Vol 21, pp 1845 – 1862 , 2001.

9. Dobson, R. T. and Harms, T. M.," Lumped parameter analysis of closed and open oscillatory heat pipes", 11th Int. Heat Pipe Conf. Tokyo, 12-16 September 1999.

10. Wong, T. N., "Theoretical modelling of pulsating heat pipe", 11th Int. Heat Pipe Conf. Tokyo, 12-16 September 1999.

11. Swanepoel, G., Taylor, A. B. and Dobson R. T., " Theoretical modelling of pulsating heat pipes", 6th International Heat Pipe Symposium.Chiang Mai, Thailand, 5 - 9 November 2000.

12. Khandekar, S. and Groll, M., "Pulsating Heat Pipes: Study on a Two-Phase Loop", Proc. 13th Int. Conf. on Thermal Engineering and Thermogrammetry (THERMO), 2003.

13. Shafii, M. B., Faghri, A. and Zhang, Y., "Thermal modelling of Unlooped and looped pulsating heat pipes",Heat Transfer Vol 123, pp.1159-1172 ,December 2001.

14. Zhang, Y. and Faghr, A., "Heat transfer in a pulsating heat pipe with open end", Int. J Heat Mass Transfer, Vol 45, pp. 755 –764, 2002.

15. Khandekar S. and Groll M., "An Insight into Thermo-Hydraulic Coupling in Pulsating Heat Pipes", Int. J. of Thermal Sciences, ISSN 1290- 0729, Vol. 43/1, pp. 13-20, 2004.

16. Khandekar S., Manyam S., Groll M. and Pandey M., " Two-phase Flow Modeling in Closed Loop Pulsating Heat Pipes", Proc. 13th Int. Heat Pipe Conf., Shanghai, China, 2004.

17. Khandekar S., " Thermo-hydrodynamics of Closed Loop Pulsating Heat Pipes," Doctoral Dissertation, Universität Stuttgart, Germany, 2004.

18. Gi. K., Sato F. and Maezawa S., "Flow Visualization Experiment on Oscillating Heat Pipe", Proc. 11th Int. Heat Pipe Conf., pp. 149- 153, Tokyo, Japan, 1999.

19. Lee W., Jung H., Kim J. and Kim J., "Flow Visualization of Oscillating Capillary Tube Heat Pipe", Proc. 11th IHPC, pp. 355-360, Tokyo, Japan, 1999.

20. Qu W. and Ma T., "Experimental Investigation on Flow and Heat Transfer of a Pulsating Heat Pipe", Proc. 12th Int. Heat Pipe Conf., pp. 226- 231, Moscow, Russia, 2002.

21. Khandekar S., Groll M., Charoensawan P. and Terdtoon P., "Pulsating Heat Pipes: Thermofluidic Characteristics and Comparative Study with Single Phase Thermosyphon", Proc. 12th Int. Heat Trans. Conf., ISBN-2-84299-307-1, Vol. 4, pp. 459-464, Grenoble, France, 2002.

22. Charoensawan P., "Heat Transfer Characteristics of Closed Loop Oscillating Heat Pipes", Ph.D. Thesis, Chiang Mai University, Chiang Mai, Thailand, 2003.

23. Khandekar S, Schneider M andGroll, M. "Mathematical modelling of pulsating heat pipes: state of the art and future challenges", 5 th ASME/ISHMT joint Heat and Mass Transfer Conference, Kolcata, India, 2002.

24. Charoensawan, P. and Terdtoon, P., "Thermal Performance of Horizontal Closed-loop Oscillating Heat Pipes", J. Appl. Thermal Engg., Elsevier, doi: 10-1016, 2007.

25. De Souza, F. A. S., Destri, J. F. A. and Colle, S., "An Experimental Investigation of a CO_2 Pulsating Heat Pipe" Proc. 14th Int. Heat Pipe Conference, pp.1-6, Brazil, 2007.

26. Gaugler, "Heat transfer device", US Patent application 21 December 1942, Published US Patent No. 2350348, 1944.

27. Grover, G M., "Evaporation-condensation heat transfer device", US Patent application 2 December 1963, Published US Patent No. 3229759, 1966.

28. Dunn, P.D. and Reay, D. A., "Heat Pipes", Third Edition, Pergamon Press, 1982.

29. Faghri, A., "Heat Pipe Science and Technology", Taylor and Francis, Bristol, Pennsylvania, USA, 1995.

30. Rittidech, S., Terdtoon, P., Murakami, M., Kamonpet, P. and Jompakdee,W., "Correlation to Predict Heat Transfer Characteristics of a Closed-End Oscillating

Heat Pipe at Normal Operating Condition", Applied Thermal Engineering, vol. 23, pp. 497–510, 2003.

.

31. Gi, K., Sato, F. and Maezawa, S., "Flow Visualization Experiment on Oscillating Heat Pipe", Proc. 11th International Heat Pipe Conference, pp. 149–153, Tokyo, Japan, 1999.

32. Zhang X. M., Xu, J. L. and Zhou, Z. Q., " Experimental Study of a Pulsating Heat Pipe using FC-72, Ethanol, and Water as Working Fluids". Vol. 12, pp. 445-472, 1999.

33. Zuo, Z. J., North, M. T. and Wert, K. L., "High Heat Flux Heat Pipes for Cooling of Electronics", IEEE Transactions on Components and Packaging Technologies, vol. 24, no. 2, pp. 220–225, 2001.

34. Holley, B. and Faghri, A., "Analysis of Pulsating Heat Pipe with Capillary Wick and Varying Channel Diameter", International Journal of Heat and Mass Transfer, vol. 48, pp. 2635–2651, 2005.

35 Dobson R. T. and Harms, T. M., "Lumped Parameter Analysis of Closed and Open Oscillatory Heat Pipes", Proc. 11th InternationalHeat Pipe Conference, pp. 12–16, Tokyo, Japan, 1999.

36 Honghai Yang, S. Khandekar, M. Groll, "Performance characteristics of pulsating heat pipes as integral thermal spreaders", International Journal of Thermal Sciences, Vol. 48, pp. 815–824, 2009.

37 Dobson, R. T., "An Open Oscillatory Heat Pipe Water Pump", Applied Thermal Engineering, vol. 25, pp. 603–621, 2005.

38. Charoensawan, P and Terdtoon, P "Thermal performance of horizontal closed-loop oscillating heat pipes", Applied Thermal Engineering, Vol. 28, issue 5-6, pp. 460-466, April 2008.

39. Faghri A. and Zhang Y., ‘Heat Transfer in a pulsating heat pipe with open end”, International Journal of Heat and Mass Transfer, Vol. 45, pp. 755-764, 2002.

40.Honghai Yang, S. Khandekar, M. Groll, “Performance characteristics of pulsating heat pipes as integral thermal spreaders”, International Journal of Thermal Sciences, Vol. 48, pp. 815–824, 2009.

Appendix A

Properties of Working Fluid and PHP Material

Table 2: Thermo Physical Properties of Working Fluid

Name of Working Fluid	Ammonia
Density of liquid at T_{sat}, ρ_l (Kg/m^3)	683.83
Density of vapor at T_{sat}, ρ_v (Kg/m^3)	.819
Boiling Point, T_{sat} (K)	240
Freezing point (K)	195
Surface tension of vapor liquid interface, $\boldsymbol{\sigma}$ (mN/m)	.044687

Table 3: Thermo Physical Properties of PHP material

Name of Material	Aluminum
Heat capacity of aluminum heating block, S_e (KJ/KgK)	900
Density, $\boldsymbol{\rho}$ (Kg/m^3)	2700
Melting point (K)	933.47

Appendix B

Data for Ammonia (Natural Convection)

Table 4: For fill ratio .4 and inclination angle 0^0 (Vertical)

fill ratio (V/Vmax)	angle (θ)	Time (min)	pressure (psi)	voltage (Volt)	current (amp)	Evaporator Temperature,Te (°C)								Max evaporator temp(°C)
						1	2	4	5	6	7	8	avg	
0.4		0	-0.09	0	0	25.4	25.4	25.4	25.4	25.4	25.4	25.4	25.40	
0.4		10	-0.06	100	0.4	28.3	28.2	28.3	28.4	28.4	28.4	28	28.29	
0.4		30	-0.03	100	0.4	32.9	32.7	32.8	32.8	33.1	32.7	32.8	32.83	
0.4		50	0	100	0.4	36.2	36.1	36.6	36	36.4	36.6	36.4	36.33	
0.4		70	1	100	0.4	39	38.6	38.9	38.7	39.3	39.5	39.2	39.03	
0.4		90	3	100	0.4	41.8	40.9	41.2	41.5	41.7	41.3	41.6	41.43	
0.4	0	120	5	100	0.4	43.9	43.5	43.5	43.6	43	43.7	43.1	43.47	47.33
0.4		150	5	100	0.4	45.6	44.9	45.3	45.1	45.2	45.1	45	45.17	
0.4		180	6	100	0.4	46.5	46	46.3	46.3	46.5	46.3	46.3	46.31	
0.4		200	7	100	0.4	46.9	46.3	47	46.7	47	46.8	46.8	46.79	
0.4		220	7	100	0.4	47	46.5	47.3	46.9	47.4	47.1	46.9	47.01	
0.4		240	8	100	0.4	47.1	46.7	47.5	47	47.7	47.3	47	47.19	
0.4		260	10	100	0.4	47.1	46.9	47.6	47.2	47.7	47.5	47.3	47.33	

Table 5: For fill ratio .4 and inclination angle 0^0 (Vertical)

fill ratio (V/Vmax)	angle (θ)	Time (min)	Condenser tipTemperature, Tc(°C)						Adiabatic Position Temperature($^\circ_C$)			Average condenser tempTc(°C)	Te-Tc (°C)
			1	2	3	4	5	avg	6	8	avg		
0.4		0	25.4	25.4	25.4	25.4	25.4	25.40	25.4	25.4	25.4	25.40	0.00
0.4		10	26.1	26.3	26.1	25.9	25.9	26.06	27.1	27	27.05	26.56	1.73
0.4		30	28.8	28.7	28.7	28.8	28.8	28.76	30.5	32.3	31.4	30.08	2.75
0.4		50	32.2	32	32.2	32.1	32	32.10	34.4	35.7	35.05	33.58	2.75
0.4		70	34	33.8	34.2	34.1	34	34.02	38.1	39.5	38.8	36.41	2.62
0.4		90	36.5	36.2	36.4	36.7	36.6	36.48	39.7	41.5	40.6	38.54	2.89
0.4	0	120	38.5	38.3	38.5	38.5	38.6	38.48	42	43.4	42.7	40.59	2.88
0.4		150	40.3	40	40.2	40.3	40.3	40.22	43.3	44.8	44.05	42.14	3.04
0.4		180	41.4	41.1	41.1	41.3	41.5	41.28	44.6	45.5	45.05	43.17	3.15
0.4		200	41.9	41.4	41.2	41.5	41.9	41.58	45.3	46	45.65	43.62	3.17
0.4		220	42	41.5	41.6	42	42.3	41.88	45.5	46.7	46.1	43.99	3.02
0.4		240	41.2	41.6	42	42.1	42.5	41.88	46	47	46.5	44.19	3.00
0.4		260	42.3	41.9	42.2	42.4	42.6	42.28	46	47.3	46.65	44.47	2.86

Table 6: For fill ratio .4 and inclination angle 30^0

fill ratio (V/Vmax)	angle (θ)	Time (min)	pressure (psi)	voltage (Volt)	current (amp)	Evaporator Temperature,Te (°C)								Max evaporator temp(°C)
						1	2	4	5	6	7	8	avg	
0.4		0	-0.09	0	0	24.8	24.8	24.8	24.8	24.8	24.8	24.8	24.8	
0.4		10	-0.06	100	0.4	27.7	27.9	27.8	27.7	27.4	27.5	27.6	27.66	
0.4		20	-0.03	100	0.4	30.4	29.8	29.9	30	29.8	30.1	30.2	30.03	
0.4		40	0	100	0.4	34.7	33.4	34.5	34.6	33.2	34.3	34.4	34.16	
0.4		60	1	100	0.4	37.6	36.7	37.5	37.8	36.9	37.5	37.5	37.36	
0.4		80	2	100	0.4	39.6	39.6	40.1	40.4	39.5	39.7	40.2	39.87	
0.4	30	100	2	100	0.4	41.2	41.3	41.5	41.6	41.6	42	42.6	41.69	46.73
0.4		130	5	100	0.4	43.5	43.7	43.1	43.1	43.7	43.8	44	43.56	
0.4		160	5	100	0.4	44.7	45.2	44.2	44.6	45.2	45.2	45.6	44.96	
0.4		190	6	100	0.4	46.5	46.9	44.9	45.2	46	45.7	46	45.89	
0.4		210	6	100	0.4	46.9	47.1	45.2	45.9	46.5	45.9	46.3	46.26	
0.4		230	7	100	0.4	47.1	47.2	45.6	46.2	46.7	46.1	46.7	46.51	
0.4		260	9	100	0.4	47.2	47.2	46	46.3	47	46.5	46.9	46.73	

Table 7: For fill ratio .4 and inclination angle 30^0

fill ratio (V/Vmax)	angle (θ)	Time (min)	Condenser tipTemperature, Tc(°C)						Adiabatic Position Temperature (°C)			Average condenser tempTc(°C)	Te-Tc (°C)
			1	2	3	4	5	avg	6	8	avg		
0.4		0	24.8	24.8	24.8	24.8	24.8	24.8	24.8	24.8	24.8	24.80	0.00
0.4		10	25.3	25.5	25.2	25.7	25.2	25.38	26.4	25.8	26.1	25.74	1.92
0.4		20	26	25.8	25.8	25.7	25.9	25.84	28.1	29.6	28.85	27.35	2.68
0.4		40	29.8	29.3	29.4	30	30.1	29.72	33.5	34.4	33.95	31.84	2.32
0.4		60	32.9	32.5	32.6	32.8	32.7	32.70	36.4	37	36.7	34.70	2.66
0.4		80	35.4	35	35.3	35.4	35.3	35.28	38.4	39.4	38.9	37.09	2.78
0.4	30	100	37.2	36.9	37.1	37.4	37.2	37.16	40.3	40.6	40.45	38.81	2.88
0.4		130	39	38.8	38.9	39.2	39.1	39.00	42.4	42.7	42.55	40.78	2.78
0.4		160	40.4	40.3	40.5	40.7	40.5	40.48	43.5	44.4	43.95	42.22	2.74
0.4		190	41.3	41	41.2	41.6	41.3	41.28	44.3	45.3	44.8	43.04	2.85
0.4		210	41.7	41.5	41.6	41.8	41.9	41.70	44.6	45.8	45.2	43.45	2.81
0.4		230	41.7	41.4	41.6	42.3	42.6	41.92	45.1	46.5	45.8	43.86	2.65
0.4		260	41.8	41.6	41.9	42.4	42.7	42.08	45.3	46.7	46	44.04	2.69

Table 8: For fill ratio .4 and inclination angle 45^0

fill ratio (V/Vmax)	angle (θ)	Time (min)	pressure (psi)	voltage (Volt)	current (amp)	Evaporator Temperature,Te(°C)								Max evaporator temp(°C)
						1	2	4	5	6	7	8	avg	
0.4		0	-0.09	0	0	24.4	24.4	24.4	24.4	24.4	24.4	24.4	24.40	
0.4		10	-0.06	100	0.4	27	26.9	27.3	27.5	27.6	27.2	27.6	27.30	
0.4		20	-0.03	100	.29.9	29.8	29.8	29.9	29.7	29.8	29.9	30	29.84	
0.4		40	0	100	0.4	34.7	33.4	34.5	34.6	33.6	34.3	34.4	34.21	
0.4		60	1	100	0.4	37.8	37.7	37.8	37.6	37	37.7	37.8	37.63	
0.4		80	2	100	0.4	40.1	40.2	39.9	40.3	39.7	40	39.9	40.01	
0.4	45	100	2	100	0.4	41.6	41.5	42.2	41.7	41.6	42	41.6	41.74	47.24
0.4		130	5	100	0.4	43.5	43.4	43.6	43.5	43.2	43.6	43.7	43.50	
0.4		160	6	100	0.4	45.2	44.8	45.8	44.9	44.5	45	45.1	45.04	
0.4		190	7	100	0.4	47	45.6	46.1	46	45.7	46	45.4	45.97	
0.4		210	8	100	0.4	47.1	46.1	46.4	46.9	46.7	46.4	46.2	46.54	
0.4		230	10	100	0.4	47.5	46.6	46.8	47	47.2	46.7	46.3	46.87	
0.4		260	11	100	0.4	47.6	47	47.4	47.4	47.3	47	47	47.24	

Table 9: For fill ratio .4 and inclination angle 45^0

fill ratio (V/Vmax)	angle (θ)	Time (min)	Condenser tipTemperature, Tc(°C)						Adiabatic Position Temperature (°C)			Average condenser tempTc(°C)	Te-Tc (°C)
			1	2	3	4	5	avg	6	8	avg		
0.4		0	24.4	24.4	24.4	24.4	24.4	24.40	24.4	24.4	24.4	24.40	0.00
0.4		10	24.9	24.9	24.9	24.8	24.9	24.88	26	26.6	26.3	25.59	1.71
0.4		20	25.6	25.7	25.4	25.6	25.5	25.56	28.1	28.2	28.15	26.86	2.99
0.4		40	29.1	29.2	29.5	29.6	29.5	29.38	35.5	35.4	35.45	32.42	1.80
0.4		60	32.3	32.1	32	32.4	32	32.16	37.4	37.6	37.5	34.83	2.80
0.4		80	34.9	35.1	34.9	34.8	34.8	34.90	38.6	39.7	39.15	37.03	2.99
0.4	45	100	36.2	36.3	36	35.9	35.8	36.04	41.7	42.4	42.05	39.05	2.70
0.4		130	37.7	37.9	37.5	37.4	37.5	37.60	42.8	43.6	43.2	40.40	3.10
0.4		160	39.5	39.6	39.1	38.9	39.4	39.30	43.5	44.3	43.9	41.60	3.44
0.4		190	40.2	40.4	40	40.6	39.9	40.22	44.6	45.6	45.1	42.66	3.31
0.4		210	40.1	41.2	40.9	40.8	40.9	40.78	45.8	46.7	46.25	43.52	3.03
0.4		230	40.4	41.4	41.1	41	41	40.98	46.4	46.5	46.45	43.72	3.16
0.4		260	40.9	41.5	41.3	41.4	41.3	41.28	46.8	47.3	47.05	44.17	3.08

Table 10: For fill ratio .4 and inclination angle 60^0

fill ratio (V/Vmax)	angle (θ)	Time (min)	pressure (psi)	voltage (Volt)	current (amp)	Evaporator Temperature,Te (°C)								Max evaporator temp(°C)
						1	2	4	5	6	7	8	avg	
0.4		0	-0.09	0	0	24.4	24.4	24.4	24.4	24.4	24.4	24.4	24.40	
0.4		10	-0.06	100	0.4	27	26.9	27.6	27.7	27.4	27.2	27.6	27.34	
0.4		20	-0.03	100	0.4	30.2	29.8	29.9	30	29.8	30.1	30	29.97	
0.4		40	0	100	0.4	34.7	33.8	34.5	34.6	33.7	34.3	34.4	34.29	
0.4		60	1	100	0.4	37.3	36.7	37.6	37.8	36.9	37.5	37.4	37.31	
0.4		80	2	100	0.4	39.8	39.6	40	39.8	39.9	39.7	40.2	39.86	
0.4	60	100	2	100	0.4	41.8	41.3	41.8	41.3	41.6	41.5	42.3	41.66	47.76
0.4		130	5	100	0.4	43.9	43.7	43.1	43.1	43.7	43.1	44.7	43.61	
0.4		160	6	100	0.4	45.4	45.3	44.8	44.9	44.7	44.1	46	45.03	
0.4		190	8	100	0.4	46.9	46.5	45.9	46	45.8	45.8	47	46.27	
0.4		210	9	100	0.4	47.5	47.4	46.7	46.9	46	46.8	47.8	47.01	
0.4		230	10	100	0.4	48	47.9	46.6	47	46.8	47.1	48.5	47.41	
0.4		260	12	100	0.4	48	48	47.9	47.1	47.2	47.6	48.5	47.76	

Table 11: For fill ratio .4 and inclination angle 60^0

fill ratio (V/Vmax)	angle (θ)	Time (min)	Condenser tipTemperature, Tc(°C)						Adiabatic Position Temperature (°C)			Average condenser tempTc(°C)	Te-Tc (°C)
			1	2	3	4	5	avg	6	8	avg		
0.4		0	24.4	24.4	24.4	24.4	24.4	24.40	24.4	24.4	24.4	24.40	0.00
0.4		10	24.9	24.9	24.7	24.8	24.9	24.84	26	25.6	25.8	25.32	2.02
0.4		20	25.6	25.4	25.3	25.6	25.7	25.52	28.1	27.2	27.65	26.59	3.39
0.4		40	29.2	28.9	28.9	29.1	29.2	29.06	33.5	34.4	33.95	31.51	2.78
0.4		60	31.9	30.9	31.7	31.8	31.5	31.56	36.4	37	36.7	34.13	3.18
0.4		80	33.6	33.5	33.5	33.5	33.3	33.48	38.1	37.9	38	35.74	4.12
0.4	60	100	35.1	35	34.7	34.6	34.9	34.86	41.2	41.4	41.3	38.08	3.58
0.4		130	37.2	37.4	36.4	36.5	36.7	36.84	43.1	43.2	43.15	40.00	3.62
0.4		160	34.2	38.3	38.2	38	38.7	37.48	44.2	45.5	44.85	41.17	3.86
0.4		190	39.5	39.6	39.8	39	39.9	39.56	45.4	46	45.7	42.63	3.64
0.4		210	40.4	40.3	40.3	39.8	40.5	40.26	45.9	46.6	46.25	43.26	3.76
0.4		230	40.9	40.5	40.6	40.3	41.3	40.72	46.8	47.2	47	43.86	3.55
0.4		260	41	40.8	40.9	41	41.7	41.08	47.1	47.5	47.3	44.19	3.57

Table 12: For fill ratio .4 and inclination angle 90^0

fill ratio (V/Vmax)	angle (θ)	Time (min)	pressure (psi)	voltage (Volt)	current (amp)	Evaporator Temperature,Te (°C)								Max evaporator temp(°C)
						1	2	4	5	6	7	8	avg	
0.4		0	-0.07	0	0	28.7	28.7	28.7	28.7	28.7	28.7	28.7	28.70	
0.4		10	-0.04	100	0.4	31.9	32.5	31.8	31.7	31.7	31.8	31.2	31.80	
0.4		30	-0.01	100	0.4	36.7	36.6	36.8	36.5	36.6	36.8	36.1	36.59	
0.4		50	0	100	0.4	40.3	40.2	40.3	40.5	40.1	40.1	40.6	40.30	
0.4		70	1	100	0.4	43	43.3	43.2	43.3	43	43.1	43.3	43.17	
0.4		90	2	100	0.4	45	45.6	45.3	45.4	45	45.2	45.6	45.30	
0.4	90	120	3	100	0.4	47.9	48.4	48.1	48.2	47.9	48.3	48.5	48.19	55.27
0.4		150	5	100	0.4	50.6	50.9	50.1	50.6	50.1	50.7	50.6	50.51	
0.4		180	7	100	0.4	52	52.5	52.4	52.7	52.5	52.7	52.6	52.49	
0.4		200	9	100	0.4	53.1	53.4	53.5	54	53.7	54	53.8	53.64	
0.4		220	11	100	0.4	54.2	54.3	54.4	54.8	54.5	54.6	54.4	54.46	
0.4		240	13	100	0.4	54.8	54.9	55.1	55.5	55	55.2	55	55.07	
0.4		260	15	100	0.4	55	55.1	55.3	55.5	55.4	55.4	55.2	55.27	

Table 13: For fill ratio .4 and inclination angle 90^0

fill ratio (V/Vmax)	angle (θ)	Time (min)	Condenser tipTemperature, Tc(°C)						Adiabatic Position Temperature (°C)			Average condenser tempTc(°C)	Te-Tc (°C)
			1	2	3	4	5	avg	6	8	avg		
0.4		0	28.7	28.7	28.7	28.7	28.7	28.70	28.7	28.7	28.7	28.70	0.00
0.4		10	29	29	28.9	29	29.1	29.00	29.8	29.1	29.45	29.23	2.58
0.4		30	30.2	30.1	30.2	30.1	30.1	30.14	31.9	31.1	31.5	30.82	5.77
0.4		50	32.4	32.3	32.1	31	32.2	32.00	32.4	33.3	32.85	32.43	7.88
0.4		70	34.2	34.1	34	33.8	34	34.02	36	36.5	36.25	35.14	8.04
0.4		90	35.3	35.2	35.1	34.5	35	35.02	39.7	39.2	39.45	37.24	8.07
0.4	90	120	37.8	37.6	37.4	37.3	37.3	37.48	42.6	41.3	41.95	39.72	8.47
0.4		150	39.9	40.2	40.1	39.8	39.7	39.94	44.2	43.5	43.85	41.90	8.62
0.4		180	41.2	41.7	41.5	41.2	40.9	41.30	46	46.5	46.25	43.78	8.71
0.4		200	41.9	42.2	42.1	42	41.8	42.00	47.7	47.1	47.4	44.70	8.94
0.4		220	42.3	42.7	42.6	42.4	42.2	42.44	50	49.5	49.75	46.10	8.36
0.4		240	42.4	43	42.9	42.6	42.3	42.64	50.7	49.5	50.1	46.37	8.70
0.4		260	43.1	43.5	43.4	43	42.9	43.18	50.8	49.6	50.2	46.69	8.58

Table 14: For fill ratio .4 and inclination angle 180^0

fill ratio (V/Vmax)	angle (θ)	Time (min)	pressure (psi)	voltage (Volt)	current (amp)	Evaporator Temperature,Te(°C)								Max evaporator temp(°C)
						1	2	4	5	6	7	8	avg	
0.4		0	-0.09	0	0	24.3	24.3	24.3	24.3	24.3	24.3	24.3	24.30	
0.4		10	-0.06	100	0.4	27.7	27.5	27.4	27.6	27.3	27.4	27.6	27.50	
0.4		30	-0.03	100	0.4	33.2	33.1	33	32.9	32.8	33.1	33.3	33.06	
0.4		50	0	100	0.4	38.2	38.1	38.1	37.7	37.5	37.9	37.6	37.87	
0.4		70	1	100	0.4	42.2	41.9	42.3	41.7	41.7	42.3	42	42.01	
0.4		90	2	100	0.4	45.7	45.1	45.1	45	45.6	46.2	45.5	45.46	
0.4	180	110	3	100	0.4	48.5	48.7	48.1	48.2	48.7	49.3	48.3	48.54	61.07
0.4		130	5	100	0.4	51.3	51.4	51	51.2	51.4	51.6	51	51.27	
0.4		160	7	100	0.4	54.6	54.8	54.7	54.5	54.4	54.7	54.2	54.56	
0.4		190	9	100	0.4	57.2	57.3	57.1	57.2	57.1	57.7	57	57.23	
0.4		220	12	100	0.4	59.4	59.5	59	59.6	59.5	59.7	59.1	59.40	
0.4		240	15	100	0.4	60.1	61.4	60.6	60.9	60.1	60.3	59.8	60.46	
0.4		260	18	100	0.4	60.5	61.7	61.7	61.4	61.2	60.8	60.2	61.07	

Table 15: For fill ratio .4 and inclination angle 180^0

fill ratio (V/Vmax)	angle (θ)	Time (min)	Condenser tipTemperature, Tc(°C)						Adiabatic Position Temperature (°C)			Average condenser tempTc(°C)	Te-Tc (°C)
			1	2	3	4	5	avg	6	8	avg		
0.4		0	24.3	24.3	24.3	24.3	24.3	24.30	24.3	24.3	24.3	24.30	0.00
0.4		10	24.9	24.8	24.8	24.7	24.8	24.80	26.6	26	26.3	25.55	1.95
0.4		30	25.6	25.7	25.8	25.5	25.6	25.64	29	28	28.5	27.07	5.99
0.4		50	26.1	26.2	26.4	26.5	26.7	26.38	30.2	30.4	30.3	28.34	9.53
0.4		70	27.3	28.9	27.2	28.4	27.4	27.84	34	31.6	32.8	30.32	11.69
0.4		90	27.6	28.5	27.9	28.9	28.4	28.26	36.7	37	36.85	32.56	12.90
0.4	180	110	28.7	28.8	28.8	28.8	30.6	29.14	38	39.1	38.55	33.85	14.70
0.4		130	30.2	30.3	30	30.4	30.1	30.20	38.5	39.5	39	34.60	16.67
0.4		160	31.9	32.2	31.8	32	31.9	31.96	39.1	39.5	39.3	35.63	18.93
0.4		190	32.3	32.3	32	32.1	31.4	32.02	40.1	40.3	40.2	36.11	21.12
0.4		220	32.1	32.8	33.4	33.2	32.8	32.86	40.6	41	40.8	36.83	22.57
0.4		240	33.5	33.4	33.9	33.7	33.9	33.68	41	41.2	41.1	37.39	23.07
0.4		260	34.2	34.3	34.9	34.6	34.6	34.52	41.8	41.3	41.55	38.04	23.04

Table 16: For fill ratio .6 and inclination angle 0^0(Vertical)

fill ratio (V/Vmax)	angle (θ)	Time (min)	pressure (psi)	voltage (Volt)	current (amp)	Evaporator Temperature,Te (°C)								Max evaporator temp(°C)
						1	2	4	5	6	7	8	avg	
0.6		0	0	0	0	25.5	25.5	25.5	25.5	25.5	25.5	25.5	25.50	
0.6		10	0	100	0.4	27.9	28.3	28.2	28.6	28.5	28.4	28.7	28.37	
0.6		20	1	100	0.4	30.9	30.8	30.9	31.2	30.8	30.8	30.9	30.90	
0.6		40	2	100	0.4	34.6	34.5	34.8	34.6	34.3	34.2	34.2	34.46	
0.6		60	4	100	0.4	37.5	37.2	37.6	37	37.4	37.2	37.9	37.40	
0.6		80	5	100	0.4	39.8	39.5	39.9	39.3	39.4	39.2	39.4	39.50	
0.6	0	100	7	100	0.4	40.7	41	41.1	41	41.3	40.8	41.2	41.01	47.19
0.6		120	8	100	0.4	42.2	42.8	42.6	42.4	42.9	42.3	42.3	42.50	
0.6		140	10	100	0.4	43.3	44.1	44	43.3	43.8	43.2	44	43.67	
0.6		180	12	100	0.4	45.2	45.4	45.3	45.3	45.4	45.1	46.2	45.41	
0.6		210	14	100	0.4	46.2	46.9	46.4	46.8	46.1	46.3	46.5	46.46	
0.6		230	15	100	0.4	46.6	47.1	46.5	47.3	46.6	46.6	47.1	46.83	
0.6		260	17	100	0.4	47	47.3	47	47.3	46.9	46.9	47.9	47.19	

Table 17: For fill ratio .6 and inclination angle 0^0

fill ratio (V/Vmax)	angle (θ)	Time (min)	Condenser tipTemperature, Tc(°C)						Adiabatic Position Temperature (°C)			Average condenser tempTc(°C)	Te-Tc (°C)
			1	2	3	4	5	avg	6	8	avg		
0.6		0	25.5	25.5	25.5	25.5	25.5	25.50	25.5	25.5	25.5	25.50	0.00
0.6		10	26	26.2	25.9	25.8	26.1	26.00	27.2	26.9	27.05	26.53	1.85
0.6		20	26.5	26.5	26.5	26.5	26.7	26.54	29.9	30	29.95	28.25	2.66
0.6		40	29.5	29.4	29.5	29.4	29.6	29.48	33	33.5	33.25	31.37	3.09
0.6		60	32.5	32.3	32.1	32.6	32.7	32.44	36.5	37.5	37	34.72	2.68
0.6		80	34.6	34.4	34.2	34.5	34.7	34.48	39	40.2	39.6	37.04	2.46
0.6	0	100	36.6	36	35.9	36.3	36.6	36.28	41.5	40.9	41.2	38.74	2.27
0.6		120	37.8	37	37.5	37.9	38.1	37.66	42.6	42.5	42.55	40.11	2.40
0.6		140	38.7	38.2	38.2	38.6	39	38.54	43.5	43.7	43.6	41.07	2.60
0.6		180	40.1	40.1	40.5	40	41	40.34	45.8	44.8	45.3	42.82	2.59
0.6		210	41.2	41.3	41.7	41	41.6	41.36	46.1	46	46.05	43.71	2.75
0.6		230	41.7	41.8	42	41.6	42	41.82	46.4	46.4	46.4	44.11	2.72
0.6		260	42	42.1	42.4	41.9	42.5	42.18	46.5	46.8	46.65	44.42	2.77

Table 18: For fill ratio .6 and inclination angle 30^0

fill ratio (V/Vmax)	angle (θ)	Time (min)	pressure (psi)	voltage (Volt)	current (amp)	Evaporator Temperature,Te (°C)								Max evaporator temp(°C)
						1	2	4	5	6	7	8	avg	
0.6		0	0	0	0	24.5	24.5	24.5	24.5	24.5	24.5	24.5	24.50	
0.6		20	2	100	0.4	29.9	30	29.7	29.8	29.8	29.7	29.9	29.78	
0.6		40	3	100	0.4	33.9	33.8	33.7	33.6	33.5	33.4	33.8	33.60	
0.6		60	4	100	0.4	37	36.9	36.8	36.6	36.5	36.9	36.2	36.60	
0.6		80	6	100	0.4	39.1	39	39.2	39.1	38.7	38.9	38.7	38.92	
0.6		100	7	100	0.4	41.6	41.2	41.3	41.2	40.7	40.8	40.7	40.94	
0.6	30	120	9	100	0.4	42.6	42.5	42.6	42.5	42.6	42.9	42.8	42.68	46.8
0.6		140	10	100	0.4	43.9	43.8	43.9	43.7	43.9	44.2	44.2	43.98	
0.6		160	11	100	0.4	44.9	44.6	44.9	44.9	45	45.3	45.1	45.04	
0.6		180	12	100	0.4	45.7	45.3	45.4	45.5	45.4	46.2	45.9	45.68	
0.6		200	14	100	0.4	46.3	46	46.1	46.2	46	46.4	46.2	46.18	
0.6		220	15	100	0.4	46.6	46.4	46.5	46.5	46.2	46.6	46.3	46.42	
0.6		260	16	100	0.4	47.1	47	46.8	46.8	46.9	46.7	46.8	46.80	

Table 19: For fill ratio .6 and inclination angle 30^0

fill ratio (V/Vmax)	angle (θ)	Time (min)	Condenser tipTemperature, Tc(°C)						Adiabatic Position Temperature (°C)			Average condenser tempTc(°C)	Te-Tc (°C)
			1	2	3	4	5	avg	6	8	avg		
0.6		0	24.5	24.5	24.5	24.5	24.5	24.5	24.5	24.5	24.5	24.50	0.00
0.6		20	26.2	26.3	26.1	26.4	26.3	26.26	28.9	28.4	28.65	27.46	2.33
0.6		40	28.6	28.8	28.6	29	28.9	28.78	30.9	30.5	30.7	29.74	3.86
0.6		60	31.5	31	31.4	31.6	31.2	31.34	35.6	34.2	34.9	33.12	3.48
0.6		80	34	33.5	34.1	34.4	34.3	34.06	39.5	38.9	39.2	36.63	2.29
0.6		100	36.3	36	36.3	36.8	35.7	36.22	41.5	41	41.25	38.74	2.21
0.6	30	120	37.7	37.3	37.6	37.7	36.9	37.44	42	42	43	40.22	2.46
0.6		140	39.2	38.9	39	39	38.1	38.84	43.8	43.4	43.6	41.22	2.76
0.6		160	40	39.7	39.6	39.7	39.3	39.66	44.8	44.5	44.65	42.16	2.89
0.6		180	40.8	40.7	40.7	40.6	40.5	40.66	45.7	45.4	45.55	43.11	2.58
0.6		200	41.1	41	41.1	41.4	41	41.12	46	45.6	45.8	43.46	2.72
0.6		220	41.5	41.3	41.4	41.5	41.3	41.40	46.3	46.2	46.25	43.83	2.59
0.6		260	41.8	41.7	41.9	41.9	41.6	41.78	46.7	46.3	46.5	44.14	2.66

Table 20: For fill ratio .6 and inclination angle 45^0

fill ratio (V/Vmax)	angle (θ)	Time (min)	pressure (psi)	voltage (Volt)	current (amp)	Evaporator Temperature,Te (°C)								Max evaporator temp(°C)
						1	2	4	5	6	7	8	avg	
0.6		0	0	0	0	24.2	24.2	24.2	24.2	24.2	24.2	24.2	24.20	
0.6		20	2	100	0.4	29.5	29.6	29.7	29.6	29.5	29.5	29.7	29.60	
0.6		40	3	100	0.4	33.8	33	33.1	33.5	33.9	33.9	34	33.60	
0.6		60	4	100	0.4	37.1	36.6	36.7	37	37.2	37.3	37.5	37.06	
0.6		80	6	100	0.4	39.7	39.2	39.3	39.6	39.6	39.8	39.8	39.57	
0.6		100	7	100	0.4	41.5	41	41.2	41.5	41.7	41.8	42.4	41.59	
0.6	45	120	9	100	0.4	43.2	42.5	42.8	43.1	43	43.3	44.1	43.14	47.47
0.6		140	10	100	0.4	44.4	43.7	44.1	44.3	44.3	44.7	45.4	44.41	
0.6		160	11	100	0.4	45.5	45	45.3	45.2	45.4	45.5	45.7	45.37	
0.6		180	12	100	0.4	46.1	45.8	46.1	45.9	46.2	46.3	46.5	46.13	
0.6		200	14	100	0.4	46.9	46.3	46.5	46.4	47	46.9	47	46.71	
0.6		220	15	100	0.4	47.3	46.7	46.8	46.9	47.3	47	47.1	47.01	
0.6		260	16	100	0.4	47.3	47.5	47.6	47.5	47.5	47.4	47.5	47.47	

Table 21: For fill ratio .6 and inclination angle 45^0

fill ratio (V/Vmax)	angle (θ)	Time (min)	Condenser tipTemperature, Tc(°C)						Adiabatic Position Temperature (°C)			Average condenser tempTc(°C)	Te-Tc (°C)
			1	2	3	4	5	avg	6	8	avg		
0.6		0	24.2	24.2	24.2	24.2	24.2	24.20	24.2	24.2	24.2	24.20	0.00
0.6		20	25.9	26.1	26.2	26.5	26.4	26.22	28.9	28.4	28.65	27.44	2.17
0.6		40	27.8	27.9	27.9	28	27.8	27.88	33.9	33.5	33.7	30.79	2.81
0.6		60	30.7	30.8	30.9	31.2	30.9	30.90	37	34.6	35.8	33.35	3.71
0.6		80	33.2	33.3	33.4	33.7	33.5	33.42	40.2	39.5	39.85	36.64	2.94
0.6		100	35.3	35.5	35.8	36	35.2	35.56	41.6	41.3	41.45	38.51	3.08
0.6	45	120	36.9	37	37.6	36.8	36.9	37.04	42.4	43.8	43.1	40.07	3.07
0.6		140	37.9	38	38.3	38.4	38.4	38.20	44.6	45	44.8	41.50	2.91
0.6		160	38.8	38.8	39.1	39.1	39.2	39.00	44.8	46.1	45.45	42.23	3.15
0.6		180	40	39.9	40.1	40	40.1	40.02	45.3	46.9	46.1	43.06	3.07
0.6		200	40.5	40.4	40.6	40.5	40.5	40.50	46	47.2	46.6	43.55	3.16
0.6		220	40.9	40.9	40.8	41	40.6	40.84	46.8	47.9	47.35	44.10	2.92
0.6		260	41.2	41.2	41.3	41.8	41.5	41.40	47	48.1	47.55	44.48	3.00

Table 22: For fill ratio .6 and inclination angle 60^0

fill ratio (V/Vmax)	angle (θ)	Time (min)	pressure (psi)	voltage (Volt)	current (amp)	Evaporator Temperature,Te (°C)								Max evaporator temp(°C)
						1	2	4	5	6	7	8	avg	
0.6		0	0	0	0	24.8	24.8	24.8	24.8	24.8	24.8	24.8	24.8	
0.6		20	2	100	0.4	30.2	30.1	30.1	30.2	30.1	30.1	30	30.10	
0.6		40	3	100	0.4	34	33.9	33.8	34.1	34	33.9	33.8	33.93	
0.6		60	4	100	0.4	37	36.9	36.7	37.6	37.1	36.9	37	37.03	
0.6		80	6	100	0.4	39.6	39.4	39.2	39.6	39.7	39.6	39.5	39.51	
0.6		100	7	100	0.4	41.5	41.3	41.2	41.4	41.8	41.6	41.5	41.47	
0.6	60	120	9	100	0.4	43.4	43.1	43	43.1	43.2	43	42.6	43.06	48.11
0.6		140	10	100	0.4	44.5	44.3	44	44.1	44.3	44.7	44.2	44.30	
0.6		160	12	100	0.4	45.5	45.3	45.1	45.3	45.6	45.7	45.3	45.40	
0.6		180	14	100	0.4	46.2	46	46.4	46.6	46.3	46.5	46.3	46.33	
0.6		200	15	100	0.4	47.5	47.4	47	47.3	46.6	47.2	46.6	47.09	
0.6		220	16	100	0.4	47.8	47.8	47.5	47.9	47	47.8	47.2	47.57	
0.6		260	18	100	0.4	48.5	48.3	48	48.3	47.4	48.3	48	48.11	

Table 23: For fill ratio .6 and inclination angle 60^0

fill ratio (V/Vmax)	angle (θ)	Time (min)	Condenser tipTemperature, Tc(°C)						Adiabatic Position Temperature (°C)			Average condenser tempTc(°C)	Te-Tc (°C)
			1	2	3	4	5	avg	6	8	avg		
0.6		0	24.8	24.8	24.8	24.8	24.8	24.8	24.8	24.8	24.8	24.80	0.00
0.6		20	26.1	29.9	26.2	26.1	26	26.86	28.9	28.4	28.65	27.76	2.35
0.6		40	28.2	28.1	27.9	28	28.1	28.06	32.9	34	33.45	30.76	3.17
0.6		60	30.7	30.7	30	30.4	30.5	30.46	36.6	37.9	37.25	33.86	3.17
0.6		80	33.2	33.1	32.8	33.1	33.2	33.08	39.5	40.2	39.85	36.47	3.05
0.6		100	35.2	35.1	34.7	35.1	35.2	35.06	41.5	42.3	41.9	38.48	2.99
0.6	60	120	36.7	36.5	36.2	36.7	36.9	36.60	42.8	44.6	43.7	40.15	2.91
0.6		140	38.1	37.9	37.3	38	38.4	37.94	44	45	44.5	41.22	3.08
0.6		160	39	38.7	38.5	39.7	39.6	39.10	44.5	46	45.25	42.18	3.23
0.6		180	40	39.7	39	40.4	40.3	39.88	45.3	46.7	46	42.94	3.39
0.6		200	40.5	40.2	40	40.9	41.3	40.58	45.9	47.3	47	43.79	3.30
0.6		220	40.7	40.6	40.7	41.3	41.3	40.92	46.3	48.1	47.7	44.31	3.26
0.6		260	41.3	41.2	41.2	41.7	41.9	41.46	47.3	48.5	47.9	44.68	3.43

Table 24: For fill ratio .6 and inclination angle 90^0

fill ratio (V/Vmax)	angle (θ)	Time (min)	pressure (psi)	voltage (Volt)	current (amp)	Evaporator Temperature,Te (°C)								Max evaporator temp(°C)
						1	2	4	5	6	7	8	avg	
0.6		0	0	0	0	25.4	25.4	25.4	25.4	25.4	25.4	25.4	25.40	
0.6		12	0	100	0.4	28.8	28.6	28.7	28.7	28.9	29	28.9	28.80	
0.6		20	3	100	0.4	30.6	30.7	30.6	31	30.9	31	31.1	30.84	
0.6		40	5	100	0.4	35	35.1	35	35.5	35.2	35.3	35.4	35.21	
0.6		60	5	100	0.4	38.2	38.3	38.2	38.5	38.1	38.3	38.2	38.26	
0.6		80	7	100	0.4	41	40.9	41	41.1	41	41.1	41	41.01	
0.6	90	100	8	100	0.4	43.2	43.1	43	43.1	43	43.2	43	43.09	49.43
0.6		120	9	100	0.4	44.8	43.9	44.2	44.7	44.3	44.4	44.7	44.43	
0.6		140	12	100	0.4	45.7	45.5	45.2	45.8	45.5	45.6	45.8	45.59	
0.6		160	15	100	0.4	46.8	46.7	46.2	46.8	46.4	46.8	46.9	46.66	
0.6		180	17	100	0.4	47.7	47.6	47.6	47.7	47.6	47.7	47.5	47.63	
0.6		220	20	100	0.4	48.7	48.7	48.5	48.6	48.6	48.7	48.7	48.64	
0.6		260	22.0	100	0.4	49.6	49.5	49.5	49.2	49.3	49.4	49.5	49.43	

Table 25: For fill ratio .6 and inclination angle 90^0

fill ratio (V/Vmax)	angle (θ)	Time (min)	Condenser tipTemperature, Tc(°C)						Adiabatic Position Temperature (°C)			Average condenser tempTc(°C)	Te-Tc (°C)
			1	2	3	4	5	avg	6	8	avg		
0.6		0	25.4	25.4	25.4	25.4	25.4	25.40	25.4	25.4	25.4	25.40	0.00
0.6		12	25.8	25.9	25.9	26	25.9	25.90	26.8	26.8	26.8	26.35	2.45
0.6		20	26.2	26.3	26	26.1	26.1	26.14	27.6	28	27.8	26.97	3.87
0.6		40	26.9	27.1	27.2	27.3	27.1	27.12	30.5	30.6	30.55	28.84	6.38
0.6		60	30.3	30.5	30.5	30.6	30.3	30.44	31.7	32.5	32.1	31.27	6.99
0.6		80	32.4	32.5	32.6	32.7	32.1	32.46	35	36.9	35.95	34.21	6.81
0.6	90	100	34	34.1	34.1	34.2	33.8	34.04	37.9	39	38.45	36.25	6.84
0.6		120	35.8	35.6	35.7	36	35.7	35.76	39	40.6	39.8	37.78	6.65
0.6		140	37.1	37.2	37.1	37.3	37.2	37.18	40.7	41.7	41.2	39.19	6.40
0.6		160	38	38.1	38	38.5	38.3	38.18	41.5	42.7	42.1	40.14	6.52
0.6		180	39.2	39.3	39.1	39.5	39.4	39.30	43.4	43.5	43.45	41.38	6.25
0.6		220	40.1	40	39.8	40.1	40	40.00	44.2	45.1	44.65	42.33	6.32
0.6		260	40.8	40.6	40.4	40.7	40.6	40.62	45.3	46.0	45.65	43.14	6.29

Table 26: For fill ratio .6 and inclination angle 180^0

fill ratio (V/Vmax)	angle (θ)	Time (min)	pressure (psi)	voltage (Volt)	current (amp)	Evaporator Temperature,Te (°C)								Max evaporator temp(°C)
						1	2	4	5	6	7	8	avg	
0.6		0	0	0	0	24.3	24.3	24.3	24.3	24.3	24.3	24.3	24.30	
0.6		10	0	100	0.4	27.2	27.4	27.4	27.3	27.2	27.5	27.3	27.33	
0.6		30	1	100	0.4	33	33.2	33.2	33.1	32.9	33.2	32.9	33.07	
0.6		50	2	100	0.4	38	37.7	38.2	37.8	38.2	37.9	38	37.97	
0.6		70	3	100	0.4	42.1	41.9	42.3	42	42.8	42	42.1	42.17	
0.6		90	4	100	0.4	45.7	45.5	45.9	46	46.1	45.7	45.6	45.79	
0.6	180	110	6	100	0.4	49.1	49	48.9	49.2	49	48.8	48.7	48.96	60.94
0.6		130	8	100	0.4	52	51.7	51.8	52	52.1	51.2	51	51.69	
0.6		160	10	100	0.4	54.8	54.4	54.7	55	55.5	54.9	54.9	54.89	
0.6		190	13	100	0.4	58	57.7	57	56.9	58	57.6	57.1	57.47	
0.6		220	16	100	0.4	58.6	58.5	59.3	59.6	60	59.3	58.4	59.10	
0.6		240	20	100	0.4	59.6	60.3	60.1	60.4	60.6	60.4	59	60.06	
0.6		260	22	100	0.4	60.7	60.5	60.6	61	61.7	61.5	60.6	60.94	

Table 27: For fill ratio .6 and inclination angle 180^0

fill ratio (V/Vmax)	angle (θ)	Time (min)	Condenser tipTemperature, Tc(°C)						Adiabatic Position Temperature (°C)			Average condenser tempTc(°C)	Te-Tc (°C)
			1	2	3	4	5	avg	6	8	avg		
0.6		0	24.3	24.3	24.3	24.3	24.3	24.30	24.3	24.3	24.3	24.30	0.00
0.6		10	24.8	24.9	24.8	24.7	24.6	24.76	26.6	26	26.3	25.53	1.80
0.6		30	25.6	25.7	25.5	25.4	25.6	25.56	29	29	29	27.28	5.79
0.6		50	26.5	26.8	26.5	26.5	26.7	26.60	34.2	34.9	34.55	30.58	7.40
0.6		70	27.3	27.9	26.8	28.4	27.1	27.50	36.8	37.9	37.35	32.43	9.75
0.6		90	27.6	28.5	28.3	28.9	29.6	28.58	38	39.3	38.65	33.62	12.17
0.6	180	110	29.1	29.1	29	29.5	30.6	29.46	39	39.8	39.4	34.43	14.53
0.6		130	30	30.1	29.9	30.4	30.7	30.22	40.4	41.2	40.8	35.51	16.18
0.6		160	31.9	31.8	30.1	31.4	31.5	31.34	40.9	41.4	41.15	36.25	18.64
0.6		190	32.6	32	31.5	32.3	32.4	32.16	41.6	42.3	41.95	37.06	20.42
0.6		220	33.4	33.6	32.9	33.3	33.8	33.40	42.2	43.2	42.7	38.05	21.05
0.6		240	34.5	34.2	34.6	34.2	34.6	34.42	42.8	43.8	43.3	38.86	21.20
0.6		260	35.3	35.8	35.8	35.1	35.5	35.50	43.1	43.8	43.45	39.48	21.47

Table 28: For fill ratio .8 and inclination angle 0^0(Vertical)

fill ratio (V/Vmax)	angle (θ)	Time (min)	pressure (psi)	voltage (Volt)	current (amp)	Evaporator Temperature,Te(°C)								Max evaporator temp(°C)
						1	2	4	5	6	7	8	avg	
0.8		0	0	0	0	26.8	26.8	26.8	26.8	26.8	26.8	26.8	26.80	
0.8		10	0	100	0.4	29.4	29.9	29.1	29.3	29.2	29.4	29.8	29.44	
0.8		30	2	100	0.4	33.4	33.8	33.5	33.4	33.6	33.5	33.7	33.56	
0.8		50	5	100	0.4	37.1	37	37.2	36.8	37.3	37.2	37.1	37.10	
0.8		70	5	100	0.4	40.2	40.1	40	39.5	40.4	40.3	40.1	40.09	
0.8		90	7	100	0.4	42.4	42.3	42.1	41.8	41.9	42	42.1	42.09	
0.8	0	120	10	100	0.4	44.3	44.4	44.6	44.5	44.6	44.7	44.8	44.56	49.04
0.8		150	12	100	0.4	46.7	46.1	45.9	45.7	46	46.1	46.1	46.09	
0.8		180	13	100	0.4	47.8	47.5	47.4	46.6	47.1	47.8	46.9	47.30	
0.8		200	14	100	0.4	48.4	48.3	48.4	47.6	47.9	48.3	47.1	48.00	
0.8		220	14	100	0.4	48.9	48.9	48.9	48.3	48.2	48.4	47.8	48.49	
0.8		240	16	100	0.4	49	49.1	49	48.6	48.7	49.1	48.1	48.80	
0.8		260	17	100	0.4	49.1	49.1	49.2	48.8	48.9	49.3	48.9	49.04	

Table 29: For fill ratio .8 and inclination angle 0^0(Vertical)

fill ratio (V/Vmax)	angle (θ)	Time (min)	Condenser tipTemperature, Tc(°C)						Adiabatic Position Temperature(°C)			Average condenser tempTc(°C)	Te-Tc (°C)
			1	2	3	4	5	avg	6	8	avg		
0.4		0	25.4	25.4	25.4	25.4	25.4	25.40	25.4	25.4	25.4	25.40	0.00
0.4		10	26.1	26.3	26.1	25.9	25.9	26.06	27.1	27	27.05	26.56	1.73
0.4		30	28.8	28.7	28.7	28.8	28.8	28.76	30.5	32.3	31.4	30.08	2.75
0.4		50	32.2	32	32.2	32.1	32	32.10	34.4	35.7	35.05	33.58	2.75
0.4		70	34	33.8	34.2	34.1	34	34.02	38.1	39.5	38.8	36.41	2.62
0.4		90	36.5	36.2	36.4	36.7	36.6	36.48	39.7	41.5	40.6	38.54	2.89
0.4	0	120	38.5	38.3	38.5	38.5	38.6	38.48	42	43.4	42.7	40.59	2.88
0.4		150	40.3	40	40.2	40.3	40.3	40.22	43.3	44.8	44.05	42.14	3.04
0.4		180	41.4	41.1	41.1	41.3	41.5	41.28	44.6	45.5	45.05	43.17	3.15
0.4		200	41.9	41.4	41.2	41.5	41.9	41.58	45.3	46	45.65	43.62	3.17
0.4		220	42	41.5	41.6	42	42.3	41.88	45.5	46.7	46.1	43.99	3.02
0.4		240	41.2	41.6	42	42.1	42.5	41.88	46	47	46.5	44.19	3.00
0.4		260	42.3	41.9	42.2	42.4	42.6	42.28	46	47.3	46.65	44.47	2.86

Table 30: For fill ratio .8 and inclination angle 30^0

fill ratio (V/Vmax)	angle (θ)	Time (min)	pressure (psi)	voltage (Volt)	current (amp)	Evaporator Temperature,Te (°C)								Max evaporator temp(°C)
						1	2	4	5	6	7	8	avg	
0.8		0	0	0	0	27	27	27	27	27	27	27	27	
0.8		10	0	100	0.4	30	30.2	29.8	29.2	29.7	29.6	30.1	29.80	
0.8		30	2	100	0.4	34.5	34.1	34.8	33.3	34.7	34	34.7	34.30	
0.8		50	5	100	0.4	37	37.5	37.9	36.4	37.9	37.1	38.1	37.41	
0.8		70	6	100	0.4	38.2	38.6	39.1	38.8	40.1	39.6	40.7	39.30	
0.8		90	7	100	0.4	40.2	40.1	40.9	40.3	42	40.9	42	40.91	
0.8	30	120	8	100	0.4	42.9	43	43.1	42.4	43.5	42.7	44	43.09	49.06
0.8		150	9	100	0.4	44.9	45	45.1	44.9	45.1	44.7	45.1	44.97	
0.8		180	11	100	0.4	46.3	46.9	46.6	46.6	46.8	46.4	46.8	46.63	
0.8		200	12	100	0.4	47.6	47.5	47.9	47.5	47.7	47.3	47.7	47.60	
0.8		220	13	100	0.4	48.6	48.6	48.1	47.5	48.4	48.3	48.6	48.30	
0.8		240	14	100	0.4	48.9	48.8	48.6	47.9	49.3	48.9	49	48.77	
0.8		260	17	100	0.4	49.3	49.1	48.9	48.1	49.6	49.1	49.3	49.06	

Table 31: For fill ratio .8 and inclination angle 30^0

fill ratio (V/Vmax)	angle (θ)	Time (min)	Condenser tipTemperature, Tc(°C)						Adiabatic Position Temperature (°C)			Average condenser tempTc(°C)	Te-Tc (°C)
			1	2	3	4	5	avg	6	8	avg		
0.8		0	27	27	27	27	27	27	27	27	27	27.00	0.00
0.8		10	27.4	27.8	27.6	27.2	27.4	27.48	27.4	27.8	27.6	27.54	2.26
0.8		30	31	31	30.7	30.8	30.7	30.84	33.2	32.5	32.85	31.85	2.46
0.8		50	33.2	33.6	33.4	33	33.9	33.42	35.3	36	35.65	34.54	2.88
0.8		70	34.5	34.6	34.7	34.2	34.1	34.42	37.1	38.9	38	36.21	3.09
0.8		90	36.1	36.4	35.6	36.3	36.8	36.24	39.2	40.7	39.95	38.10	2.82
0.8	30	120	38.7	38.1	38.9	39.3	38.1	38.62	42.5	41.8	42.15	40.39	2.70
0.8		150	40.6	40.9	40.1	41.1	40.5	40.64	43.2	44.5	43.85	42.25	2.73
0.8		180	41	41.2	40.9	41.9	41	41.20	45.1	46.4	45.75	43.48	3.15
0.8		200	41.5	41.7	41.1	42	42	41.66	46	47.3	46.65	44.16	3.45
0.8		220	41.9	42	41.5	42.2	42.3	41.98	47.6	48.6	48.1	45.04	3.26
0.8		240	42	42.2	41.9	42.4	42.3	42.16	48.2	49.2	48.7	45.43	3.34
0.8		260	42.2	42.3	42	42.4	43.5	42.48	48.5	49.2	48.85	45.67	3.39

Table 32: For fill ratio .8 and inclination angle45^0

fill ratio (V/Vmax)	angle (θ)	Time (min)	pressure (psi)	voltage (Volt)	current (amp)	Evaporator Temperature,Te (°C)								Max evaporator temp(°C)
						1	2	4	5	6	7	8	avg	
0.8		0	0	0	0	27.1	27.1	27.1	27.1	27.1	27.1	27.1	27.10	
0.8		10	0	100	0.4	30.2	30.4	29.9	29.7	29.9	29.6	30.1	29.97	
0.8		30	2	100	0.4	34.6	34.8	34	34.1	34.7	34.1	35	34.47	
0.8		50	5	100	0.4	37.2	38.6	37.3	37.8	37.4	37.6	38	37.70	
0.8		70	6	100	0.4	38.9	40.2	39.7	39.1	40.1	39.6	40.6	39.74	
0.8		90	7	100	0.4	41.1	41.1	42	41	41.4	41.3	41.9	41.40	
0.8	45	120	8	100	0.4	43.7	43.4	43.7	43.3	43.6	43.2	43.8	43.53	49.37
0.8		150	11	100	0.4	45.2	45.1	45.8	45.5	45.7	45.1	45.9	45.47	
0.8		180	12	100	0.4	47.1	46.4	48.2	46.8	47	47.1	47.5	47.16	
0.8		200	13	100	0.4	47.9	47	48.5	47.8	48.2	47.9	48	47.90	
0.8		220	14	100	0.4	48.3	47.9	50.1	48.1	49.3	48.6	48.9	48.74	
0.8		240	16	100	0.4	48.6	48.7	50.2	48.3	49.4	48.9	49.4	49.07	
0.8		260	18	100	0.4	49.1	49.1	50.2	48.9	49.4	49.3	49.6	49.37	

Table 33: For fill ratio .8 and inclination angle45^0

fill ratio (V/Vmax)	angle (θ)	Time (min)	Condenser tipTemperature, Tc(°C)						Adiabatic Position Temperature (°C)			Average condenser tempTc(°C)	Te-Tc (°C)
			1	2	3	4	5	avg	6	8	avg		
0.8		0	27.1	27.1	27.1	27.1	27.1	27.10	27.1	27.1	27.1	27.10	0.00
0.8		10	27.4	27.8	27.6	27.2	27.4	27.48	27.4	27.8	27.6	27.54	2.43
0.8		30	31.1	32	29.8	29.6	31.6	30.82	33.2	32.5	32.85	31.84	2.64
0.8		50	32.4	32.6	31.6	30.9	31.8	31.86	34.3	35	34.65	33.26	4.44
0.8		70	33.7	33.7	33.4	32.9	33.1	33.36	35.4	35.9	35.65	34.51	5.24
0.8		90	34	35.4	34.1	34.2	34.8	34.50	37.1	37.6	37.35	35.93	5.47
0.8	45	120	36.3	37.1	36.2	36.2	36.8	36.52	37.5	38	37.75	37.14	6.39
0.8		150	38.1	38.6	38	38.5	38.2	38.28	38.2	39	38.6	38.44	7.03
0.8		180	39.9	39.5	39.1	40.2	39.9	39.72	39.3	40.9	40.1	39.91	7.25
0.8		200	40.5	40.2	40.1	41.1	40.3	40.44	41	41.9	41.45	40.95	6.95
0.8		220	41.5	41.6	40.8	41.3	41	41.24	42.6	43.1	42.85	42.05	6.70
0.8		240	41.8	41.4	41.1	42	41.1	41.48	44.2	45.2	44.7	43.09	5.98
0.8		260	42	41.5	41.4	42.3	41.4	41.72	44.9	45.3	45.1	43.41	5.96

Table 34: For fill ratio .8 and inclination angle 60^0

fill ratio (V/Vmax)	angle (θ)	Time (min)	pressure (psi)	voltage (Volt)	current (amp)	Evaporator Temperature,Te (°C)								Max evaporator temp(°C)
						1	2	4	5	6	7	8	avg	
0.8		0	0	0	0	28	28	28	28	28	28	28	28.00	
0.8		10	0	100	0.4	31.2	31.4	30.9	30.3	30.9	30.6	31.1	30.91	
0.8		30	2	100	0.4	35	35.2	35.9	36.3	35.8	35.1	36.9	35.74	
0.8		50	5	100	0.4	38.1	38.4	38.7	39.4	38.8	38.9	39.4	38.81	
0.8		70	6	100	0.4	39.8	40	40.2	41	41.3	40.8	41.8	40.70	
0.8		90	7	100	0.4	41.8	42.2	41.1	41.6	42.7	44.1	42.9	42.34	
0.8	60	120	9	100	0.4	44.2	44.6	44.2	44.5	44.1	46	46	44.80	51.06
0.8		150	11	100	0.4	47	48.1	47.1	46.6	46.7	47	47.8	47.19	
0.8		180	12	100	0.4	49.4	49.8	48.8	47.3	48.3	49.1	48.9	48.80	
0.8		200	14	100	0.4	50.4	50.6	49.6	49.7	49.3	49.9	50.1	49.94	
0.8		220	14	100	0.4	51.3	50.8	50.1	50.5	50.1	50.4	50.7	50.56	
0.8		240	18	100	0.4	51.5	51	50.3	50.6	50.6	50.8	50.9	50.81	
0.8		260	20	100	0.4	51.7	51.3	50.8	50.8	50.7	51	51.1	51.06	

Table 35: For fill ratio .8 and inclination angle 60^0

fill ratio (V/Vmax)	angle (θ)	Time (min)	Condenser tipTemperature, Tc(°C)						Adiabatic Position Temperature (°C)			Average condenser tempTc(°C)	Te-Tc (°C)
			1	2	3	4	5	avg	6	8	avg		
0.8		0	28	28	28	28	28	28	28	28	28	28.00	0.00
0.8		10	28.4	28.8	28.6	28.3	28.3	28.48	29.4	29.8	29.6	29.04	1.87
0.8		30	32.1	33	30.8	30.6	32.6	31.82	32	32.5	32.25	32.04	3.71
0.8		50	33.4	33.6	32.6	30.9	32.8	32.66	33.1	34	33.55	33.11	5.71
0.8		70	34.7	35.1	34.4	32.2	34.1	34.10	33.9	34.9	34.4	34.25	6.45
0.8		90	35	36.4	35.1	33.2	35.8	35.10	35.1	35.7	35.4	35.25	7.09
0.8	60	120	36.3	38.9	37.9	37.1	38	37.64	36.9	36.7	36.8	37.22	7.58
0.8		150	37.1	39.1	38.4	37.2	38.2	38.00	38.1	38.6	38.35	38.18	9.01
0.8		180	37.9	39.7	39.7	38.3	38.9	38.90	39.3	40.1	39.7	39.30	9.50
0.8		200	38.8	40	40.1	39.5	39.4	39.56	40.2	41.6	40.9	40.23	9.71
0.8		220	39	40.5	40.6	40.1	40.2	40.08	41.2	42.7	41.95	41.02	9.54
0.8		240	39.5	40.6	41	40.4	40.4	40.38	43	44.6	43.8	42.09	8.72
0.8		260	40.5	40.9	41.2	40.7	40.7	40.80	44	44.1	44.05	42.43	8.63

Table 36: For fill ratio .8 and inclination angle 90^0

fill ratio (V/Vmax)	angle (θ)	Time (min)	pressure (psi)	voltage (Volt)	current (amp)	Evaporator Temperature,Te(°C)								Max evaporator temp(°C)
						1	2	4	5	6	7	8	avg	
0.8		0	0	0	0	27 .2	27.2	27.2	27.2	27.2	27.2	27.2	27.20	
0.8		10	0	100	0.4	30	30.1	30.1	30.3	30.2	30	30.1	30.11	
0.8		30	1	100	0.4	34.7	34.8	34.9	34.6	35.2	34.9	35	34.87	
0.8		50	4	100	0.4	38.9	39.1	38.6	38.8	38.7	38.9	39	38.86	
0.8		70	5	100	0.4	42.1	42	41.8	42.4	42.5	42.1	42.2	42.16	
0.8		90	9	100	0.4	45.1	45	45.3	45	45.2	45.1	45.3	45.14	
0.8	90	130	15	100	0.4	49.7	49.6	50.4	50	50.7	50.9	50.1	50.20	58.61
0.8		160	22	100	0.4	53.6	53.4	53.2	53.8	53.6	53.9	53.4	53.56	
0.8		180	25	100	0.4	55.5	55.4	55.5	55.7	55.6	55.7	55.4	55.54	
0.8		200	28	100	0.4	57.5	57.6	57.5	57.4	57.4	57.1	57.1	57.37	
0.8		220	30	100	0.4	57.9	58.1	57.9	58.2	58.3	57.6	57.9	57.99	
0.8		240	32	100	0.4	58.3	58.4	58.2	58.3	58.5	58	58.7	58.34	
0.8		260	33	100	0.4	59	58.7	58.7	58.3	58.6	58.1	58.9	58.61	

Table 37: For fill ratio .8 and inclination angle 90^0

fill ratio (V/Vmax)	angle (θ)	Time (min)	Condenser tipTemperature, Tc(°C)						Adiabatic Position Temperature(°C)			Average condenser tempTc(°C)	Te-Tc (°C)
			1	2	3	4	5	avg	6	8	avg		
0.8		0	27.2	27.2	27.2	27.2	27.2	27.20	27.2	27.2	27.2	27.20	0.00
0.8		10	27.3	27.6	27.5	27.5	27.9	27.56	28.5	28	28.25	27.91	2.21
0.8		30	28	28.3	28.4	28.2	28.5	28.28	30.1	30	30.05	29.17	5.71
0.8		50	29.9	29.8	29.8	28.9	29.1	29.50	35.1	35.5	35.3	32.40	6.46
0.8		70	30.9	30	31.2	29.5	30.1	30.34	36.2	36.6	36.4	33.37	8.79
0.8		90	31.7	30.9	31.9	30.4	31	31.18	37.8	38.3	38.05	34.62	10.53
0.8	90	130	32.4	31.5	32.1	31.2	31.9	31.82	39.6	39.4	39.5	35.66	14.54
0.8		160	33.5	32.7	33	32.5	32.8	32.90	40.9	41.1	41	36.95	16.61
0.8		180	34.2	33.4	34	33.7	33.8	33.82	42.4	42.3	42.35	38.09	17.46
0.8		200	34.5	34.6	35.1	34.7	34.9	34.76	43.7	43.7	43.7	39.23	18.14
0.8		220	35.4	35.5	36	35.4	35.3	35.52	44.6	44.8	44.7	40.11	17.88
0.8		240	36	35.9	36.1	35.9	35.8	35.94	45.5	46	45.75	40.85	17.50
0.8		260	36.4	36.2	36.3	36	36.1	36.20	46.1	46.8	46.45	41.33	17.29

Table 38: For fill ratio .8 and inclination angle180^0

fill ratio (V/Vmax)	angle (θ)	Time (min)	pressure (psi)	voltage (Volt)	current (amp)	Evaporator Temperature,Te (celcius)								Max evaporator temp(°C)
						1	2	4	5	6	7	8	avg	
0.8		0	0	0	0	24.5	24.5	24.5	24.5	24.5	24.5	24.5	24.50	
0.8		10	0	100	0.4	27.4	27.4	27.3	27.5	27.3	27.5	27.5	27.41	
0.8		30	1	100	0.4	32.3	32.4	32.2	32.2	32.4	32.4	32.3	32.31	
0.8		50	4	100	0.4	36.7	36.5	36.5	36.6	36.7	36.2	36.5	36.53	
0.8		70	8	100	0.4	40.4	40.3	40.2	40.3	40.5	40.2	40.3	40.31	
0.8		90	12	100	0.4	44	43.8	43.4	43.5	44	43.5	43.8	43.71	
0.8	180	120	15	100	0.4	48.3	48	47.8	48	48.2	47.9	48.2	48.06	61.26
0.8		150	21	100	0.4	51.9	52	51.2	51.8	52	51.8	51.9	51.80	
0.8		180	26	100	0.4	55	55.1	54.7	54.9	55.1	54.8	55.2	54.97	
0.8		210	29	100	0.4	57.7	57.8	57.5	57.6	57.8	57.3	57.9	57.66	
0.8		230	32	100	0.4	59.3	59.4	59.2	59.3	59.5	59	59.2	59.27	
0.8		250	33	100	0.4	60.9	61	60.7	60.8	60.1	60.5	60.3	60.61	
0.8		260	35	100	0.4	61.4	61.8	61.2	61.4	61.1	61	60.9	61.26	

Table 39: For fill ratio .8 and inclination angle180^0

fill ratio (V/Vmax)	angle (θ)	Time (min)	Condenser tipTemperature, Tc(°C)						Adiabatic Position Temperature (°C)			Average condenser tempTc(°C)	Te-Tc (°C)
			1	2	3	4	5	avg	6	8	avg		
0.8		0	24.5	24.5	24.5	24.5	24.5	24.50	24.5	24.5	24.5	24.50	0.00
0.8		10	24.9	24.7	24.8	24.8	24.8	24.80	25.5	25.6	25.55	25.18	2.24
0.8		30	25.1	25.4	25.7	25.5	25.4	25.42	27.4	27.5	27.45	26.44	5.88
0.8		50	25.9	26.5	26	26.2	25.4	26.00	29.5	29.1	29.3	27.65	8.88
0.8		70	26.7	27.1	26.2	26.3	26.2	26.50	31.7	30.2	30.95	28.73	11.59
0.8		90	28	28.9	27	27.9	28.5	28.06	33.9	33	33.45	30.76	12.96
0.8	180	120	28.6	29.1	28.6	27.9	28	28.44	35.1	34.9	35	31.72	16.34
0.8		150	29.5	29.9	29.9	28.8	28.9	29.40	36.4	36.1	36.25	32.83	18.98
0.8		180	31	29.8	30.2	29.5	29.5	30.00	37.1	37.2	37.15	33.58	21.40
0.8		210	32.4	30	31.2	30.5	30.1	30.84	38	38.2	38.1	34.47	23.19
0.8		230	33.6	31.1	31.9	31.3	31.4	31.86	38.8	39	38.9	35.38	23.89
0.8		250	34	31.9	32.6	32.1	32.6	32.64	39.8	40.1	39.95	36.30	24.32
0.8		260	33.9	32.2	33.2	32.6	32.9	32.96	40.4	40.7	40.55	36.76	24.50

CALCULATION FOR HEAT TRANSFER

Condenser length : 4680.00 mm Surface area of condenser A_c sq : 0.0588 sq m

Adiabatic length : 1680 .00 mm Surface area of evaporator A_e sq : 0.0314 sq m

Q : 36 Watt

Table 40: For fill ratio .4 and inclination angle 0^0(Vertical position)

fill ratio (V/Vmax)	angle (θ)	Time (min)	Q elect (W)	Q block (W)	Q wall (W)	Qphp (W)	Qcon (W)	R (°C/W)	Overall U_{php} (W/m² °C)
0.4	0	0	36	0.000	0.000	0.000	0.000	0.000	0.000
0.4		10		32.464	0.357	3.179	1.341	0.544	119.661
0.4		30		25.554	0.652	9.794	6.225	0.281	232.143
0.4		50		19.688	0.678	15.635	11.336	0.176	369.899
0.4		70		15.188	0.803	20.010	15.377	0.131	497.812
0.4		90		13.500	0.793	21.707	18.516	0.133	489.556
0.4		120		7.661	0.800	27.539	21.522	0.105	622.634
0.4		150		6.375	0.794	28.831	23.799	0.105	618.573
0.4		180		4.286	0.807	30.907	25.299	0.102	639.350
0.4		200		2.652	0.834	32.514	25.933	0.098	668.035
0.4		220		1.286	0.823	33.891	26.496	0.089	730.053
0.4		240		0.964	0.850	34.185	26.762	0.088	743.408
0.4		260		0.804	0.809	34.387	27.207	0.083	782.308

Table 41: For fill ratio .4 and inclination angle 30^0

fill ratio (V/Vmax)	angle (θ)	Time (min)	Q elect (W)	Q block (W)	Q wall (W)	Qphp (W)	Qcon (W)	R (°C/W)	Overall U_{php} (W/m² °C)
0.4	30	0	36	0.000	0.000	0.000	0.000	0.000	0.000
0.4		10		32.143	0.365	3.492	1.016	0.549	118.667
0.4		20		26.679	0.671	8.650	3.069	0.310	209.989
0.4		40		23.223	0.711	12.066	9.627	0.192	338.493
0.4		60		18.000	0.746	17.254	13.802	0.154	423.012
0.4		80		14.143	0.736	21.121	17.325	0.132	494.698
0.4		100		10.205	0.725	25.069	19.855	0.115	566.930
0.4		130		7.018	0.730	28.252	22.745	0.098	661.537
0.4		160		5.250	0.718	30.032	24.874	0.091	713.491
0.4		190		3.482	0.738	31.780	26.066	0.090	727.522
0.4		210		2.089	0.730	33.180	26.676	0.085	770.023
0.4		230		1.446	0.736	33.817	27.273	0.078	830.000
0.4		260		0.804	0.745	34.451	27.529	0.078	834.782

Table 42: For fill ratio .4 and inclination angle 45^0

fill ratio (V/Vmax)	angle (θ)	Time (min)	Q elect (W)	Q block (W)	Q wall (W)	Qphp (W)	Qcon (W)	R (°C/W)	Overall U_{php} (W/m² °C)
0.4		0		0.000	0.000	0.000	0.000	0.000	0.000
0.4		10		32.625	0.388	2.987	1.361	0.572	113.801
0.4		20		28.607	0.686	6.706	2.921	0.446	146.224
0.4		40		24.589	0.775	10.636	11.003	0.169	385.090
0.4		60		19.205	0.876	15.918	14.451	0.176	370.548
0.4		80		13.420	0.820	21.761	17.733	0.137	474.234
0.4	45	100	36	9.723	0.914	25.363	20.607	0.106	612.443
0.4		130		6.589	0.946	28.465	22.567	0.109	598.190
0.4		160		5.786	0.920	29.294	24.355	0.118	554.301
0.4		190		3.482	0.922	31.596	25.912	0.105	621.592
0.4		210		3.214	0.924	31.862	27.166	0.095	685.530
0.4		230		1.848	0.944	33.208	27.440	0.095	685.376
0.4		260		1.393	0.956	33.651	28.089	0.091	712.268

Table 43: For fill ratio .4 and inclination angle 60^0

fill ratio (V/Vmax)	angle (θ)	Time (min)	Q elect (W)	Q block (W)	Q wall (W)	Qphp (W)	Qcon (W)	R (°C/W)	Overall U_{php} (W/m² °C)
0.4		0		0.000	0.000	0.000	0.000	0.000	0.000
0.4		10		33.107	0.401	2.492	0.951	0.812	80.246
0.4		20		29.571	0.713	5.715	2.497	0.593	109.944
0.4		40		24.268	0.838	10.895	9.603	0.255	255.237
0.4		60		17.036	0.922	18.042	13.376	0.176	369.115
0.4		80		14.304	1.022	20.674	15.642	0.199	327.133
0.4	60	100	36	10.125	1.089	24.786	19.014	0.144	451.389
0.4		130		7.339	1.086	27.575	21.831	0.131	496.341
0.4		160		5.304	1.210	29.487	23.427	0.131	497.191
0.4		190		4.661	1.076	30.264	25.714	0.120	541.423
0.4		210		4.179	1.083	30.739	26.625	0.122	532.685
0.4		230		2.25	1.0729	32.6771	27.52396	0.109	598.934
0.4		260		1.285714	1.0702	33.6441	28.01165	0.106	614.436

Table 44: For fill ratio .4 and inclination angle 90^0 (Horizontal position)

fill ratio (V/Vmax)	angle (θ)	Time (min)	Q elect (W)	Q block (W)	Q wall (W)	Qphp (W)	Qcon (W)	R (°C/W)	Overall U_{php} (W/m² °C)
0.4		0		0.000	0.000	0.000	0.000	0.000	0.000
0.4		10		32.550	0.449	3.001	0.323	0.858	75.930
0.4		30		25.125	1.033	9.842	2.082	0.586	111.203
0.4		50		19.500	1.330	15.170	4.144	0.519	125.492
0.4		70		15.075	1.467	19.458	7.990	0.413	157.735
0.4		90		11.175	1.648	23.177	10.895	0.348	187.218
0.4	90	120	36	10.100	1.716	24.184	14.471	0.350	185.994
0.4		150		8.150	1.695	26.155	17.696	0.330	197.686
0.4		180		6.900	1.793	27.307	20.360	0.319	204.226
0.4		200		6.075	1.866	28.059	21.646	0.319	204.401
0.4		220		4.275	1.926	29.799	23.636	0.281	232.152
0.4		240		3.225	1.992	30.783	23.974	0.283	230.464
0.4		260		1.050	1.938	33.012	24.499	0.260	250.612

Table 45: For fill ratio .4 and inclination angle 180^0

fill ratio (V/Vmax)	angle (θ)	Time (min)	Q elect (W)	Q block (W)	Q wall (W)	Qphp (W)	Qcon (W)	R (°C/W)	Overall U_{php} (W/m² °C)
0.4		0		0	0.0000	0.0000	0	0.000	0.000
0.4		10		33.6	0.4327	1.9673	1.404169	0.991	65.723
0.4		30		29.175	1.1888	5.6362	2.881819	1.062	61.328
0.4		50		25.275	1.8417	8.8833	4.09512	1.073	60.716
0.4		70		21.75	2.2717	11.9783	6.574786	0.976	66.728
0.4		90		18.075	2.7562	15.1688	9.374687	0.851	76.591
0.4	180	110	36	16.2	3.1097	16.6903	10.91686	0.881	73.977
0.4		130		14.325	3.3771	18.2979	11.75892	0.911	71.502
0.4		160		11.5	3.6217	20.8783	13.028	0.907	71.862
0.4		190		9.35	4.0402	22.6098	13.31483	0.934	69.746
0.4		220		7.6	4.2536	24.1464	14.1595	0.935	69.696
0.4		240		5.55	4.2916	26.1584	14.94442	0.882	73.876
0.4		260		3.225	4.2554	28.5196	15.92844	0.808	80.652

Table 46: For fill ratio .6 and inclination angle 0^0(Vertical position)

fill ratio (V/Vmax)	angle (θ)	Time (min)	Q elect (W)	Q block (W)	Q wall (W)	Qphp (W)	Qcon (W)	R (°C/W)	Overall U_{php} (W/m² °C)
0.6		0		0.000	0.000	0.000	0.000	0.000	0.000
0.6		10		32.304	0.380	3.316	1.126	0.557	117.008
0.6		20		28.446	0.699	6.855	3.335	0.387	168.197
0.6		40		20.009	0.798	15.193	7.821	0.204	320.098
0.6		60		16.554	0.795	18.651	12.754	0.144	453.384
0.6		80		11.813	0.805	23.383	16.154	0.105	619.230
0.6	0	100	36	8.518	0.759	26.723	18.698	0.085	765.480
0.6		120		8.357	0.776	26.867	20.687	0.089	730.809
0.6		140		6.589	0.822	28.588	22.058	0.091	715.919
0.6		180		4.902	0.813	30.285	24.639	0.086	760.496
0.6		210		3.911	0.817	31.272	25.936	0.088	740.248
0.6		230		2.089	0.803	33.108	26.545	0.082	793.377
0.6		260		1.339	0.802	33.858	26.994	0.082	796.091

Table 47: For fill ratio .6 and inclination angle 30^0

fill ratio (V/Vmax)	angle (θ)	Time (min)	Q elect (W)	Q block (W)	Q wall (W)	Qphp (W)	Qcon (W)	R (°C/W)	Overall U_{php} (W/m² °C)
0.6		0		0.000	0.000	0.000	0.000	0.000	0.000
0.6		20		29.700	0.564	5.736	3.778	0.405	160.717
0.6		40		21.488	0.773	13.740	6.928	0.281	231.893
0.6		60		16.875	0.843	18.282	11.824	0.190	342.241
0.6		80		13.050	0.779	22.171	17.046	0.103	630.724
0.6		100		11.363	0.756	23.881	20.162	0.092	705.557
0.6	30	120	36	9.787	0.840	25.373	22.261	0.097	671.922
0.6		140		7.313	0.824	27.864	23.747	0.099	657.684
0.6		160		5.963	0.862	29.175	25.082	0.099	658.804
0.6		180		3.600	0.805	31.595	26.536	0.081	799.346
0.6		200		2.813	0.811	32.377	27.051	0.084	775.442
0.6		220		1.350	0.805	33.845	27.594	0.077	849.670
0.6		260		1.069	0.805	34.127	28.057	0.078	835.796

Table 48: For fill ratio .6 and inclination angle 45^0

fill ratio (V/Vmax)	angle (θ)	Time (min)	Q elect (W)	Q block (W)	Q wall (W)	Qphp (W)	Qcon (W)	R (°C/W)	Overall U_{php} (W/m² °C)
0.6		0		0.000	0.000	0.000	0.000	0.000	0.000
0.6		20		30.375	0.542	5.083	4.212	0.426	152.959
0.6		40		22.500	0.917	12.583	8.767	0.223	291.725
0.6		60		19.446	0.987	15.567	12.459	0.238	273.556
0.6		80		14.143	0.986	20.871	17.288	0.141	463.038
0.6		100		11.330	0.966	23.704	20.056	0.130	501.252
0.6	45	120	36	8.759	0.978	26.263	22.343	0.117	556.787
0.6		140		7.152	0.996	27.852	24.427	0.105	622.610
0.6		160		5.384	1.021	29.595	25.467	0.106	612.755
0.6		180		4.259	0.979	30.762	26.736	0.100	653.080
0.6		200		3.295	0.996	31.709	27.439	0.100	652.830
0.6		220		1.688	0.990	33.323	28.247	0.088	743.626
0.6		260		1.286	0.973	33.741	28.821	0.089	733.575

Table 49: For fill ratio .6 and inclination angle 60^0

fill ratio (V/Vmax)	angle (θ)	Time (min)	Q elect (W)	Q block (W)	Q wall (W)	Qphp (W)	Qcon (W)	R (°C/W)	Overall U_{php} (W/m² °C)
0.6		0		0.000	0.000	0.000	0.000	0.000	0.000
0.6		20		29.813	0.519	5.668	3.823	0.414	157.468
0.6		40		21.536	0.941	13.524	7.810	0.235	277.610
0.6		60		17.438	1.053	17.510	12.254	0.181	359.434
0.6		80		13.982	1.031	20.987	16.111	0.145	448.366
0.6		100		11.009	1.028	23.964	19.075	0.125	521.866
0.6	60	120	36	8.920	1.035	26.045	21.522	0.112	583.651
0.6		140		6.991	1.019	27.990	23.110	0.110	592.016
0.6		160		6.188	1.010	28.803	24.523	0.112	581.825
0.6		180		5.223	1.034	29.743	25.624	0.114	571.820
0.6		200		4.259	1.043	30.698	26.864	0.107	606.811
0.6		220		2.732	1.066	32.202	27.604	0.101	643.221
0.6		260		1.527	1.066	33.407	28.148	0.103	633.702

Table 50: For fill ratio .6 and inclination angle 90^0(Horizontal)

fill ratio (V/Vmax)	angle (θ)	Time (min)	Q elect (W)	Q block (W)	Q wall (W)	Qphp (W)	Qcon (W)	R (°C/W)	Overall U_{php} (W/m² °C)
0.6		0		0.000	0.000	0.000	0.000	0.000	0.000
0.6		12		31.875	0.465	3.660	0.931	0.669	97.326
0.6		20		28.728	0.754	6.519	1.553	0.594	109.650
0.6		40		24.589	1.297	10.113	3.751	0.631	103.280
0.6		60		17.116	1.253	17.631	7.373	0.396	164.387
0.6		80		15.509	1.371	19.120	11.568	0.356	182.926
0.6	90	100	36	11.652	1.450	22.898	14.487	0.299	218.068
0.6		120		7.554	1.389	27.057	16.803	0.246	265.119
0.6		140		6.509	1.347	28.144	18.917	0.227	286.670
0.6		160		6.027	1.359	28.615	20.302	0.228	286.034
0.6		180		5.464	1.335	29.201	22.141	0.214	304.197
0.6		220		2.853	1.385	31.762	23.486	0.199	327.512
0.6		260		2.210	1.412	32.378	24.650	0.194	335.155

Table 51: For fill ratio .6 and inclination angle 180^0

fill ratio (V/Vmax)	angle (θ)	Time (min)	Q elect (W)	Q block (W)	Q wall (W)	Qphp (W)	Qcon (W)	R (°C/W)	Overall U_{php} (W/m² °C)
0.6		0		0.000	0.000	0.000	0.000	0.000	0.000
0.6		10		34.071	0.412	1.517	1.396	1.186	54.944
0.6		30		30.150	1.204	4.646	3.175	1.247	52.263
0.6		50		25.725	1.823	8.452	7.399	0.875	74.448
0.6		70		22.050	2.351	11.599	9.588	0.840	77.526
0.6		90		18.975	2.758	14.267	10.931	0.853	76.369
0.6	180	110	36	16.650	3.125	16.225	11.761	0.895	72.761
0.6		130		14.325	3.440	18.235	13.033	0.887	73.438
0.6		160		11.200	3.774	21.026	13.780	0.887	73.483
0.6		190		9.050	4.057	22.893	14.687	0.892	73.049
0.6		220		5.700	4.119	26.181	16.087	0.804	81.026
0.6		240		5.025	4.109	26.866	17.287	0.789	82.569
0.6		260		4.650	4.078	27.272	18.222	0.787	82.760

Table 52: For fill ratio .8 and inclination angle 0^0(Vertical position)

fill ratio (V/Vmax)	angle (θ)	Time (min)	Q elect (W)	Q block (W)	Q wall (W)	Qphp (W)	Qcon (W)	R (°C/W)	Overall U_{php} (W/m² °C)
0.8		0		0.000	0.000	0.000	0.000	0.000	0.000
0.8		10		27.750	0.369	7.881	0.358	0.273	239.034
0.8		30		21.600	0.525	13.875	5.669	0.183	355.560
0.8		50		18.600	0.574	16.826	11.381	0.129	506.310
0.8		70		15.675	0.648	19.677	15.729	0.109	598.796
0.8		90		10.500	0.831	24.669	17.538	0.113	576.900
0.8	0	120	36	8.650	0.881	26.469	19.736	0.141	462.646
0.8		150		5.350	0.995	29.655	21.952	0.124	526.309
0.8		180		4.250	1.045	30.705	23.885	0.115	565.859
0.8		200		3.675	1.096	31.229	24.591	0.119	546.889
0.8		220		2.550	1.120	32.330	24.854	0.124	525.142
0.8		240		1.650	1.148	33.202	25.811	0.110	591.794
0.8		260		1.275	1.154	33.571	26.318	0.106	616.425

Table 53: For fill ratio .8 and inclination angle 30^0

fill ratio (V/Vmax)	angle (θ)	Time (min)	Q elect (W)	Q block (W)	Q wall (W)	Qphp (W)	Qcon (W)	R (°C/W)	Overall U_{php} (W/m² °C)
0.8		0		0.000	0.000	0.000	0.000	0.000	0.000
0.8		10		29.400	0.372	6.228	0.422	0.363	179.531
0.8		30		23.625	0.555	11.820	6.565	0.208	313.668
0.8		50		16.350	0.640	19.010	10.433	0.151	430.112
0.8		70		9.900	0.782	25.318	12.752	0.122	533.773
0.8		90		8.475	0.749	26.776	15.555	0.105	618.717
0.8	30	120	36	7.600	0.716	27.684	18.954	0.098	667.794
0.8		150		6.600	0.694	28.706	21.709	0.095	685.904
0.8		180		5.800	0.870	29.330	23.340	0.108	605.894
0.8		200		5.100	0.952	29.948	24.258	0.115	566.326
0.8		220		3.675	1.013	31.312	25.497	0.104	625.723
0.8		240		2.475	1.060	32.465	26.024	0.103	632.960
0.8		260		1.500	1.054	33.446	26.374	0.101	642.327

Table 54: For fill ratio .8 and inclination angle 45^0

fill ratio (V/Vmax)	angle (θ)	Time (min)	Q elect (W)	Q block (W)	Q wall (W)	Qphp (W)	Qcon (W)	R (°C/W)	Overall U_{php} (W/m² °C)
0.8		0		0.000	0.000	0.000	0.000	0.000	0.000
0.8		10		30.150	0.399	5.451	0.247	0.446	146.042
0.8		30		23.625	0.585	11.790	6.373	0.224	291.325
0.8		50		16.950	0.936	18.114	8.109	0.245	265.479
0.8		70		10.725	1.023	24.252	9.859	0.216	301.635
0.8		90		8.700	1.106	26.194	11.863	0.209	311.679
0.8	45	120	36	7.450	1.123	27.427	13.623	0.233	279.459
0.8		150		6.800	1.153	28.047	15.512	0.251	259.859
0.8		180		5.900	1.192	28.908	17.633	0.251	259.860
0.8		200		3.900	1.196	30.904	19.150	0.225	289.475
0.8		220		4.425	1.202	30.373	20.759	0.221	295.415
0.8		240		1.725	1.217	33.058	22.281	0.181	360.051
0.8		260		1.575	1.226	33.199	22.742	0.180	362.793

Table 55: For fill ratio .8 and inclination angle 60^0

fill ratio (V/Vmax)	angle (θ)	Time (min)	Q elect (W)	Q block (W)	Q wall (W)	Qphp (W)	Qcon (W)	R (°C/W)	Overall U_{php} (W/m² °C)
0.8		0		0.000	0.000	0.000	0.000	0.000	0.000
0.8		10		30.600	0.390	5.010	1.138	0.374	174.131
0.8		30		25.350	0.629	10.021	5.301	0.370	176.071
0.8		50		16.125	0.986	18.889	6.516	0.302	215.530
0.8		70		9.900	1.058	25.042	8.127	0.258	252.930
0.8		90		8.625	1.161	26.214	9.493	0.271	240.770
0.8	60	120	36	8.600	1.148	26.252	12.401	0.289	225.626
0.8		150		8.350	1.472	26.178	13.480	0.344	189.261
0.8		180		5.650	1.587	28.763	15.019	0.330	197.244
0.8		200		6.000	1.664	28.336	16.308	0.343	190.055
0.8		220		3.225	1.679	31.096	17.447	0.307	212.297
0.8		240		1.350	1.672	32.978	19.033	0.265	246.251
0.8		260		1.275	1.644	33.081	19.554	0.261	249.660

Table 56: For fill ratio .8 and inclination angle 90^0

fill ratio (V/Vmax)	angle (θ)	Time (min)	Q elect (W)	Q block (W)	Q wall (W)	Qphp (W)	Qcon (W)	R (°C/W)	Overall U_{php} (W/m² °C)
0.8		0		0.000	0.000	0.000	0.000	0.000	0.000
0.8		10		32.786	0.409	2.805	0.627	0.788	82.709
0.8		30		26.759	1.056	8.185	1.831	0.697	93.438
0.8		50		22.420	1.500	12.081	6.142	0.535	121.882
0.8		70		18.563	1.894	15.544	7.173	0.565	115.237
0.8		90		16.795	2.238	16.968	8.659	0.620	104.994
0.8	90	130	36	14.223	2.946	18.831	9.486	0.772	84.372
0.8		160		12.589	3.311	20.100	11.017	0.826	78.848
0.8		180		11.170	3.482	21.349	12.514	0.818	79.666
0.8		200		10.286	3.624	22.090	14.054	0.821	79.327
0.8		220		3.455	3.601	28.944	15.371	0.618	105.483
0.8		240		2.009	3.591	30.401	16.461	0.576	113.184
0.8		260		1.527	3.592	30.881	17.165	0.560	116.359

Table 57: For fill ratio .8 and inclination angle 180^0

fill ratio (V/Vmax)	angle (θ)	Time (min)	Q elect (W)	Q block (W)	Q wall (W)	Qphp (W)	Qcon (W)	R (°C/W)	Overall U_{php} (W/m² °C)
0.8		0		0.000	0.000	0.000	0.000	0.000	0.000
0.8		10		32.786	0.419	2.795	0.573	0.801	81.321
0.8		30		27.563	1.105	7.333	1.739	0.802	81.249
0.8		50		23.705	1.687	10.607	2.942	0.837	77.830
0.8		70		21.295	2.214	12.491	3.995	0.928	70.217
0.8		90		19.125	2.509	14.366	6.683	0.902	72.218
0.8	180	120	36	16.286	3.144	16.570	7.466	0.986	66.075
0.8		150		14.036	3.590	18.374	8.644	1.033	63.083
0.8		180		11.893	4.002	20.105	9.334	1.064	61.214
0.8		210		10.071	4.298	21.631	10.353	1.072	60.773
0.8		230		9.080	4.393	22.526	11.595	1.061	61.424
0.8		250		7.554	4.483	23.963	12.850	1.015	64.191
0.8		260		7.232	4.535	24.233	13.474	1.011	64.429

Table 58: Table of Q(W), U(W/m_2°C) and R(°C/W) at different inclination and fill ratio

Fill ratio		0°	30 °	45 °	60 °	90°	180 °
	Q(W)	34.387	34.451	33.651	33.644	33.012	28.52
	U(W/m² °C)	742.3	834.8	712.3	614.4	282.7	80.65
0.4	R(°C/W)	0.083	0.078	0.091	0.106	0.23	0.808
	Q(W)	33.858	34.127	33.741	33.407	32.378	27.272
	U(W/m² °C)	796.10	835.8	733.60	633.7	335.2	82.76
0.6	R(°C/W)	0.082	0.078	0.09	0.103	0.194	0.787
	Q(W)	33.571	33.556	33.20	33.081	30.881	24.232
	U(W/m² °C)	616.40	642.3	362.80	249.7	116.4	64.42
0.8	R(°C/W)	0.106	0.11	0.18	0.261	0.56	1.011

Table 59: Table for thermocouple calibration.

Thermocouple No	1	2	3	4	5	6	7
Thermocouple Reading	-5	-4.4	-3.6	-3.6	-3	-2.8	-3.6
	18.8	19	19.1	18.8	18.9	18.8	19.3
	44.2	44.2	43.2	44.5	44.4	44.5	44.8
	93.5	94.3	94.5	93.6	94.8	95.3	94.7
Thermometer Reading	-1	-1.1	-1.1	-1	-0.8	-0.5	-0.8
	24.1	24.1	24.2	24.1	24.2	24.3	24.4
	51.3	50.3	50.2	50.3	50.4	50.4	50.5
	99.3	99.4	99.3	99.4	99.5	99.6	99.7

Table 60: Table for thermocouple calibration.

Thermocouple No	8	9	10	11	12	13	14
Thermocouple Reading	-2.9	-2.9	-4.4	-4	-4.3	-3.9	-2.8
	19.1	19.5	19.3	19.4	19.5	19.4	19.3
	45	44.6	44.9	44.2	44.7	44.5	44.9
	93.2	94.5	92.7	93.4	94.1	93.5	92.6
Thermometer Reading	-0.7	-0.6	-0.4	-0.4	-0.3	-0.3	-0.4
	24.5	24.5	24.6	24.6	24.7	24.7	24.7
	50.5	50.5	50.6	50.6	50.7	50.7	50.7
	99.8	99.7	99.8	99.9	99.8	99.4	99.6

Table 61: Table for pressure gauge calibration.

No of data	1	2	3	4	5	6	7
Applied pressure(psig)	0	5	10	15	20	25	30
Pressure gauge reading(psig)	0	5	10	15	20	25	30

Table 62: Table for Vacuum pump calibration.

No of data	1	2
Assumed value(Psig)	14.7	0
Actual value(Psig)	14.7	3.7

Appendix C

Uncertainty Analysis

Experimental Uncertainty Analysis

Experimental uncertainty analysis provides a method for predicting the uncertainty of a variable based on its component uncertainties

Suppose we measure Jphysical quantities (or variables, like voltage, resistance, power, torque, temperature, etc.), X_1, X_2, ..., X_J. Also suppose that each of these quantities has a known *experimental uncertainty* associated with it, which we shall denote by U_{xi}, i.e $X_i=X[\ _i \pm U_{Xi}$

Furthermore, unless otherwise specified, each of these uncertainties has a confidence level of 95%. Since the *xi* variables are components of the calculated quantity, we call the uncertainties *component uncertainties*.

Suppose now that some new variable, *r*, is a function of these measured quantities, i.e., $r= r(X_1, X_2, ...,X_J.)$ The goal in experimental uncertainty analysis is to estimate the uncertainty in *r* to the same confidence level as that of the component uncertainties, i.e., we want to report *r* as $r= r[\ \pm U_r$, where U_r is the predicted uncertainty on variable *r*. There are two types of uncertainty on variable *r*

Maximum uncertainty – We define the maximum uncertainty on variable r as

$$U_{r,max} = \sum_{i=1}^{i=J} \left| U\square\square \frac{\partial r}{\partial Xi} \right|$$

Expected uncertainty– We define the expected uncertainty on variable *r* as

$$U_{r\,RSS} = \sqrt{\sum_{i=1}^{i=J} \left(U\square\square \frac{\partial r}{\partial Xi}\right)^2}.$$

General form of uncertainty

We use the RSS uncertainty as the standard for experimental uncertainty analysis in this course.

A simpler formula for RSS results if the functional form of $r = r(X_1, X_2, \ldots, X_J)$ (1) and the uncertainty in the experimental result is given by

$$U_r^2 = \left(\frac{\partial r}{\partial X_1}\right)^2 U_{X_1}^2 + \left(\frac{\partial r}{\partial X_2}\right)^2 U_{X_2}^2 + \cdots + \left(\frac{\partial r}{\partial X_J}\right)^2 U_{X_J}^2 \quad (2))$$

whereU_r is the uncertainty in the result, U_{XI} is the uncertainty in the variable X_1, etc. This is the most general form of the uncertainty propagation equation (Coleman and Steele 1999). When applying the uncertainty propagation equation, the individual uncertainties should all be expressed with the same odds, e.g., at 95% confidence. In the planning phase, this assumption is implicit. In addition, the measured variables and their uncertainties are assumed to be independent of one another.

Uncertainty in voltage

The electric power is calculated as

P = EI

where E and I are measured as

E = 100 V +/- 2 V

I =.4A +/- 0.01 A

The nominal value of the power is 100 x .4 = 40W. The uncertainty in this value is calculated by applying Eq. (2). The various terms are

$\partial P/\partial E = I = .4$

$\partial P/\partial I = E = 100$

$U_E = 2$ V

$U_I = 0.01$ A

Thus, the uncertainty in the electric power is

$U_p = [(.4)^2(2)^2 + (100)^2(0.01)^2]^{1/2}$ .8 W or 2.01 percent.

Uncertainty Analysis of Thermocouple, Type K, Chromel-Alumel

Thermocouple manufacturers adhere to the American Society for Testing Materials (ASTM) specification for calibration accuracy ("limits of error") for Type K TCs

0-1250°C (32-2300°F): ±2.°C or 0.75% of reading in °C, whichever is greater.

This is normally considered a systematic uncertainty. Random uncertainties are "fossilized" into the calibration bias. Specially calibrated thermocouple wire that can

provides accuracy to ±1.1°C or ±0.4% of reading in °C, whichever is greater "the 'limits of error' stated are definitive, not statistical. The above uncertainties should be considered a maximum, or 3σ (99.7%) limits.

Summary for Type K thermocouples:

B (systematic uncertainty) = ± 2°C and

S (random uncertainty) = 0

a. Thermocouple Connector

For a detailed analysis of potential thermocouple connector errors. it is assumed that there is a 2°F change in temperature along the length of the pin of the TC connector, and that the TC connector pins are made of material close to but not the same as the TC. In this case, a 2°F ΔT along the TC connector pins corresponds to about a 2°F error . This is a systematic uncertainty (B) because it can be reduced by reducing the ΔT along the connector pins. For this analysis, it will be assumed that there is a smaller change in temperature across the connector of only 0.3°C, and that the uncertainty scales linearly so the uncertainty is also about 0.3°C.

Summary for Type K thermocouple connectors:

B = ±0.3°C, and S = 0

b. Thermocouple Extension Wire

TC extension wire is used for two reasons: (1) to improve mechanical properties and (2) to use material that is less costly. ASTM specifications for TC extension wire are as follows: ±1.5°C (±4°F) between 0-200°C (32–400°F). Therefore, the extension wire uncertainty limits are the same as that for TC wire in the temperature range of 0-200°C (32–400°F). There is no guarantee that the error is ±1.5°C outside the 0-200°C range, and in fact the extension wire junction to the TC wire has to be kept "below the upper limit of the extension wires or considerable errors may be introduced." This is a systematic uncertainty (B).

Summary for Type K thermocouple extension wires:

B = ±1.5°C, and S = 0

c. Thermocouple Installation Method or Type and Shunting ErrorsThere is often a significant systematic error related to the installation of the TC or TC type used. The temperature of the measuring junction of the TC is never equal to the

temperature of the test item. The TC exchanges energy with the test item and with the environment so an error is always present. Estimating the error associated with mounting the TC to the test item is the key to accurate TC measurements in typical "abnormal" environments. This type of error can be called "mounting error" and is ±.3

Type K TC ±2°C or ±0.75% of reading (in °C), whichever is greater, from 0-1250°C (32 – 2300°F). Summary for TC B = ± 2 °C or ± 3/4% of reading S = 0 TC Type or Installation Errors: S = 0 B = ±.3	TC Connector Approximate error is same as ΔT across connector Summary for TC connector B = ± .3 S = 0	Extension Wire For cable temperature 0-200°C (32 - 400°F): ± 1.5°C Summary for extension cable B = ± 1.5°C S = 0

$B=[B_1^2+B_2^2+B_3^2+B_4^2+\ldots..]^{½}$

$=[2.0^2+.3^2+1.5^2+.3^2]^{½}$

$=6.43$

$S=[S_1^2+S_2^2+S_3^2+S_4^2+\ldots.]^{½} \quad =0$

So the uncertainty of thermocouple reading is

$U=\pm[B^2+S^2]^{½}$

$=\pm[6.43^2+0]^{½}$

$=\pm 6.43°C$

$=10.20\%$ of the reading

Uncertainty Analysis of heat capacity

Calculate the specific heat of the metal Cp using the following equation:

i. Temperature

(absolute uncertainty is ‡ distance between smallest mark, for this thermometer which measures to the nearest *f*C, uncertainty is 0.5^{o}C)

1. T_i (metal) = 24.3 ± 0.1^{o} C
2. T_f (metal) = 63 ± 0.1 ^{o}C
3. T_f (condenser)= 30.9± 0.1
4. ΔT (metal) = (63.9-24.3) ± (0.1 + 0.1) = 39.6 ± .2 ^{o}C % =.2/39.6*100 =.51%
5. ΔT(condenser)= (30.9-24.3) ± (.01+.01) = 6.6 ± .2°C % = .2/6.6 *100 = 3.03%

ii. Mass

1. metal = 7500 ± 50 g % = .66%

iii. specific heat capacity

1. (metal) add % uncertainties for all quantities involved in the calculation of the heat capacity 0.51 + 3.03 + .66 = 4.2 % of 0.9 J/g °C (±4.2) = .9 ±.04 J/g°C

Appendix D

Sample Calculation

1. For determining heat flux

$$\dot{Q}_{block}(W) = \frac{mass\ of\ Aluminium\ block\ X\ Specific\ Heat\ X\ Temp\ diff}{Time\ diff}$$

$$= \frac{M_{Al} S_{Al} \Delta \bar{T}_{Al}}{\Delta t}$$

The mass of Aluminiun block M_{Al} =7.5 kg

Specific Heat of Aluminium S_{Al} = 900 J/kg˚C

Temperature of Aluminium block after 210 min is 46.46˚C(For .6 fill ratio and 0˚ inclination)

Temperature of Aluminium block after 230 min is 46.83˚C (For .6 fill ratio and 0˚ inclination)

So Temperature difference $\Delta \bar{T}_{Al}$ = (46.83˚C-46.46˚C) = 0.37˚C

and time interval Δt = (230-210) min = 20 min =20 X 60 sec = 1200 sec

Heat absorbed by Aluminium block

$\dot{Q}_{block}(W)$ = (7.5 kgX 900 J/kg˚C X 46.83-46.46.46)˚C/(230-210)X60 sec

= 2.089 J/sec

= 2.089 W

$$\dot{Q}_w(W) = k_{Al} \frac{n\pi(d_o^2 - d_i^2)}{4} \frac{(\bar{T}_e - \bar{T}_c)}{L_{ad}}$$

Where

n = No of Aluminium pipes = 14

d_o = Outer dia of Aluminium pipes = .004 m

d_i = Inner dia of Aluminium pipes = .003 m

$\bar{T}_e$ = Average temperature of evaporator section = 46.83 °C (For .6 fill ratio, inclination angle 0˚ and after 230 min of heating)

$\bar{T}_c$ = Average temperature of condenser section = 41.82 °C (For .6 fill ratio, inclination angle 0˚ and after 230 min of heating)

L_{ad}= Distance between evaporatorr and condenser section = .12 m

k_{Al} = Thermal conductivity of Aluminium = 250 W/m ˚C

$\dot{Q}_w(W)$ = 250*14*3.14*(0.004^2-0.003^2)*(46.83-41.82)/(4*0.12)

= 0.803 W

$$\dot{Q}_{php}(W) = \dot{Q}_{elec} - \dot{Q}_{block} - \dot{Q}_w$$

= (36-2.089 -0.803)W

=33.108 W

2. For determining overall heat transfer coefficient

$$U_{php}\left(\frac{W}{m^2}{}^{\circ}C\right) = \frac{\dot{Q}_{php}}{\bar{T}_e - \bar{T}_c}\left(\frac{1}{A_{ei}} + \frac{1}{A_{ci}}\right)$$

Where average evaporator temperature $\bar{T}_e$

Average condenser temperature $\bar{T}_c$

Surface area of evaporator A_{ei}

Surface area of Condenser A_{ci}

Heat Input $\dot{Q}_{php}$

For .4 fill ratio and 0˚ inclination at steady state condition

$\bar{T}_e$=47.33˚C

$\bar{T}_c$=44.47˚ C

A_{ei}=.0236 sq mm

A_{ci}=.0441 sq mm

$\dot{Q}_{php}$=33.858 W

U_{php}=782.308W/m² ˚C

3. For determining Thermal Resistance.

The thermal resistance of the CLPHP is calculated as, $R_{combined}(°C/W) = \frac{\bar{T}_e - \bar{T}_c}{\dot{Q}_{php}}$

For .4 fill ratio and 0˚ inclination at steady state condition

$\bar{T}_e$=47.33˚C

$\bar{T}_c$=44.47˚ C

$\dot{Q}_{php}$=33.858 W

R=.083 °C/W